c.3

RESEARCH AND DEVELOPMENT BRANCH
DEPARTMENT OF NATIONAL DEFENCE
CANADA

DEFENCE RESEARCH ESTABLISHMENT OTTAWA

DREO REPORT NO. 736
DREO R 736

THE FLOW OF WATER AND HEAT THROUGH NARES STRAIT

by

H.E. Sadler

PROJECT NO.
97-67-05

DECEMBER 1976
OTTAWA

CAUTION

This information is furnished with the express understanding that proprietary and patent rights will be protected.

RESEARCH AND DEVELOPMENT BRANCH

DEPARTMENT OF NATIONAL DEFENCE
CANADA

DEFENCE RESEARCH ESTABLISHMENT OTTAWA

REPORT NO. 736

THE FLOW OF WATER AND HEAT THROUGH NARES STRAIT

by

H.E. Sadler

Earth Sciences Division

PROJECT NO.
97-67-05

PUBLISHED FEBRUARY 1976
REPRINTED DECEMBER 1976
OTTAWA

76-207

TABLE OF CONTENTS

ABSTRACT

The flow of water from the Polar Ocean through Nares Strait is described by means of observations of water characteristics in the Strait and current meter observations in Robeson Channel. The mean annual volume discharge of water from the Polar Ocean is estimated to be 2.1 x 10^4 km^3 $year^{-1}$ which is a higher value than previous estimates. The mean annual transport of salt out of the Polar Ocean through the Strait is estimated to be 6.7 x 10^{14} kg $year^{-1}$.

Thermograph records and observations of ice movement are used to derive a value for the mean annual heat flux into the Polar Ocean of 2.1 x 10^{19} cal.$year^{-1}$, which is also a higher value than previous estimates.

A discussion of tidal variations shows that the tides in Robeson Channel are mixed diurnal/semidiurnal with maximum current velocities along the axis of the channel of the order of 1.5 $m.s.^{-1}$ at 100 m depth.

A new explanation is proposed for the origin of Baffin Bay Bottom Water which depends on the assumption of a greater than usual amount of ice formation in the North Water polynya.

RESUME

Les observations des charactéristiques de l'eau dans le détroit Nares et les résultats obtenus par les compteurs de flot dans le canal Robeson servent à décrire le flux de l'eau provenant de la mer polaire. Ici on évalue ce flux à 2.1 x 10^4 mètres cubes par an. Cette estimation est plus grande que les estimations antérieures. On trouve aussi que le transport de sel par le canal se monte à 6.7 x 10^{14} kilograms par an.

Les courbes enregistrées par les thermographes et les observations des mouvements de la glace servent à estimer le flux annuel de chaleur dans le mer polaire à 2.1 x 10^{19} calories par an, une estimation qui est aussi plus grande que les antérieures.

On discute aussi les marées au canal Robeson. Elles sont du types diurne/semidiurne et leurs velocités axiales atteignent approximativement 1.5 mètres par seconde.

Une nouvelle theorie est proposèe pour expliquer l'origine de l'eau profonde de la baie de Baffin. Cette théorie suppose que la génération de la glace dans le polynia North Water est beaucoup plus grande que celle des regions voisines.

SYMBOLS AND ABBREVIATIONS

A	Cross-sectional area of channel in square metres.
ΔA_i	Area of the i^{th} element of the cross-sectional area.
C_I	Specific heat of ice in calories per kilogram per degree Celsius.
C_p	Specific heat of water in calories per kilogram per degree Celsius.
CPH	Cycles per hour.
f	Coriolis factor.
h	Ice thickness.
L	Characteristic length.
L_I	Latent heat of fusion of ice in calories per kilogram.
$\hat{Q}$	Total heat flow in calories per year.
Q_I	Heat transported by sea ice in calories per year.
$\hat{Q}_I$	Annual heat transport by sea ice in calories per year.
Q_w	Heat transported by water in calories per second.
$\overline{Q}_w$	Mean transport of heat by water in calories per second.
$\hat{Q}_w$	Annual heat transport by water in calories per year.
S	Salinity in parts per thousand.
S'	Salinity of sea ice in parts per thousand.
T	Time period of integration.
T	Temperature in degrees Celsius.
T_I	Mean temperature of sea ice.

T_i	Mean temperature of water at a given point in the cross-section.
T_R	Reference or 'sink' temperature.
U	Mean water velocity in metres per second.
U_x	Mean axial water velocity in metres per second. Positive values indicate a flow into the Arctic Ocean.
U_y	Mean cross-channel velocity in metres per second. Positive values indicate a flow to the south-east.
u	Instantaneous water velocity at a given point.
u'	The variation of the instantaneous velocity around the mean value U.
u_o	Characteristic velocity.
$\overline{V}$	Mean rate of volume transport of water in cubic metres per second.
$\overline{V}_i$	Mean rate of volume transport of water through the i^{th} element of the cross-section.
v	Axial velocity in metres per second.
V_I	Rate of volume export of ice in cubic metres per second.
ρ_o	Density of water in kilograms per cubic metre.
ρ_I	Density of sea ice in kilogrammes per cubic metre.
ρ_p	Density of water at constant pressure.
σ_T	Density of sea water.
ϕ	Latitude.
ω	Earth's angular velocity.

LIST OF FIGURES

LIST OF FIGURES - continued

LIST OF FIGURES - continued

LIST OF FIGURES - continued

LIST OF FIGURES - continued

LIST OF FIGURES - continued

LIST OF TABLES

ACKNOWLEDGEMENTS

The support and assistance of several organizations and of many people are essential to the successful conclusion of oceanographic investigations in Arctic regions. In the present case, the work was supported by the Defence Research Board with ship time made available by the Canadian Coast Guard (Transport Canada). In particular I wish to acknowledge the support and encouragement given by Mr. T.A. Harwood, Miss Moira Dunbar and Dr. J.H. Greenblatt all of the Defence Research Establishment Ottawa, Geophysical Division.

The observational work at the ice stations could not have been completed without the ungrudging assistance of Messrs. H.V. Serson, J.E. Keys and D. Finlayson in particular, while the assistance of R. Herlingveaux and the support of Captain Paul Fournier of the CCGS Louis S. St. Laurent and his crew enabled me to complete the planned summer programme in full.

Finally I would like to acknowledge the valuable assistance of Dr. C.R. Garrett of Dalhousie University, Dr. C.R. Mann and Dr. W.D. Forrester of the Bedford Institute and Dr. A.E. Collin of Environment Canada who read and commented on the text.

FIGURE 1 *General Map of the Canadian Archipelago showing the main passages between the Polar Ocean and Baffin Bay.*

Chapter I

INTRODUCTION

The Arctic Ocean, surrounded by the great land masses of the earth, has only three connections with the rest of the World Ocean. Of these three, by far the largest is the gap between Greenland and the Eurasian continent. Its width is 1450 km and its maximum sill depth is 3400 m and through this opening flows by far the greater part of the water entering or leaving the Arctic Ocean.

The Bering Strait provides a much more constricted passage; it is about 65 km wide and its limiting depth is only about 50 m. The third connection is via the network of passages through the Canadian Archipelago into Baffin Bay and the Labrador Sea (Fig. 1). While the transports in this region are certainly much smaller than those through the Greenland Sea and the Denmark Strait, their effects on conditions in Baffin Bay and within the archipelago itself are critical, and their measurement presents a more complex problem than that in most regions. However, this area is one of growing importance and interest for scientific and other reasons, and it is becoming ever more desirable that the effects of these interchanges of water and heat be well understood.

In the past decade movement into the Arctic regions each summer has increased by a factor of three or four and there is every sign that this expansion of interest in the region has not yet reached its peak. Every summer a small armada of ships sails north, carrying supplies for military bases, airfields, meteorological stations and centres of population. Equipment for mining and oil companies flows in by sea and by air as the search for materials in increasingly short supply progresses. Work is being undertaken in the engineering aspects of the recovery and export of oil through off-shore wells and underwater pipelines. The Mackenzie delta is now the proud possessor of an artificial island and in the Queen Elizabeth Islands the drilling rigs are hard at work. It seems to be unavoidable that in a very few years oil, gas and iron ore and other metals will be moving south through this region and that considerable changes to the whole ecosystem are possible. In much of the area there is little or no definitive knowledge which could be used to estimate the effects of any changes, or indeed to permit rational design factors to be applied to the facilities themselves.

It therefore becomes important to obtain knowledge of the mechanism of water movement and exchange processes between the Arctic Ocean and Baffin Bay. These exchanges are confined to the three channels, Lancaster Sound, Jones Sound and Smith Sound which open into Baffin Bay (Fig. 1). Some flow takes place west and south of Baffin Island through Fury and Hecla Strait, via Foxe Basin and Hudson Strait, but the magnitude of the volume transport through this constricted channel is not known. The only current velocity measurements available are a 24 hour series obtained by Barber (1964) and because of the large tidal variations which occur no valid estimate of the relative importance of the volume transport can be made. The transport through Fury and Hecla Strait is thus undetermined but has been incorporated in most previous estimates of the total flow through Lancaster Sound. In passing it may be observed that we propose to make direct measurements of the currents and transports in the Strait over a period of 6 weeks in 1976.

While some work has been done on the three main channels there are insufficient data to give any definite answers and the data available are largely confined to the summer months from July to September. The work reported on here is an attempt to provide some understanding of exchange processes through Nares Strait, one of these three channels, using data obtained in April and May as well as summer data.

GENERAL BACKGROUND

The Arctic Ocean lies in a deep basin almost completely surrounded by land and continental shelf. The main bathymetric features are indicated in Figure 2. The more obvious characteristics of the ocean may be listed:

1. its connections with the world oceans are very restricted;
2. it is completely circum-polar;
3. it receives more fresh water run-off in comparison to its volume than any other ocean, and this run-off is highly seasonal;
4. it is situated almost entirely north of the Arctic Circle and thus the insolation received is also highly seasonal;
5. it is largely covered with heavy pack ice throughout the year - almost completely so in winter and spring;
6. precipitation is generally small but still exceeds evaporation;
7. air temperatures are below freezing point for most of the year;

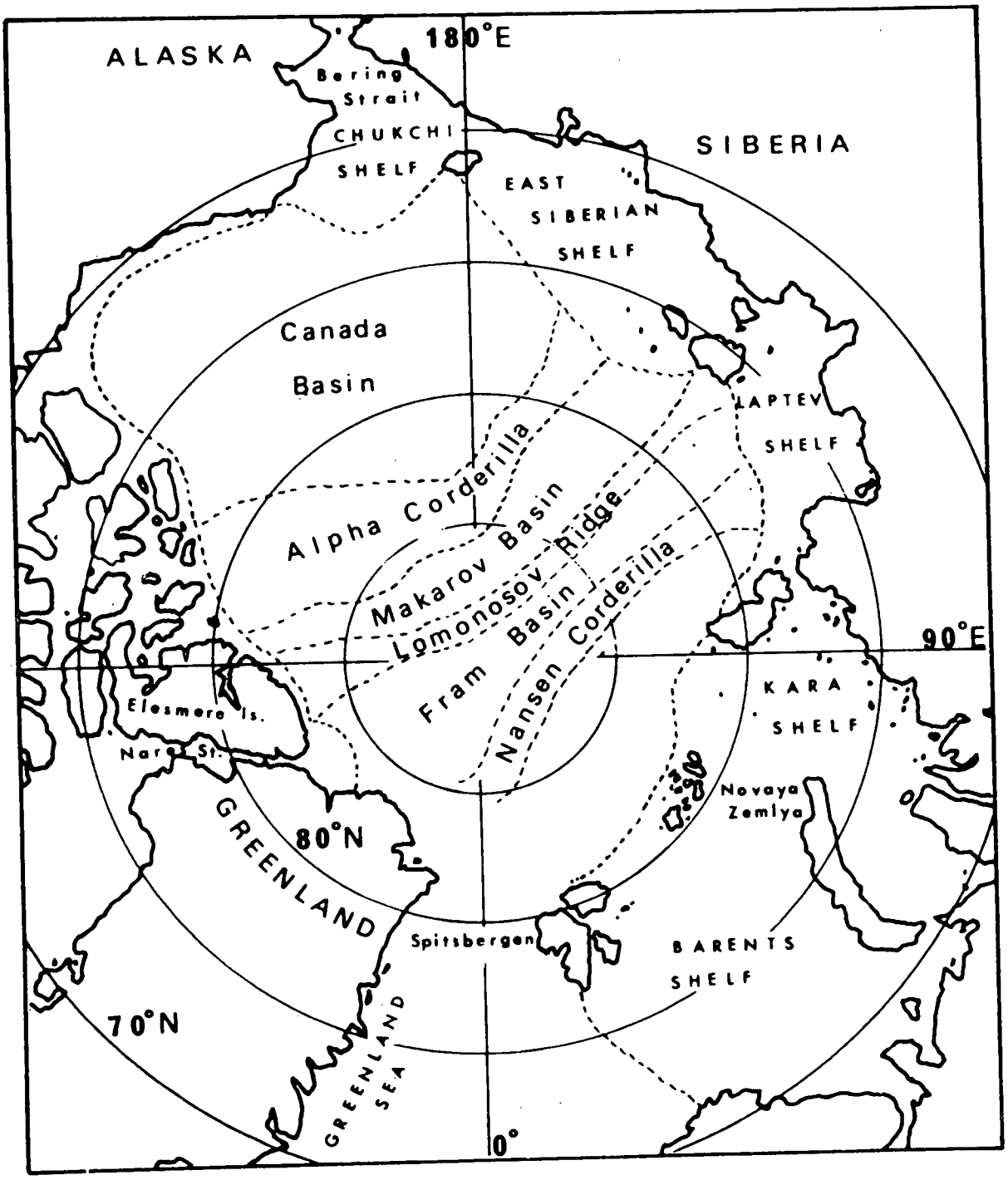

FIGURE 2 *Map of the Arctic Ocean showing the General Bottom Structure.*

8. the continental shelves surrounding it comprise a much higher proportion of its total surface area than is the case for any other ocean.

The combination of these and other factors renders the Arctic Ocean very different from any other and some of the features which affect the object of this investigation must be discussed briefly.

THE CONTINENTAL SHELVES

While the area of the Polar Ocean* is about 14 x 10^6 km^2, about five times as large as the Mediterranean, its volume of 17 x 10^6 km^3 is only about three times as large. Over 35% of its area overlies the continental shelves and this 35% of area contains only 2% of the total volume. The most extensive of these shelves, that bordering the Eurasian continent, extends up to 1000 km from the land. This section, covering roughly 180° of longitude east from the prime meridian, is divided by headlands and islands into five marginal seas, the Chukchi, East Siberian, Laptev, Kara and Barents Seas. These shallow seas receive the out-flow from all but two of the major rivers flowing into the Arctic Ocean (Coachman and Barnes 1962). Antonov (1958) estimates the total run-off from the Eurasian rivers at just under 3000 km^3 per year which is only 0.8% of the volume of the marginal seas. However, most of this river water is discharged over a period of only a month or so and at this time in some places the water over the shelf may contain as much as 5% river water. Zubov (1943) found that most of the south-western part of Kara Sea, for example, had surface salinities less than 30 °/oo during the run-off period.

The shelf on the American side of the basin is much narrower, from 15 to 50 km off the Alaskan peninsula and round the western margin of the Canadian Archipelago. It widens to about 250 km off northwest Greenland. Two large rivers enter the Arctic Ocean on the American side of the polar basin, the Yukon, most of whose waters flow north through the Bering Strait into the Chukchi Sea, and the Mackenzie which drains into the Beaufort Sea. Antonov (1958) estimated the run-off from the North American continent at 1000 km^3 per year. The shallow waters of the channels through the archipelago interpose a barrier several hundred kilometres wide between the Arctic Ocean and the deep waters of Baffin Bay, with sill depths of the order of one or two hundred metres.

---

* The Polar Ocean as used in this paper means the Arctic Ocean less the Norwegian and Barents Seas but including the other marginal seas.

THE WATER-MASSES OF THE ARCTIC OCEAN AND THE NEIGHBOURING SEAS

The characteristics of the Arctic Ocean waters are remarkably constant in distribution below the surface layer, and the seasonal changes in the surface layer are repeated very closely from year to year. Typical salinity and temperature curves are given by Sater et al (1971) and these are reproduced in Figure 3. Together with the T-S curves in Figure 4, they indicate that the water structure is almost identical below 350 m for stations in several parts of the Arctic Ocean and the North Atlantic while the water in Baffin Bay is similar but 0.5 $^{o}/oo$ less saline. Above 350 m local processes become important. The major processes are seasonal but are confined to the surface layers down to 200 m or so. For example, the only winter data which is known from Baffin Bay (Muench and Sadler 1973) indicates that except near the surface there is no significant difference between the summer T-S curve shown in Figure 4 and that shown in Figure 5A which was obtained in February. The seasonal effects may be summarized as follows:

SUMMER PROCESSES

a) Addition of fresh water by river run-off.

b) Addition of fresh water from melting ice.

c) Solar heating.

d) Increased evaporation from the surface.

The first three of these processes decrease the density of the surface layer, mainly by decreasing the salinity. The temperature near the surface never rises much above freezing point in the Arctic Ocean proper although in some of the marginal seas, such as Baffin Bay, where large stretches of open water are found, the surface temperature may rise 3 or 4 degrees above freezing point. Over most of the ocean the heat absorbed by the surface water is converted into latent heat of melting ice, while that absorbed by the surface of the ice itself produces melt pools on the floes which eventually drain into the sea. About 30-40 cm of ice are ablated from the surface of the floes each summer, ice whose salinity is less than 4 $^{o}/oo$. Almost all of the evaporation occurs between May and September and, using values given by Vowinkel and Orvig (1970) may be estimated to be about 500 km^3 per year. The precipitation is more evenly distributed through the year and was estimated by Sverdrup (quoted by Vowinkel and Orvig 1970) as about 3300 km^3 per year. Thus during the five month period from May to September the excess of precipitation over evaporation is of the order of 100 km^3 which is equivalent to a layer of fresh water about 0.1 metres in thickness. The final result is a highly stable surface layer of comparatively fresh water which greatly reduces the vertical convection of water and heat between the upper few metres and that below.

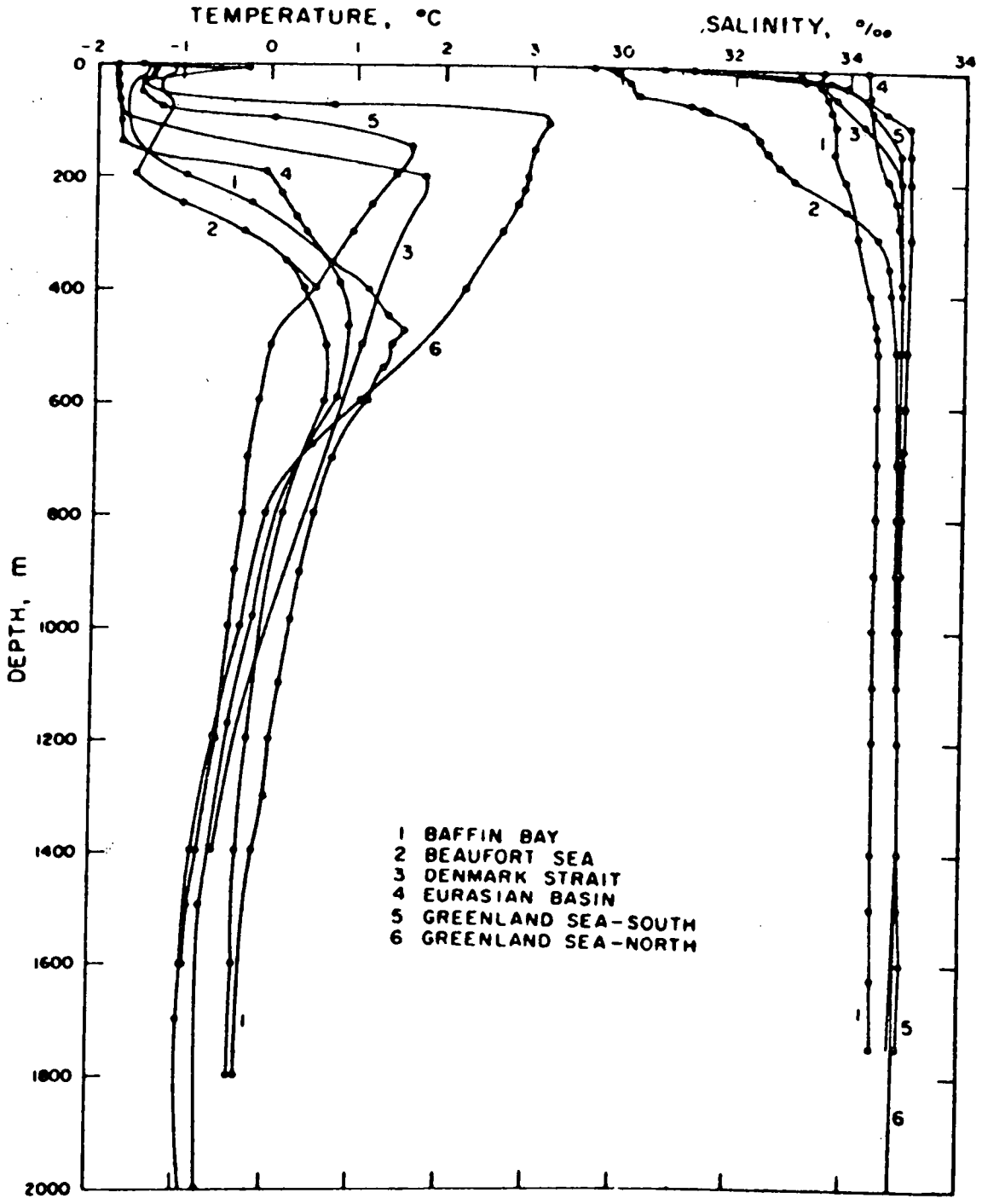

FIGURE 3 *Temperature and Salinity Profiles for a number of Stations in the Arctic Ocean (After Sater 1971).*

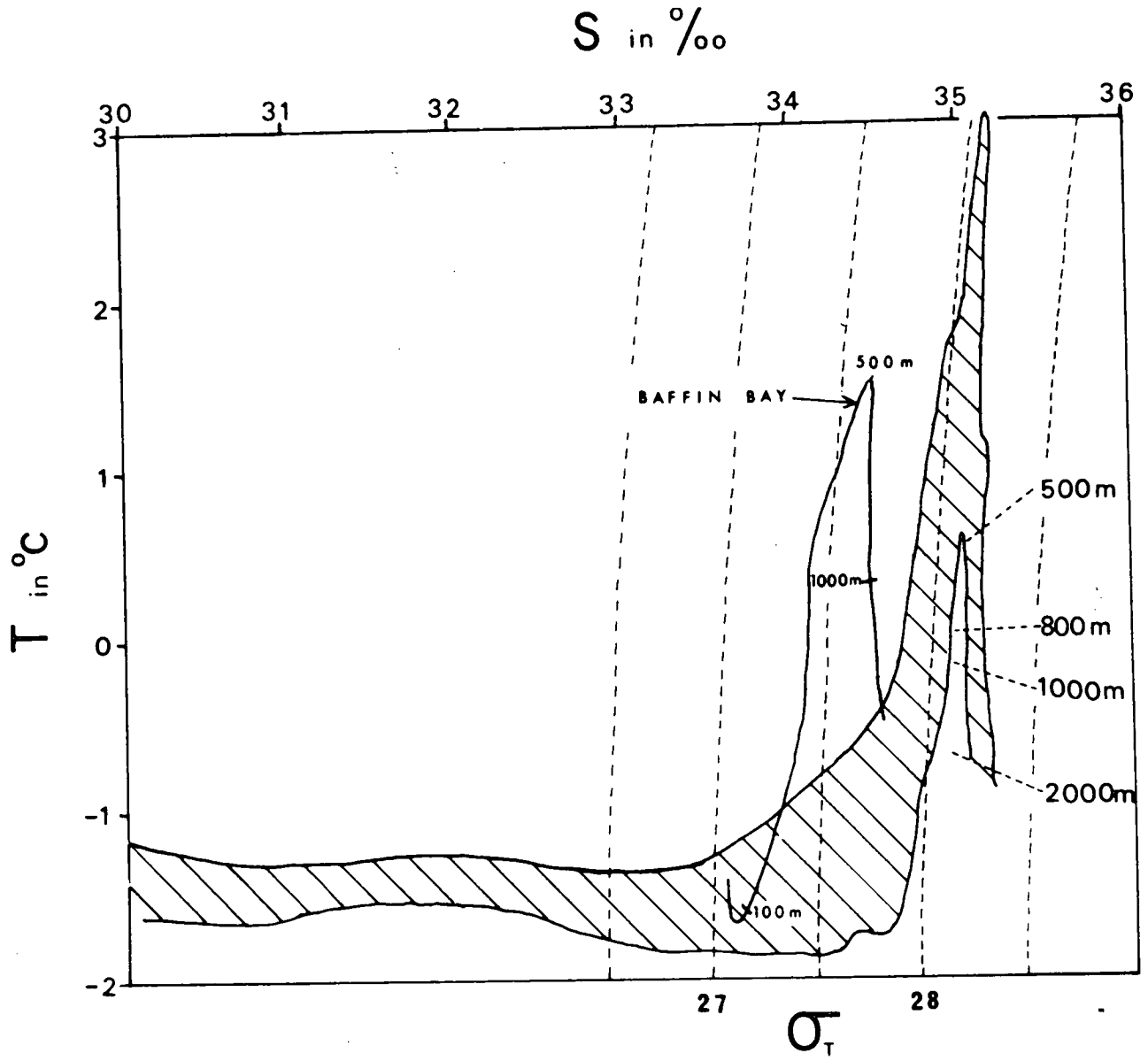

FIGURE 4 *Envelopes of the T-S Curves for the stations shown in Figure 3. The T-S Curve for Baffin Bay is drawn separately.*

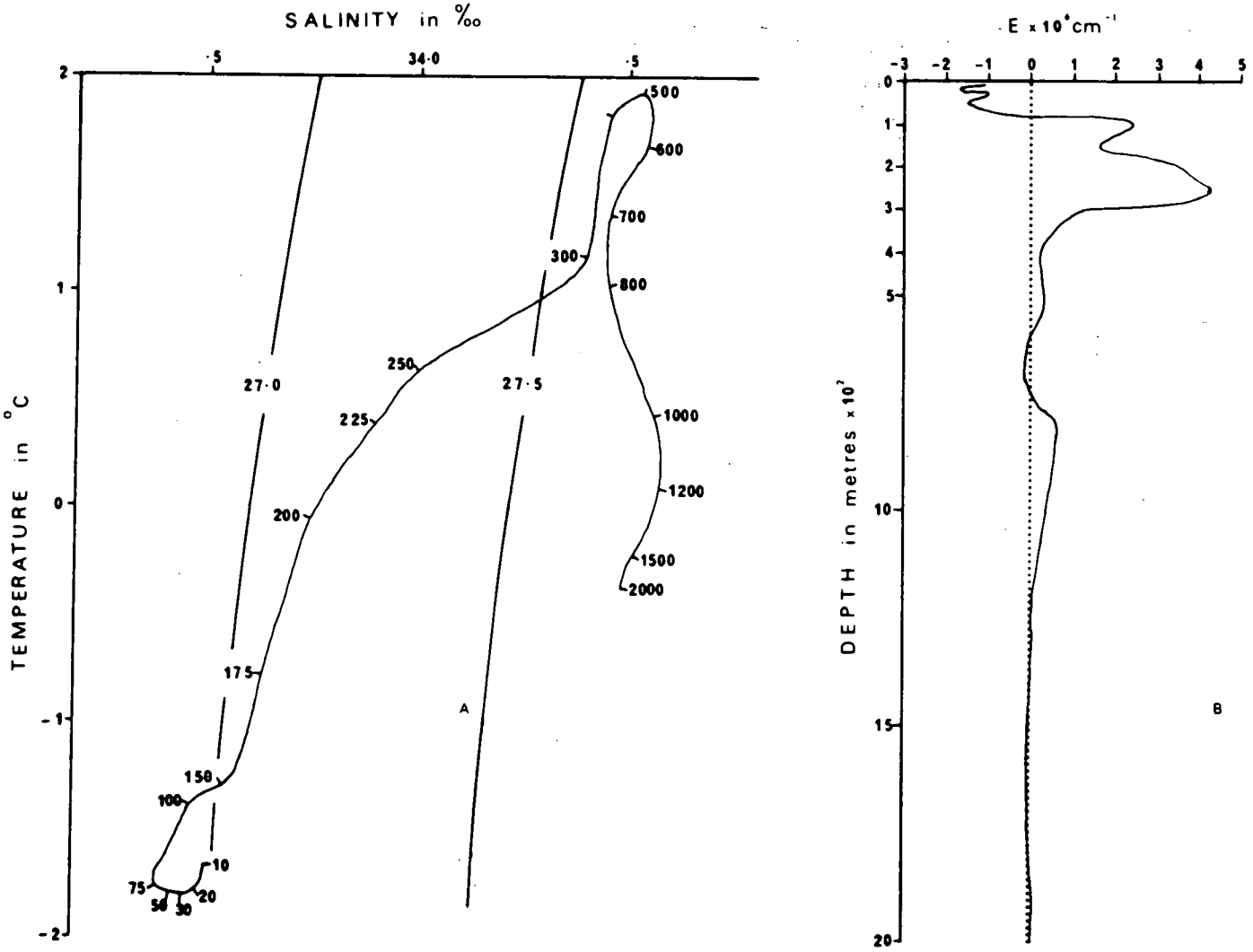

Figure 5A *A T-S Curve in Baffin Bay in February 1972 (From Muench and Sadler 1973).*

B *Stability Curve for water volume in Fig 5A.*

WINTER PROCESSES

a) Freezing of surface water causing local increases in salinity.

b) Rapid loss of heat to the atmosphere from open water areas and loss of heat from ice surfaces due to radiation.

The result of both of these processes is to increase the density of the water near the surface and a vertical convection process is set up. Coachman (1966a) described the formation of supercooled water under areas of freezing and the subsequent formation of convection cells.

The surface instability under conditions of rapid freezing is illustrated in Figures 5A and 5B. Figure 5A shows the T-S curve for a station in Baffin Bay in February 1972 (Muench and Sadler 1973). The surface water down to 75 metres appears to be unstable with other possible regions of instability around 700 m and below 1200 m. Figure 5B shows the variation with depth of the stability factor E in $cm^{-1} \times 10^6$. E is defined as the ratio of the acceleration experienced by a water particle displaced from its rest position by a distance of 1 cm to the acceleration of gravity, and is given by Defant (1929) in the form

$$E = \frac{1}{\rho}\left[\frac{\partial \rho}{\partial S}\frac{dS}{dz} + \frac{\partial \rho}{\partial T}\left(\frac{dT}{dz} - \frac{d\theta}{dz}\right)\right] \qquad 1.1$$

where ρ is the density in situ in $gm.cm^{-3}$

S is the salinity in $^{o}/oo$

T is the temperature in situ in ^{o}C

and $\frac{d\theta}{dz}$ is the adiabatic temperature gradient in $^{o}C.cm^{-1}$.

The curve in Figure 5B was calculated from this expression using tables developed by Hesselburg and Sverdrup (1914, 1915). The surface instability above 75 m shows up clearly as negative values of E but the magnitudes of negative E at 700 m and between 1400 and 1800 m are very small. They do not indicate regions of actual overturn since the derivation of Equation 1.1 neglects the effects of heat conduction, friction, diffusion and horizontal pressure gradients around a displaced particle. Neumann (1948) showed that stability vanishes only when E attains a small negative value and the column below 75 m is in fact stable. The large decrease in stability at 300 m is an indication of the boundary between the layer of the Arctic Surface Water and the underlying Atlantic Layer. Above 75 m it appears that overturn was occurring. The air temperature at the time of the observations was $-30^{o}C$ with a 10 $m.s.^{-1}$ wind and the water in the lead was freezing very rapidly.

Such processes, however, are usually insufficient in the open ocean to cause mixing to extend to a depth greater than about 200 m and water from below this is advected almost unchanged from the peripheral seas.

As we shall discuss later in more detail the relatively shallow and constricted passages through the Bering Strait and the Canadian Archipelago prevent the free advection of water deeper than 200 m or so. However, the third passage, through the Greenland-Eurasian Gap has a maximum sill depth of 3400 m and it thus provides a passage for water above that depth between the Polar Ocean and the Greenland Sea. As a result, the structure of the Arctic Ocean is in three layers.

Arctic water:- The layer from the surface to some 200 m depth is subject to seasonal change and may have differing characteristics with change in geographical position. These changes usually repeat very closely from year to year. The temperature of the layer is always near its freezing point rising a few degrees above this temperature only in areas which are generally ice free during the northern summer. Similarly the salinity of the surface water may vary quite widely with changing season and location but it increases rapidly with depth and reaches almost a uniform value of about 34.5 ^{o}/oo at a depth of 200 m.

The Atlantic layer:- This layer, between 200 and 1000 m, is generally warmer than the water above or below it. The temperature is above 0^{o}C at 350 - 500 m. The salinity increases with depth until at about 400 m, roughly the same depth as the temperature maximum, it reaches a value of 34.9 ^{o}/oo to 35.1 ^{o}/oo which is constant through the rest of the layer and almost uniform over the whole of the Arctic Ocean.

The Arctic Bottom Water which lies below the Atlantic Layer has temperatures below 0^{o}C and a similar salinity to that in the Atlantic Layer being essentially uniform between 34.98 ^{o}/oo and 34.99 ^{o}/oo. The deep Arctic Ocean is subdivided into four separate basins (Figure 2). The Lomonosov Ridge running from Ellesmere Island over the pole to Siberia divides the ocean into the Eurasian Basin and the Canadian Basin. The Eurasian Basin is again subdivided by the northern extension of the mid-Atlantic ridge while a less well defined feature, the Alpha Rise, separates the Canadian Basin into two parts. These features, particularly the Lomonosov Ridge whose peaks reach to within 1500 m of the surface, must have a profound effect on the movements of the bottom waters. One indication of this is that the temperature in the bottom waters of the Canadian Basin are about -0.3^{o}C while in the Eurasian Basin the equivalent temperatures are about -0.7^{o}C.

DENSITY STRUCTURE

The extreme range of temperature in the water column is small and is confined to within one or two degrees of 0^{o}C. In this temperature

region $\partial\sigma/\partial T$ is small and as a result the variations in density which occur are almost entirely due to salinity changes. The result is a basic two layer structure for the whole ocean, a water mass with a σ_T value of about 28.0 being overlain by a relatively thin layer with a σ_T value of about 26.5 separated by a fairly sharp pycnocline. These highly stable conditions in effect put a lid on the Arctic Ocean and severely limit vertical convection and the loss of heat from the main water mass of the ocean to the atmosphere during the winter.

CURRENTS IN THE ARCTIC OCEAN

In some respects the Polar Basin may be considered as a kind of estuary, at least during the two months when the major part of the annual influx of fresh water occurs. During this short period the influx of fresh water is distributed around half the circumference, between the Beaufort and Barents Seas, while at the same time more fresh water is formed by the melting of the sea ice which occurs fairly uniformly over the whole area. The surface flow is directed generally towards the outlet at the "seaward" end and this is balanced by a general influx of more saline water below 200 metres mainly from the Greenland Sea. During the summer run-off the surface salinity around the "head" of the estuary may fall as low as 27 $^{o}/oo$ increasing to seaward until it meets the surface waters of the Atlantic in the Greenland Sea. In the winter, with no run-off and with ice forming rather than melting, the near-surface salinities increase everywhere, up to 2 $^{o}/oo$ in the peripheral seas and 1 $^{o}/oo$ in the central ocean, while the general relative distribution remains much the same as that during the summer.

Baffin Bay during the summer months presents a similar picture. While no major rivers drain into it, it is fed near its northern end with less saline Arctic Surface Water through the channels from the Arctic Ocean and this flow is combined with the fresh water run-off in the form of both glacier melt-water and glacier ice. The surface salinity in northern Baffin Bay may fall as low as 30 $^{o}/oo$ while in winter values as high as 34 $^{o}/oo$ may be encountered (Muench and Sadler 1973).

However, the estuary analogy is of doubtful value in discussing the currents in the Arctic Ocean since many such phenomena occupy only a small fraction of the year.

Arctic Water: The surface circulation shown in Figure 6 is taken from Sater, Ronhovde and Van Allen (1971) and is based on all available data from manned ice islands, floe stations and ships and on the mean dynamic topography estimated from 300 stations. They describe a general drift of surface water from the Eurasian shelf towards the pole with a magnitude of 2 or 3 $cm.s^{-1}$. Beyond the pole this drift becomes concentrated

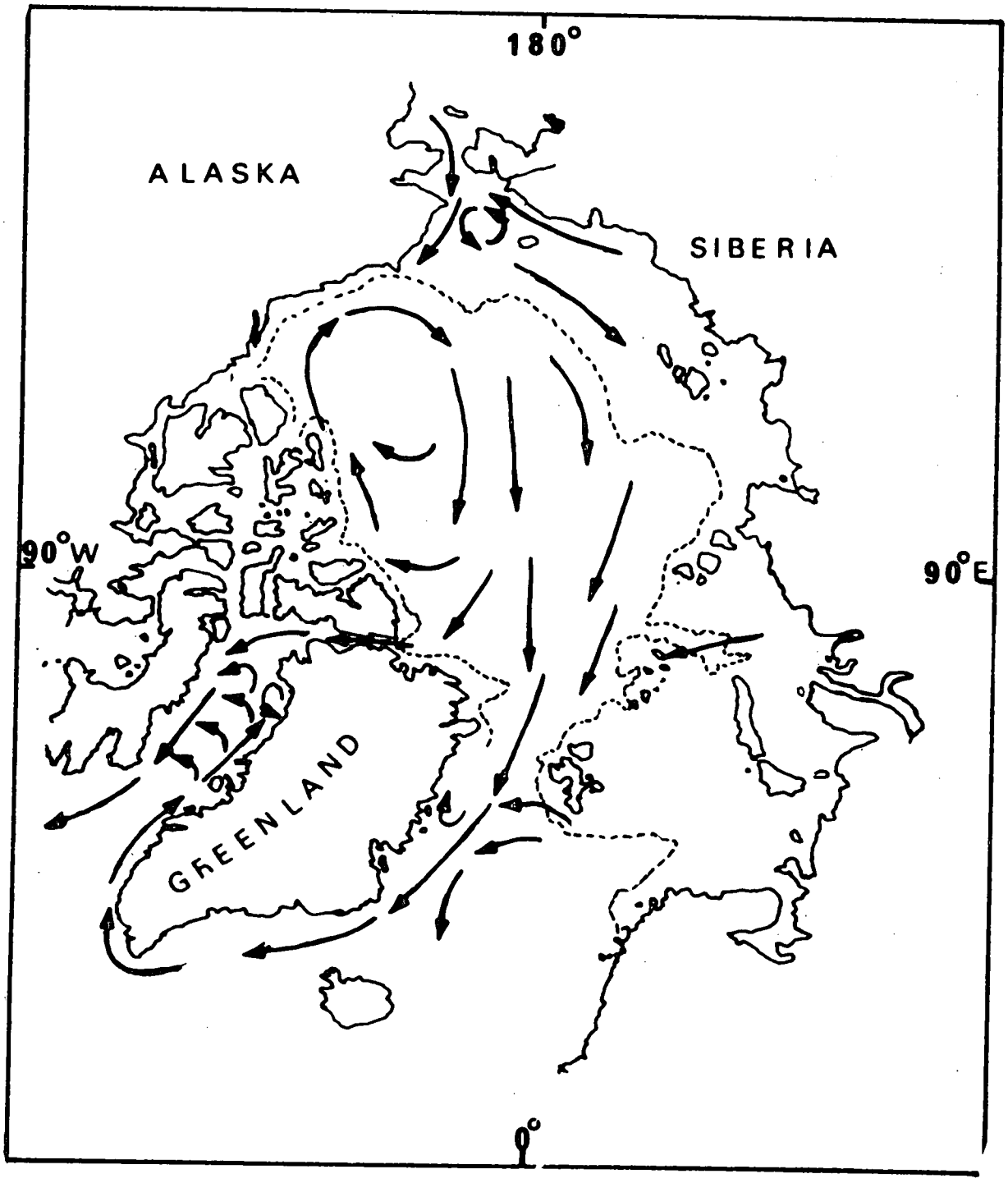

FIGURE 6 *General Surface Circulation in the Arctic Ocean.*

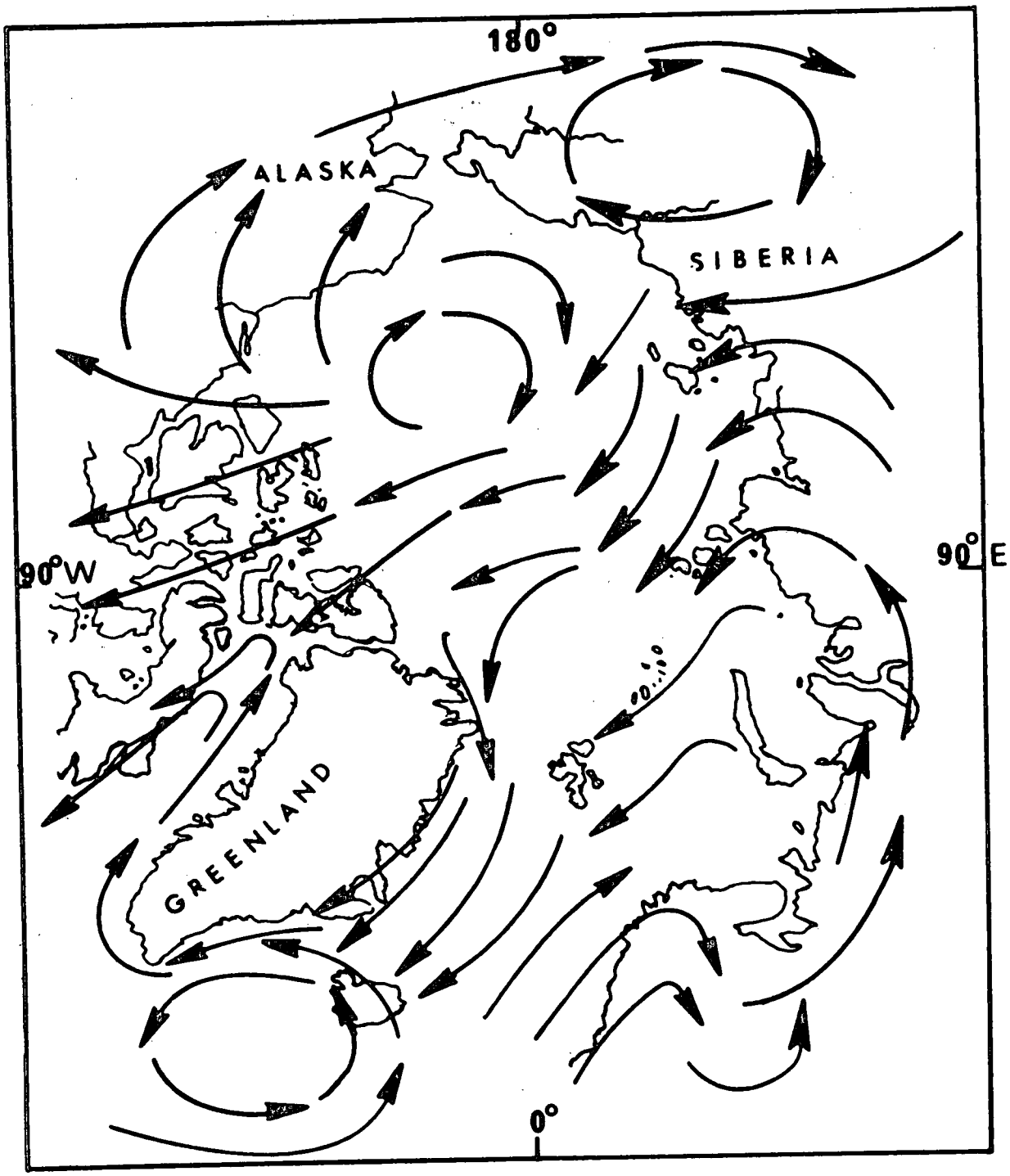

FIGURE 7 *Mean Annual Wind Pattern Over the Arctic Regions.*

towards the exit where it forms part of the East Greenland Current. Mixing with the Atlantic Surface Water in the large cyclonic gyre in the Greenland Sea it flows south-westward along the coast of Greenland at speeds up to 40 $cm.s^{-1}$. Almost isolated from this general circulation, the waters of the Beaufort Sea form a large clockwise gyre off the western shores of the Canadian Archipelago. In Baffin Bay a general counter-clockwise circulation exists formed by the West Greenland Current running north along the Greenland coast and the Canada Current flowing south off Baffin Island.

The probable origin of this current pattern is indicated in Figure 7 which is a representation of the mean annual wind directions taken from the mean annual isobars given by Vowinkel and Orvig (1970 p. 212). The correlation between the surface currents shown in Figure 5B and the mean annual winds is clear and it seems probable that the surface circulation in the Arctic Ocean is largely, if not entirely, wind driven. The only region where this is not entirely true is in the Bering Strait where a northward flow is found (Coachman and Aagaard 1966) which includes the run-off from the Yukon River.

The Atlantic Layer:- The circulation in this layer was deduced by Sater (1971) from the density structure and partially confirmed by direct current readings from ice islands (Hunkins 1966). It appears that water entering from the Greenland Sea crosses the Lomonosov Ridge and forms a generally cyclonic circulation with an anticyclonic gyre in the Beaufort Sea. Outflowing Atlantic water forms the deeper waters of the East Greenland Current as described by Coachman and Barnes (1963) and Aagaard and Coachman (1968).

The Arctic Deep Water:- Even less is known about movements in the deep layer of the Arctic Ocean. The few direct readings available (Hunkins 1966) indicate that the current velocities are similar to those in the Atlantic Layer, but the circulation will obviously be governed largely by bottom morphology.

Currents in Baffin Bay:- These follow an analagous pattern to those in the Arctic Ocean and have been described by Muench (1971). The surface circulation is cyclonic with water entering from the Atlantic through the Davis Strait as the West Greenland Current. Some water also enters via Smith, Jones and Lancaster Sounds, and the combined outflow, known as the Canadian Current, runs southerly along the eastern shores of Baffin Island. This current gathers speed as it flows south past Hudson Strait, being now known as the Labrador Current. The Atlantic Layer has essentially the same pattern of movement as the surface waters although too few direct readings are available to estimate speeds. The motions of the bottom water in Baffin Bay are not known.

ADVECTION BOUNDARIES

The Greenland-Spitzbergen Gap: The Greenland Sea is separated from the Arctic Ocean at about 79°N by a rise which extends from Greenland to the shelf near Spitzbergen at a depth of about 2800 m. This feature, the Nansen Rise, is cut transversely by the Lena Trench which has a least depth of 3400 m. To the south in about 71°N the Greenland Sea is separated from the Atlantic by the Jan Mayen Ridge with a sill depth of about 1500 m. The resulting connection between the Arctic Ocean and the Atlantic is by far the biggest of the three and most of the flow of water in and out of the Arctic Ocean occurs here. Measurements of water transport are few and inconsistent but the influx of Atlantic Water is probably of the order of 3×10^6 $m^3 s^{-1}$. Observations from the ice island ARLISS II which drifted into the Greenland Sea in 1965 gave the volume transport of the East Greenland Current as $283 \times 10^6 m^3$ sec^{-1}. This large transport is mainly due to the counterclockwise circulation in the Greenland Sea, the interchange with the Arctic Ocean being only a marginal effect, a small fraction of the total circulation.

The Bering Strait is the best known of the advection boundaries, in the summer months at least. The summer transport north through the Strait is about 0.75×10^6 $m^3 s^{-1}$ (Coachman and Aagaard 1966b). The transport in winter is probably less.

The Canadian Archipelago: The flow is generally from the Arctic through the channels into Baffin Bay but there have been few direct current readings. Collin (1963) estimated the total mass transport through the Archipelago at 0.1×10^6 $m^3.s^{-1}$ and that via Robeson Channel as 0.04×10^6 $m^3.s^{-1}$ calculated from water density data. However, other estimates have varied by more than an order of magnitude from this. Timofiev (1965) estimated the total flow as 0.95×10^6 $m^3 s^{-1}$ while Treshnikov (1959) gave a value of 0.25×10^6 $m^3 s^{-1}$. Forrester (1972) has pointed out the limitations of using a geostrophic approximation from isolated data points. Only rough estimates have been made of heat transport into Baffin Bay and then only during the summer, although this parameter may be of some importance in the formation of the North Water, the large permanent polynya in the northern end of Baffin Bay.

NARES STRAIT AND ROBESON CHANNEL

THE BATHYMETRY OF NARES STRAIT

As is the case for much of the Archipelago, Nares Strait is not well surveyed over most of its length. It runs (Figure 8) NE to SW between Greenland and Ellesmere Island for a distance of some 550 km.

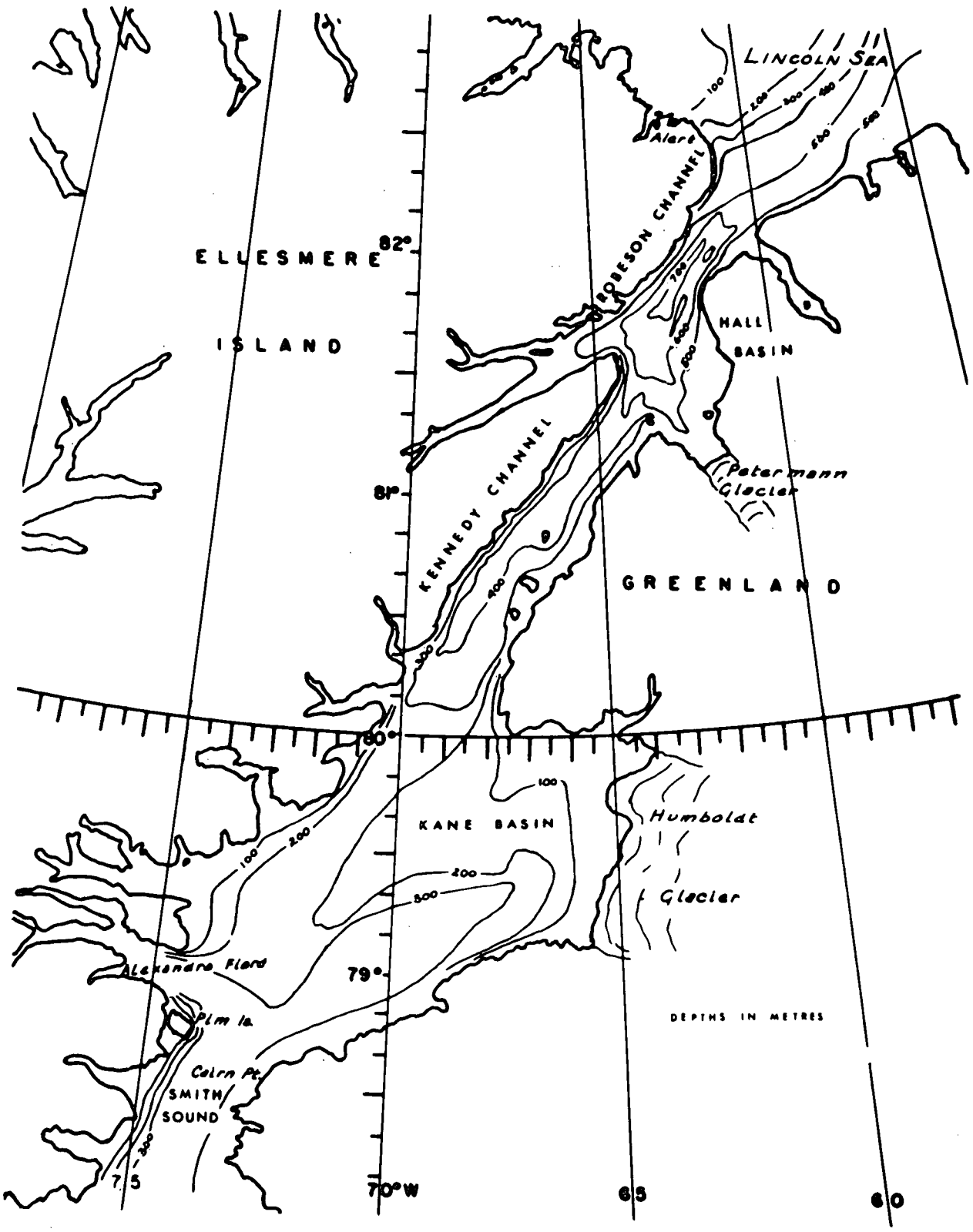

FIGURE 8 A General Map of Nares Strait.

It is divided from north to south into Robeson Channel, Hall Basin, Kennedy Channel, Kane Basin and Smith Sound. Robeson Channel is about 80 km long from the Lincoln Sea to Hall Basin and is as narrow as 20 km in one place. The Lincoln Shelf and Robeson Channel were surveyed recently by the Hydrographic Service of the Department of the Environment of Canada, the survey being finished in 1971, and the bathymetry is reasonably well known as far south as Hall Basin.

Hall Basin has two large fiords opening into it, Lady Franklin Bay on the west and Petermann Fiord on the east side. It reaches a depth of nearly 700 m which is 300 m deeper than the channel across the shelf into the Lincoln Sea. Immediately south of Hall Basin, the strait narrows again to Kennedy Channel which is roughly 25 km wide and 100 km long. The depths decrease steadily from 600 metres at the north end to about 300 m at the entrance to Kane Basin. Kane Basin is roughly rectangular and measures about 250 km by 120 km. Most of the eastern shoreline is occupied by the 90 km front of the Humboldt Glacier while on the west side lie the entrances to a number of fiords which penetrate deeply into the mountains of Ellesmere Island and which hold a number of glaciers fed by the Ellesmere Island Ice Cap.

Kane Basin is generally shallow, with a typical depth of about 200 m. A deeper channel lies on the Ellesmere side and the limiting sill depth of 250 m is in the western part of Kane Basin. From this point on the depth gradually increases through Smith Sound into Baffin Bay.

THE MORPHOLOGY OF ROBESON CHANNEL (Figure 10)

Robeson Channel runs for some 80 km in a NE - SW direction between the Lincoln Sea and Hall Basin. It is approximately rectangular, its width varying from 20-27 km. The greatest depth is about 700 m and the channel continues to the north across the Lincoln Shelf with a depth of 450 m. The depression across the shelf does not appear to have the cross-section typical of off-shore canyons but rather is consistent with the theory that the channels in the archipelago are a drowned drainage system which has been overdeepened by ice in many places. The cross-section of Robeson Channel itself is approximately rectangular although the bottom topography is irregular. The shore-lines are steep-to and the channel is bordered on both sides by a line of cliffs which are typically 500 to 800 metres in height. Partly because of these cliffs, the winds near the surface tend to blow directly up or down channel. There are few breaks in the line of cliffs; on the Ellesmere side Lincoln Bay is a triangular bay open to north-easterly winds while Wrangel Bay, 15 kilometres further south has a narrow entrance and is more sheltered. On the Greenland side Newman Bay lies about halfway down the channel directly opposite Lincoln Bay. Immediately beyond both ends of the channel the shore-line opens up rapidly.

CLIMATIC CONDITIONS

The Canadian Weather Station at Alert is only about 30 km NW of Robeson Channel and general climatic conditions in the Channel are of course similar to those at Alert. However, the weather in this region is often a purely local phenomenon, and wind direction and velocity, visibility and precipitation may change completely in a comparatively short distance. During the summer of 1972 conditions near Lincoln Bay for three days were too bad for a helicopter to take off on the 20 minute flight to Alert while at the same time the runway at Alert was being used by large Hercules aircraft with no difficulty.

In general the area is a polar desert and most of the total precipitation occurs during the short summer as rain so that the annual snowfall is small. However, drifting may be severe due to high winds, particularly in locations such as that occupied by the Lincoln Bay camp which lies half a mile back from the cliff edge at 600 m elevation on the high point of the ridge. On the ice in Robeson Channel in the spring of 1972 the snow was less than 5 cm deep everywhere except in drifts in the lee of pressure ridges. The winter temperatures are normally higher than $-40^{\circ}C$ although a minimum of $-53^{\circ}C$ was recorded during the winter of 1971-72 at the Lincoln Bay camp. After the sun returns in spring the temperature rises toward $-20^{\circ}C$ and high winds become much less frequent. At this time of year the weather is often calm with almost unlimited visibility. Later in the summer the visibility deteriorates due to fog forming over the open water and during June and July of 1972 for example only one day in three was completely fog-free both on the cliff and on the sea ice. In late August and September gales become more frequent and snow remains permanently on the ground from early September onwards. The best months for working in this area are usually April and May when the visibility is good and the flying weather is excellent.

SEA ICE CONDITIONS

During the early part of the winter multi-year floes are in motion in Robeson Channel. The ice usually becomes fixed at some time between early January and late February (Moira Dunbar 1972) and most of the channel is then blocked by a heavily ridged conglomerate of multi-year and one-year ice. By April the first-year ice is about 2 metres thick and suitable landing strips for STOL aircraft can usually be found. The confused, heavy ridging, however, almost prohibits surface movement in the northern part of the Channel. In both 1970-71 and 1971-72 the

the ice a few kilometres south of Wrangel Bay was free of ridges and travel on the sea-ice in that region may be possible in most years.

By the middle of June the increasing insolation has begun to melt the surface of the sea-ice and melt pools become frequent on the multi-year floes. These melt pools gradually deepen until in many cases they thaw right through the floes. Sometime in July usually, the ice breaks up and begins to move under the influence of current, tidal motions and wind. Generally the ice to the south of Robeson Channel breaks up a little earlier leaving an open path to the south. During July 1972 the mean drift of the sea-ice in Robeson Channel was observed to be about 19 km per day. However, in the summer of 1974 a large floe (about 8 km in diameter) wedged across Kennedy Channel and blocked most of the southerly movement of the ice. As a result the mean drift velocity was reduced to only a 4 km per day. In spite of the movement of ice to the southwards, the channel is rarely ice free since more pack ice drifts into the channel from the north, depending on conditions in the Lincoln Sea. The channel thus has appreciable amounts of ice within it for most of the summer. The details of the drift of ice through the channel are the subject of a current investigation by Dunbar, Keys, Sadler, Serson and others.

Chapter II

GENERAL OBJECTIVES

As discussed in Chapter I there is too little information available to derive realistic values for exchanges between the Arctic Ocean and Baffin Bay through the Canadian Archipelago. Reasonably accurate values for mass and energy transports are required for the solution of problems in several fields, in particular, the obtaining of a better understanding of conditions in Baffin Bay and the Labrador Sea. Measurement of total exchanges presupposes measurement in all three of the main channels opening into Baffin Bay and this would require either a multi-year programme or a large project. However, measurements obtained in a single channel may be crucially important in the investigation of more localized problems such as the provenance of the semi-permanent polynyas in northern Baffin Bay, Jones Sound and Lancaster Sound. A large scale investigation is in preparation into the oceanography and ice régime of northern Baffin Bay and a knowledge of mass and energy transports through Smith Sound is required for this project.

Another problem to be investigated is the origin of the bottom water in Baffin Bay. This water has a characteristic in situ temperature of $-0.4^{o}C$ and a salinity of 34.5 $^{o}/oo$. Water with similar in situ characteristics is found in Nares Strait at depths greater than the sill depth of 250 m. (Collin 1965, Palfrey and Day 1968), and the suggestion has been made (Collin 1965) that this water might pass over the sill in Smith Sound in discrete slugs. Muench (1971), however, pointed out that, because of the large difference in depth between the Baffin Bay Bottom Water and the water in Nares Strait, the potential temperature should be used to allow for adiabatic heating. When this is done it becomes apparent that the water in Nares Strait of the correct salinity is $0.2^{o}C$ or more too warm and that the nearest water with the required characteristics is found in the Eurasian Basin at depths of 200 m. (See Fig. 25). Thus any transport of unchanged water to the depths of Baffin Bay would require a slug to travel the full length of Nares Strait.

The objectives of the work reported on here were therefore formalized as follows:

i) to measure water transport through Nares Strait,

ii) to measure sensible heat and salt transport through Nares Strait,

iii) to measure the water characteristics and determine the origin of water in the Strait,

iv) to investigate the distribution in the Strait of water having the same T-S characteristics as Baffin Bay Deep and Bottom Waters.

There are, of course, a number of terms in the heat-budget equation which could not be measured during this investigation, such as the effects of sensible heat transfer and evaporation between the air and water, and the effects of land run-off, particularly that in the form of icebergs. It is probable, however, that these effects are sufficiently small compared with the transport of heat by a water column of a depth greater than 250 metres that they may be neglected when seeking a first order value for heat transport. The relative importance of these terms will be discussed later.

Similarly the effects of wind stress on the flow of water through the Strait have been neglected since this factor is operative over most of Nares Strait for only a small part of the year.

PLANNED OBSERVATIONS

It was clear that the obtaining of the necessary data would be somewhat of a long drawn out process and that observations would have to be made piecemeal as opportunity occurred. Standard oceanographic stations in two consecutive years were considered desirable together with continuous current readings over at least one cross-section of the Strait for a minimum period of one month. The obvious limitation of previous data was that almost all of them were obtained during the short summer period from July to September which is the only season when even an icebreaker is able to penetrate the Strait. There is, however, considerable difficulty in extending this short observational period.

Although a large icebreaker might well be able to operate in Baffin Bay through October or even into November, to attempt this in Nares Strait would be foolhardy because the ice north of a line joining Pim Island and Cairn Point (Figure 8) is normally about 9/10 concentration. It consists largely of heavy multi-year floes which are frequently under pressure from the prevailing north easterly winds (Figure 5B) and they form a barrier which is completely impassable. As Zubov observes, "the ship which is in pack ice when freezing conditions <u>begin</u> is likely to spend all winter there."

An obvious alternative method available in the other months of the year, is the use of recording instruments. This method, however,

is limited in its application. Even in the summer months submerged moorings must be used with sufficient clearance to avoid being disturbed by floating ice. In the northern half of Nares Strait, with no large glaciers calving into the water, the limiting depth is the keel depth of pressure ridges. Insufficient direct measurements have been made to allow a statistical estimate to be made of the probable maximum depth of ridges, but Kovacs (1973) working in the Beaufort Sea reported normal "bummock" depths as 12 to 15 metres and described one ridge with a keel depth of 57 metres. Pieces of the Ward Hunt Ice Shelf have also passed south through the Strait and these would be expected to draw up to 50 metres of water. Consequently a submerged array in Robeson Channel would need to be at least 50 metres below the surface, thus failing to obtain data in just the layer which might be expected to be most active. Finally, it is by no means certain that moorings laid from a ship could be recovered even two or three weeks later since fields of pack ice are continually shifting. While it may be possible by using dye release and sonar to recover a mooring in the middle of pack ice the operation is by no means simple or certain. South of Robeson Channel the problems are compounded by the movement of icebergs, from the Humboldt Glacier and from other glaciers which are small only in comparison. Even bottom mounted instruments in 700 m of water have been destroyed and a moored array in Smith Sound, for example, would be in continuous danger. Thus, while it was hoped that an array of meters recording for a full year could be placed in Nares Strait later on, it was necessary to plan on a different method for the measurement of currents during this investigation.

Fixed ice provides a working surface which is better in some ways than a ship. There is normally no movement, except the unnoticeable rise and fall with the tides, and equipment can be hung from the ice itself. The station may be occupied by using air transport, by powered sledges or even by using a self-contained laboratory unit mounted on an air-cushion vehicle. There are of course limitations. In many areas around the Queen Elizabeth Islands the ice does not become fixed until well on into the winter. For example, the ice in Robeson Channel in 1970 did not consolidate until late February. (M. Dunbar 1972). Even when consolidated the ice may not be completely motionless. Wind stress or tidal movements may distort the surface causing ridgings or the formations of cracks and leads, and such motions would prevent the use of taut wire moorings between the ice and the sea bottom. Further, the ice must be sufficiently smooth to allow power sledges to be used from a shore camp out to the stations or have areas of smooth ice of sufficient diameter to permit landing of STOL aircraft. If aircraft are used the operation cannot be scheduled before the return of the sun, in practice until there is 24 hours of daylight. This ensures that in an emergency the aircraft can land at a station site at short notice whenever the weather is fit for flying, and also delays the operation until the air temperatures have begun to rise to a level where unpleasant conditions do not cause a loss of efficiency.

Because of these conditions it was decided to combine oceanographic observations obtained from icebreakers during the summer with observations and current readings taken through the fixed ice in Robeson Channel in the spring.

NARRATIVE OF FIELD OBSERVATIONS

ROBESON CHANNEL, APRIL 1971

In April 1971 a two-man team under Finlayson was landed by a STOL aircraft on the sea ice in the middle of Robeson Channel off Lincoln Bay. They were intended to occupy a number of stations on the cross-section and to suspend current meters through the ice, partly as a test of the methods of deploying the gear and also to obtain current readings at depths near the bottom of the ice in an attempt to estimate horizontal stresses on the ice. However, the very badly ridged and hummocked ice prevented them from moving heavy gear more than a few hundred metres from the original camp site and the only stations occupied are those shown in Figure 10. Stations 1, 2 and 3 were all near the original camp site while Stations 4 and 5 were obtained towards the end of the six weeks' stay by using the STOL aircraft. The current meter results were of questionable value for transport calculations and have not been used in this paper.

In addition, a tide gauge was established in Lincoln Bay and the records from this instrument were analysed by the Tides and Water Levels Section of the Department of the Environment. The resulting tidal constants are discussed later (Table 1) and the station records from the sample bottle casts are given in Appendix 2.

CRUISE IN *CCGS LOUIS S. ST. LAURENT*, AUGUST 1971

On August 16, 1971 the CCGS Louis S. St. Laurent sailed from Resolute on Cornwallis Island with a mixed scientific party, which included the writer and two technicians. On the 18th August oceanographic observations were begun in Nares Strait (Fig. 8) and continued until 29th August. The 24 stations occupied are shown in Figures 9 and 10 and the station records in Appendix 3.

The ship steamed north through Smith Sound stopping for only one station there since the ship's programme required her to be in Robeson Channel as soon as possible. The ice conditions were exceptionally good, with the western half of the Strait being almost clear. The eastern half of Kane Basin was covered with fairly close pack, 7 to 9 tenths, but a cross-section of 3 stations was obtained in latitude 79°45'N without too much difficulty. In Kennedy Channel there was again very little ice and Station 5 was occupied near Hans Island. The clear water extended northwards

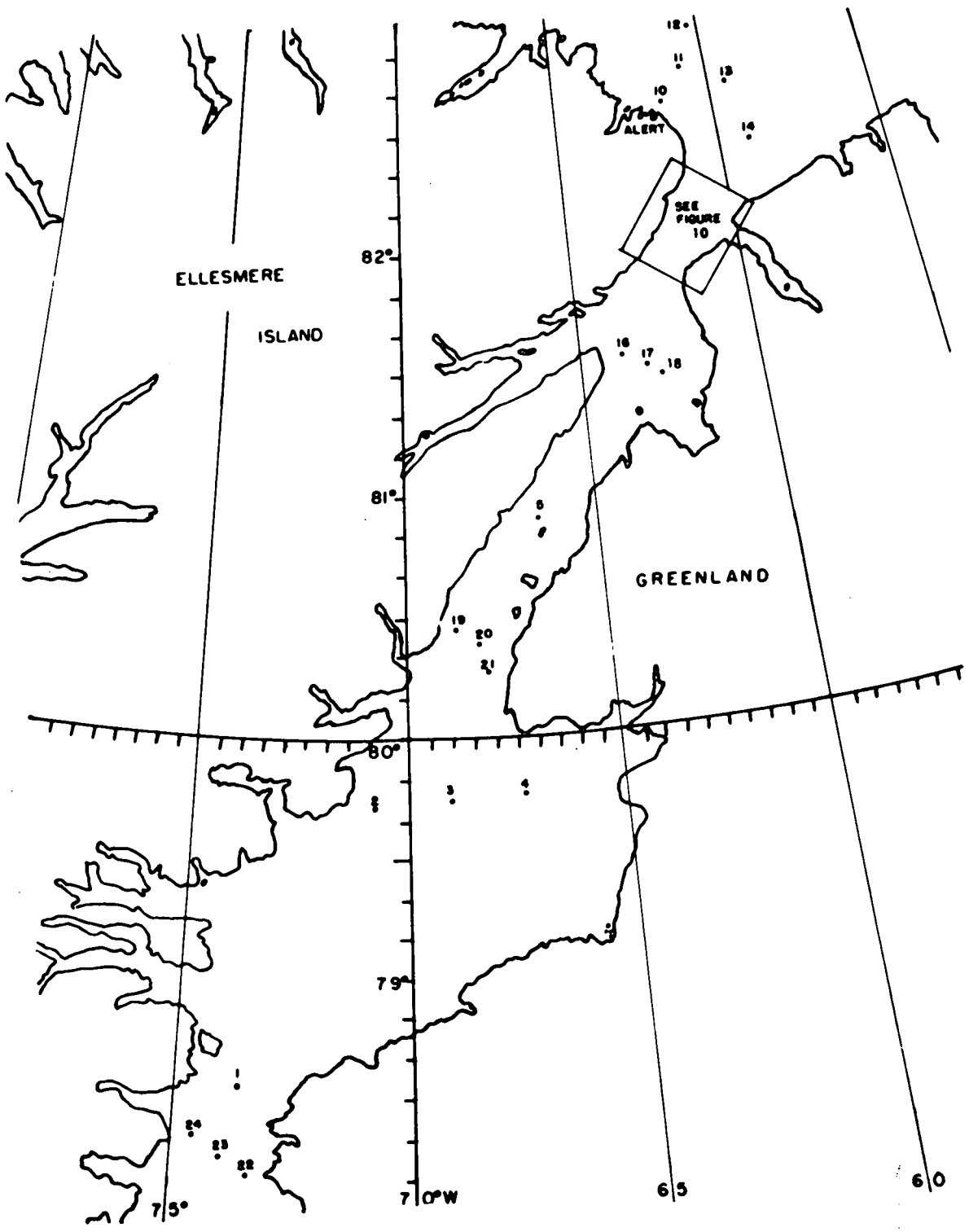

FIGURE 9 *Map of Nares Strait showing the stations occupied between 18th August and the 29th August 1971.*

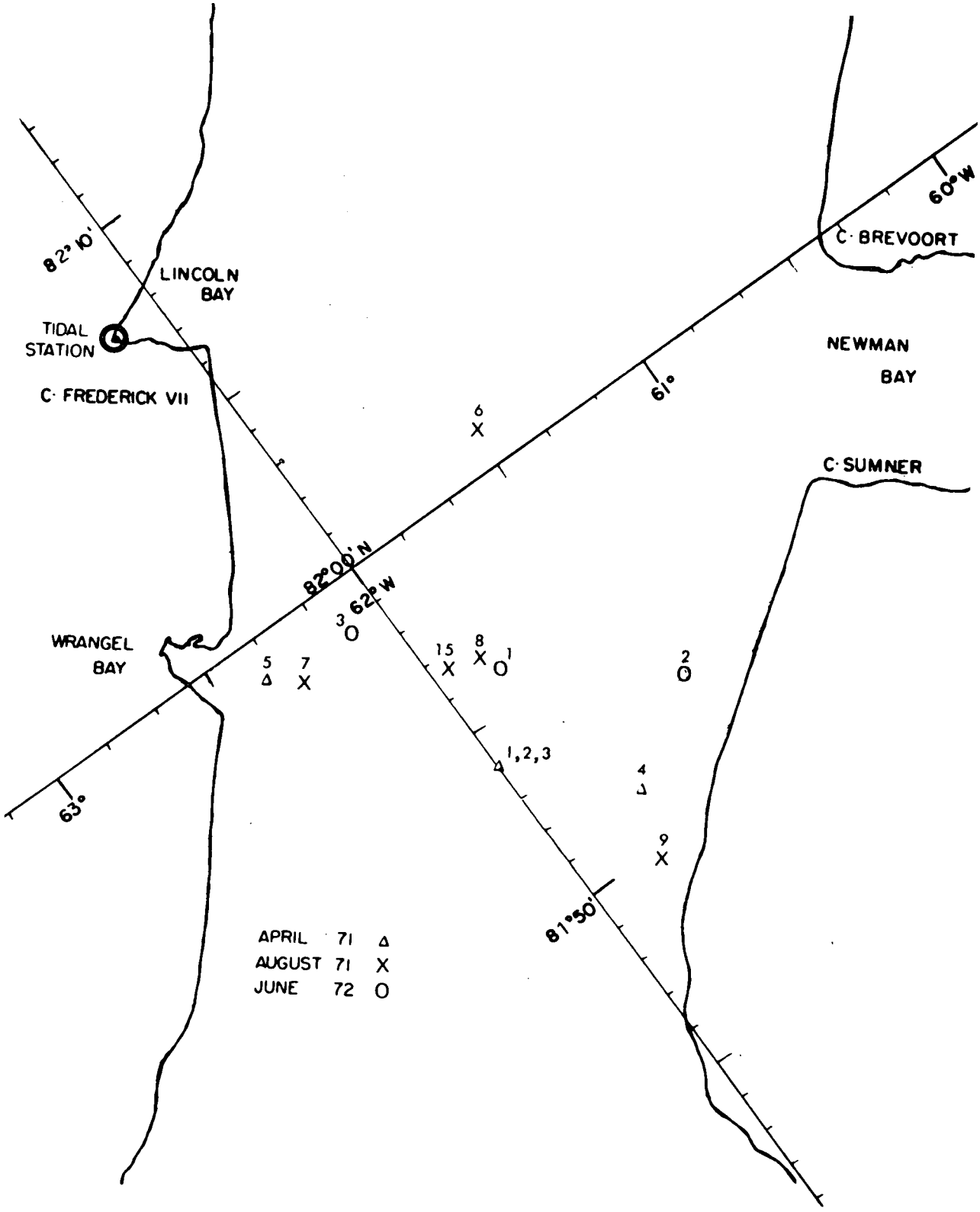

FIGURE 10 *Map of Robeson Channel showing the positions of all stations occupied in 1971 and 1972.*

through Hall Basin and Robeson Channel was clear of ice over most of its width. In Robeson Channel the ship was engaged in other work and only four stations were occupied in the next three days (Fig. 10). On the 20th August the ship left for Alert where most of the scientific party was landed by helicopter.

The ice conditions deteriorated north of Robeson Channel, the concentration rising to 8/10 or more. All the floes encountered here were multi-year ice from the arctic pack and the speed of advance of the ship was reduced to one or two knots. After landing the people in Alert the opportunity was taken to run a line of stations north across the shelf, Stations 10, 11 and 12 (Fig. 9). After completing Station 11 the ice closed to 9/10 coverage and by the time Station 12 had been completed the wind direction was changing. It was decided that it would be imprudent to go any further north since most of the work in Nares Strait still remained to be completed. Station 12 was taken in latitude 82°56'N which is the highest latitude yet attained by a ship under control in this half of the Arctic Ocean. The station was completed during an inappropriate "Scotch mist" with the air temperature above the freezing point.

On the way back into Robeson Channel, two more stations, Stations 13 and 14, were occupied, but ice prevented us from taking a station in the deep channel which cuts across the shelf from Robeson Channel north-eastwards. In the clearer waters of Robeson Channel, Station 15 was occupied near the centre station of the cross-section obtained earlier. Ice conditions in the eastern half of the channel prevented a second full cross-section being made.

On the way south cross-sections of the channel were obtained in Hall Basin, Kennedy Channel and Smith Sound although ice prevented them being extended as widely across the channel as was desired, particularly in Kennedy Channel. The ship then returned to Thule where the last of the scientific party, except for the writer, left. She then crossed to Makinson Inlet on Ellesmere Island where a short reconnaissance was made (Sadler 1972).

The success of the cruise was due to the exceptional capabilities of the ship and her crew. Although 1971 was a "good" ice year, and there were many long stretches of open water, the requirement for properly spaced stations forced the ship, on several occasions, into encounters with heavy pack ice. A less well found or well-handled ship would have spent days doing things which only took us a few hours.

OBSERVATIONS

At each station Knudsen bottle casts were made. The temperatures were measured using two reversing thermometers mounted on each bottle, supplied, as was most of the equipment by the Bedford Institute of Oceanography. The thermometers were calibrated in September 1970 and the final values are considered accurate to ± 0.02°C. Salinities were determined to 0.005 °/oo after returning south, using a Bisset-Burman Conductivity Meter. However, this does not allow for uncertainties due to the transfer and storage of samples and the salinity values are assumed to be accurate only to 0.02 °/oo. Dissolved oxygen was estimated on board using a modified Winkler titration (Strickland and Parsons 1965) and are considered accurate to ± 0.2 ml. l^{-1}. The depths of samples were measured using a meter wheel and checked by using unprotected reversing thermometers on some of the bottles. The results agreed closely and the depths are considered accurate to ± 1m or ± 1% of the indicated depth.

Bathythermograph slides were obtained at each station but they have not been reproduced as they add nothing to the other data. The temperature gradients in the Arctic are usually so small that in most cases the bathythermograph is too insensitive to give much useful information. The positions of the station were determined by using the ship's navigational radar and are accurate to ± 0.2 km relative to the Canadian coastline. The discrepancies in the charted positions of the Canadian Islands and the Greenland coast are surprisingly large on different maps and charts, the Greenland side of Robeson Channel being at least 5 km out of position on the National Topographic Series as compared with the navigational charts. These differences are a result of the extension of the surveys from the Canadian base line on one side and the European grid on the other in the topographical series and are now being resolved to some degree. The charts used in this work were the Canadian Hydrographic Service Charts No. 7072 and 7071, 1971 Edition and, in Robeson Channel two unpublished field sheets CHS 3499 and CHS 3696 supplied by the Hydrographic Service of the Department of the Environment. Apart from the area covered by these field sheets, the only bathymetry is that obtained from ships' echo sounder records, which are naturally restricted to those waters which have been found to be reasonably free of hazard. These soundings are generally track soundings obtained on passage and the cross-sections used here largely depend on bathymetry measured during the operation itself. Soundings were obtained throughout the operation using the Kelvin-Hughes echo-sounder fitted in the oceanographic laboratory of the ship. The echo-sounder trace was marked every 15 minutes and the ship's position at that moment recorded. These records have been forwarded to the Hydrographic Service of the Department of the Environment and the corrected values have been used in drawing the profiles and cross-sections below. The echo-sounder records were maintained by two Danish students under the direction of Dr. Milan Thamsborg of the Danish Oceanographic Centre.

Meteorological data were recorded using the ship's instruments, read by one of the oceanographic party. Wind velocities may be in error in some cases due to masking of the anemometer.

In addition to the observations required for this investigation a number of snow samples for isotope determinations were taken from the tops of tabular icebergs, using one of the ship's helicopters.

Some data obtained before August 1971 have also been used in this paper, particularly those from stations already mentioned which were occupied in April 1971 by Finlayson (1971) in Robeson Channel and those obtained by Seibert over the Lincoln Sea Shelf in April 1966 (Seibert 1968). These latter data were all obtained through holes drilled through fixed ice cover.

OBSERVATIONS IN ROBESON CHANNEL APRIL-JUNE 1972

In April 1972 an array of current meters and thermographs was established in Robeson Channel. The party was based in the Defence Research camp on the cliff top one mile south of Lincoln Bay and a De Havilland Twin Otter aircraft was used to ferry men and equipment to the station positions on the fixed ice (Figure 10). The line chosen for the stations ran SE from Wrangel Bay as it was hoped that the smooth ice observed in this area in 1971 would recur but the surface in 1972 was heavily ridged for some miles south of this line. However, there were a sufficient number of level areas to enable the aircraft to land fairly close to the predetermined station positions.

The instruments were suspended through holes blown in the ice which was about 1.8 metres thick at the station positions. A collapsible derrick and a small gasoline powered winch were used to lay the moorings and the details of the methods used for this and for the blasting of the holes are discussed in Appendix 1. Because of the limited power of the winch the instruments at Stations 1 and 2 were divided into two separate moorings to make recovery easier, the two holes being 100 metres apart on a line parallel to the axis of the channel.

The array consisted of 14 Braincon Recording Current Meters (8 Type 381 and 6 Type 316) and 6 Braincon Recording Thermographs. The location of these instruments is indicated in Figure 26 below. The instruments were all in position by 26th April and were recovered on the 5th and 6th of June. No difficulties were encountered and the techniques developed for this operation were very successful. A high rate of data returns was achieved largely because of the care taken to prevent the meters becoming 'cold-soaked'. They were prepared (cameras loaded, etc.) in a heated workshop hut and transported in insulated boxes to the ice stations only when the equipment to moor them was assembled. They were thus not exposed to the ambient air temperature (-30^{o}C) for more than one or two minutes before immersion. In addition the comparative scarcity of fouling organisms

in these waters ensured that all of the external parts of the instruments remained clean and only two of the meters showed any sign of corrosion on recovery.

As each string of meters was recovered a number of temperature-salinity samples were obtained at each station using Knudsen bottles and reversing thermometers. The station records are displayed in Appendix 4. An attempt was also made to obtain further tidal records in Lincoln Bay using an Otman tide gauge but the records were lost when the gauge was destroyed by moving ice. General breakup of the ice in the Channel occurred on 26th July when a separate investigation on the dynamics of moving ice began.

CRUISE IN *CCGS LOUIS S. ST. LAURENT*, FEBRUARY 1972

An attempt was made during the winter of 1972-73 to penetrate the ice in Baffin Bay through to the area of the semi-permanent 'North Water' polynya and Smith Sound. Because of the unusually severe ice conditions and a delay of three weeks in the date of sailing the ship was unable to proceed much further north than Disko Island (71° N) and only one station was obtained in the deeper central part of Baffin Bay. (Muench and Sadler 1973).

Chapter III

RESULTS OF OBSERVATIONS OF WATER CHARACTERISTICS

The results of observations taken during the cruise of the CCGS Louis S. St. Laurent, between 18th August and 29th August 1971 are tabulated in Appendix 3 and have been abstracted from the Canadian Oceanographic Data Centre Preliminary Data Report. The positions of the profiles and cross-sections obtained are shown in Figure 11. Curves showing the variations of temperature, salinity and density with depth for each station have not been reproduced here but the resulting profiles and cross-sections for temperature and salinity are shown in Figures 12 to 18. No diagrams have been included showing the variations in σ_T as these are almost identical in form to those for salinity. The greatest range of temperature at any station was from $-1.8^{\circ}C$ to $\pm 1.6^{\circ}C$ and in this range the variation of density with temperature is very small. The density was therefore essentially a function of salinity.

It should perhaps first be emphasized that 1971 was an unusually "good" ice-year. The ice covered less than half the waters of Nares Strait throughout the period of observations and the extent of wind mixing in the upper layers was probably greater than would normally be found. There is of course no such thing as a "typical" ice-year and the results given below show that the conditions near the surface are sensitive both to the wind and to the amount of ice in the neighbourhood of the station.

The weather was calm during the northward leg from Smith Sound (R71 in Fig. 11) into Robeson Channel, the winds being less than 5 kts. Thus Stations 1 to 9 (Figs. 9 and 10) were taken in undisturbed water. Most of the sea-ice during this leg was confined to the eastern side of the channel and the eastern half of Kane Basin.

The winds in the Lincoln Sea (Stations 10 to 14) were very light, the air temperatures were four or five $^{\circ}C$ above freezing point, there was continuous low cloud and the most northerly station, in $82^{\circ}56'N$, was occupied in light drizzle. During the time spent in Robeson Channel on other investigations from the 23rd - 26th August, the wind blew from the S.W. at speeds up to 60 kts. Even in the comparatively restricted waters of Robeson Channel the seas became two metres high and the ice in the channel was jammed onto the Greenland shore. The effects of this wind will be discussed later in a comparison of the profiles of the north and south legs.

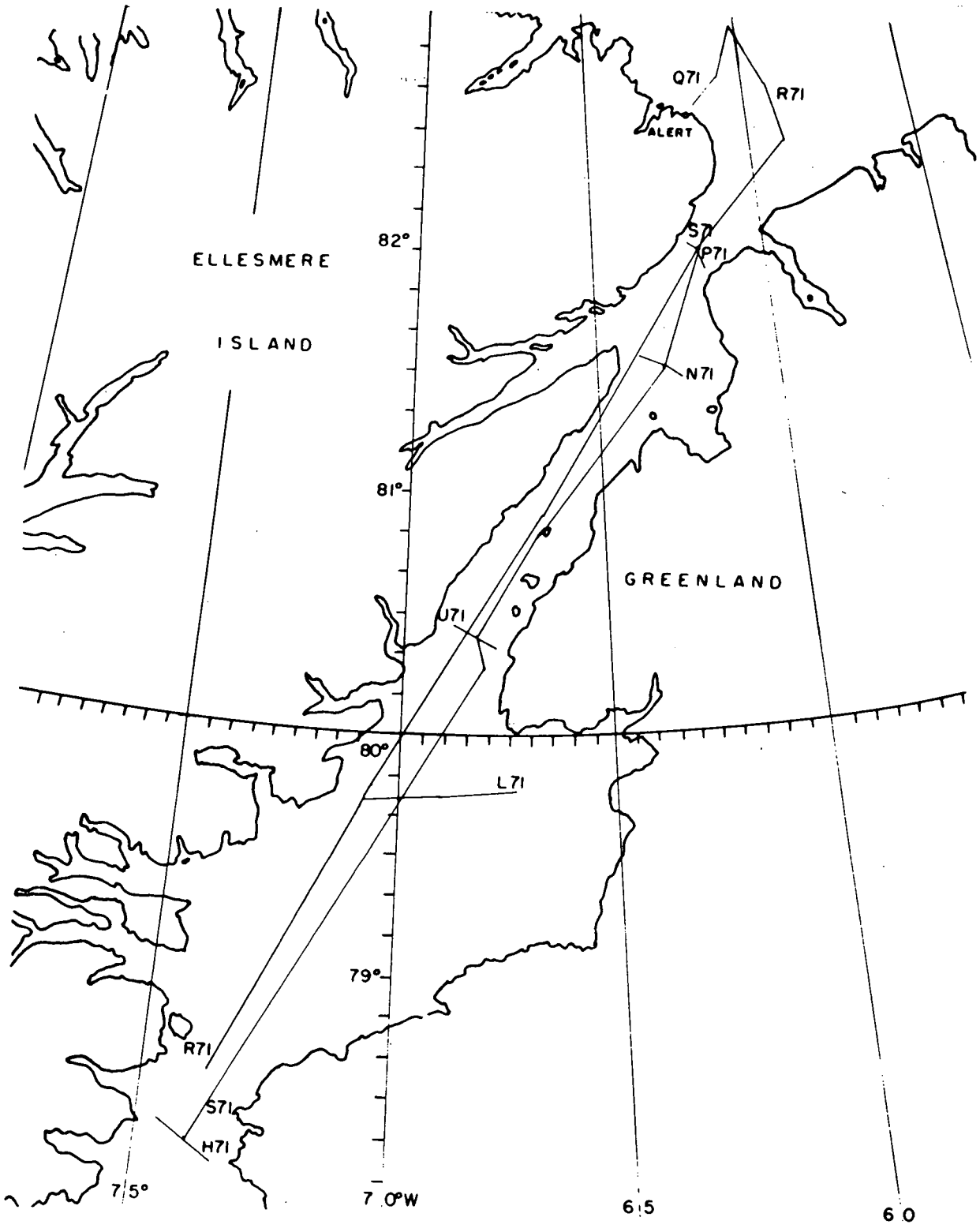

FIGURE 11 *Map of Nares Strait showing the position of the longitudinal profiles and cross-sections obtained in 1971.*

During the southern leg which is shown as S71 in Figure 11 (Stations 15 to 24) the winds were from the north and north-east at speeds up to 29 kts while the air temperature remained within a few tenths of a degree of the freezing point. The ice was more of an obstacle than it had been on the way north and some of the stations in the cross sections were displaced from the planned positions because of pack ice.

TEMPERATURE - SALINITY - DISSOLVED OXYGEN PROFILES

The cross-sections and profiles presented below are of course not obtained from instantaneous observations. The data for the longitudinal profile (R71) heading north was obtained over a period of four days and that heading south (S71) over six days. Station 15 shown on the cross-section P71 was occupied four days after the other three stations. The remaining cross-sections were completed in two to four hours. Thus the longitudinal profiles in particular are affected by any time variations which may have occurred. However, the changes with time for the water deeper than 30 metres are likely to be very small. The weather conditions were consistent for all stations in each separate profile that is, generally calm overcast weather while heading north and generally windy conditions while heading south, with a period of high winds between the two. The near surface structures are thus considered to be a reasonable approximation to instantaneous profiles under two different sets of conditions.

The profiles for the northern leg from Smith Sound to the Lincoln Sea (R71 in Fig. 11) are displayed in Figure 12. The bathymetry, as is the case for all the diagrams, is drawn from a combination of the echo-sounder records obtained in the ship and the best available published charts and field sheets. The broken line between Stations 1 and 2 indicates the maximum depth over the sill north of Smith Sound while that north of Station 6, shows the depth of the deep channel crossing the shelf north-east from the northern entrance of Robeson Channel.

The temperature profile indicates that there was a layer of relatively cold water between 20 metres and 100 metres depth with the minimum isotherm at about 75 metres, while the minimum temperature in the layer increased from north to south. In Robeson Channel (Stations 6 and 8) the water at 75 metres was close to the freezing point of $-1.75^{\circ}C$ and in Smith Sound (Station 1) the minimum temperature was $-1.30^{\circ}C$. Overlying this layer of cold water was a surface layer which, in the southern half of the profile, reached temperatures of about $0^{\circ}C$. In Robeson Channel (Stations 8 to 14) this surface layer disappeared and the surface temperature was below $-1^{\circ}C$. The closure of the $-1.7^{\circ}C$ isotherm indicated between Stations 13 and 14 in Figure 9 is probably due to the fact that the profile north of Station 14 crosses the continental shelf. It will be shown later that the cold layer is probably continuous through the deep channel with the waters of the Lincoln Sea.

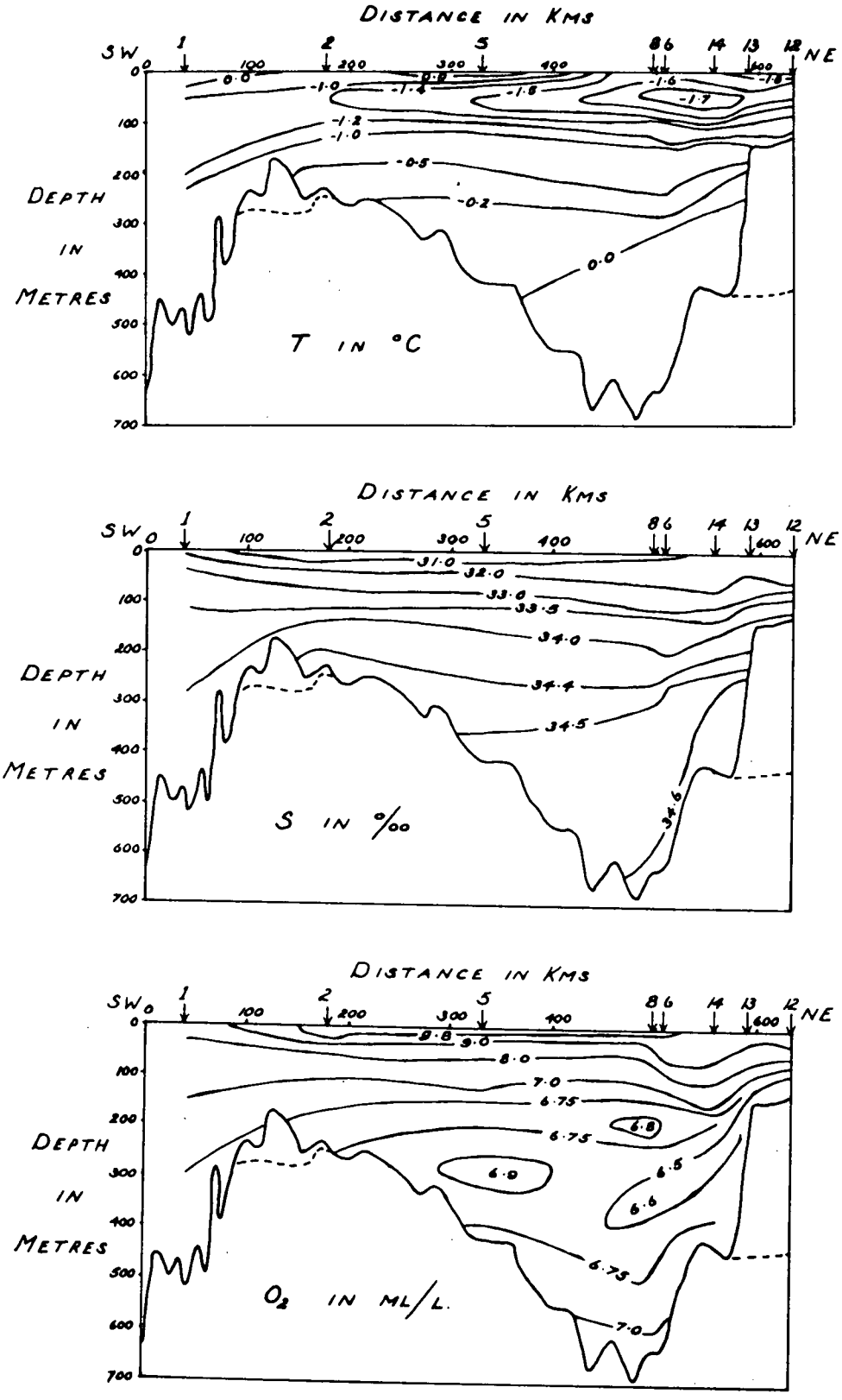

FIGURE 12 *Temperature, Salinity and Dissolved Oxygen profiles on the north bound leg (Profile R71).*

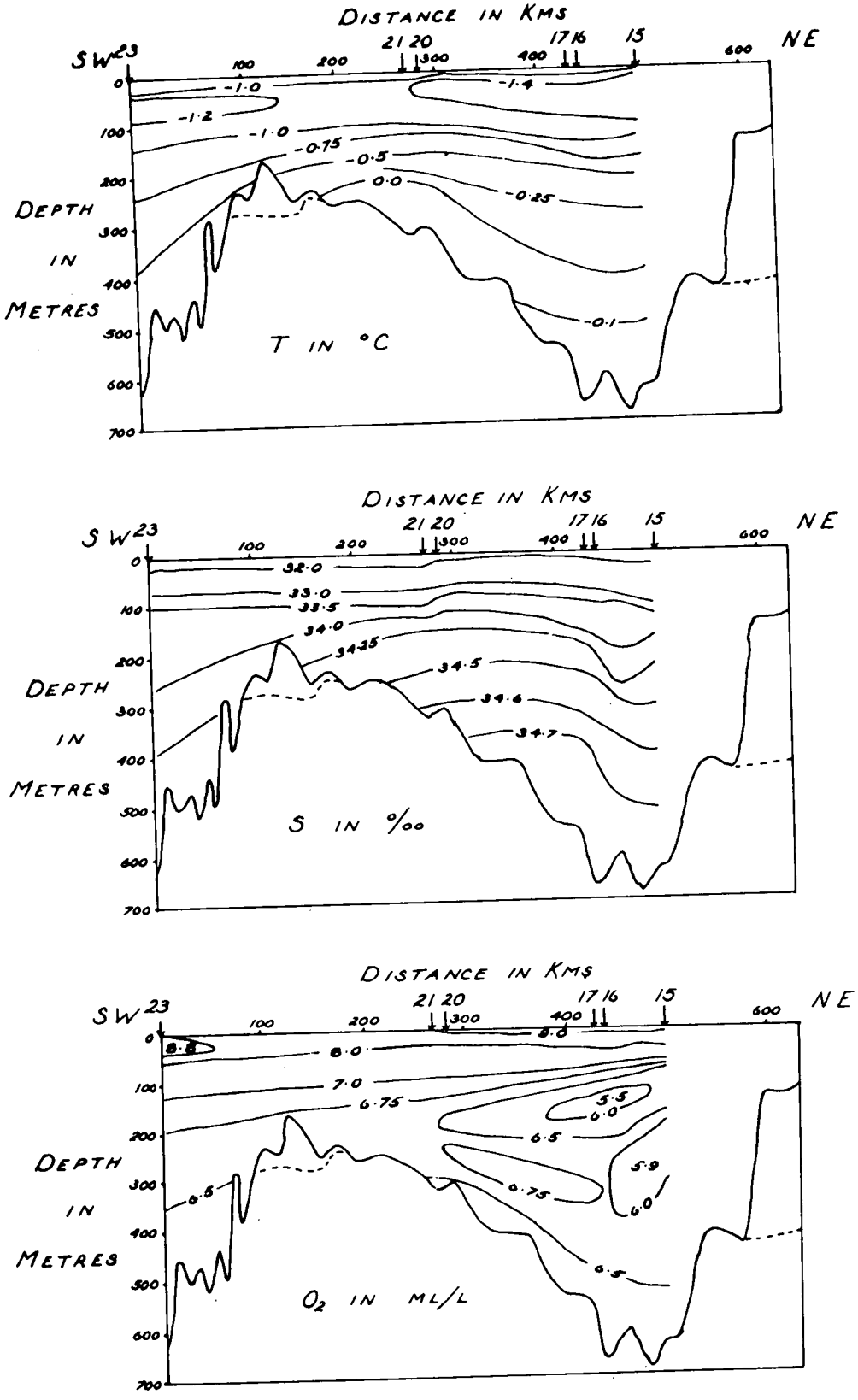

FIGURE 13 *Temperature, Salinity and Dissolved Oxygen profiles on the south bound leg (Profile S71).*

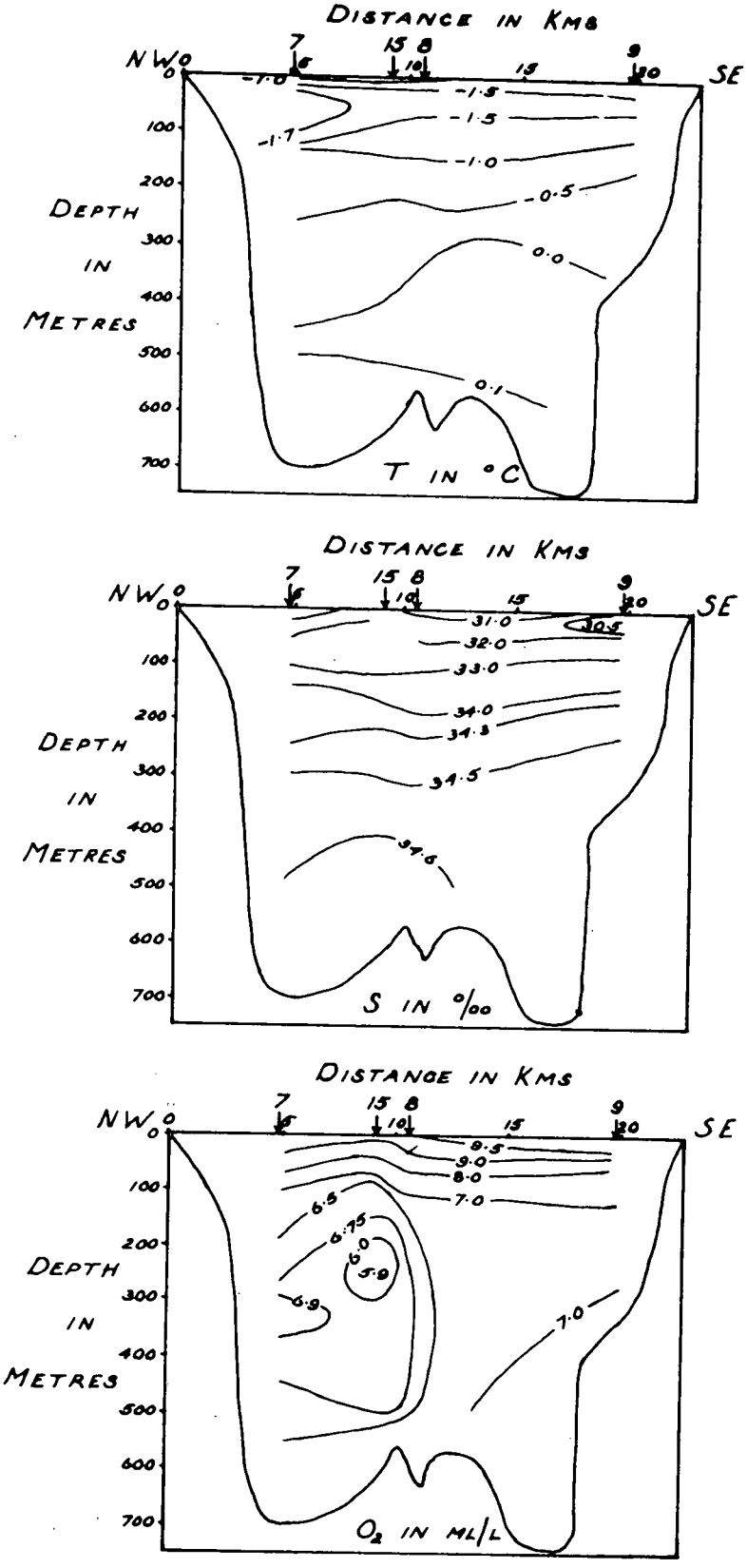

FIGURE 14 *Temperature, Salinity and Dissolved Oxygen cross-sections in Robeson Channel (P71).*

The warmer surface layer in the southern half of profile R71 was probably the result of insolation in the prevailing calm weather in regions with little sea ice. The surface temperature in the Lincoln Sea at the north end of this profile varied between -0.8°C and + 1.0°C. This was a region of heavy multi-year ice whose upper sections were of low salinity due to one or more summers leaching of salt. The melt water from these floes being almost fresh tends to lie on the surface and consequently the temperature there cannot fall much below 0°C.

In Robeson Channel south of Station 14 the warmer surface layer was not evident and this was probably mostly a result of wind mixing. The land formation at the sides of this channel tends to canalize the surface winds up or down channel and a calm day here is a rarity at this time of year. No comprehensive records are available at sea level in Robeson Channel but the mean wind speeds appear to be higher than those experienced at Alert which is only 40 km away but which fronts north onto the Lincoln Sea.

Below the cold layer, the temperatures vary little with latitude until Smith Sound and the Baffin Bay are reached.

The salinity profile remains fairly uniform along the channel except for the lower surface salinity between Stations 6 and 1. This section of the Strait is the receptacle in July and August for a great deal of land ice and run-off; from Lady Franklin Bay and Petermann Fiord in Hall Basin, from Alexandra Fiord in Kane Basin and above all from the 90 km front of the Humboldt Glacier on the eastern shore of Kane Basin. The melt water at the surface produced salinities as low as 29 °/oo at Station 2 for example and the large positive salinity gradients with increasing depth in the upper 50 metres or so is the result.

The effects of this melt water can also be seen in the dissolved oxygen profile. Glacier ice has a large air content which is released as tiny bubbles during the melting process, resulting in a near-saturation level of dissolved oxygen in the surface layers. Below 100 metres the oxygen levels were essentially constant at about 7 $m.l^{-1}$.

Comparing these profiles with those observed between 27th and 29th August on the southern leg (S71 in Fig. 11) which are shown in Fig. 13, we notice a number of changes. The mixing in ice-free regions caused by high winds of 20th - 22nd August has mixed down the surface layer of relatively warm fresh water and the surface temperatures in the southern half of the profile are about 0.5°C lower than they were on the 19th and 20th August. This mixing is also indicated in the salinity profile where the very low salinity surface water has been mixed down and the surface salinities are about 1 °/oo higher than those found on the way north. Similarly the oxygen content near the surface has fallen about 1 $ml.l^{-1}$.

The cold layer has also warmed up very slightly, but the significant changes are confined to the surface layer.

The cross-section P71 shown in Figure 14 lies across Robeson Channel (see Fig. 11). The surface temperatures are all below 0°C and the temperature falls to -1.5°C at a depth of 20 metres. Between 25 and 125 m

on the western side there is a core of water whose temperature at -1.7°C is very little above freezing. The salinity profile indicates that the salinity of this core lies between 31 °/oo and 33°/oo while there is some sign of slightly lower salinity near the surface on the eastern side of the channel. However, this particular observation was taken in a gap in a field of almost continuous pack ice which filled the eastern third of the channel, and could be due to local melting and reduced turbulence. The dissolved oxygen curves show lower values in the western half of the channel below 100 m, while the low near-surface salinities on the eastern side are accompanied by somewhat higher values for dissolved oxygen content, probably also caused by local melting.

The cross-section south (N71, Fig 15) lies at the south end of Hall Basin and is affected by the discharges of ice and water from Lady Franklin Bay to the west and from Petermann Fiord on the east. Little horizontal structure is visible in the cross-sections except for the tongue of slightly colder water at 75 m between Stations 17 and 18 which was seen in the longitudinal profiles. The surface salinities and dissolved oxygen levels are slightly lower at both ends of the cross-section than in the middle but this effect, probably due to melting ice in Lady Franklin Bay and Petermann Fiord, was much reduced by the high winds of the previous days.

Cross-section U71 (Fig. 16) was taken at the southern end of Kennedy Channel. Here the core of colder water lies between 25 and 75 metres in the centre of the channel. There was an average of about 3/10 ice cover when this cross-section was taken and the surface salinities of less than 31.5 °/oo and the high dissolved oxygen values reflect this.

Cross section L71 (Fig. 17) was obtained in Kane Basin on the way north on 19th August in calm sunny weather. The cross-section is at right angles to the Humboldt Glacier and the cold water core at 50 metres spreads right across the Basin with the lowest temperatures in the vicinity of the glacier at 75-100 m. As was the case in the presence of close pack on the Lincoln Sea, the surface temperatures lie close to 0°C as the insolation is absorbed in melting ice rather than warming the water. The surface salinities are low, particularly in the station nearest to the glacier where the values fall below 28 °/oo. Similarly the dissolved oxygen values are near saturation from the melting of glacier ice. Below 50 metres the water structure is much the same as that in cross-sections further north.

The most southerly cross-section H71 (Fig. 18) was obtained in Smith Sound on 29th August. The cold layer is now centred at about 100 m and the water is about 1 °/oo more saline than that in this layer further north. It is now overlain by warmer water, the temperatures being above 0°C down to 50 metres. These values, the salinities of about 32.5 °/oo and the dissolved oxygen contents of 8 to 8.5 ml.l are near the typical values in the surface of northern Baffin Bay at this time of year.

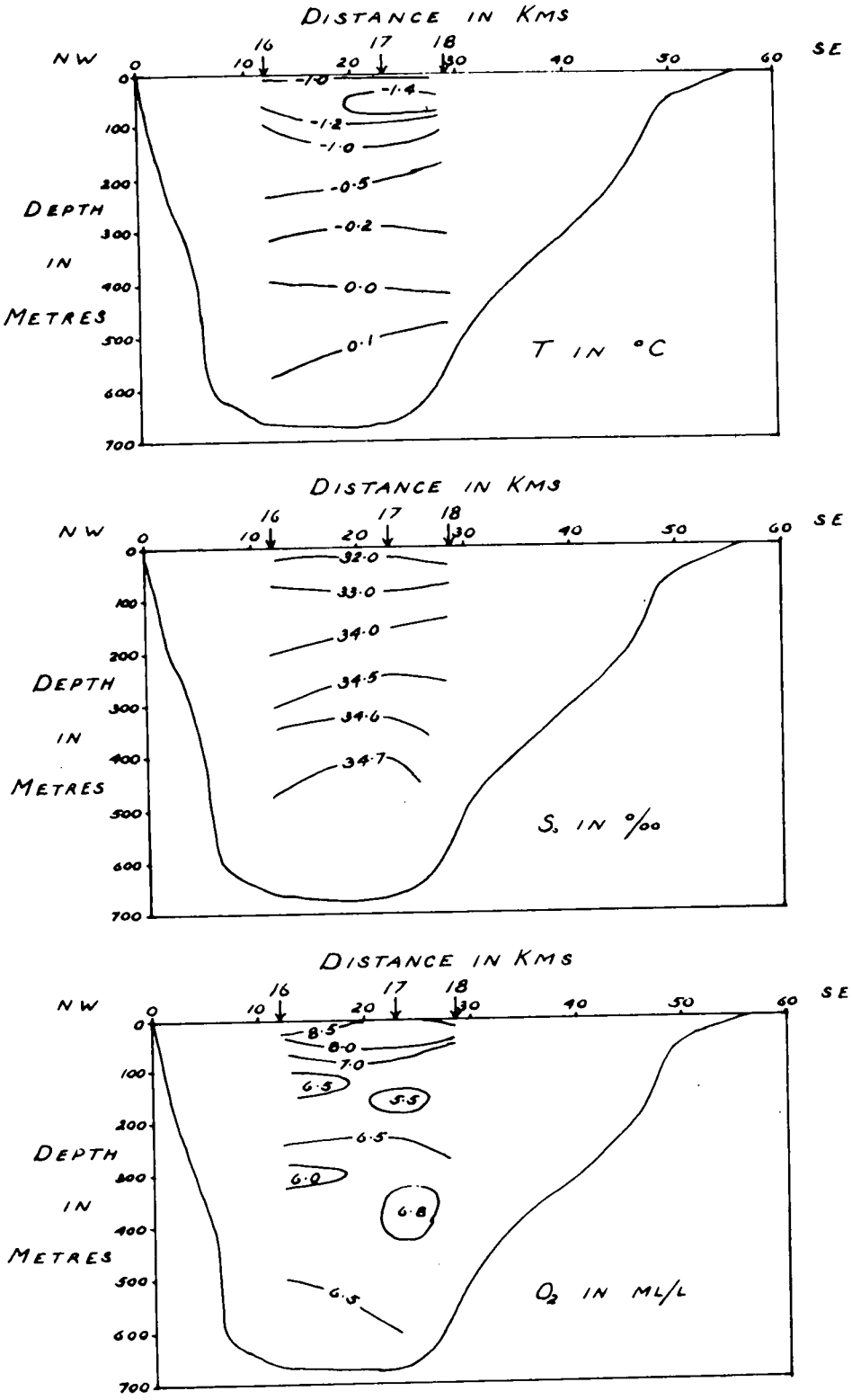

FIGURE 15 *Temperature, Salinity and Dissolved Oxygen cross-sections in Hall Basin (N71).*

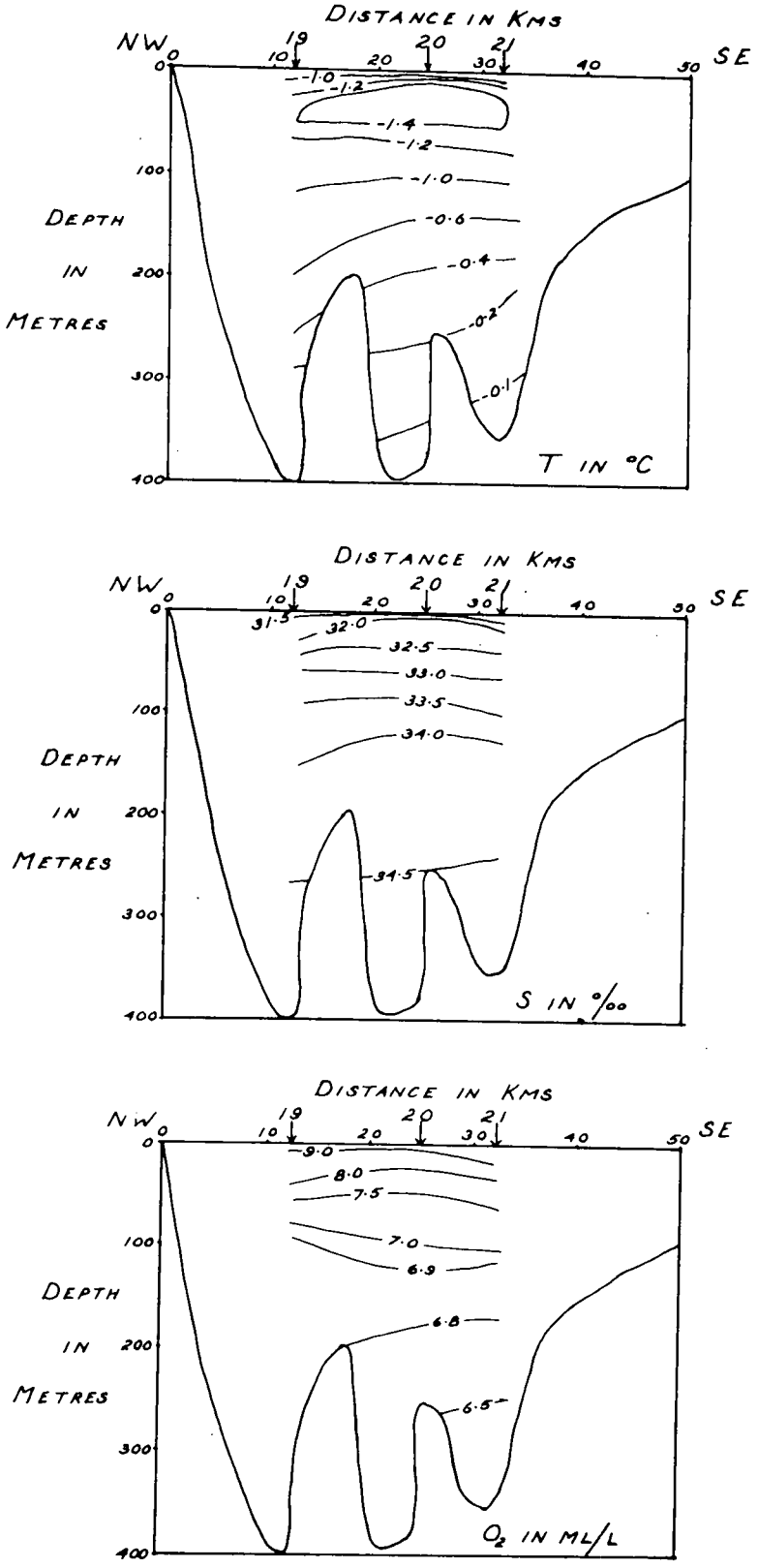

FIGURE 16 *Temperature, Salinity and Dissolved Oxygen cross-sections in Kennedy Channel (U71).*

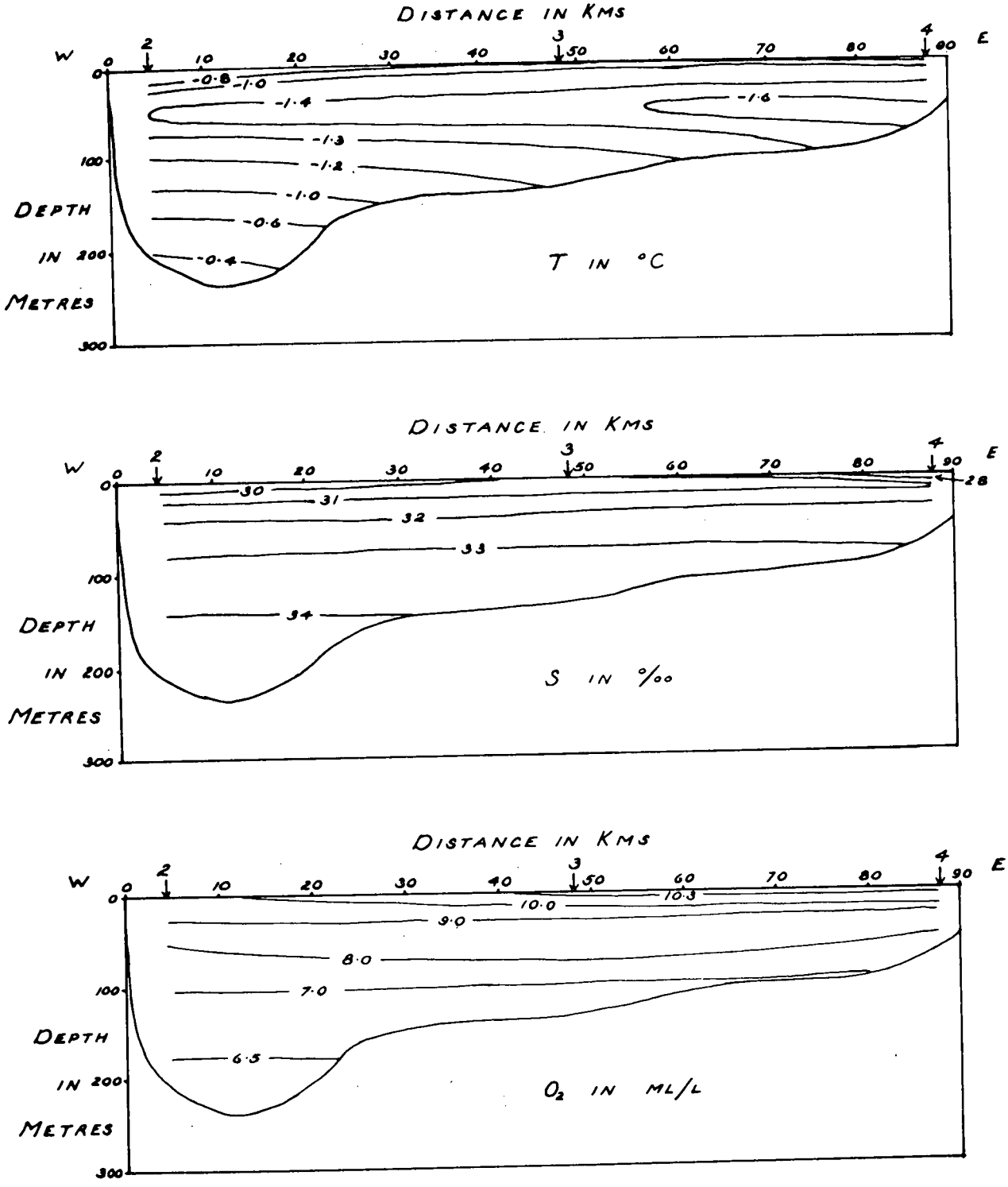

FIGURE 17 *Temperature, Salinity and Dissolved Oxygen cross-sections in Kane Basin (L71).*

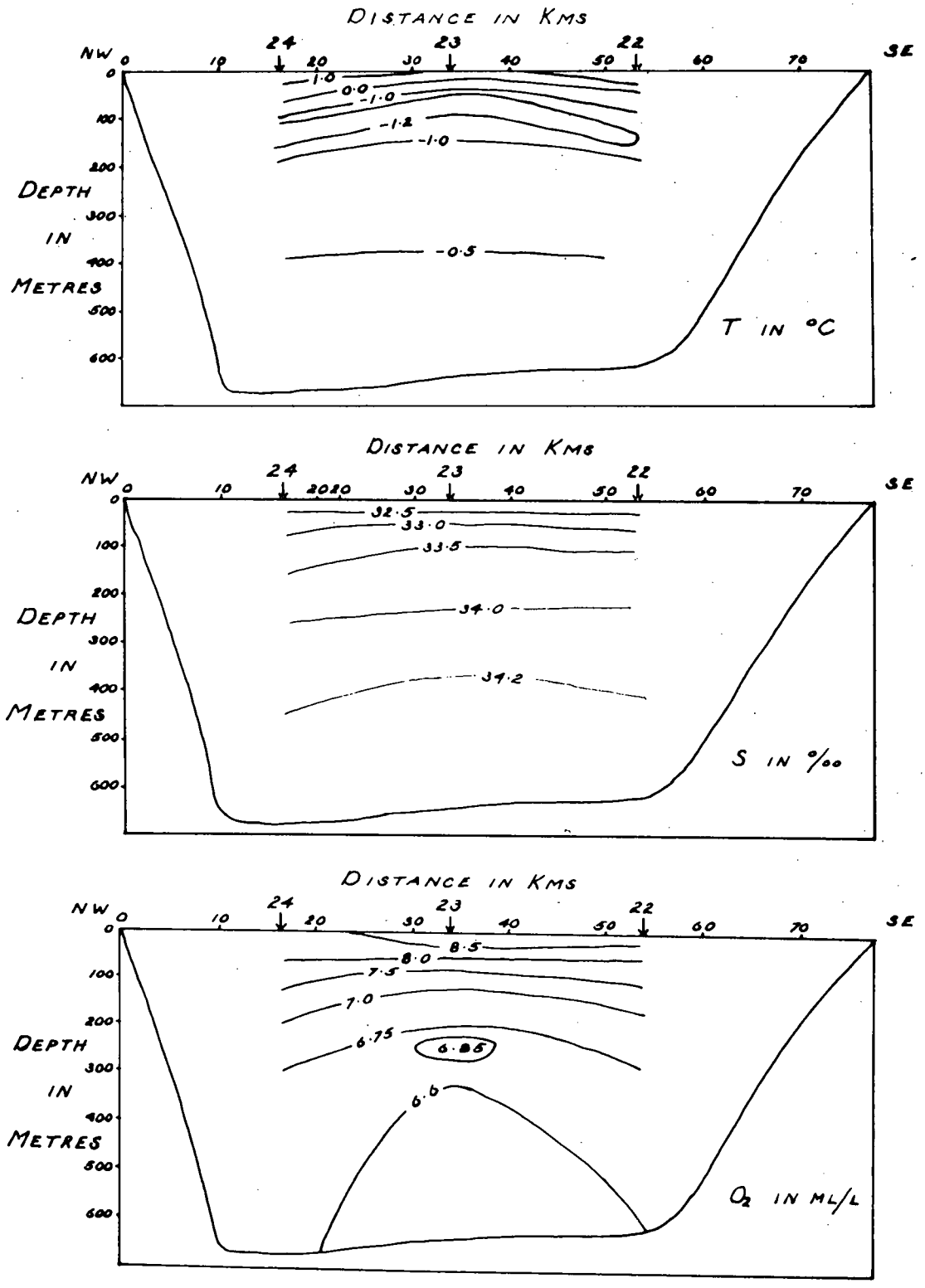

FIGURE 18 *Temperature, Salinity and Dissolved Oxygen cross-sections in Smith Sound (H71).*

T-S DIAGRAMS

The envelope of the T-S curves for the stations used in the north-bound profile (R71, Fig. 11) are shown in Figure 19. All the curves fit within a well defined envelope except that for Station 1 which is shown separately and which will be discussed later. In Figure 20, the envelope for the T-S curves obtained during the southerly leg are shown and in Figure 21 that for the T-S curves drawn from Seibert's (1968) data obtained in the Lincoln Sea in June 1967. These three envelopes are almost identical below 50 metres the only difference being the summer heating near the surface which appears in Figures 19 and 20. Similarly in Figure 22 the envelope of the observations made in Robeson Channel in April 1971 by Finlayson is compared with the envelope of Figure 20 taken in the late summer and this again shows close correspondence between the two except for near surface summer heating.

Finlayson's data (Figure 22) show sharp temperature maxima at about 20 metres depth which may be seen more clearly in Figure 23 where the envelopes of S, T and σ_T curves for these observations are shown. Similar temperature maxima have been observed before in several areas where they have been attributed to the advection of a surface layer of cold water entrained with moving ice floes on top of water whose temperature has been raised by insolation. In this case such surface advection cannot be responsible for the temperature peaks since the ice cover is fixed. The origin of the temperature maxima in this case probably lies in the rapidly increasing insolation in March and April. The sun returns about the 1st March in this latitude and by 7th April there is 24 hours of sunlight. The amount of solar energy which enters the ice varies widely with the character and thickness of the ice. There is no surface melting because of the low air temperature (typically $-30^{\circ}C$) but the heat energy which penetrates the ice will cause some melting at the bottom surface where the ice temperature is at the freezing point. Since the temperature of the water layer in contact with the ice cannot rise much above the freezing point ($\simeq -1.7^{\circ}C$) a cold but slightly less saline layer forms. The remaining radiant energy which penetrates several metres further into the water raises the temperature of this sub-surface layer. Because of the lower salinity of the water immediately below the ice and the insensitivity of the density to small changes in temperature near the freezing point this structure remains stable, until eventually the rise in temperature of the water at the temperature maximum is sufficient to cause an overturn. It may be seen in Figure 23 that the water column down to 50 metres depth is at least neutrally stable in spite of the temperature maxima.

It is now time to discuss the anomalous T-S curve at Station 1. In Figure 24 two T-S curves have been drawn from data obtained by Muench (1970) in August 1969 at his Stations 34 and 35. These two stations were approximately 100 km south of the position of Station 1. The dotted curve in the diagram is the T-S curve for Station 1 and it may be seen that there is good general agreement between the curves, so that it appears likely that the waters have a common origin. On the same cruise

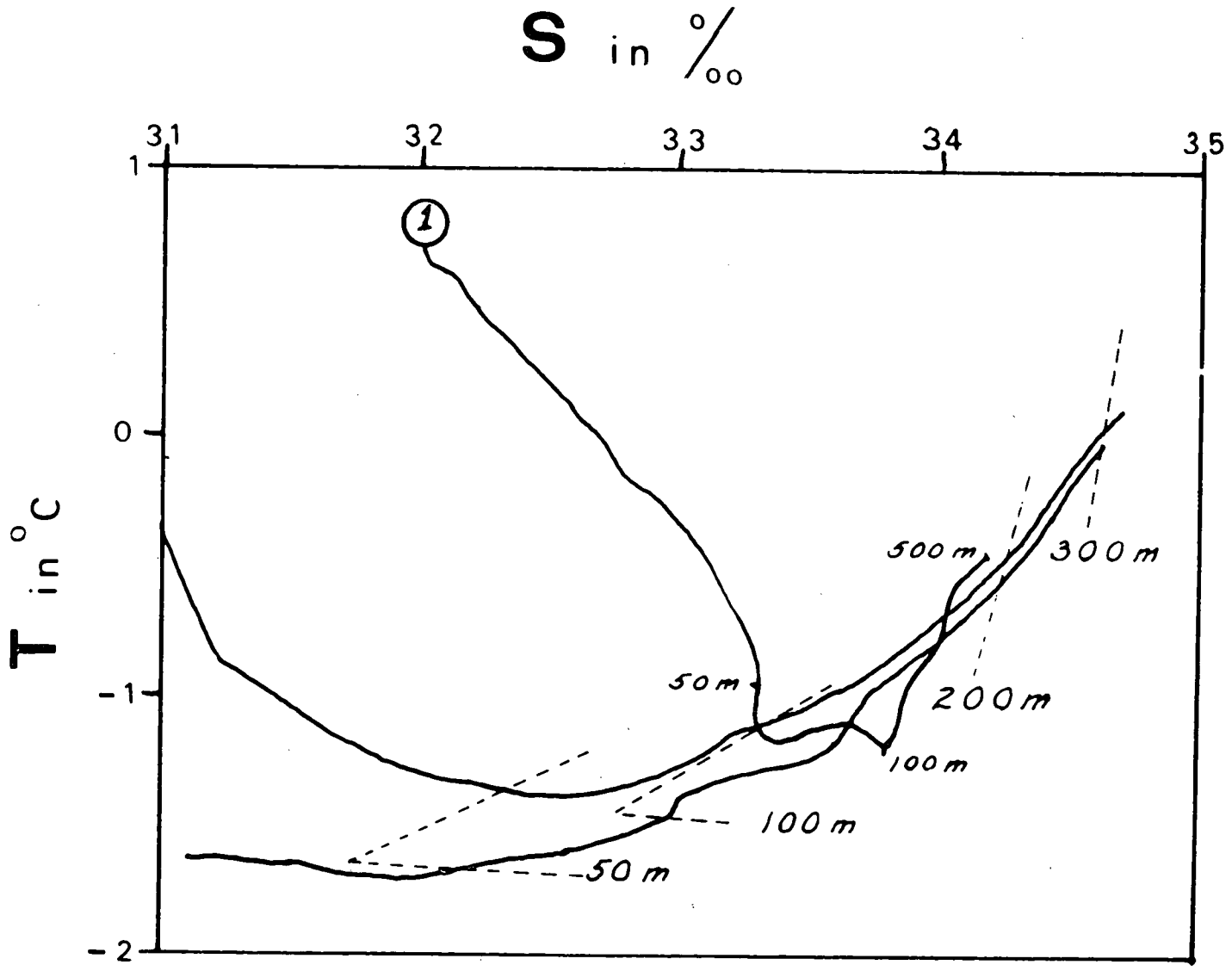

FIGURE 19 *Envelope of T-S curves from stations on the north bound leg (R71). The curve from Station 1 is drawn separately.*

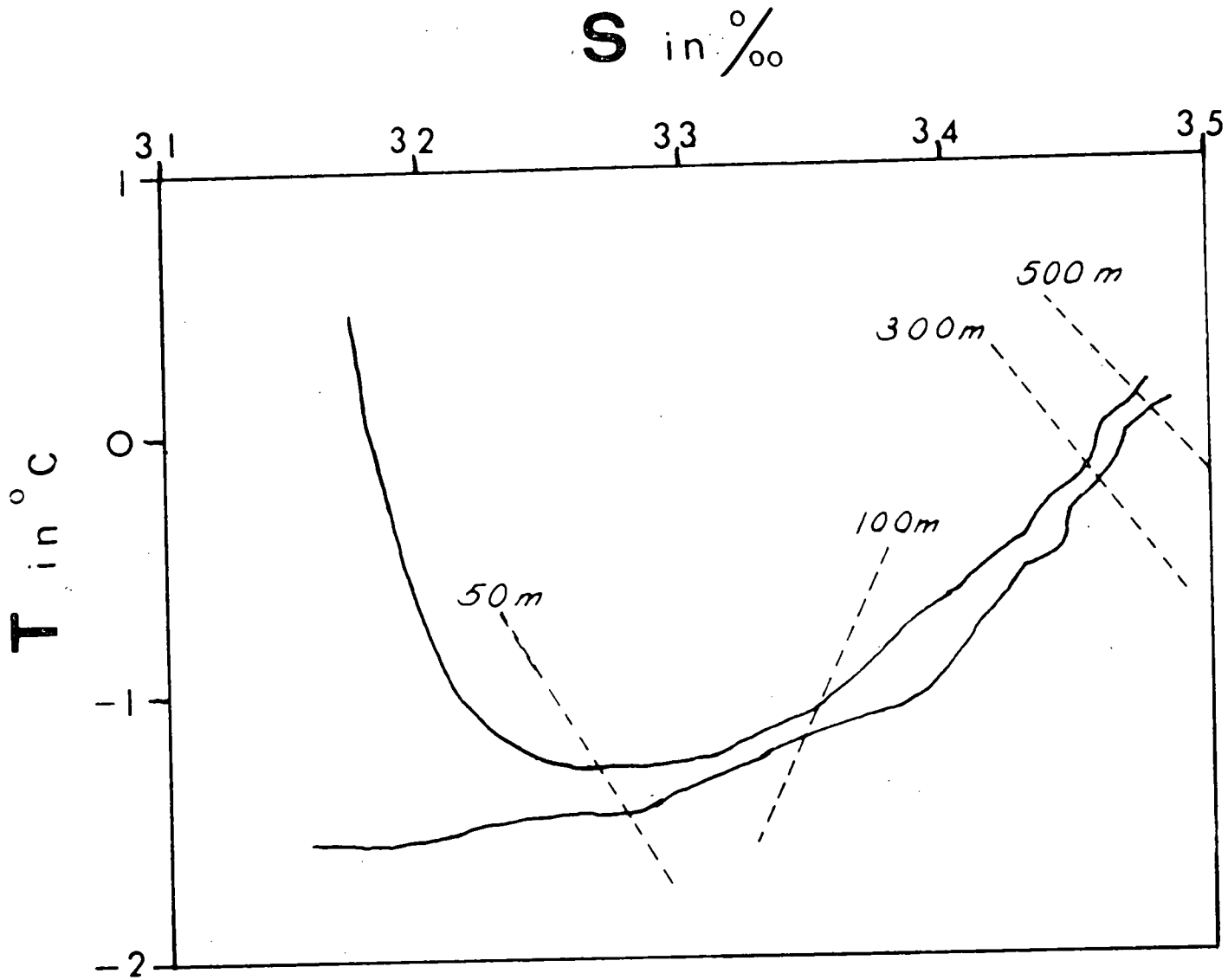

FIGURE 20 *Envelope of T-S curves from stations on the south bound leg (S71).*

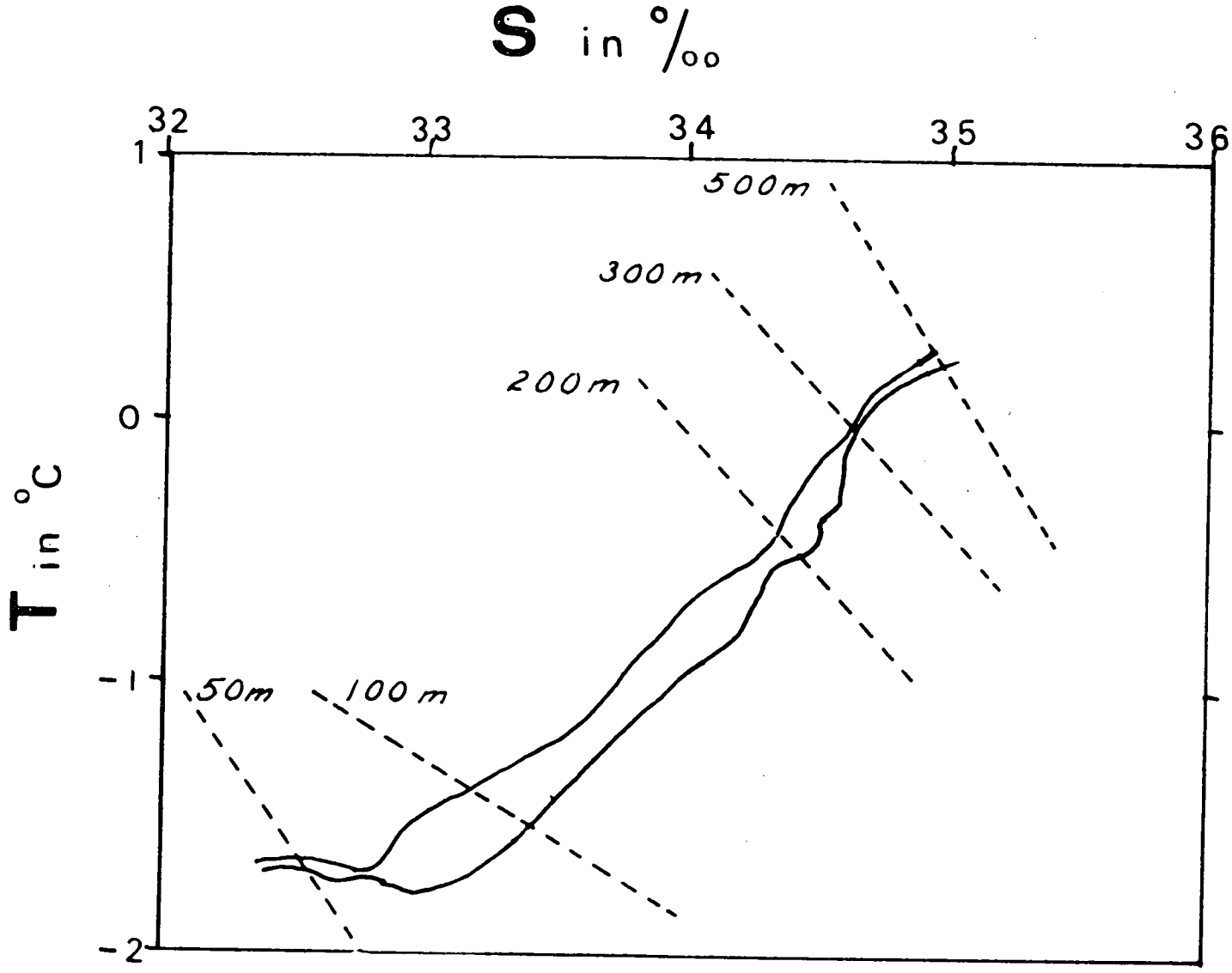

FIGURE 21 *Envelope of T-S curves from stations in the Lincoln Sea. Drawn from data obtained by Siebert (1967).*

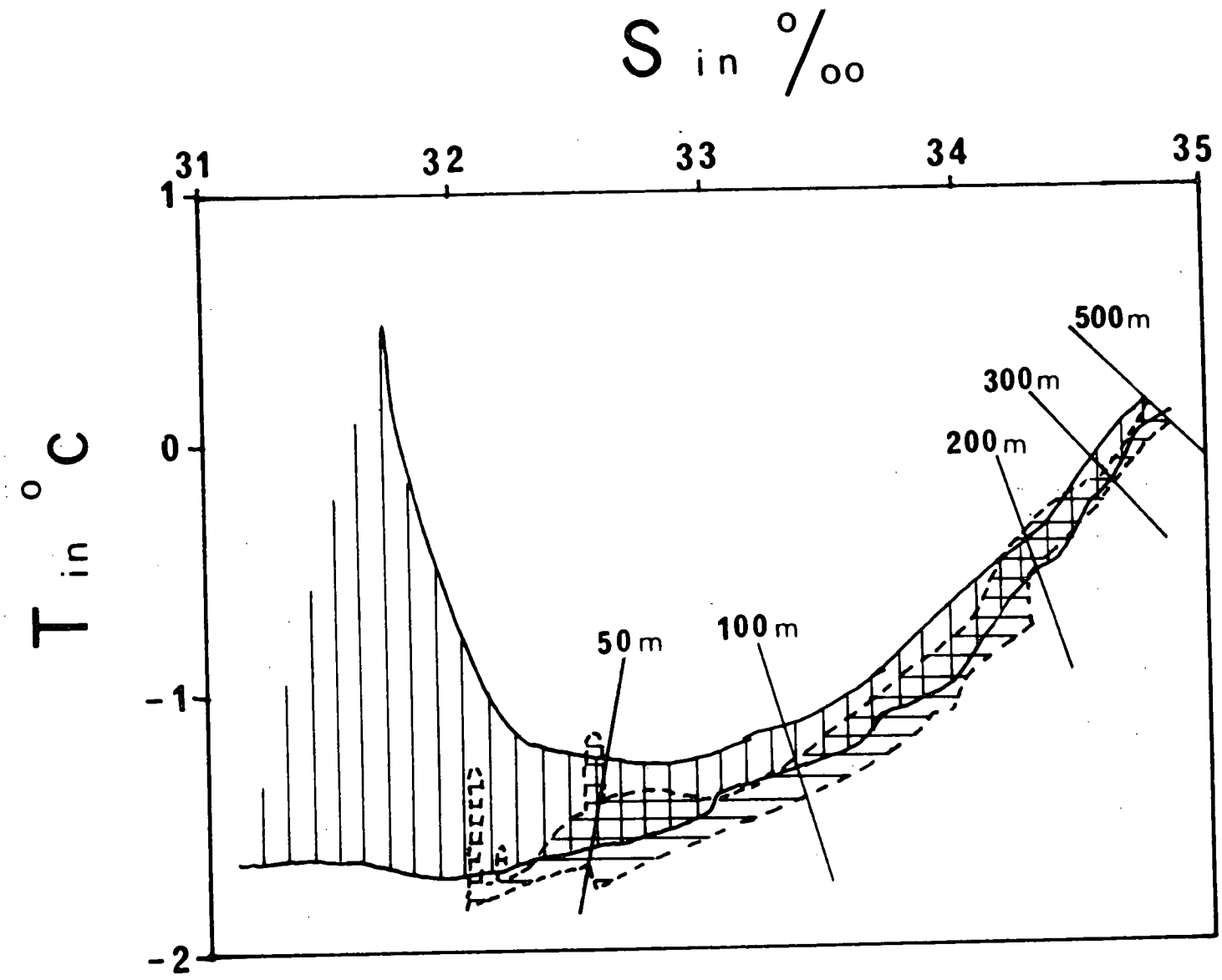

FIGURE 22 *A comparison of the envelopes of T-S curves obtained in Robeson Channel in April 1971 (horizontal shading) and in August 1971 (vertical shading).*

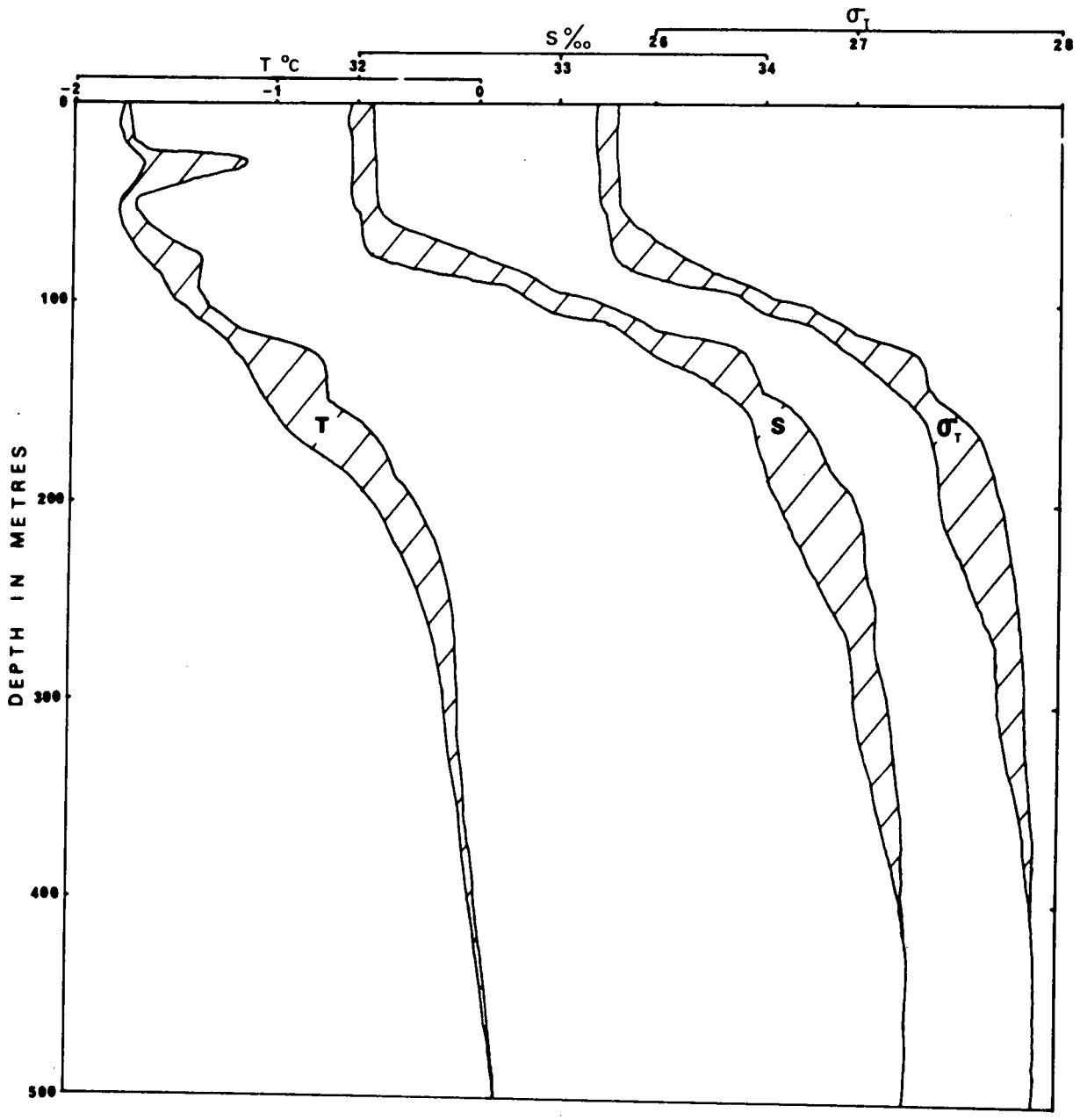

FIGURE 23 *Envelope of the Temperature, Salinity and Density profiles in Robeson Channel in April 1971. (From data obtained by Finlayson).*

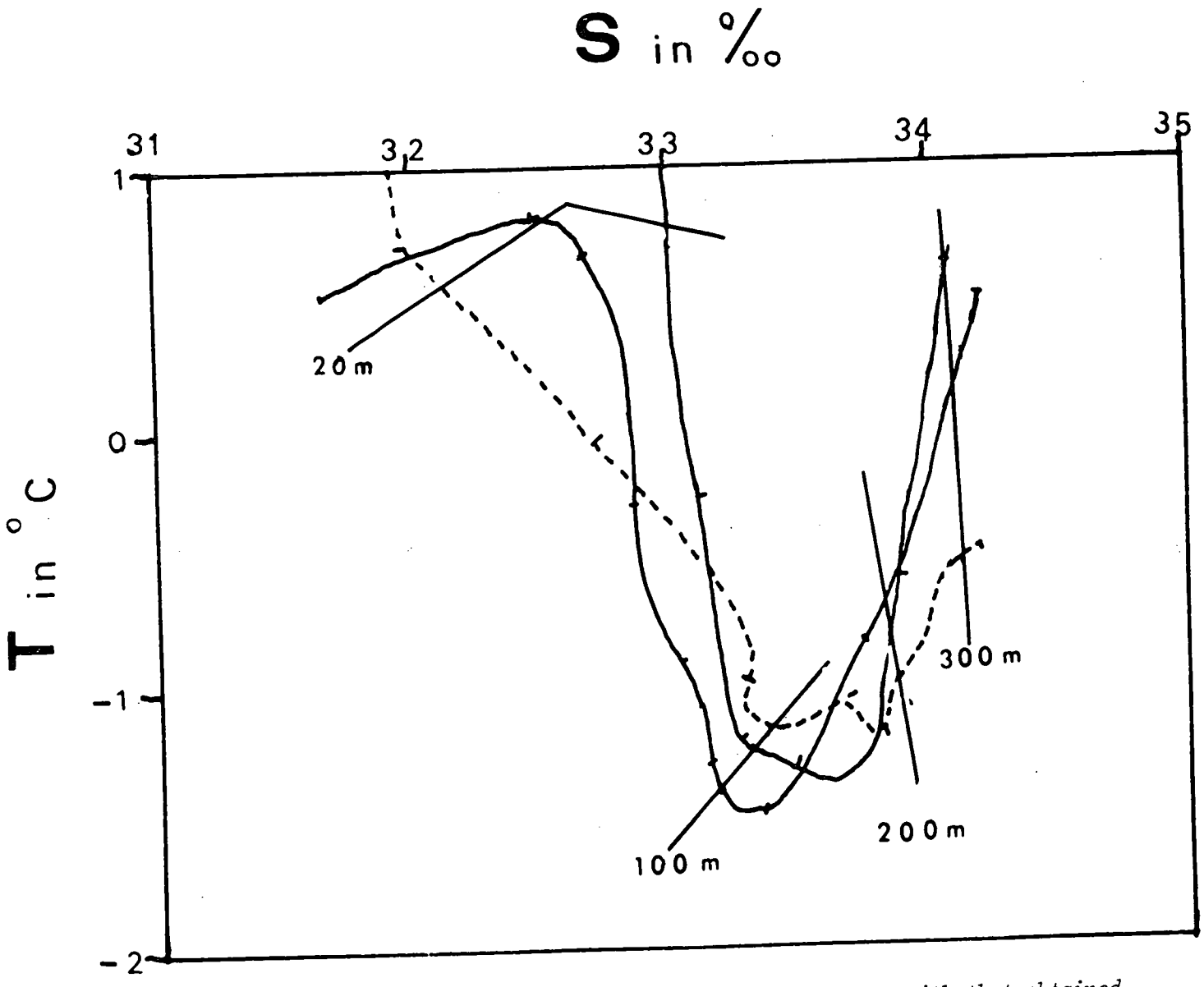

FIGURE 24 *Comparison of T-S curves obtained in Baffin Bay with that obtained in Station 1. (Station 1 shown by broken line).*

Muench obtained a cross-section in about the same position in Smith Sound as the cross-section H71 obtained here and Muench's results match quite closely the envelopes in Figure 19 and 20. It seems probably then that the results obtained in Station 1 were due to an influx of water from Baffin Bay. Both Nares (1878) and Bessels (1884) reported northerly drifts in the Smith Sound region and Nutt (1966) found northerly currents and ice drift well up into Nares Strait. Previous geostrophic estimates of flow through Smith Sound have varied widely. Collin (1965) quoted Kiilerich's(1928) value of 0.42×10^6 m^3 s^{-1} southwards. Bailey (1956) calculated a net northerly flow of $0.42 \times 10^6 \times m^3$ s^{-1} in 1954. Collin (1965) found an average southerly flow of 0.24×10^6 m^3 s^{-1} and Moynihan (1972 a and b) found a northerly flow of 0.48×10^6 m^3 s^{-1} in 1969. It is clear that the flow of water through Smith Sound may be variable and may be affected by wind, tide and barometric gradient, but the inherent errors in the determinations of the geostrophic flows are likely to be larger than any of these effects. However, the water column at Station 1 was very probably the result of a northerly incursion of Baffin Bay water into Smith Sound.

The incursion of Baffin Bay water at Station 1 was found in a position which was slightly further north than those reported by Muench (1971). Although a number of authors (Palfrey and Day 1968) have found reversals of current with tidal frequencies in Smith Sound it is difficult to explain the present findings by this factor alone Station 1 being several times the distance of a tidal excursion to the north of Station 23. Further, the two stations were occupied at almost identical phases of the tide, both being taken within ten minutes of Lower High Water at Pim Island and within two days of neap tides. (Anon 1971).

A possible explanation might be looked for in the atmospheric pressure gradients over Nares Strait but little data is available in the immediate area of Smith Sound. At the time of Station 1 the barometer at Alert 500 km north of Smith Sound was 3.4 mb higher than that at the US Air Base in Thule 250 km to the south and the pressure was rising at both places. At the time of Station 23 the gradient was reversed with the barometer at Alert being 1.9 mb/lower than that at Thule with the pressures moving towards equality. Thus at the time of Station 1 we might expect little or no current due to changing barometric pressure if the changes in the pressure gradients in Smith Sound can be assumed to be the same as those from Alert to Thule. With the same proviso, any current in Smith Sound at the time of Station 23 would be towards the south west. It seems doubtful that the displacement of Baffin Bay water found at Station 1 could have been due to this effect.

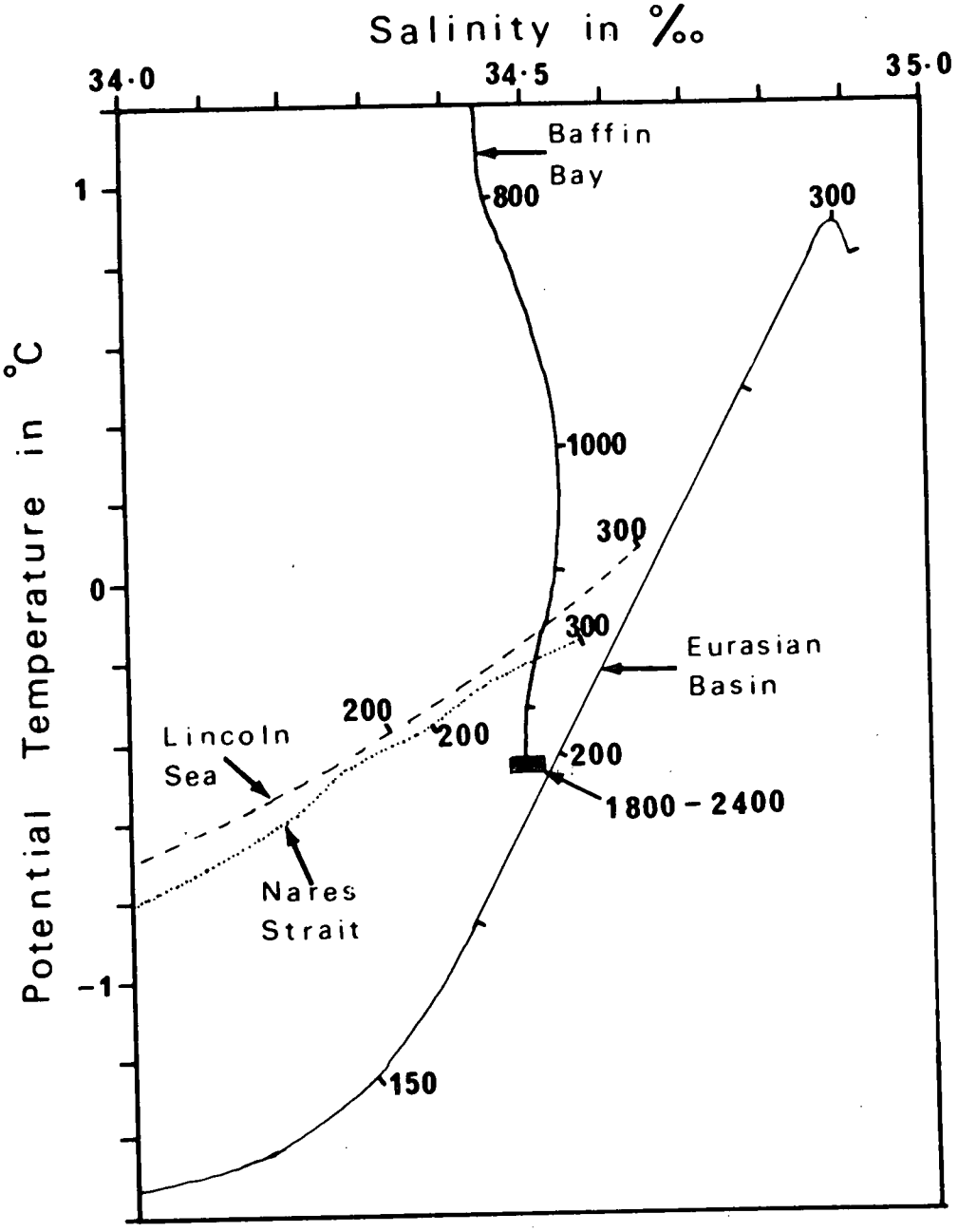

FIGURE 25 *T-S Diagram illustrating a possible origin for Baffin Bay Bottom Water.*

THE BOTTOM WATER OF BAFFIN BAY

The Deep Water of Baffin Bay lies between about 1200 metres and 1800 metres in depth. Its in situ temperature decreases from about 0°C at 1200 metres to -0.4°C at 1800 metres while the salinity is uniform from 1200 metres down at 34.5 °/oo ± 0.04 °/oo. The Bottom Water below 1800 metres has characteristic in situ temperature and salinity of -0.4°C ± 0.02°C and 34.50 °/oo ± 0.02 °/oo.

Collin (1956) and Palfrey and Day (1968) suggested that water with the same characteristics as Baffin Bay Bottom Water could be found in Nares Strait at depths greater than the sill depth at 250 metres. Water with in situ temperatures below -0.2°C and salinities of 34.5 °/oo were in fact observed by them and also in 1972 (Figure 12). Moynihan (1972) suggested that the southward slope of the 34 °/oo isohaline lines and the 27.5 isopycnal lines which he obtained indicate a flow of water over the sill at the south end of Kane Basin. A similar configuration was observed in August 1972 (Fig. 12). This appears to support Collin's suggestion that water from below sill depth might pass into Baffin Bay in discrete slugs as a result of unusual tidal or meteorological conditions.

However, the potential temperature of Baffin Bay Bottom Water from 2000 metres is -0.7°C and water of this potential temperature in Nares Strait has a salinity of only 34.0 °/oo which is 0.5 °/oo too low. Muench (1971) observes that the nearest water of the correct salinity and potential temperature to form the Bottom Water is found in the Eurasian Basin at 180 - 200 metres and that water with this characteristic has been observed in Nares Strait only once, at the Godthaab Station #98 in 1928 (Fig. 25). If the Bottom Water were to be produced by the passage over the sill of discrete parcels of water this would imply that such parcels might pass almost unchanged through a channel 600 kms long. No evidence has become apparent of the passage of such a parcel in any data obtained up to the present.

An alternative explanation is suggested:

Kupetskiy (1962) discussing the origin of the North Water and noting that the most likely mechanism for its formation is that the area is swept clear of ice by the strong off-shore winds, suggested that the total thickness of ice formed in this region could well be greater than that normally found in this latitude by a factor of four or five and gave a value for total thickness of ice of 9 m. This implies that the rapid cooling in regions of open water or thin ice and the excess of salinity produced by freezing will increase the instability of the surface layers to such an extent that the convection layer may extend to greater depths than the normal 200 m of the Polar Ocean and possibly through the layer of Atlantic Water to the bottom in about 500 m. That such a process could well produce water of the same characteristics as Baffin Bay Bottom Water is seen below.

We consider the mixing of water from Nares Strait above sill depth (250 m) with Atlantic Water from 250 m to 500 m which is the typical depth in the North Water region. The salinity and temperature of the water leaving Nares Strait may be assumed to be the same as that found in the spring in Robeson Channel. The mean temperature and salinity from the underside of the fixed ice down to 250 metres, weighted for the volume transports found in May 1972 are -1.22^{o}C and $33.0^{o}/oo$. The mean temperature and salinity of the Atlantic Layer of Baffin Bay between 250 m and 500 metres taken from Muench and Sadler (1973) are $+ 1.50^{o}$C and $34.4^{o}/oo$. A mixture of these waters would give a 500 m column from surface to bottom with a mean temperature of $+ 0.14^{o}$C and a mean salinity of $33.7^{o}/oo$.

Now consider the salt rejected when freezing 9 metres thickness of ice. Malmgren (1927) gives values for the salinity of new sea ice. In the case of the North Water we may assume that the mean thickness of ice formed before it is blown away is 0.5 metres or less. The resulting estimated salinity of the ice is $4.0^{o}/oo$. As a result, the freezing of a total thickness of 9 metres of ice will release about 270 kgms.m^{-2}. The excess salt distributed through a water column 500 metres deep will increase the salinity by about $0.6^{o}/oo$ resulting in a mean salinity of $34.3^{o}/oo$ which is reasonably close to the $34.5^{o}/oo$ of the Bottom Water.

At the same time there will be a considerable heat loss at the surface to the atmosphere in the form of evaporation and sensible heat since the surface temperature of the water is approximately 30^{o}C warmer than the air. If we suppose that the heat loss is sufficient to freeze 9 metres of ice and also to cool a 500 metre column of water by ΔT from $+ 0.14^{o}$C to the potential temperature of the Bottom Water of -0.6^{o}C then the total heat loss of Q in cal.m^{-2} over the winter period must be approximately

$$Q = 9 \times 10^{6}L + 500 \times 10 \times C_{p} \times \Delta T$$

and assuming $C_{p} = 1$ and L the latent heat of freezing $= 80$ cal.gm^{-1}

$$Q = 1.1 \times 10^{9} \text{ cals.m}^{-2}.$$

Using Vowinkel and Orvig's (1971, page 174, 177) estimated values for evaporation and sensible heat losses over the period November to May we have approximately an evaporative heat loss of 1×10^{9} cal.m^{-2} and a sensible heat loss of 0.3×10^{9} cal.m^{-2} for a total of 1.3×10^{9} cal.m^{-2}, and in good agreement with the value above.

It is therefore possible to explain the production of Baffin Bay Bottom Water by mixing and cooling of Arctic Surface Water advected through Smith Sound with water of the Baffin Bay Atlantic Layer. If such water is produced it will be much denser than water at the same level surrounding the North Water area and will subside down the slope into the deep basin of Baffin Bay, replacing Bottom Water which is slowly mixed up into the Deep Water Layer.

We have from Dunbar (1973b) that the mean area of the North Water is approximately $2 \times 10^{10}m^{2}$. However, most of this area is not open water, the greater part of it being covered by more or less concentrated

pack ice. The concentration increases from zero in Smith Sound to approximately 10/10 at the southern boundary and a reasonable estimate of the amount of open water over the whole area is probably 3/10. Neglecting the freezing and cooling which occurs in the ice covered areas, since the cooling through ice is about two orders of magnitude less than that through an open water surface, we find an area of about $6 \times 10^9 m^2$ which may be considered to be producing Bottom Water. With a typical depth of 500 metres, the annual production of this water is then approximately $3 \times 10^{12} m^3$. The volume of the deep basin of Baffin Bay below 1800 metres is approximately $5 \times 10^{13} m^3$ which indicates a residence time for Bottom Water of the order of 20 years.

This removes a further objection to the proposed mechanism, namely that the oxygen content of Bottom Water is much lower than that of a mixture of Arctic Surface Water and Atlantic Layer water. The dissolved oxygen level in Atlantic Water between 250 and 500 metres deep is approximately 5.5 $ml.l^{-1}$ and that of Arctic Surface Water in Smith Sound between the surface and 250 metres is 7.0 $ml.l^{-1}$. The mixture should therefore have a dissolved oxygen content of about 6.2 $ml.l^{-1}$ while that in the Bottom Water is near 3 $ml.l^{-1}$. A twenty year residence as suggested above would allow plenty of time for the oxygen level to be reduced to half by biological processes, but would imply a negative gradient in dissolved oxygen content from north to south in the basin as the Bottom Water is replaced by water creeping down the slope. There is insufficient data available to determine whether such an oxygen gradient exists and its magnitude would also depend on the length of time that the new Bottom Water is in transit before reaching the basin.

A simple test of this theory would consist of observations to determine the thickness of the convection layer in the North Water in winter to decide whether it does in fact extend to the bottom in 500 m.

SUMMARY

We may summarize the results for the waters of Nares Strait in August as follows:

1. The water column has characteristics which indicate that its origin is in the Lincoln Sea. A layer of Arctic Surface Water ($<0.0^{o}C$ and $<3.4\ ^{o}/oo$) about 200 metres thick overlies water from the Atlantic Layer of the Arctic Ocean ($>0^{o}C$ and $>34.6\ ^{o}/oo$), which is evident in Hall Basin.

2. The near surface layer (<50 metres) is strongly affected by the seasonal factors of insolation, run-off and wind-driven turbulence during the open period, and is characteristically warmer and less saline than the Arctic water below it.

3. No evidence was found for the existence of water in Nares Strait having the necessary characteristics to form Baffin Bay Bottom Water. It is suggested that the Bottom Water is formed by the mixing in the North Water of water from Nares Strait at depths above sill depth (250 cm) with Atlantic Water entering Baffin Bay from the south. The mixture has its salinity increased by the exceptionally large amount of ice produced in the North Water and its temperature reduced by the intense cooling which takes place over the open water area.

4. There are at least occasional incursions of Baffin Bay water northwards into Smith Sound at depths between the surface and the sill depth of 250 m.

5. In view of these northerly incursions, the constant characteristics of the water in Nares Strait indicate that there is a general southerly drift from the Lincoln Sea which maintains these characteristics. While this flow may be irregular in some areas and may be halted or even reversed by tidal and wind effects, there is in general a southerly flow of Arctic Surface Water from the Lincoln Sea southwards which is somewhat more concentrated on the westerly side of the Channel. The magnitude of this flow is demonstrated below from direct measurements of the currents.

Chapter IV

RESULTS FROM CURRENT METER ARRAY, MAY 1972

GENERAL REMARKS

The array of 14 current meters and 6 thermographs was installed on the 24th and 25th April 1972 through first-year ice floes about 2 metres thick frozen into the fixed ice of Robeson Channel. The exact locations of the three stations were dictated by the need to find an area of smooth ice sufficiently large to allow the landing of a De Havilland Twin Otter among the chaotic pressure ridges in the channel. Three suitable areas were located by a prior reconnaissance flight in approximately the desired positions. The snow cover on these level areas was generally less than 5 cms thick and the aircraft, fitted with oversized wheels, had no difficulty in landing or take-off with full load.

The stations were spaced equi-distantly across the channel (Fig. 10) and their positions were fixed by theodolite angles of points on Ellesmere Island with reference to the coastline on the Topographic Series Map with an uncertainty of ± 100 metres. However, the positions shown are only approximate relative to the coast of Greenland as shown on the topographic map due to the discrepancies between the two surveys. The cross-section shown in Figure 26 was drawn from the Hydrographic Field Sheet CHS 3696 but the charted depths at the specific positions of the stations are possibly in error.

This is because the field sheet does not show a surveyed coast line but only a number of survey base points. In the time available and under the prevailing conditions of snow cover it was not possible to recover these survey markers and coastal features were used as survey marks. This gives rise to errors in the station positions relative to the survey markers and thus to the surroundings shown on the field sheet. It is considered that these errors in position were less than ± 200 m in the worst case. In some parts of the channel a horizontal error of this magnitude may be equivalent to an error in charted depth of ± 30 metres.

The possibility of errors in estimating the depth of the planned station location caused other problems. The method of mooring employed requires that the wire be cut to length and shackles inserted at appropriate

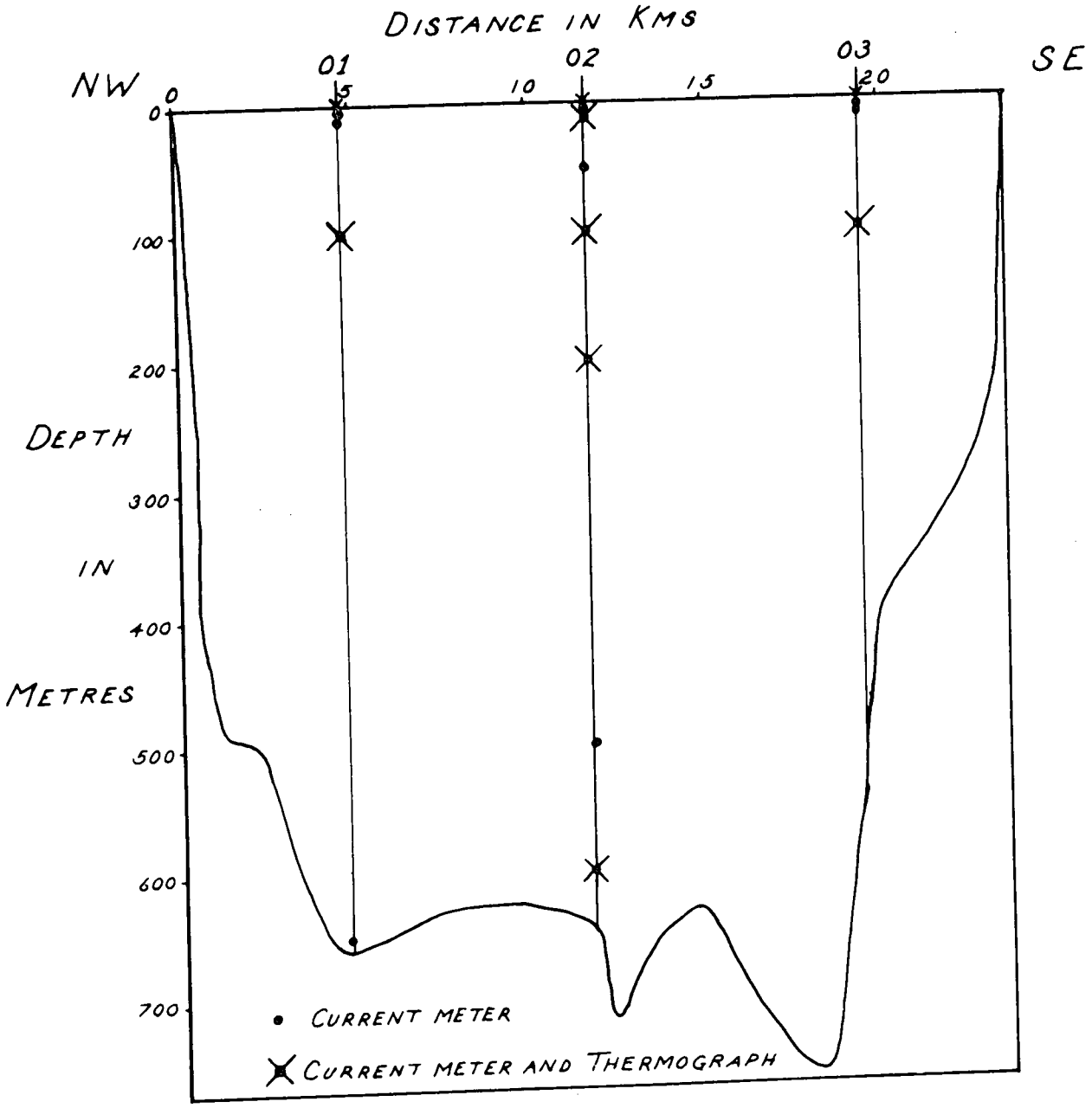

FIGURE 26 *Cross-section of Robeson Channel showing the positions of current meters and thermographs in the array.*

points before going into the field. There is thus little flexibility in establishing the positions of stations if it is desirable to mount meters near the bottom and errors in the survey may cause such meters to hit sea bed. Because of this no deep meter was planned at Station 3, nearest to Greenland, where the uncertainties are particularly serious. Before the moorings were laid, a portable echo-sounder was used through the holes in the ice to obtain soundings. Unfortunately no results could be obtained with this instrument at Station 1 and it was only after analysis of meter records for tilt and current that it was realized that the meter in this station at 650 metres depth was fouling the bottom at slack water. Consequently the records obtained by this meter have had to be ignored.

The positioning of the meters in the array is illustrated in Figure 26. Since only 14 recording current meters were available it was decided to employ 7 of them at the centre station to obtain a good estimate of the current profile and to place the meters at the other two stations at three of the same depths to provide a cross-channel velocity gradient. Three meters were established just below the ice at 5 metres depth to provide in addition some idea of the sheer stresses acting on the fixed ice due to water movement. A similar principle was used in positioning the six thermographs, four of them being used in Station 2 and the other two being placed so as to provide a cross-channel gradient.

The instruments and the length of the records obtained are listed in Table 1. The nominal depths listed in the second column are the actual wire lengths. However, it is obvious that a suspended array will be deflected from the vertical if the currents are strong and thus the instantaneous depth is a function of the drag forces on all the meters and on the suspending wire. No depth recorders were available but estimates of the maximum amplitude of the tidal oscillations in depth have been made by using the tilt angles recorded by the current meters. These amplitudes vary from about half a meter at a nominal depth of 10 metres to 6 metres at a nominal depth of 600 metres. The ranges in depth for each meter have been listed in the third column.

In the fourth and fifth columns are listed the serial number and type of the current meter. The meters used were of two types. The Type 316 Braincon Recording Meters were borrowed from Bedford Institute. This type is heavier and much more bulky than is the newer Type 381 and this bulk necessitated a larger hole than would otherwise have been required. It will be seen from column 6 that two of the Type 316's and one of the Type 381's produced no record at all. The failure in all three cases was in the film drive, but no reason could be found for these failures when the meters were examined upon recovery. Meter #271, the Type 381 which failed during this experiment was in fact re-loaded and used with satisfactory results in another experiment two weeks later.

TABLE 1

Thermograph and Current Meter Records Obtained

St. No.	Nominal Depth (Metres)	Range in m	Current Meter Number	Current Meter Type	Record Length (days)	Thermograph Number	Record Length (days)
1	5	0	234	381	41	--	--
	10	0.5	139	316	0	--	--
	100	4	182	316	41	5310048	41
	650	6	200	316	41*	--	--
2	5	0	237	381	39	--	--
	10	0.5	233	381	39	310051	39
	50	1.5	238	381	39	--	--
	100	4	235	381	39	5310030	39
	200	5	140	316	0	5310046	39
	500	6	232	381	39	--	--
	600	6	236	381	39	5310055	30
3	5	0	271	381	0	--	--
	10	0	193	316	37	--	--
	100	2	201	316	37	5310047	37

* The record from Current Meter #200 has not been used as the meter apparently fouled the bottom at slack water.

The commonest failure when using this type of meter under arctic conditions is that the film breaks. This usually occurs when the temperature of the film has fallen so low before immersion that the film becomes stiff and brittle and it then breaks when the drive motor operates to shift it one frame. This was avoided by loading film and storing the meters in a heated hut and taking the meter, wrapped in insulation, out to the station only when all preparations were complete, so that it was immersed in a very few minutes. Similar precautions are necessary when handling the recording thermographs which made use of a special green-sensitive 70 mm film.

DATA PROCESSING

The analogue records from the Braincon current meters are in the form of 16 mm film. The film was processed and then digitized using a system devised by Keys (1973). Some delays were encountered while setting up the system but it eventually proved to be fast and accurate in operation.

At this point difficulty was encountered in reading the records from two meters (Numbers 182 and 193) both Type 316 meters on loan from Bedford Institute. Since both these meters had already been returned to Bedford it was not until June 1973 that it could be confirmed that they had both been assembled with the Savonius rotor upside down. While this did not affect the magnitude of the observed current vector reading it meant that the bearing angle had been measured in the wrong sense. No correction was made for this during the computer processing, the necessary adjustment being made to the computer output.

The initial processing of the current meter data was completed on the Xerox 7 computer at DREO. In June 1973 the data was transferred, with some difficulty, to the CDC 3100 computer at Bedford Institute where the analysis was continued using the programme package developed for that computer (Rudderham and Lively 1970). This was accomplished by November 1973 but a check of final calculations in May 1974 led to the discovery of a programming error in the package which affected all the Type 316 meter results. The analysis of the results from these meters was repeated, being finished by the end of August 1974. Some further processing was then completed on the Xerox 7 at DREO.

DISCUSSION OF OBSERVATIONAL ERRORS

CURRENT RATE

Both types of Braincon current meters have, according to the manufacturer, an accuracy of ± 2% in recording the current rate. Over a period of five or six weeks in the field this is probably optimistic and the current recordings are not assumed to have an accuracy of better than ± 4%. In addition the uncertainties involved in digitizing the film records must be considered. The arc length measured by the system devised by Keys (1973) is reproducible by different observers to 1^{o} at each end. For an arc length of 120^{o} this is equivalent to about 1.5% error while for an arc length of 10^{o} the uncertainty is about 16%. The

uncertainty in rate measurement therefore varies from about 20% for rates of 0.5 m.s.$^{-1}$ to about 6% for a rate of 1 m.s.$^{-1}$. While these errors may be presumed to be random errors and thus to have little effect on the long term averages used later in transport calculations, they must be considered when discussing details of the tidal flow.

BEARING ACCURACY

There are a number of sources of error which reduce the bearing accuracy.

i) The area of operations is comparatively near the north magnetic pole and the horizontal component is weak thus exaggerating the effects of any deviation induced by the material of the meter itself.

ii) Similarly the weakness of the horizontal field allows considerable changes to occur due to the unknown magnetic composition of the surface rock below the channel and, more important, because of changes in magnetic variation due to secular or short term changes in the earth's field.

iii) The large tidal currents of the region change very quickly when the tide is turning while the record on the film is the result of a 20 minute exposure. If the current direction should stay constant to within two or three degrees for say 15 minutes of this period a very short arc will appear on the film as a result. If then during the last 5 minutes of the exposure the current swings through thirty or forty degrees the mid-point of the resulting arc will not give a true 20 minute mean of direction. In any case, the mean current speed and mean direction as given by the Braincon meters does not give an exact value for the mean vector.

iv) Uncertainties in the measurement of the end bearings of the arc.

Of these four main sources of error the second is probably the more serious. The deviation due to the meter itself was measured for eight of the meters used, two of them in the base camp at Lincoln Bay, and was found to be always less than 2^{o}. The effects on transportation calculations of the rapid swinging of the meter at the turn of the tide are minimized by the fact that these periods coincide with low values for the magnitude of the velocity. The errors in reading are random and will have no systematic effect on the residual. The variation on the other hand may change by as much as 5^{o} per <u>day</u> in this area, according to information obtained from the Hydrographic Service of Canada. Consequently only two adjustments were made to the direction as read by the meter;

i) allowance for a mean magnetic variation of 75°W.

ii) a rotation of the reference point to the axis of the channel at 045°.

The uncertainties in the current directions observed as a result of all these factors is approximately ± 8° for bearings near the channel axis, i.e. during the periods of strong flow while for small currents around the turn of the tide the bearing errors may be as high as ± 30°. The resultant errors in the down-channel component are small, averaging ± 0.01 metres per second, or less than 2% at full tide. However, the uncertainties in the cross-channel components due to bearing uncertainties are much higher. They vary from ± 0.05 $m.s.^{-1}$ (or ± 10%) during full flood or ebb tide to ± 0.05 $m.s^{-1}$ (or ± 50%) near slack water. The cross channel components must therefore be accepted with reservations.

TILT CORRECTIONS

Both types of Braincon meter are designed so that the degree of tilt of the instrument is recorded for each period. This tilt angle must be applied to the recorded rate to obtain the true horizontal rate. Unfortunately an error existed at this stage in the computer program for Type 316 meters which was not discovered until processing was complete. The tilt angle was read and entered in circular degrees but the program treated these as units of 5° each in accordance with an obsolete method of digitizing from the film record. Consequently all the tilt calculations were carried out with the tilt angle too large by a factor of 5. To further confuse the interpretation the exact relation

$$\text{True Rate} = \text{Observed Rate}/\cos(\text{Tilt})$$

was approximated in the program by a linear relationship,

$$\text{True Rate} \simeq \text{Observed Rate}\ (1 + k.\ (\text{Tilt Angle}))$$

since the Tilt angle is normally small. Consequently a tilt of 20° (a fairly common value at full tide in this case) was treated as 100° and the calculated True Rate was too high by about 30% whereas the exact relationship would have produced an obviously incorrect result.

The error did not affect the results from the Type 381 meters as the program had been corrected for that type of meter several years before, but the output from the Type 316 meters had to be recalculated.

Observational errors in tilt reading are considered to be less than 5° or less than 0.8% of the value of True Rate. The total uncertainty

in the magnitudes of the down channel components are therefore assumed to be ± 10% while those for the cross channel components may be as high as ± 30%.

TIME INACCURACIES

The times of starting and stopping of the film drive in the current meters were recorded as were the times of immersion and recovery. A frame count over the whole period allowed time corrections to be applied but it still was not possible to fix exactly the time of any specific frame, particularly in the case of the Type 316 meters. The film in the latter type is cycled only when the meter is upright in its suspended position. Normally the working of the clock drive can be verified after the meter has been suspended on the mooring cable but before immersion, as the functioning of the drive is audible. In the conditions in which this mooring was made it was undesirable to wait up to 20 minutes for the drive to function as the instrument would have been 'cold-soaked' in the interval. Consequently the clock was started and the functioning checks carried out in the work hut and since there was plenty of spare film the clocks were left functioning for two or three days before they were submerged. Unfortunately the film record was confused at the time of immersion, with a number of overlapping and blurred images, and it was not possible to fix the time of the first valid record to within 20 minutes. As a result it is impossible to compare the times of exposures from two different meters with an uncertainty of less than 40 minutes. While this is not important in the calculations of tidal frequencies or mass transports, it prevents the drawing of instantaneous current velocity profiles. For future operations the Type 381 meters have been rearranged so that the watch face will be photographed onto the recording film. In addition a set of current profiles will be obtained by means of a direct reading current meter to provide a direct check on the recording meters.

MEASURED CURRENTS

An example of the curves of rate and true direction is given in Figure 27 from the records obtained by Meter #235 at 100 metres depth in Station 2. It may be seen that the current shows semi-diurnal and diurnal

tidal constituents with the maximum flows being toward the southwest. The spring-neap variation is also pronounced.

In Figure 28 a typical two days records from the same meter are shown on an expanded scale and it may be seen that the current direction is in fact bipolar, running for most of the time in the direction of 225^{o} or 045^{o}, that is, up and down channel.

In Figure 29 to 48 are shown the plots of current components, axial (major) and cross-channel (minor) for all the meter records. The major axis is positive towards 045^{o} and the minor towards 135^{o}. The first diagram of each pair displays the full record while the second shows an expanded plot for 2 days, 13th and 14th May. The records indicate clearly the preponderantly semi-diurnal nature of the tides in the channel but with a distinct diurnal constituent and a prominent spring-neap effect. The maximum velocity amplitudes for the major components (approximately 0.45 $m.s.^{-1}$) are found at the 100 metre level at each station (Figure 31, 39 and 47) with smaller amplitudes (0.25 $m.s.^{-1}$) at the shallow positions near the ice. Station 3 near the Greenland coast has slightly smaller amplitudes than those at the other two stations.

The minor components in general have smaller amplitudes (0.1 $m.s.^{-1}$) at 100 metres and the semi-diurnal constituents are less clearly marked (Fig. 40) but at shallow depths the amplitudes are approximately 0.15 $m.s.^{-1}$ and are more clearly semi-diurnal in form (Fig. 36).

It will be observed from the two-day current diagram in Figures 34, 36, 38, 40, 42 and 44 that the axial components are in phase at all the current metres in Station 2 and that the amplitudes are approximately equal at all depths. This indicates that the tides are almost entirely barotropic in the Channel even though the residual current varies with depth and station position. The existence of these residual currents is indicated by the displacement of the mean which can be seen in most of the plots of the major (axial) components. The displacements are mainly towards the negative or south-westerly side of the zero line and are particularly obvious in Figures 31, 38 and 39 indicating that an appreciable south-westerly residual current existed at those positions. The minor components are irregular in amplitude and relative phase partly due to the large percentage uncertainties in measurement discussed above. Figures 41, 43 and 47 are much more symmetrically placed and any residual axial velocity is small.

The residual current is more clearly shown in Figures 49 and 50 which are the progressive vector diagrams from 100 metres in Station 2, Figure 50 being an expansion of two days of the complete record. Figure 49 shows a total drift of some 400 km in a period of 38 days, approximately 10 km per day at this position. In Figure 50 there is no trace of a regular tidal turning pattern both clockwise and counter-clockwise rotation being observed, and this may be more clearly seen in Figure 51 which gives the tidal hodographs for four levels in Station 2 for the tidal cycle from 0600 14th May to 1900 14th May. All of these curves are folded and have sections indicating turns in opposite senses.

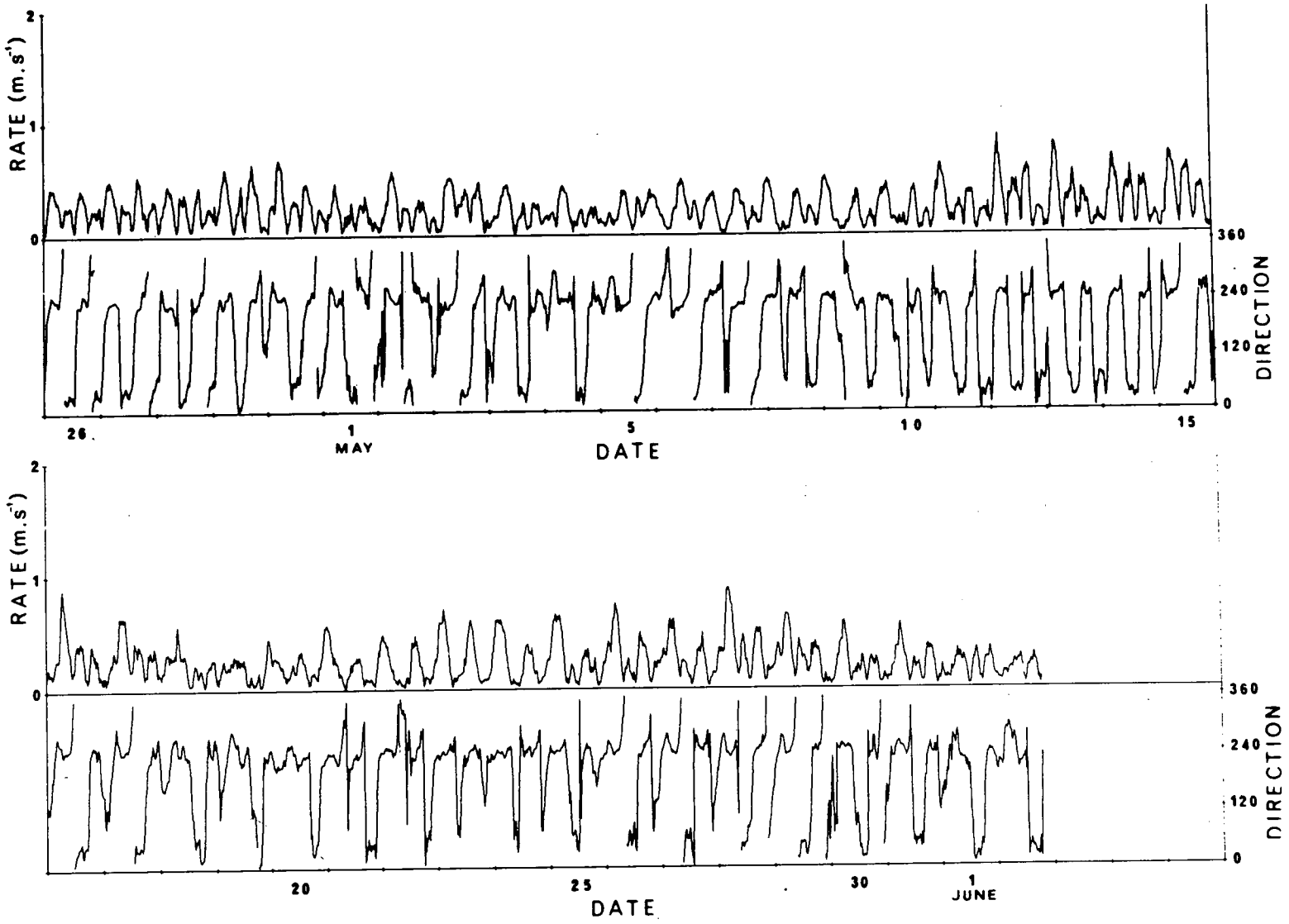

FIGURE 27 *Plots of rate and direction of the current measured by Meter #235 in Station 2 at 100 metres depth over the whole period.*

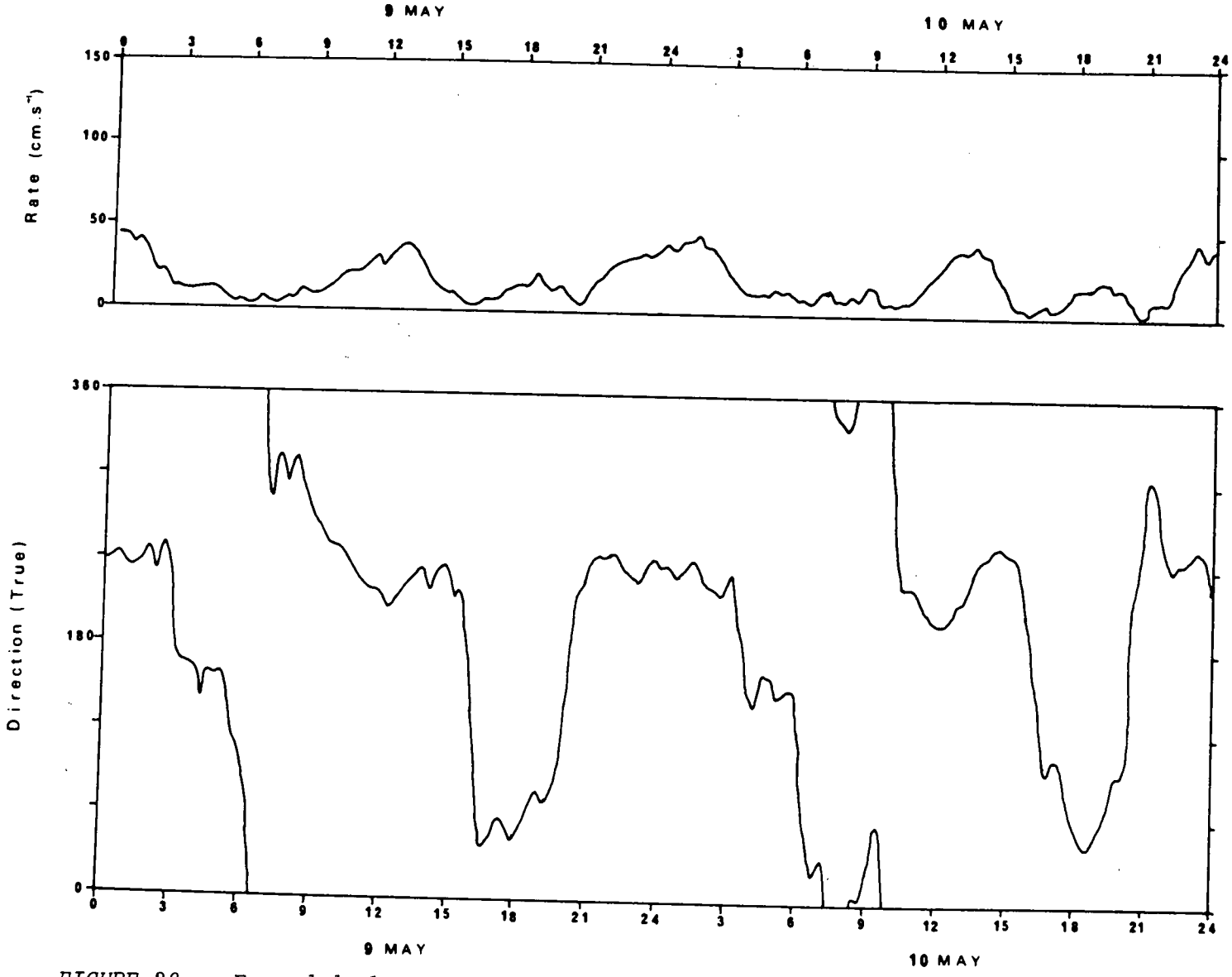

FIGURE 28 *Expanded plots of rate and direction measured by Meter #235 in Station 2 at 100 metres depth for 9th - 10th May 1974.*

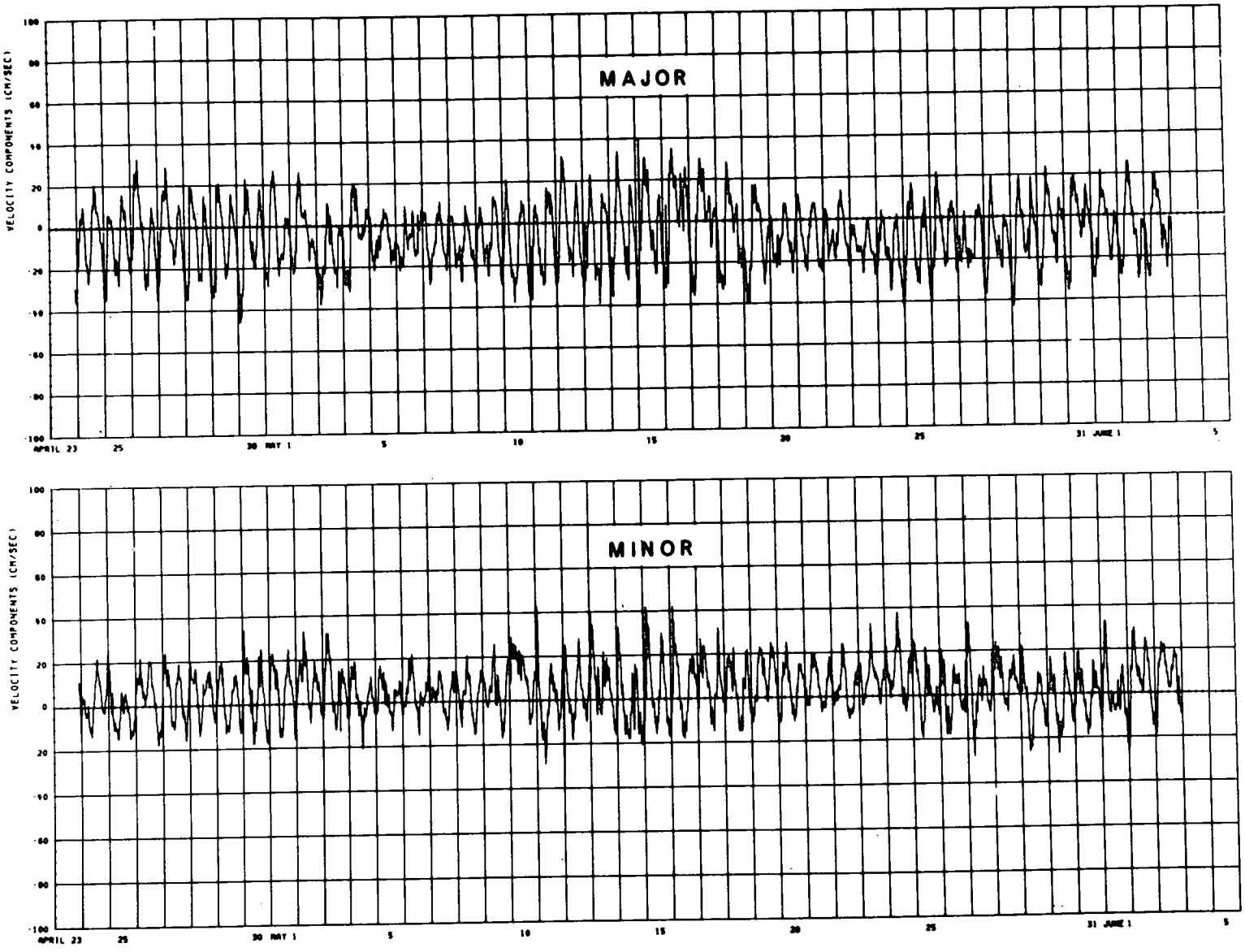

FIGURE 29 *Plots of Current components at 5 metres depth in Station 1 (Meter #234) over the full record period.*

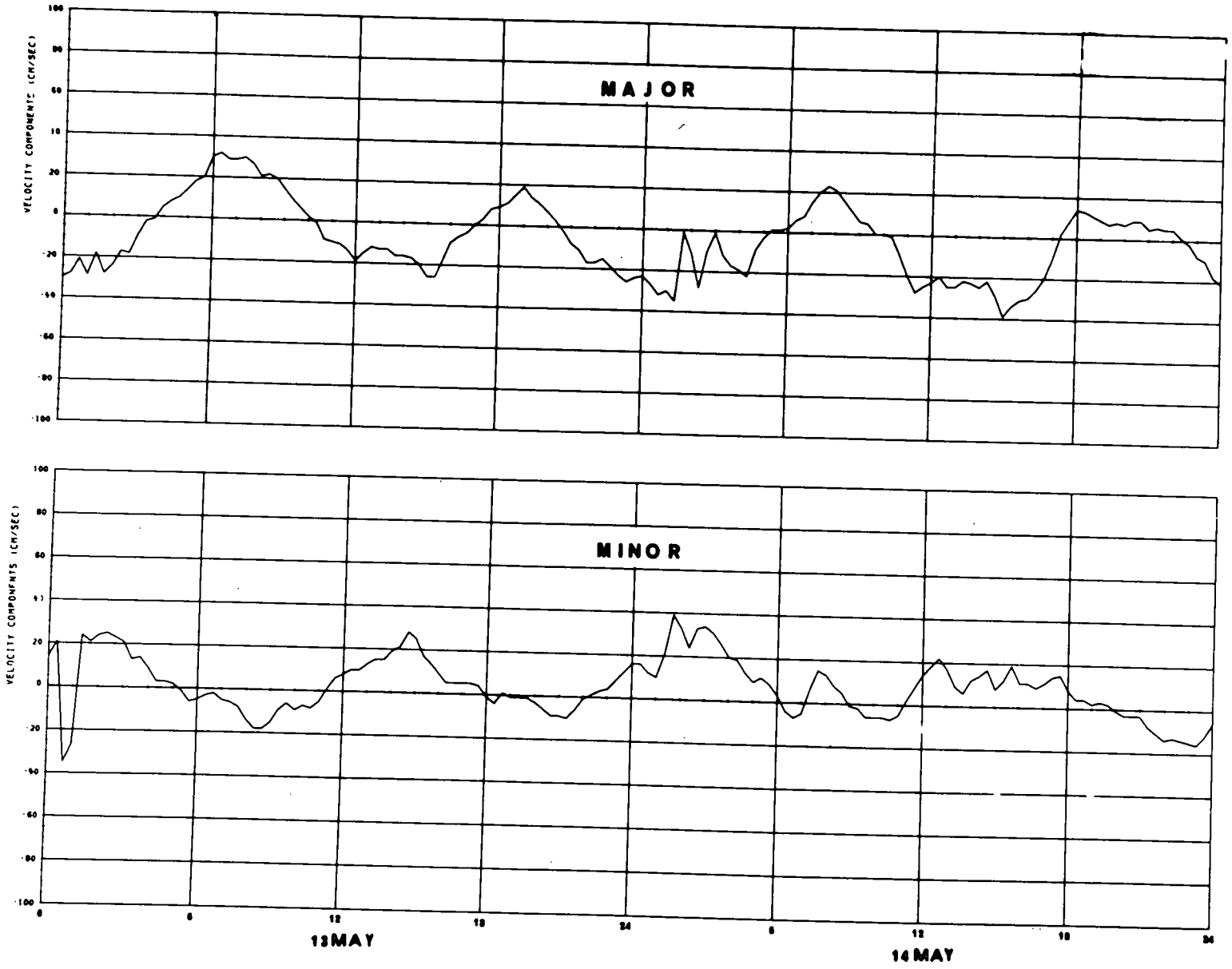

FIGURE 30 *Plots of Current components at 5 metres depth in Station 1 (Meter #234) over a two-day period.*

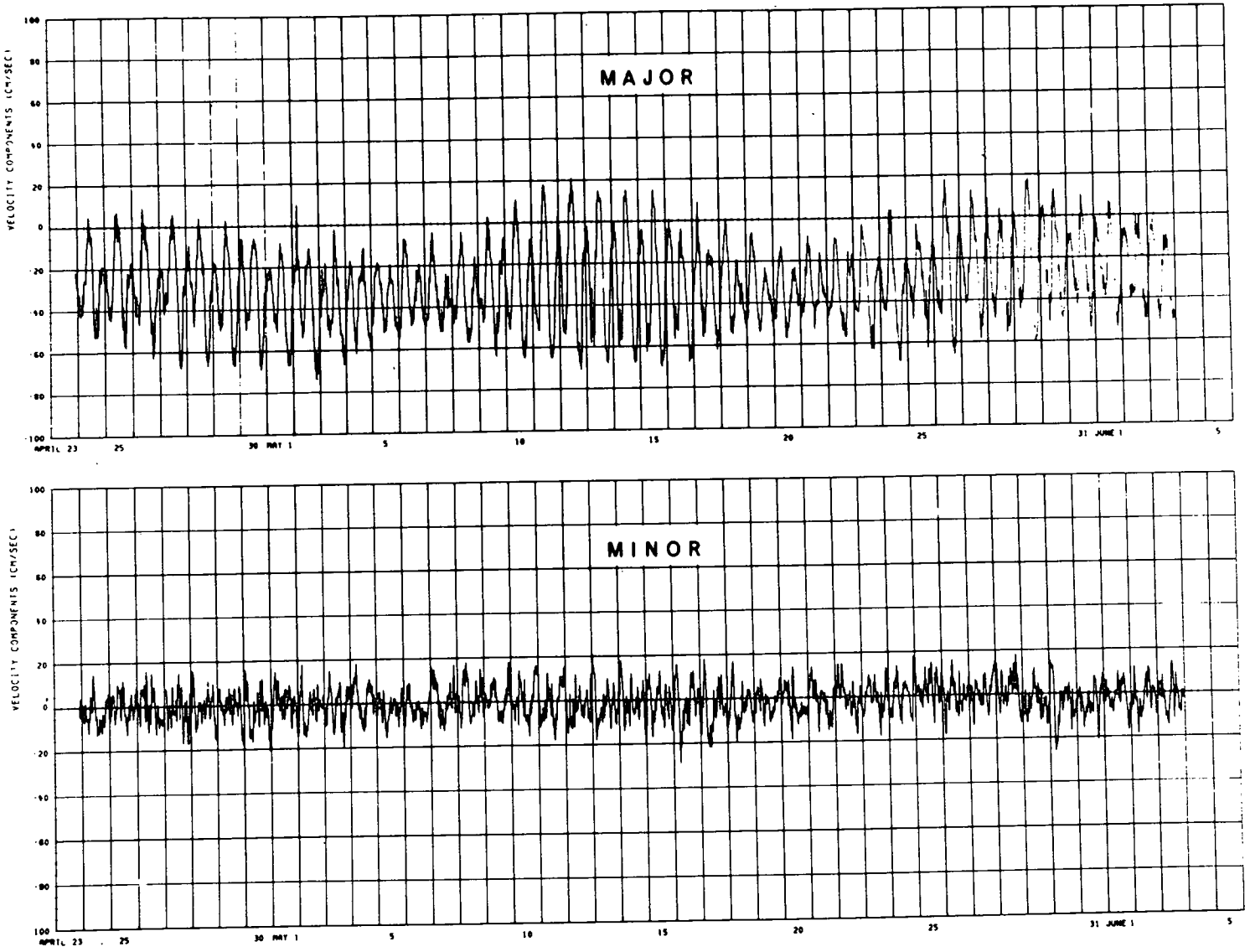

FIGURE 31 *Plots of Current components at 100 metres depth in Station 1 (Meter #182) over the full record period.*

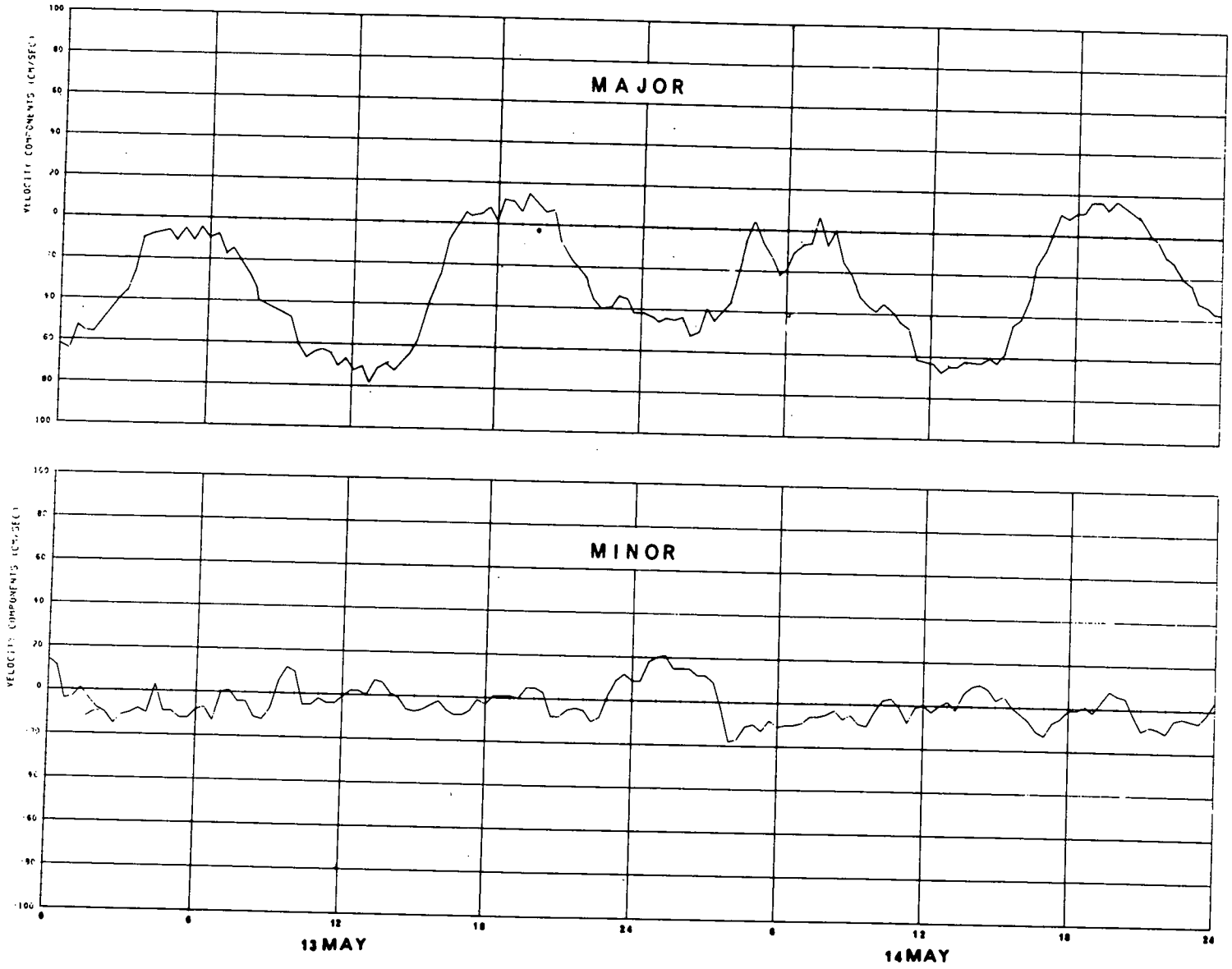

FIGURE 32 *Plots of Current components at 100 metres depth in Station 1 (Meter #182) over a two-day period.*

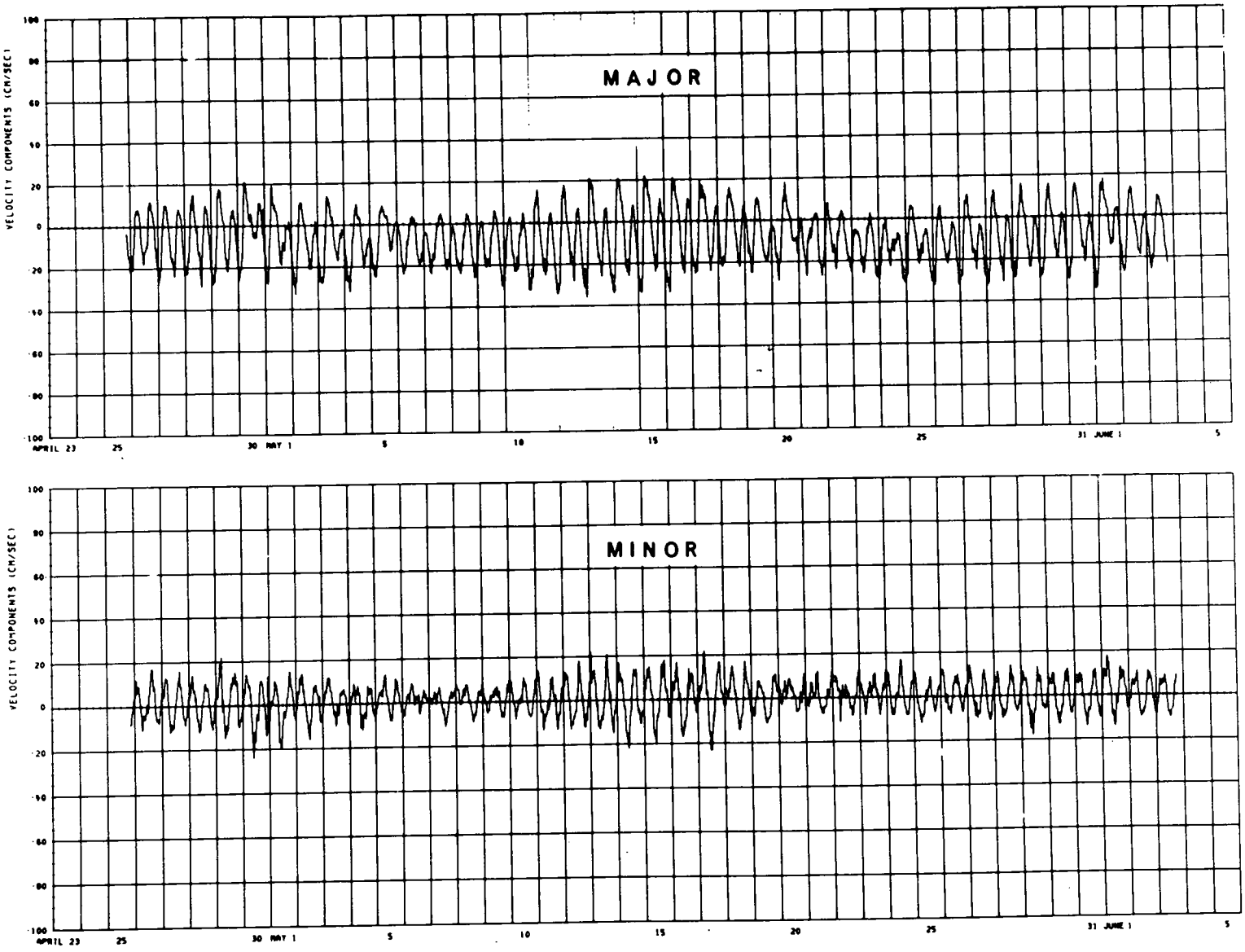

FIGURE 33 *Plots of Current components at 5 metres depth in Station 2 (Meter #237) over the full record period.*

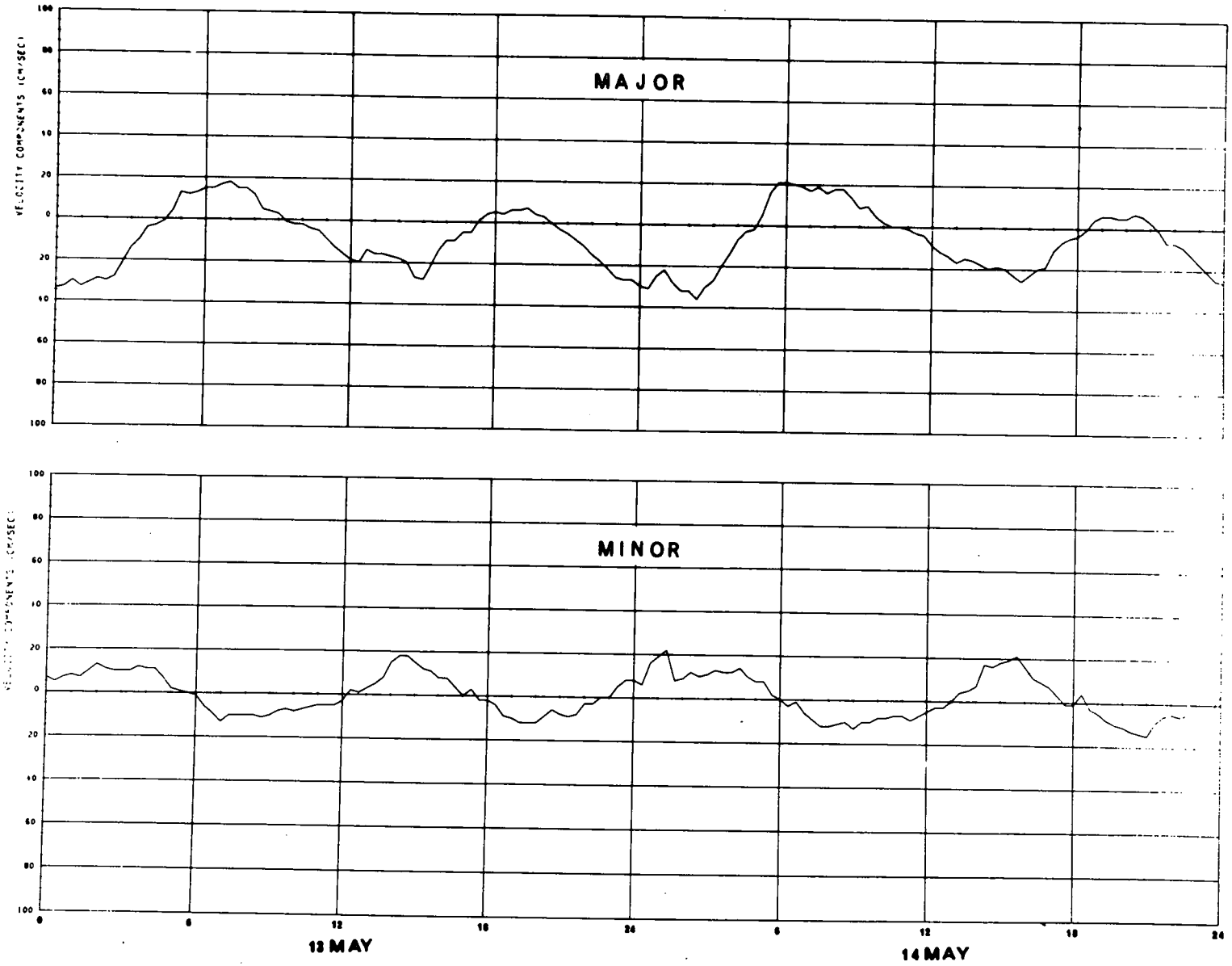

FIGURE 34 *Plots of Current components at 5 metres depth in Station 2 (Meter #237) over a two-day period.*

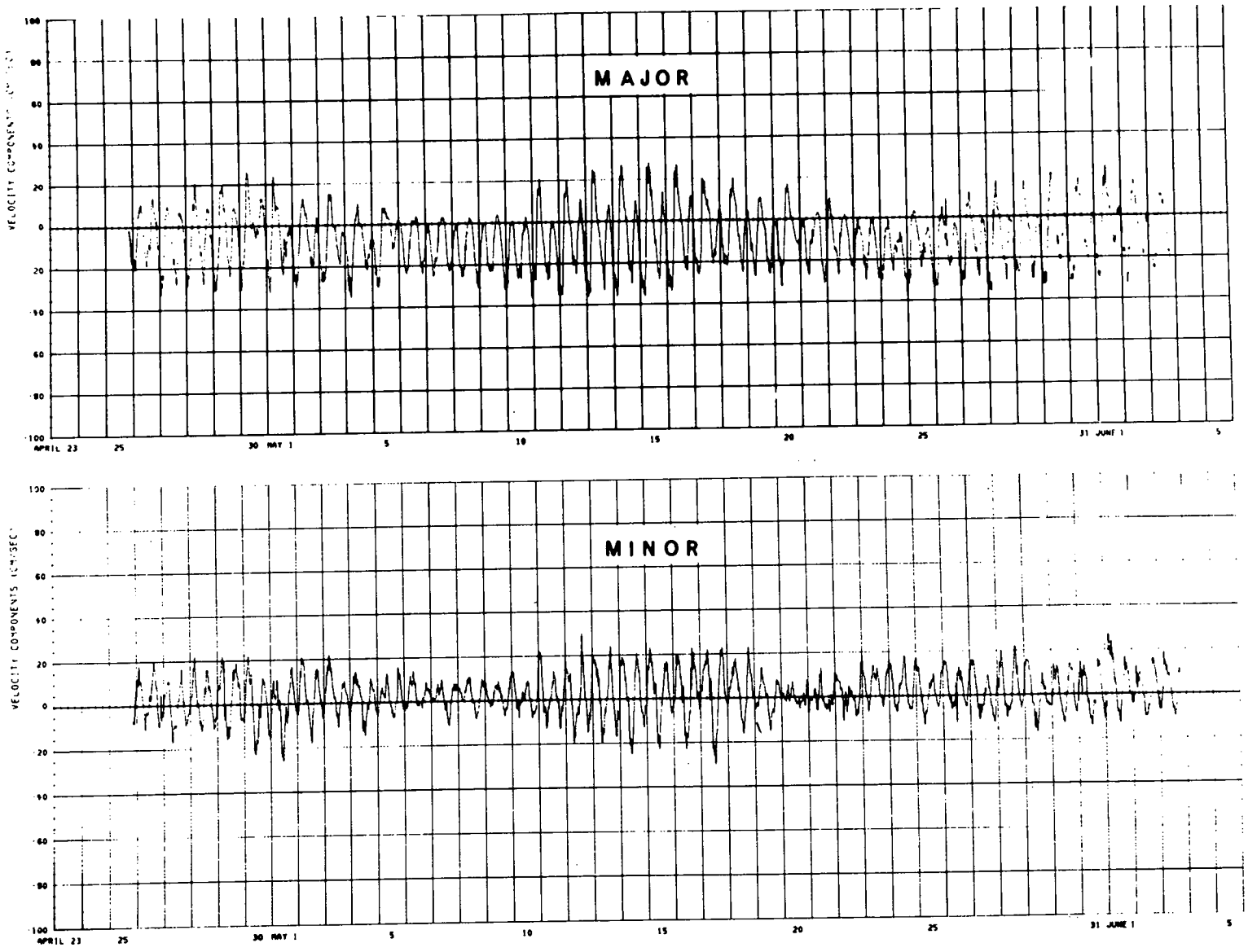

FIGURE 35 *Plots of Current components at 10 metres depth in Station 2 (Meter #233) over the full record period.*

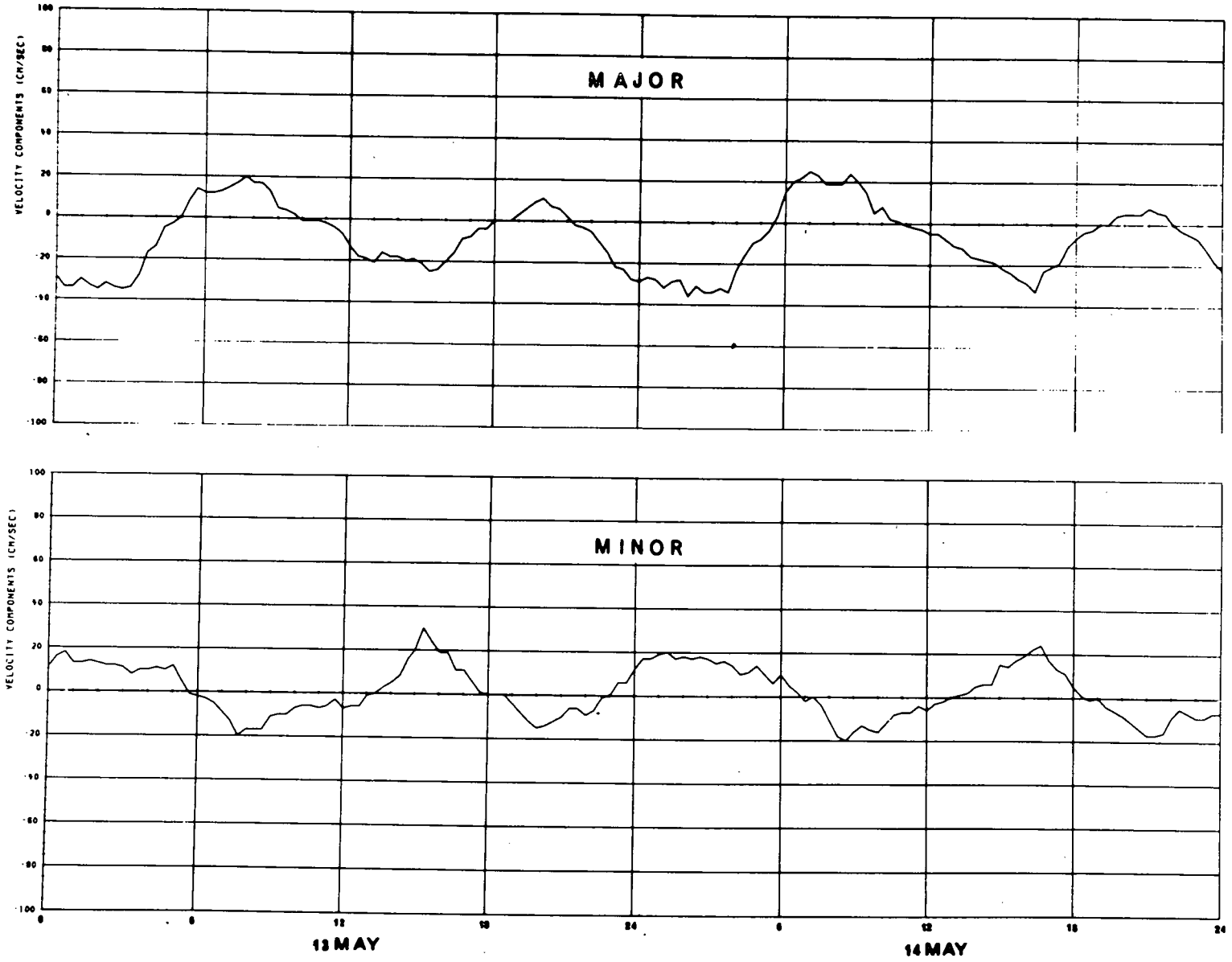

FIGURE 36 *Plots of Current components at 10 metres depth in Station 2 (Meter #233) over a two-day period.*

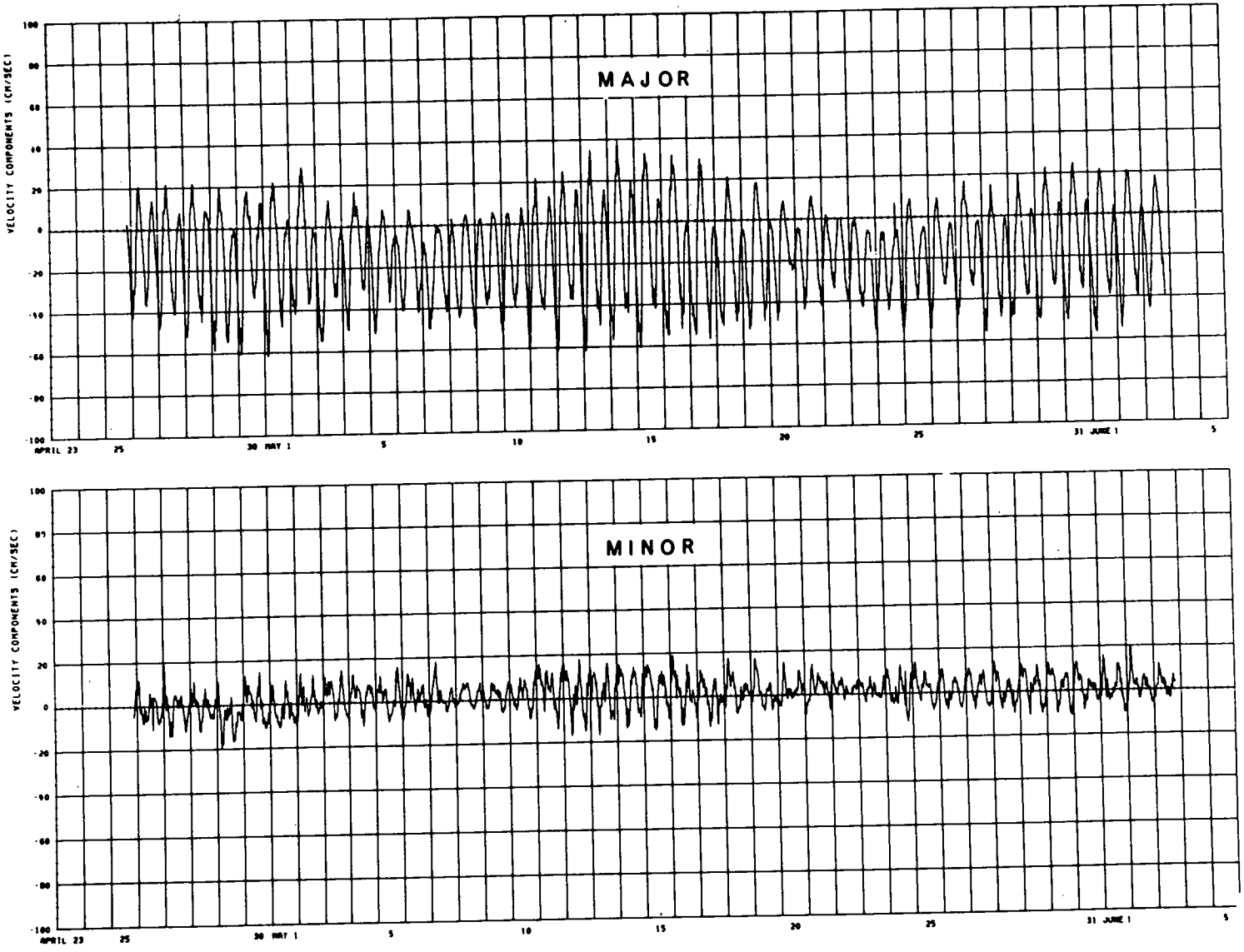

FIGURE 37 *Plots of Current components at 50 metres depth in station 2 (Meter #238) over the full record period.*

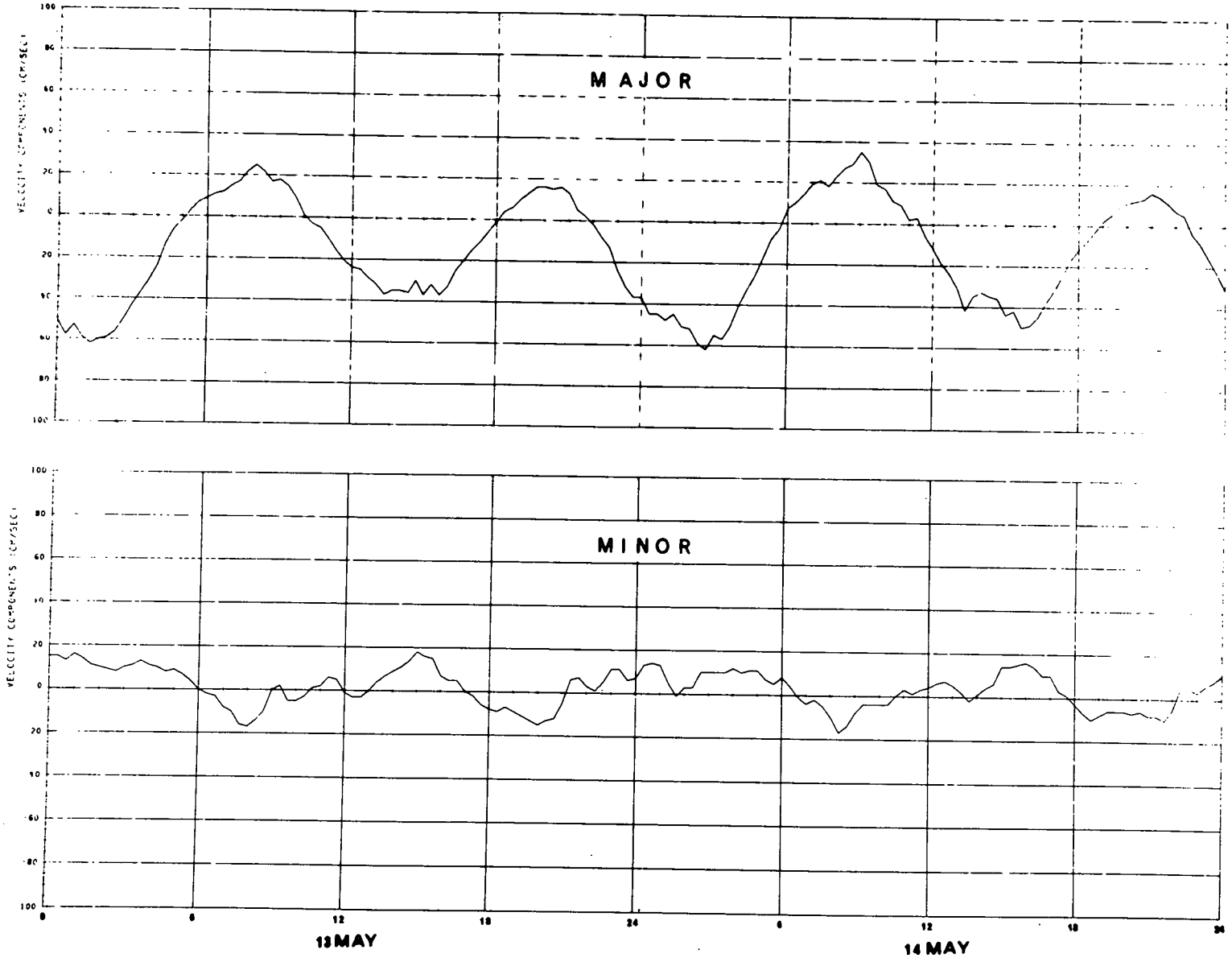

FIGURE 38 *Plots of Current components at 50 metres depth in Station 2 (Meter #238) over a two-day period.*

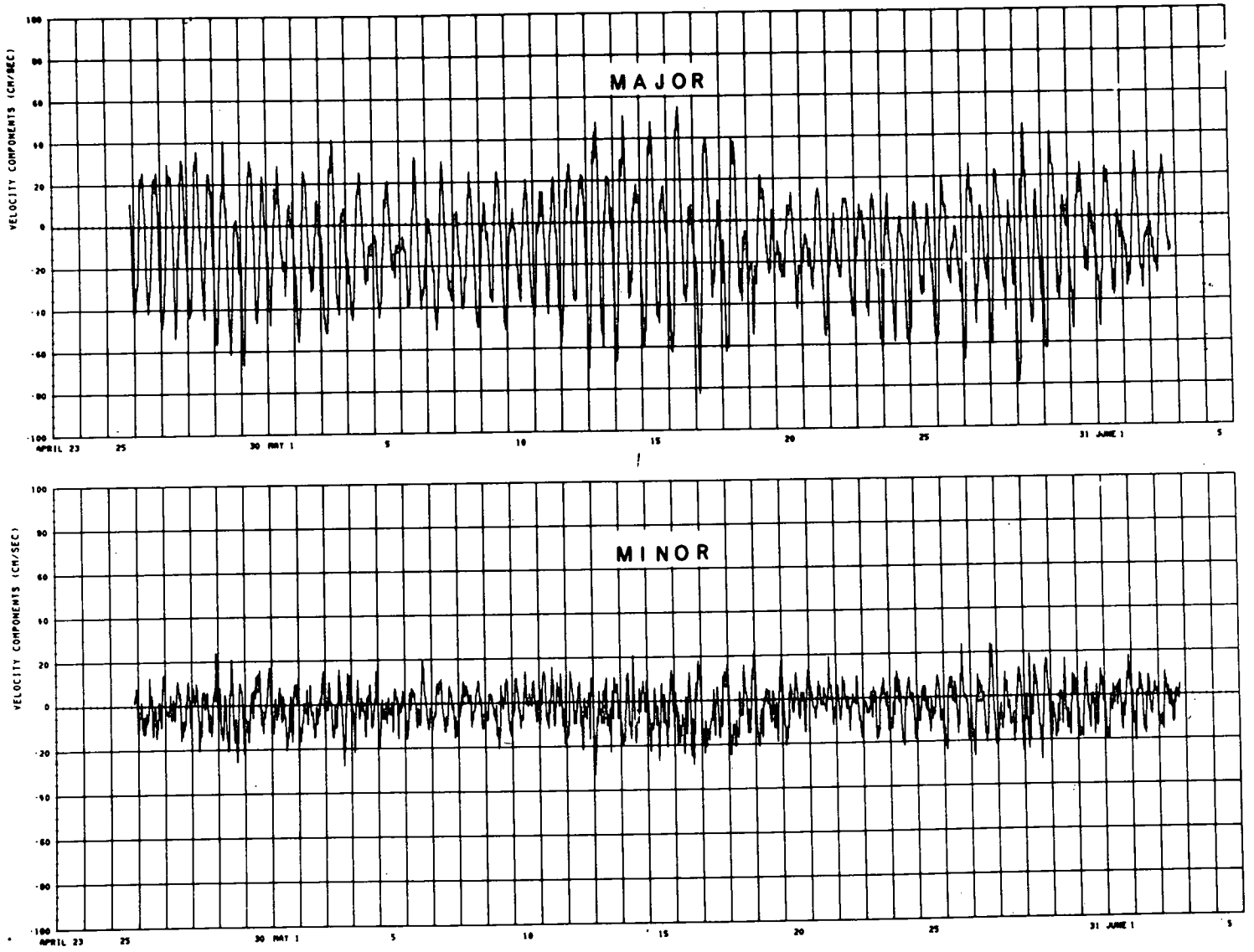

FIGURE 39 *Plots of Current components at 100 metres depth in Station 2 (Meter #235) over the full record period.*

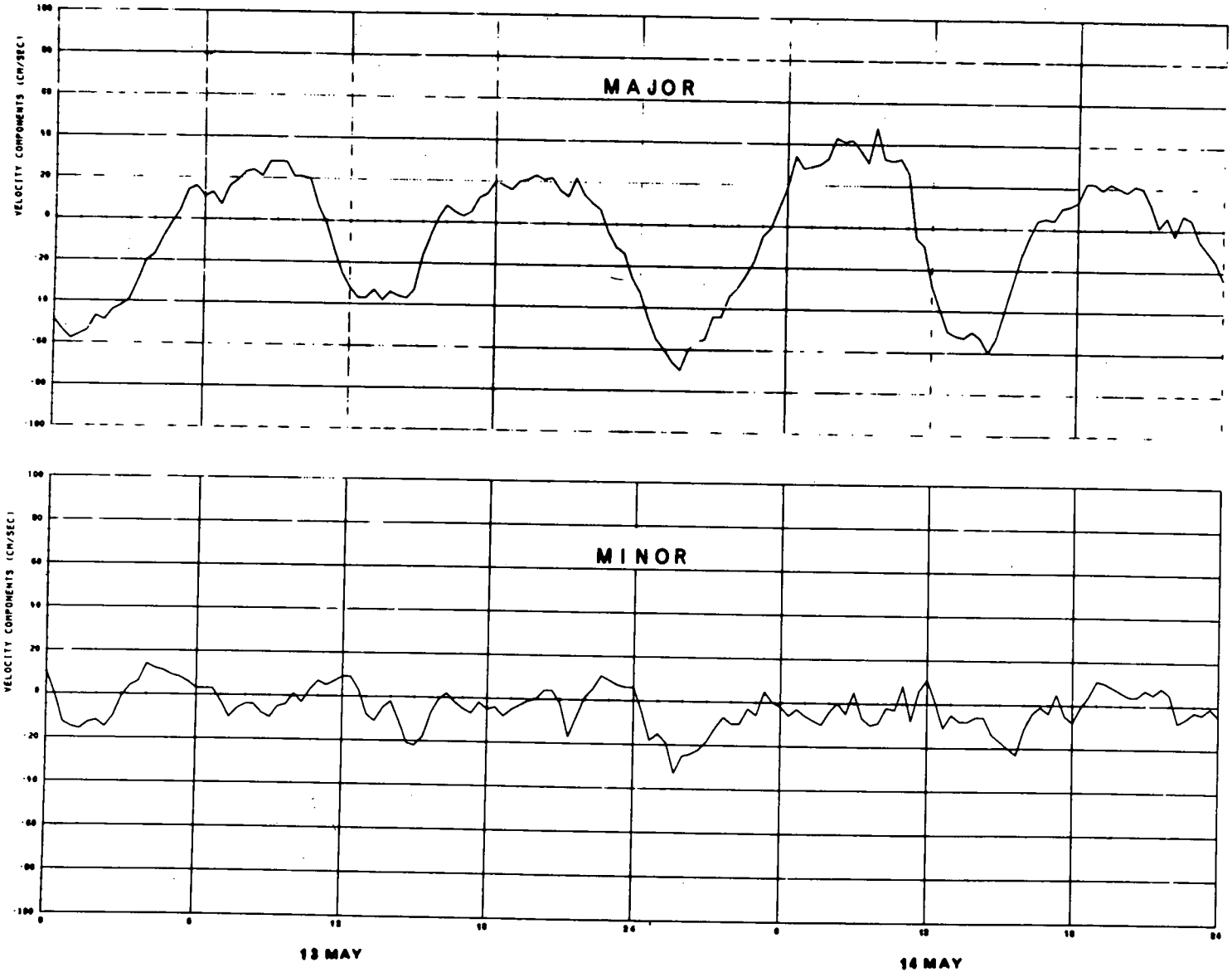

FIGURE 40 *Plots of Current components at 100 metres depth in Station 2 (Meter #235) over a two-day period.*

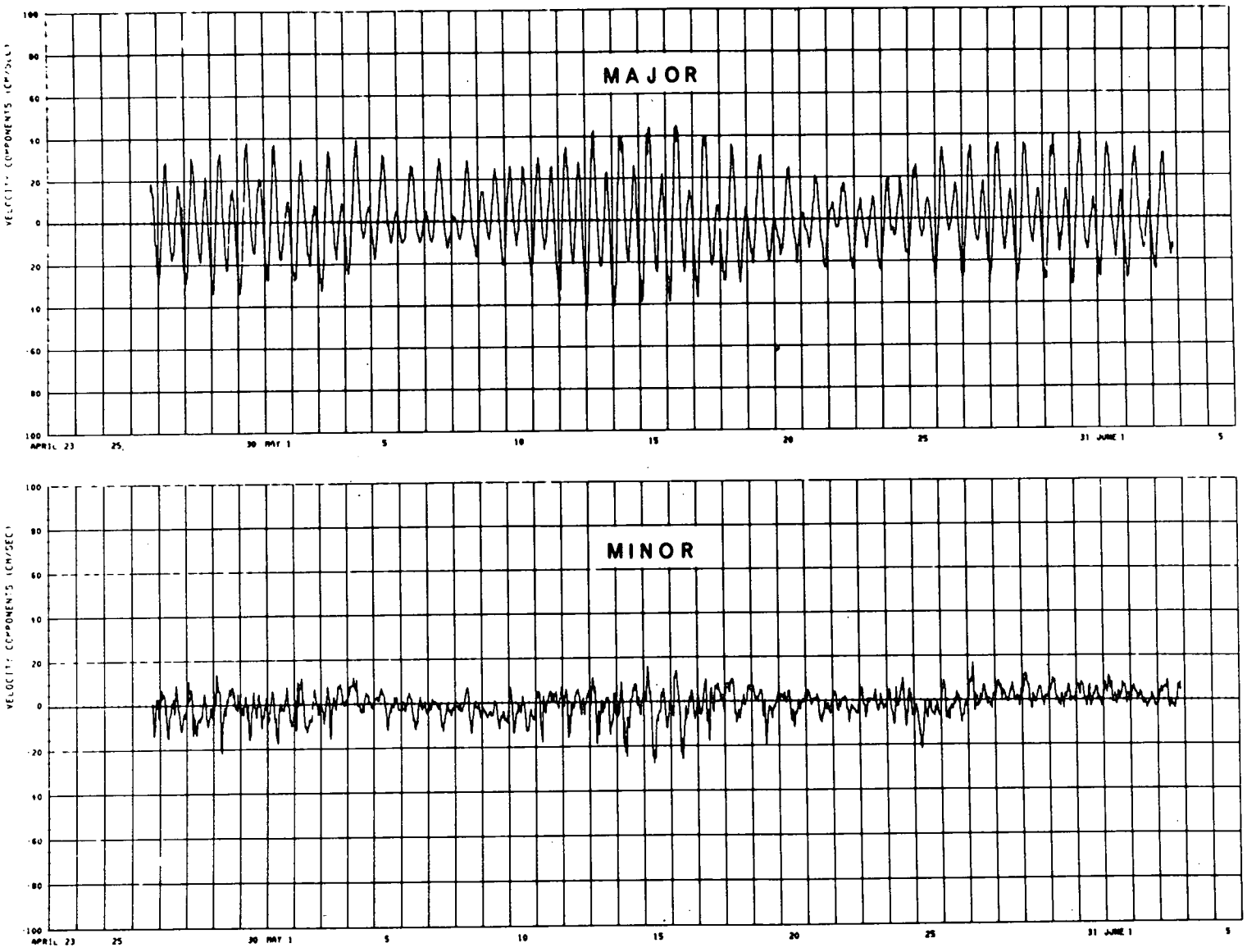

FIGURE 41 *Plots of Current components at 500 metres depth in Station 2 (Meter #232) over the full record period.*

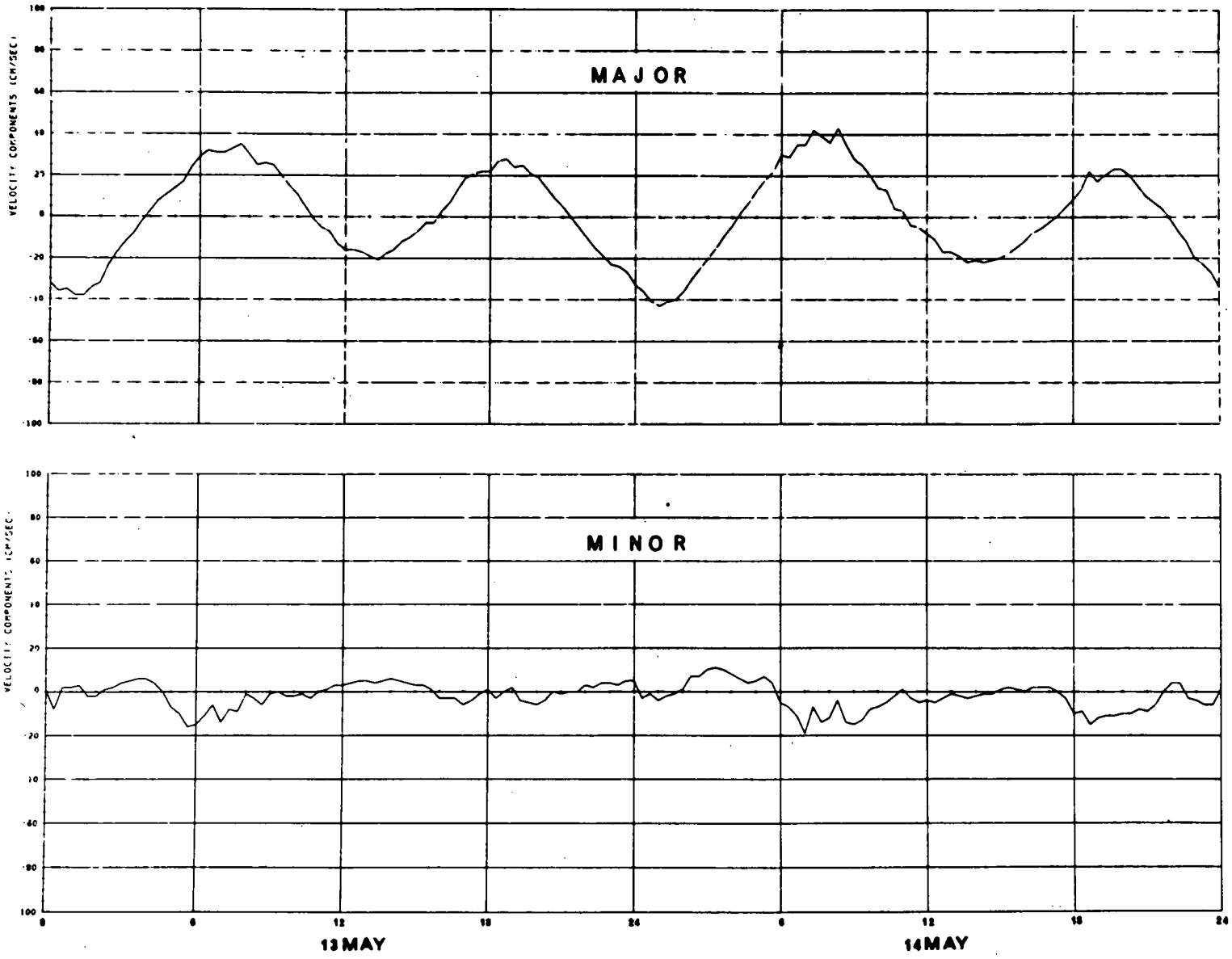

FIGURE 42 *Plots of Current components at 500 metres depth in Station 2 (Meter #232) over a two-day period.*

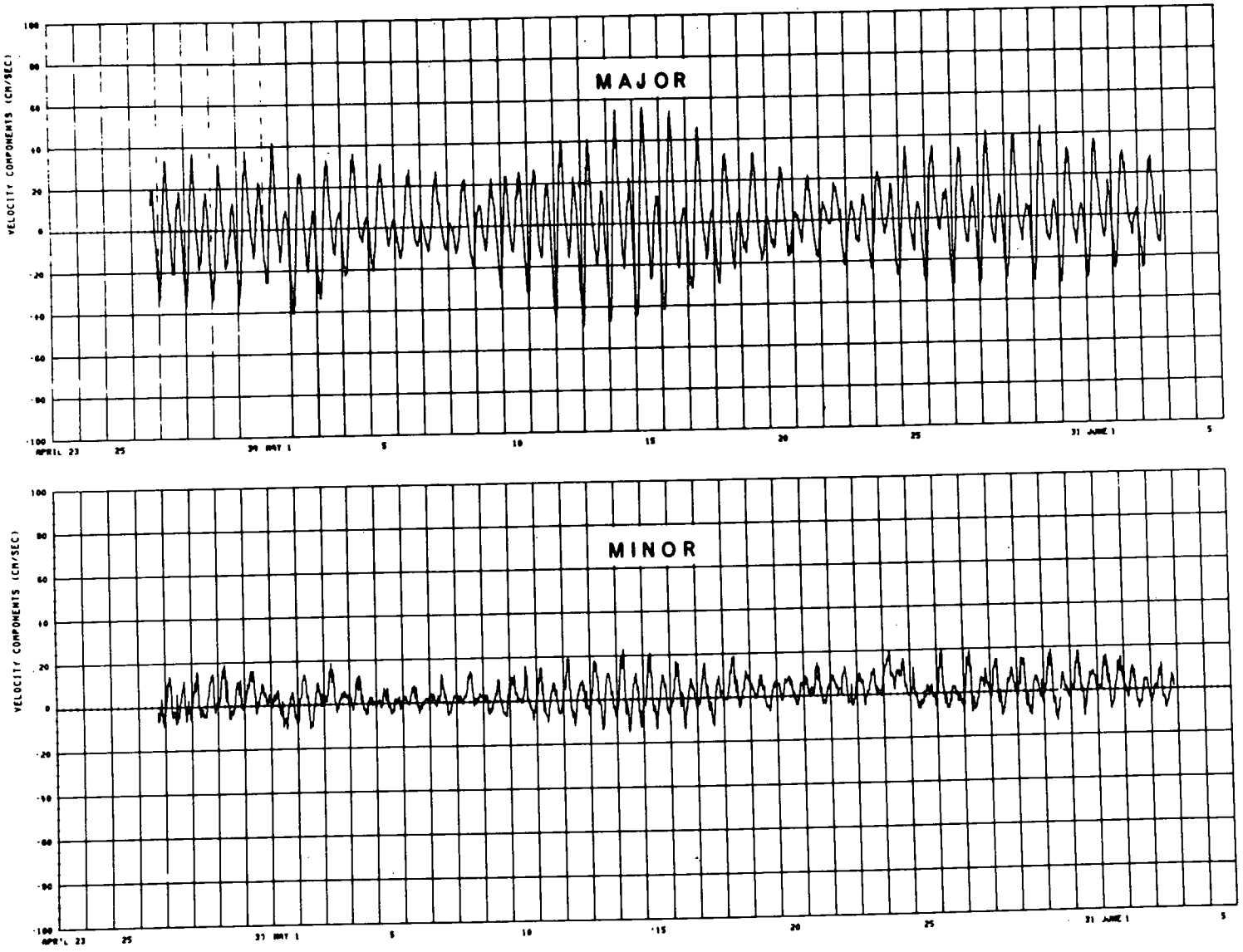

FIGURE 43 *Plots of Current components at 600 metres depth in Station 2 (Meter #236) over the full record period.*

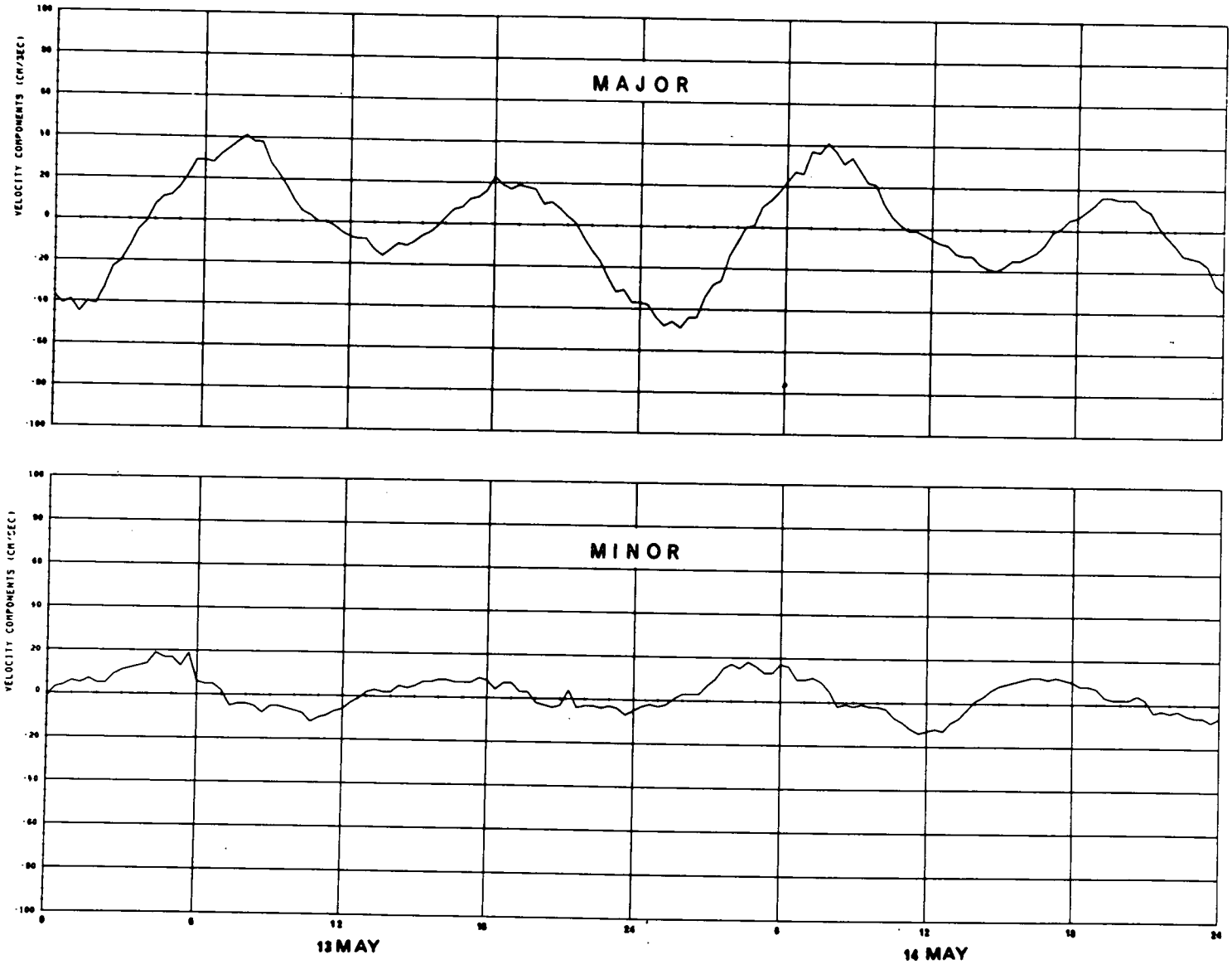

FIGURE 44 *Plots of Current components at 600 metres depth in Station 2 (Meter #236) over a two-day period.*

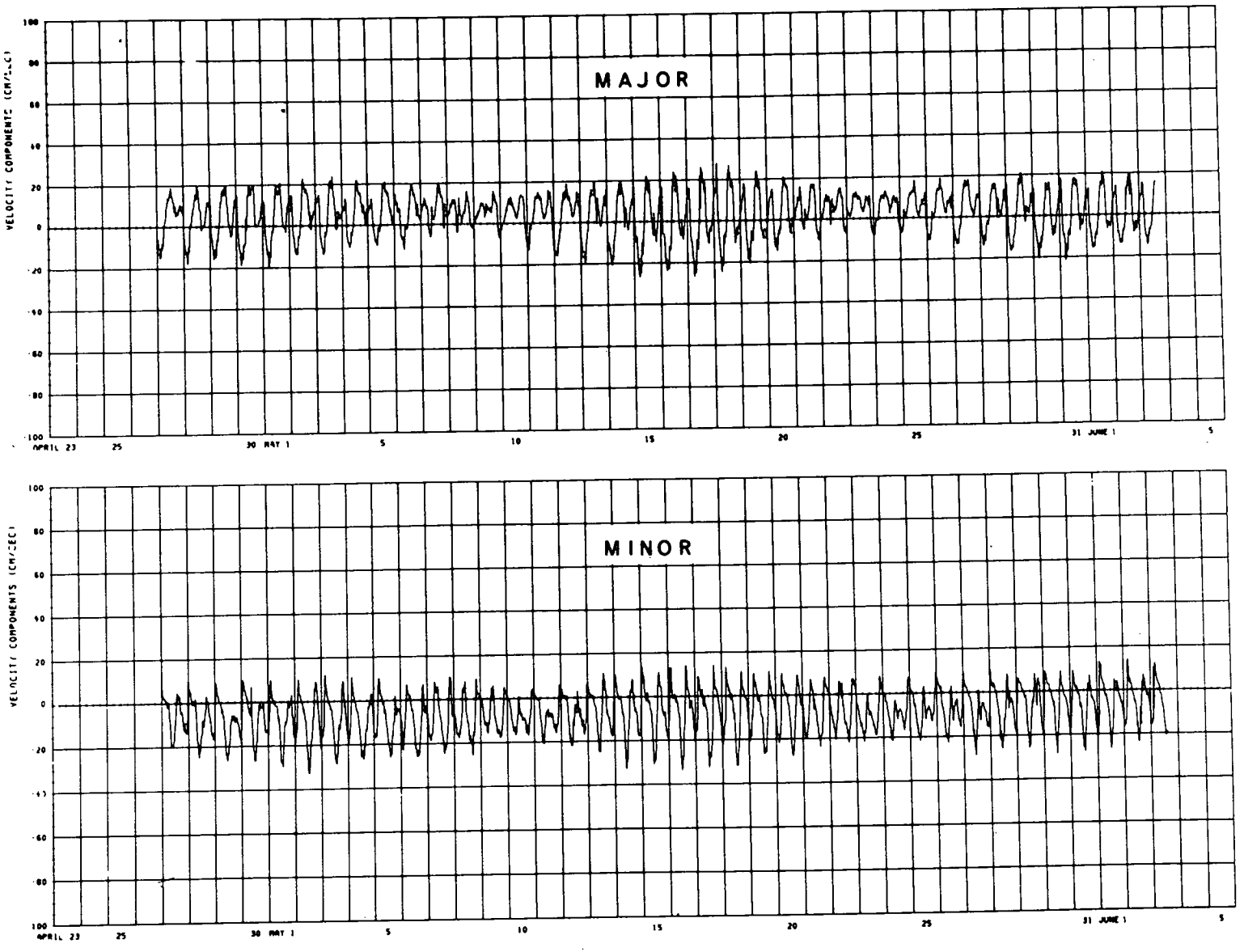

FIGURE 45 *Plots of Current components at 10 metres depth in Station 3 (Meter #193) over the full record period.*

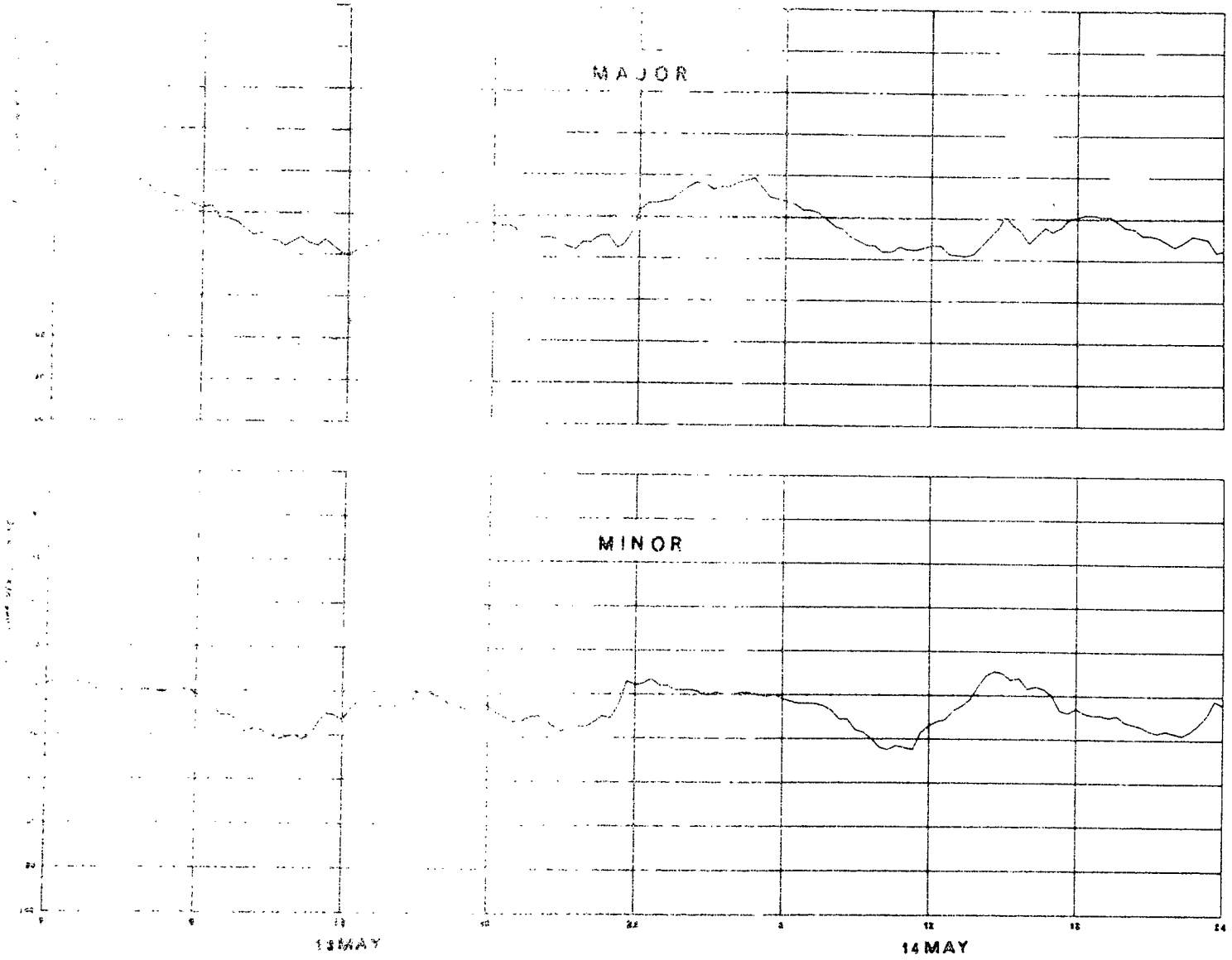

[illegible] meters depth in Station 3 (Meter #193)

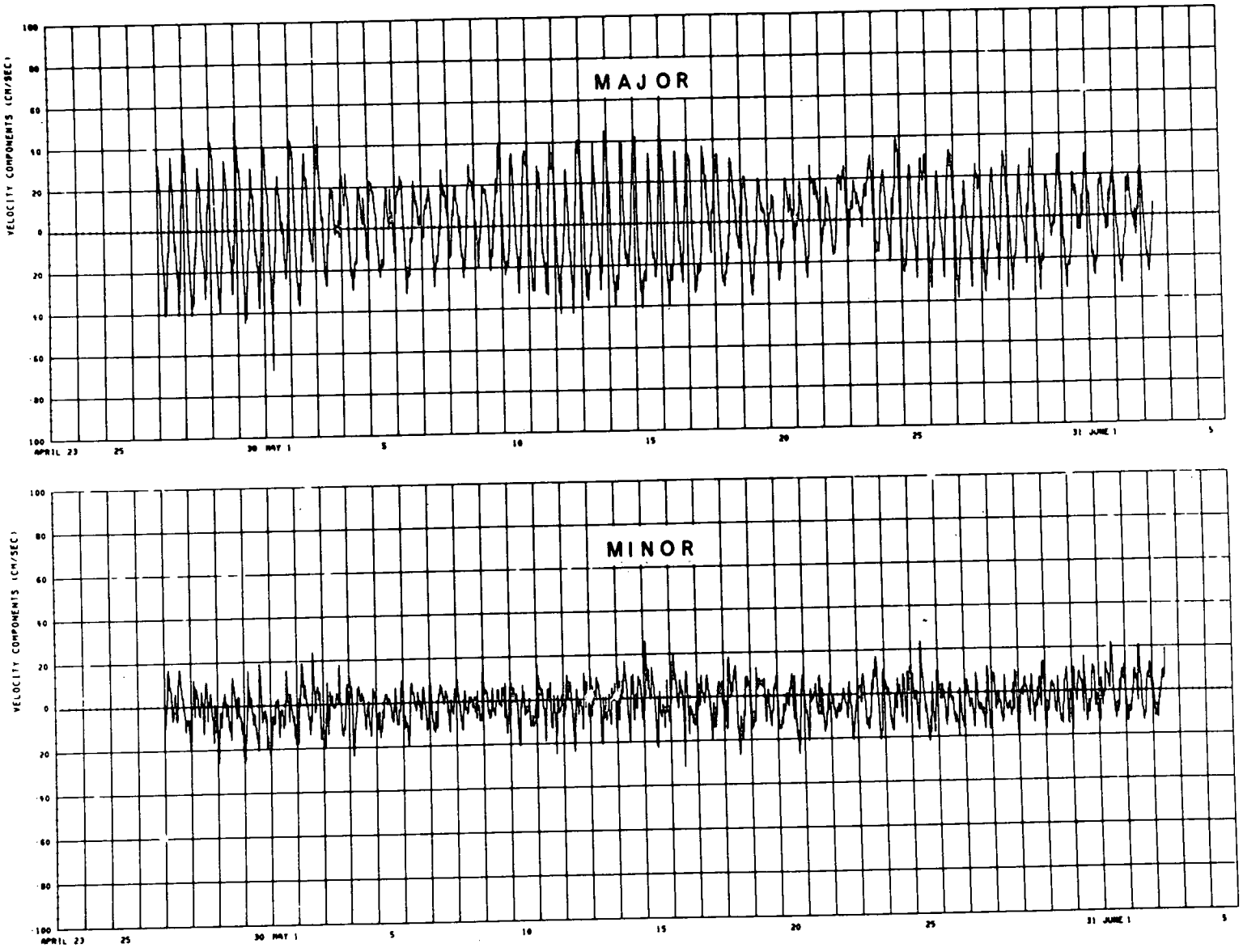

FIGURE 47 *Plots of Current components at 100 metres depth in Station 3 (Meter #201) over the full record period.*

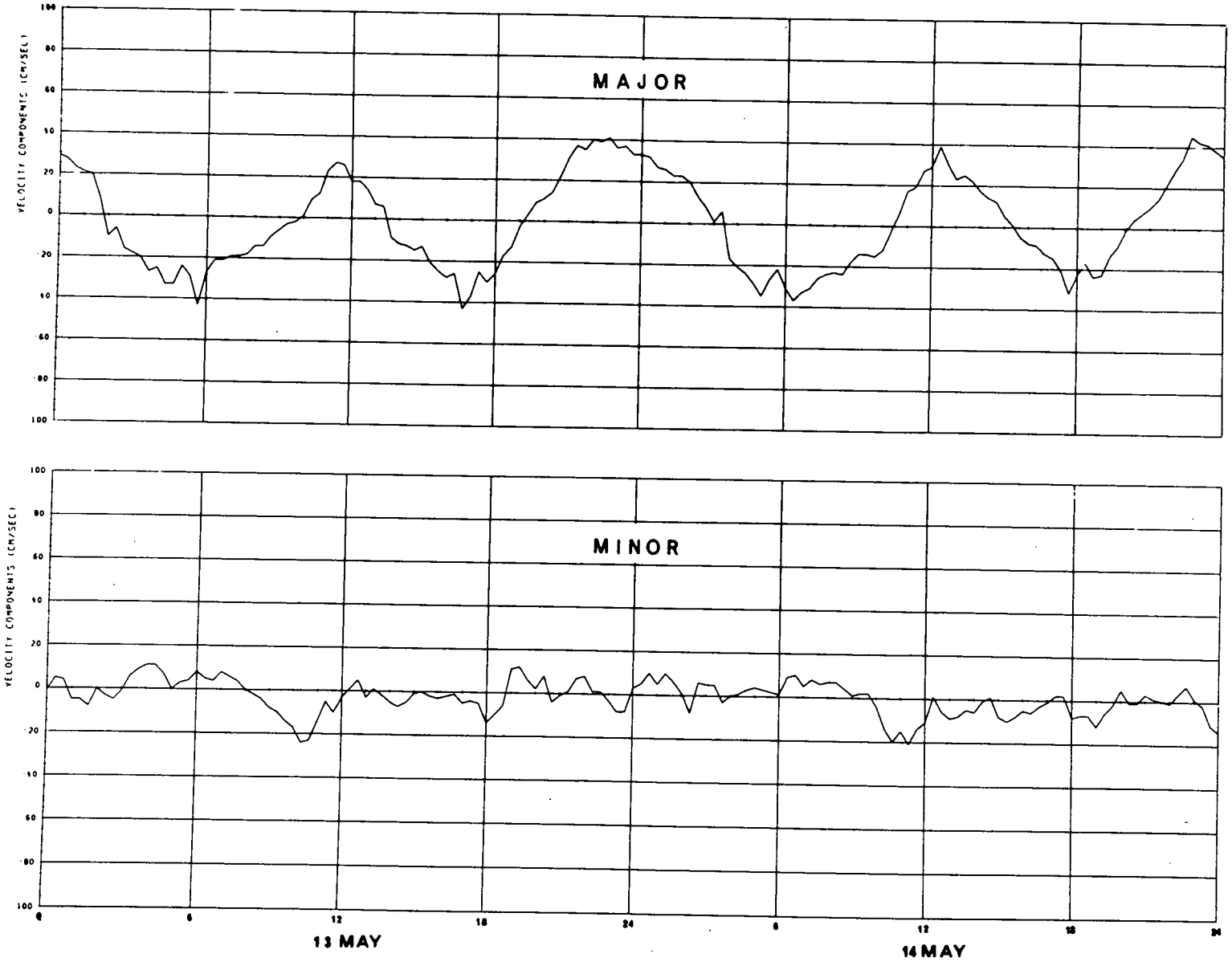

FIGURE 48 *Plots of Current components at 100 metres depth in Station 3 (Meter #201) over a two-day period.*

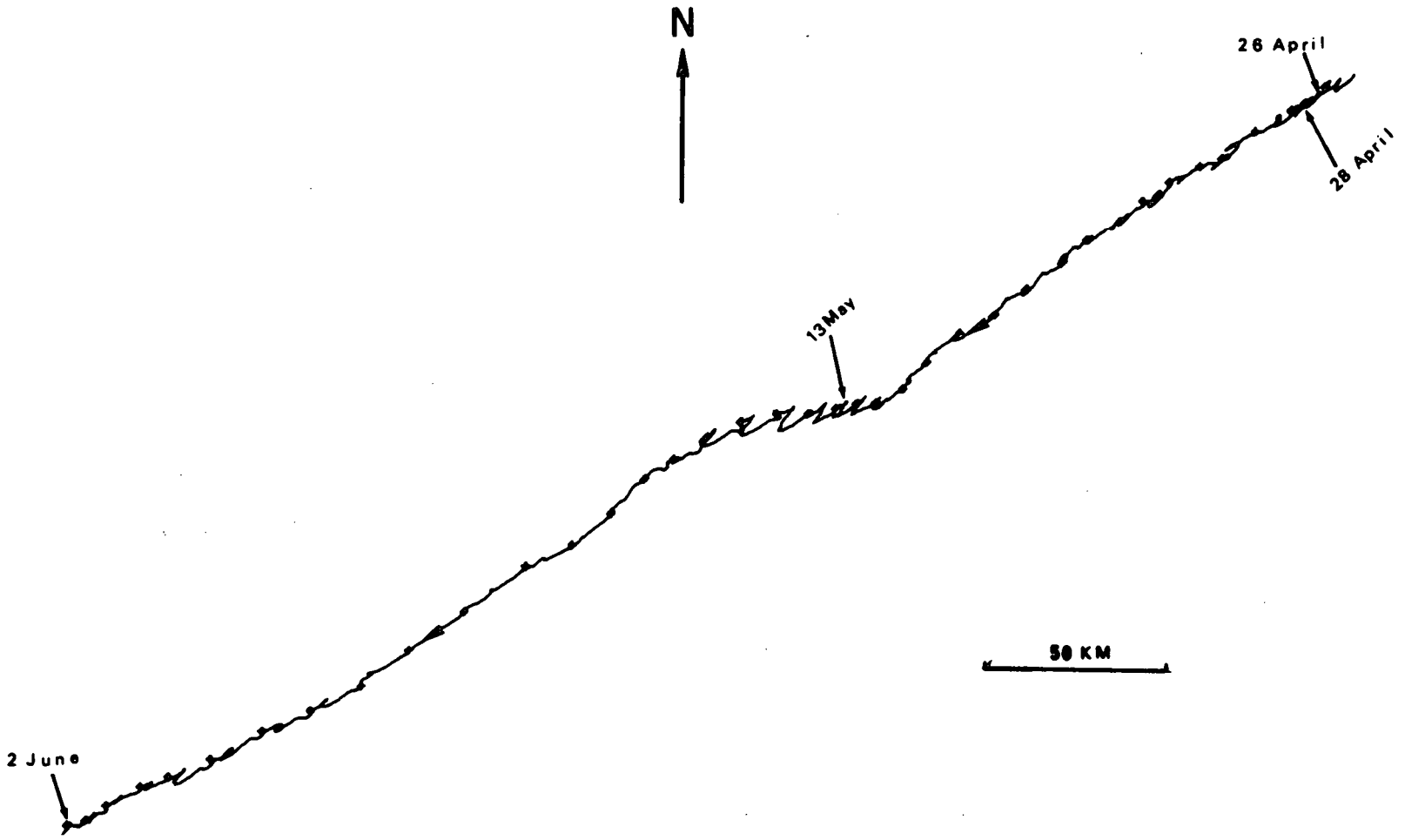

FIGURE 49 *Progressive vector diagram for currents measured by Meter #235 in Station 2 at 100 metres depth over the whole period.*

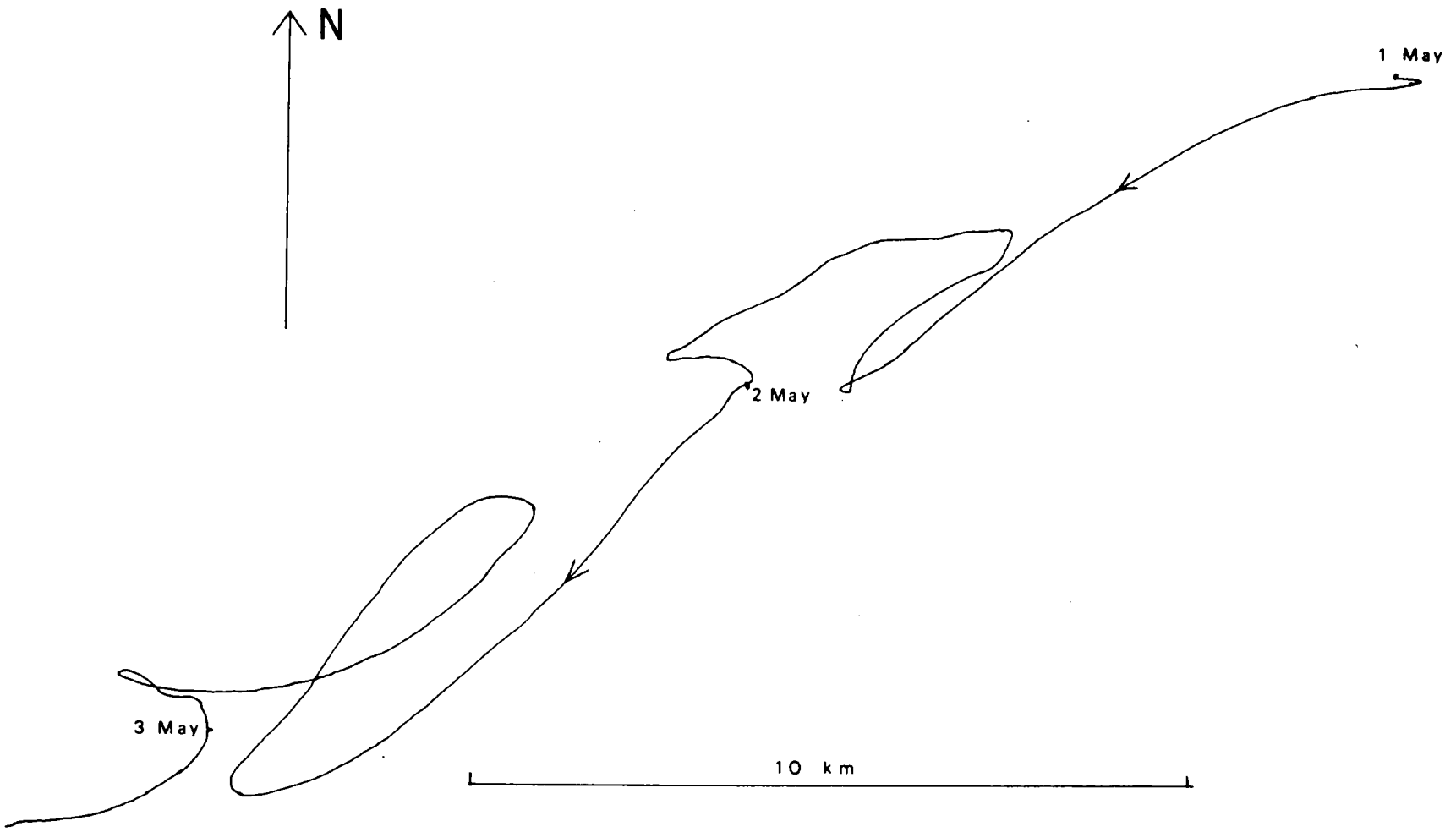

FIGURE 50 *Progressive vector diagram for currents measured by Meter #235 in Station 2 at 100 metres depth on the 1st - 2nd May 1971.*

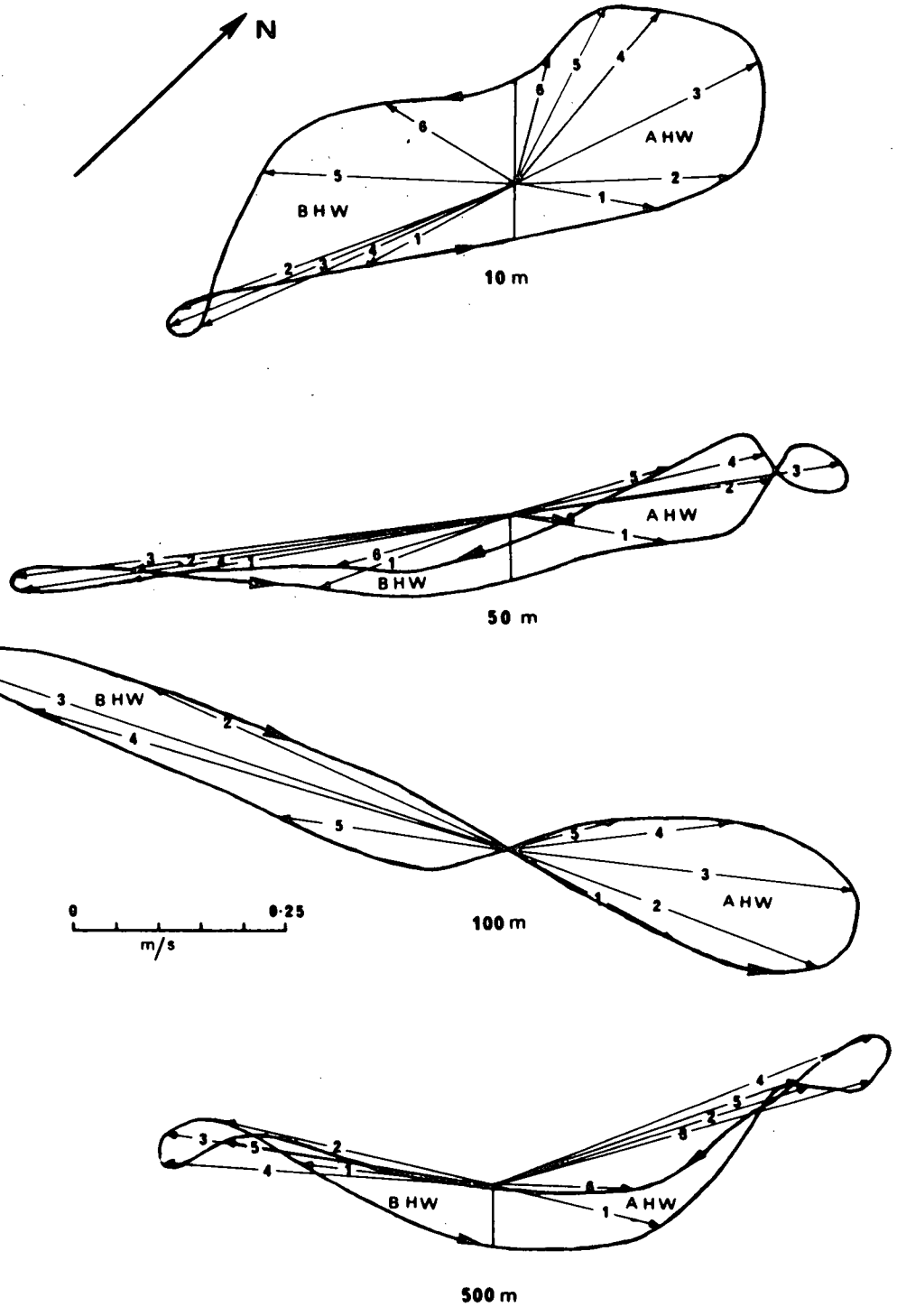

FIGURE 51 Tidal hodographs at 4 depths in Station 2.

TIDAL ANALYSIS

The only water-level information available from Robeson Channel is a single month's record in April 1971 obtained with an Ott recording gauge employing a submerged pressure sensor. This was placed in the S.W. corner in Lincoln Bay through fixed ice. An attempt to obtain more data in May 1972 failed when the tide gauge was destroyed by ice movement. A further investigation employing five water level gauges is planned for April 1975. The tidal constituents derived from the 1971 data by the Tidal Section of the Department of the Environment are given in Table 2.

The tide levels in Lincoln Bay are related to those recorded at Alert with a time lag of 1 hour and 22 minutes, the range at Lincoln Bay being 0.9 times that at Alert. The maximum southerly currents are 2 hours and 30 minutes ahead of high water in Lincoln Bay.

PERIODOGRAMS

The periodograms for axial and cross-channel components were derived separately by the method of Blackman and Tukey (1958). If u(t) is a continuous velocity component then it can be represented by the frequencies given by the Fourier transform

$$U(f) = \int_{-\infty}^{\infty} u(t) \exp(2\pi i f t).dt \qquad 4.1$$

where U(f) is the Fourier component of u(t) at the frequency f. Setting u(t) = 0 outside the period (0, T) of the finite length record we have

$$U(f) \simeq \int_{0}^{T} u(t) \exp(2\pi i f t).dt \qquad 4.2$$

TABLE 2

TIDAL ANALYSIS FROM RECORDS OBTAINED IN LINCOLN BAY 1971

STATION 3782 LINCOLN BAY NWT			ZONE +7	LAT 82 7 NORTH	LONG 62 4 WEST	ANALYSIS 1 x 29 DAYS
NAME	AMPL.	PHASE	C.T.	NAME	AMPL.	PHASE	C.T.
ZO	5.488	0.0	571				
MM	.072	234.5	571	MSF	.024	265.0	571
SIG1	.002	59.9	571	Q1	.007	286.4	571
01	.034	296.6	571	P1	.039	307.2	571
K1	.112	303.0	571				
OQ2	.003	87.5	571	N2	.111	64.2	571
M2	.609	92.2	571	L2	.028	39.7	571
S2	.295	137.5	571	K2	.085	134.5	571
MSN2	.019	80.4	571	2SM2	.009	256.2	571
MO3	.014	94.8	571	M3	.012	263.3	571
MK3	.020	81.0	571	SK3	.006	296.3	571
MN4	.003	296.8	571	M4	.005	334.9	571
MS4	.008	261.5	571	SK4	.003	322.0	571
2MN6	.003	337.7	571	M6	.007	61.5	571
2MS6	.004	84.1	571	2SM6	.004	113.2	571
M8	.003	68.1	571				

AGE	M2/S2	AGE	K1/01	DL-S1	DL	SD	DL/SL	DL±SD
45	2.06	6	3.29	255	.10	.65	.15	.75

MEAN TIDE, TIMES AND HEIGHTS

1620	6.2	325	6.1	2220	4.9	938	4.7
HHW		LHW		HLW		LLW	

LARGE TIDES		RANGES		ZO
6.6	4.2	1.5	2.4	5.5
HHW	LLW	MT	LT	

U(f) here is phase sensitive and noise sensitive (i.e. U(f) will be different if the limits of integration are changed to (-T/2, + T/2) for example. The 'power' density p(f) defined by

$$p(f) = \frac{1}{T} \left| U(f) \right|^2 \qquad 4.3$$

is relatively independent of T.

Replacing the continuous function u(t) by the discrete sampling values $u(t_k)$ where $t_k = k\Delta t$ and $k = 0,1....(N-1)$ where $(N-1)\Delta t = T$, we substitute the integral in 4.2 by the summation

$$U(f) = \sum_{k=o}^{N-1} u(t_k)\exp(2\pi i f t_k)\Delta t \qquad 4.4$$

A Fast Fourier Transform may be used to carry out this summation but introduces certain restrictions on u(t) and U(f). First N must equal 2^j where j is integral and this means that the length of the record which can be used for the frequency analysis is usually shorter than the full record. For a sampling interval of 20 minutes with j = 11 the maximum length of the available record which can be used is only 2048 intervals or just over 28 days. Second the power density p(f) is folded at f = o and at the Niquist frequency $F = \frac{1}{2\Delta t}$

$$\text{i.e. } p(f + 2k\,F) = p(f) \quad 0 < f < f_{max}$$

For 2048 intervals F ≃ 1.4 cycles per hour.
Third, the resolution of p(f) as calculated by a FFT is limited to

$$\Delta f = \frac{1}{2T} = \frac{1}{2^{j+1}\Delta t} = 7 \times 10^{-4} \text{ cycle per hour or } 0.36 \text{ on}$$

the horizontal scale of the power spectra below.

The function p(f) was then normalized, using a normalization constant C defined by

$$C \int_o^\infty p(f).df = 1 \qquad 4.5$$

$$P(f) = \frac{p(f)}{\int_0^\infty p(f)df} = Cp(f) \qquad 4.6$$

The horizontal scale of these diagrams is in frequency steps of 1.953×10^{-3} cycles per hour and the resolution is 7×10^{-4} cycles per hour or 0.36 scale units. The cut-off for the diagram is at 0.5 cycles per hour which is one third of the Niquist frequency since there is almost no energy beyond this frequency.

COMPARISON OF PERIODOGRAMS

Since the long term constituents have not been removed from the spectra shown in Figures 52 to 61 positive identification of many of the peaks cannot be made. The tidal height components from Table 2 have been relisted in Table 3 in period groups and the locations of tidal level constituents have been marked in Figure 57, the velocity spectrum in Station 2 at 100 metres.

TABLE 3

Tidal Components In Robeson Channel

Component	Name	Amplitude	Period in Hours	Scale Reading
Monthly	MM	.072	27.55 days	0.77
Fortnightly	MSF	.024	13.66 days	1.56
Diurnal	K1	.112	23.93	21.40
	P1	.039	24.07	21.27
	O1	.034	25.83	19.83
	Q1	.007	24.83	20.62
	S1G1	.002	24.00	21.33
Semi Diurnal	M2	.609	12.42	41.23
	S2	.295	12.00	42.67
	N2	.111	12.66	40.44
	K2	.085	11.97	42.77
	L2	.028	12.19	42.00
	MSN2	.019	12.20	41.97
	2SM2	.009	12.42	41.23
	OQ2	.003	12.42	41.23
8 Hourly	MK3	.020	7.98	64.16
	MO3	.014	8.61	59.45
	M3	.012	8.28	61.84
	SK3	.006	8.00	64.00
6 Hourly	MS4	.008	6.10	83.94
	M4	.005	6.21	82.45
	MN4	.003	6.10	83.94
	SK4	.003	6.00	85.34
4 Hourly	M6	.007	4.14	123.68
	2MS6	.004	4.07	125.81
	2SM6	.004	4.14	123.68
	2MN6	.003	4.07	125.81
Inertial Period			12.12	42.25

The periodograms were obtained by using 2016 values (28 days) in one group and the 80% confidence limits (χ^2 distribution) for 1 degree of freedom are 0.016 and 2.71. At this level the only constituents which may be firmly identified are the diurnal and semi-diurnal constituents. Several other peaks which appear in the records are worth mentioning.

Low Frequency Constituents. A peak at low frequencies is prominent in all the periodograms except those at 500 m and 600 m in the centre of the channel, where the residual current is small. Any monthly constituent will also be included in this peak.

Fortnightly (MSF) Constituent. This can be seen in all records at or above 100 m depth and appear to be reduced in power from west to east at 100 m. The lower bound of the 80% confidence limits is, however, below noise level.

Diurnal Constituents. The five constituents listed in Table 3 are just at the limit of resolution and no separate lines are visible except for the O1/Q1 and K1/P1 constituents of the cross-channel components in Figures 53 and 61.

Semi-Diurnal Frequencies. These are resolved at all the meters into an M2/N2 peak and an S2/K2/L2 peak. The inertial frequency at this latitude is very close to that of the S2 constituent and is not resolved.

The "8-hour" and "6-hour" Constituents. Peaks are visible in the spectra from all but the deep meters near the MK3, MO3, M3 and SK3 frequencies but only the cross-channel M3 has a lower probability limit (60 cm^2s^{-2}) which is greater than the noise level in Fig. 57. Similarly the peak at M4 has a lower probability limit of 50 cm^2s^{-2} which is just above noise level. Recent unpublished analyses of tide levels in Robeson Channel also indicate M3 and M4 constituents which are just above the uncertainty levels.

Other Frequencies. A peak is visible on most of the record at a period of 4-9 hours which is most prominent in Fig. 57. The lower probability limit is below the noise level but it is interesting to note that this frequency is close to the seiche period for Nares Strait.

SEICHE PERIODS

Merian's formula for the n^{th} modal seiche period for a channel open at both ends is

$$T = \frac{2L}{n\sqrt{gh}} \qquad 4.7$$

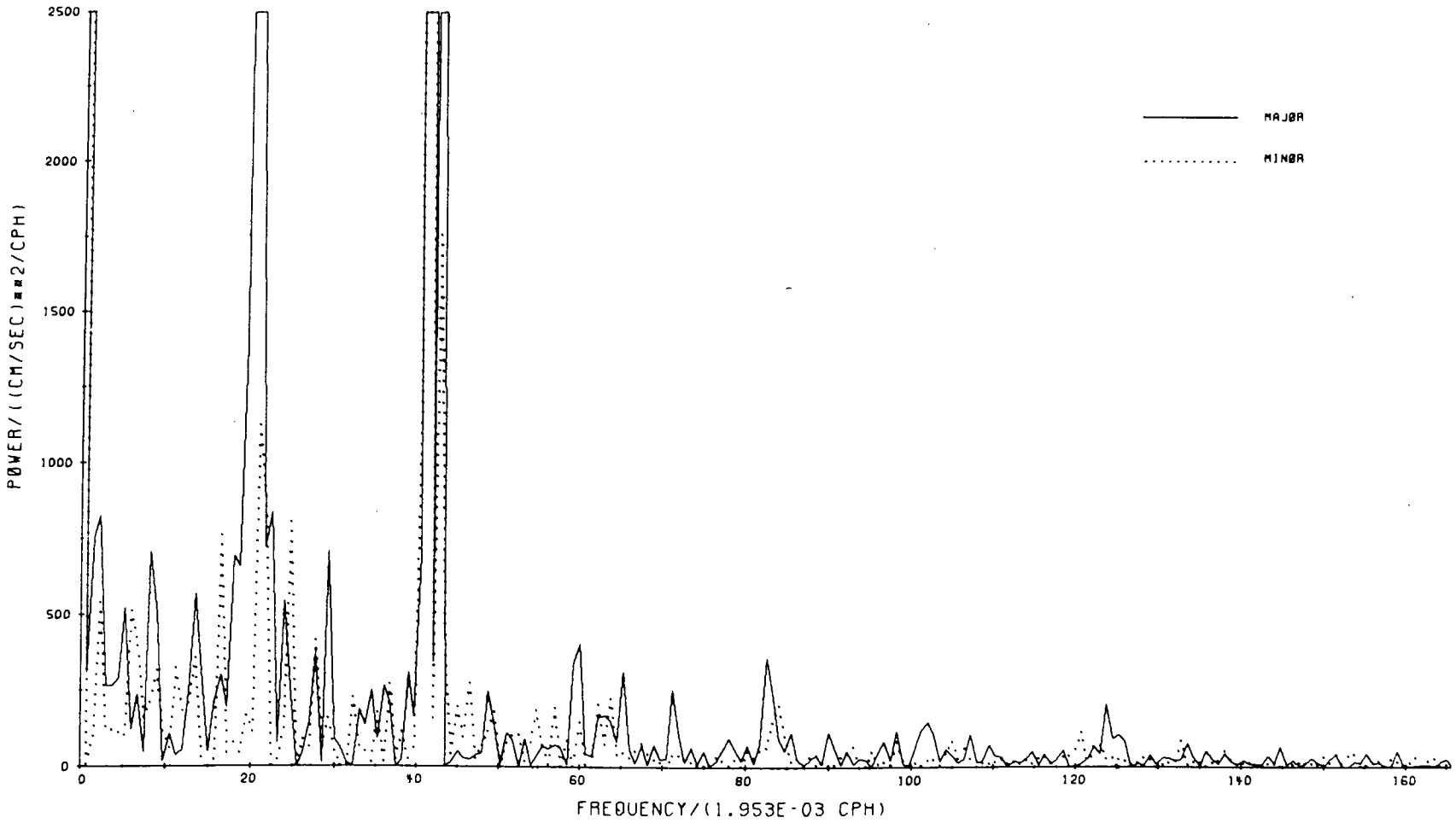

FIGURE 52 *Power spectrum of current velocity components at Meter #234 in Station 1 at 5 metres depth.*

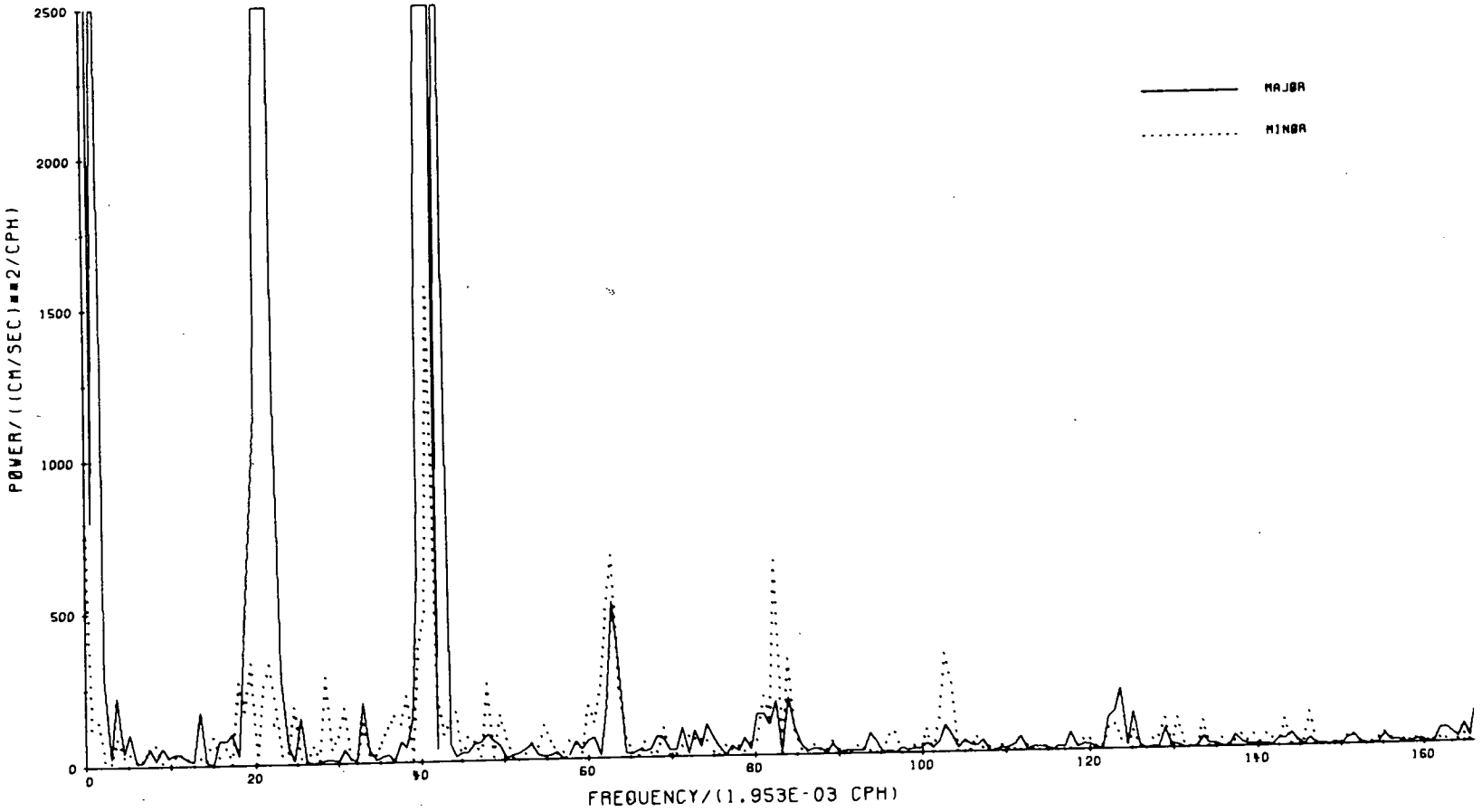

FIGURE 53 *Power spectrum of current velocity components at Meter #182 in Station 1 at 100 metres depth.*

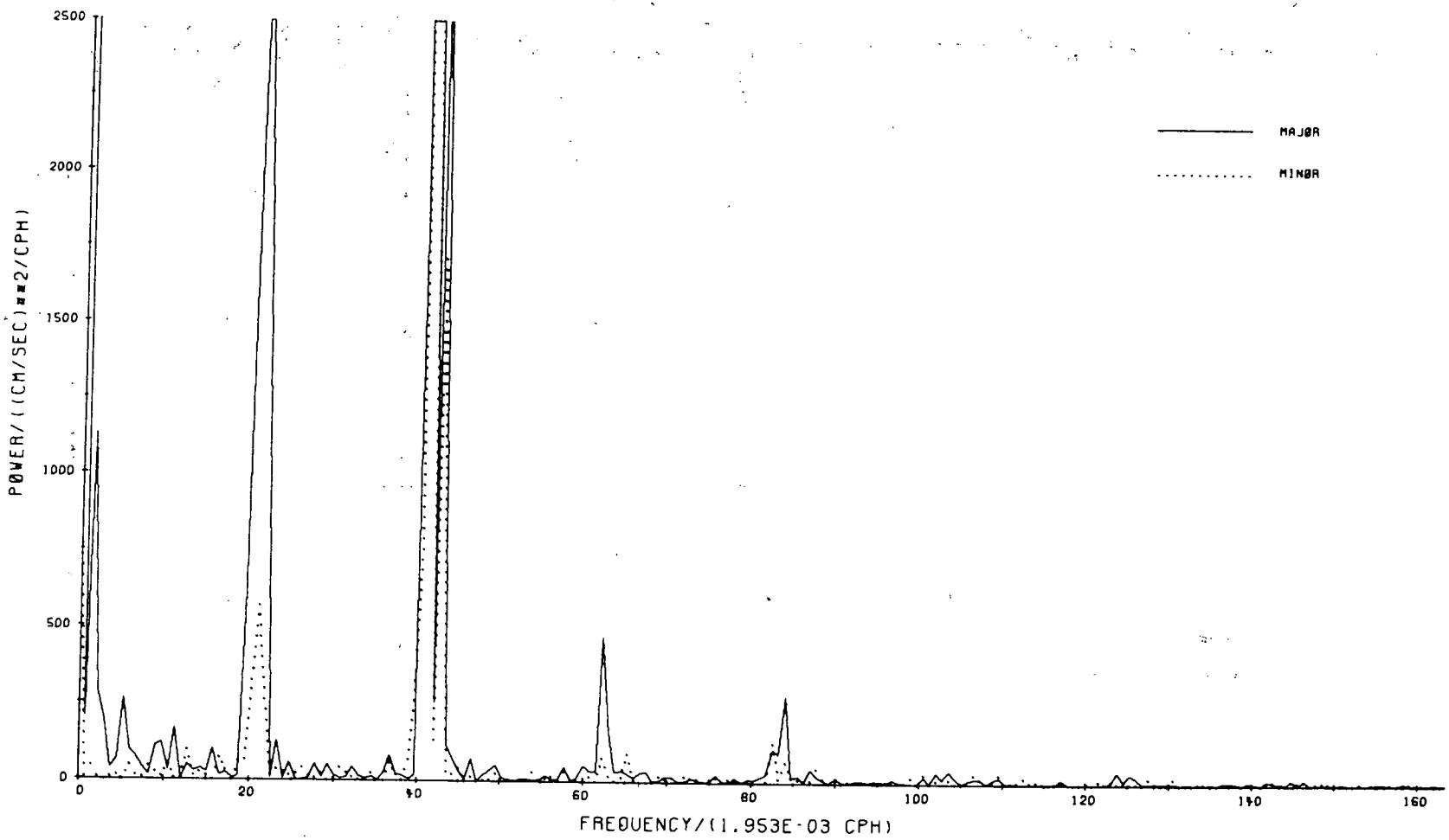

FIGURE 54 *Power spectrum of current velocity components at Meter #237 in Station 2 at 5 metres depth.*

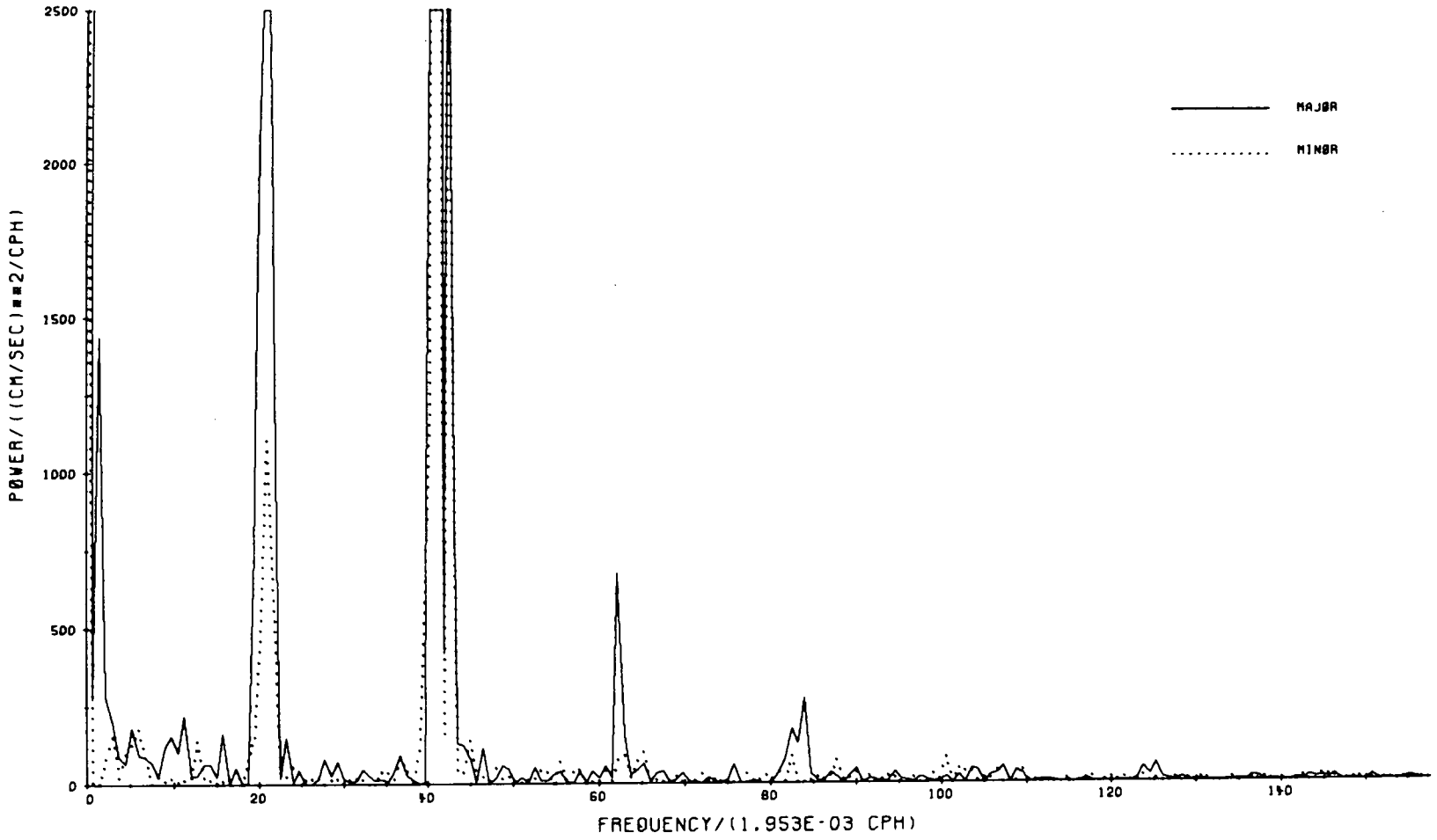

FIGURE 55 *Power spectrum of current velocity components at Meter #233 in Station 2 at 10 metres depth.*

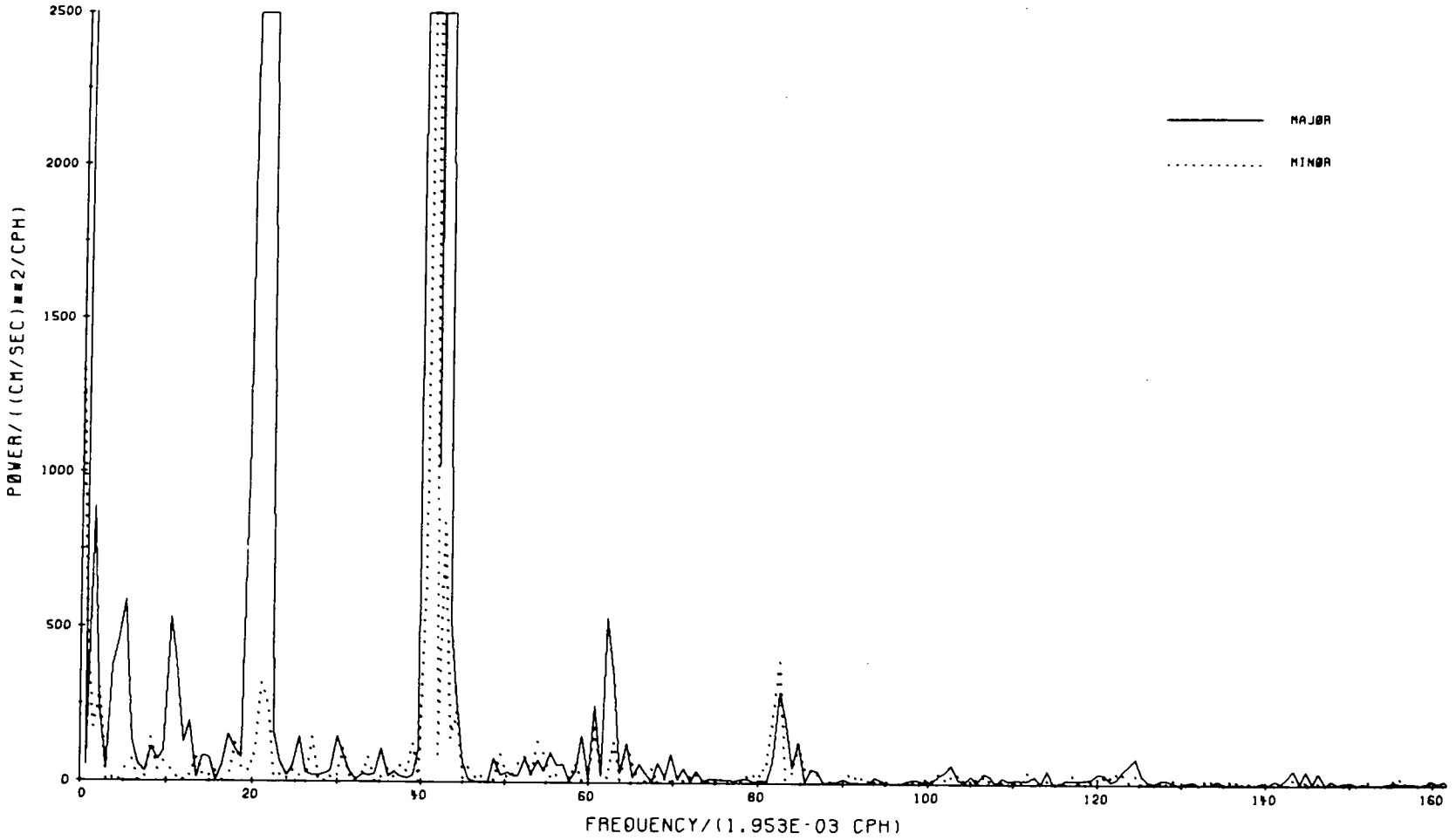

FIGURE 56 *Power spectrum of current velocity components at Meter #238 in Station 2 at 50 metres depth.*

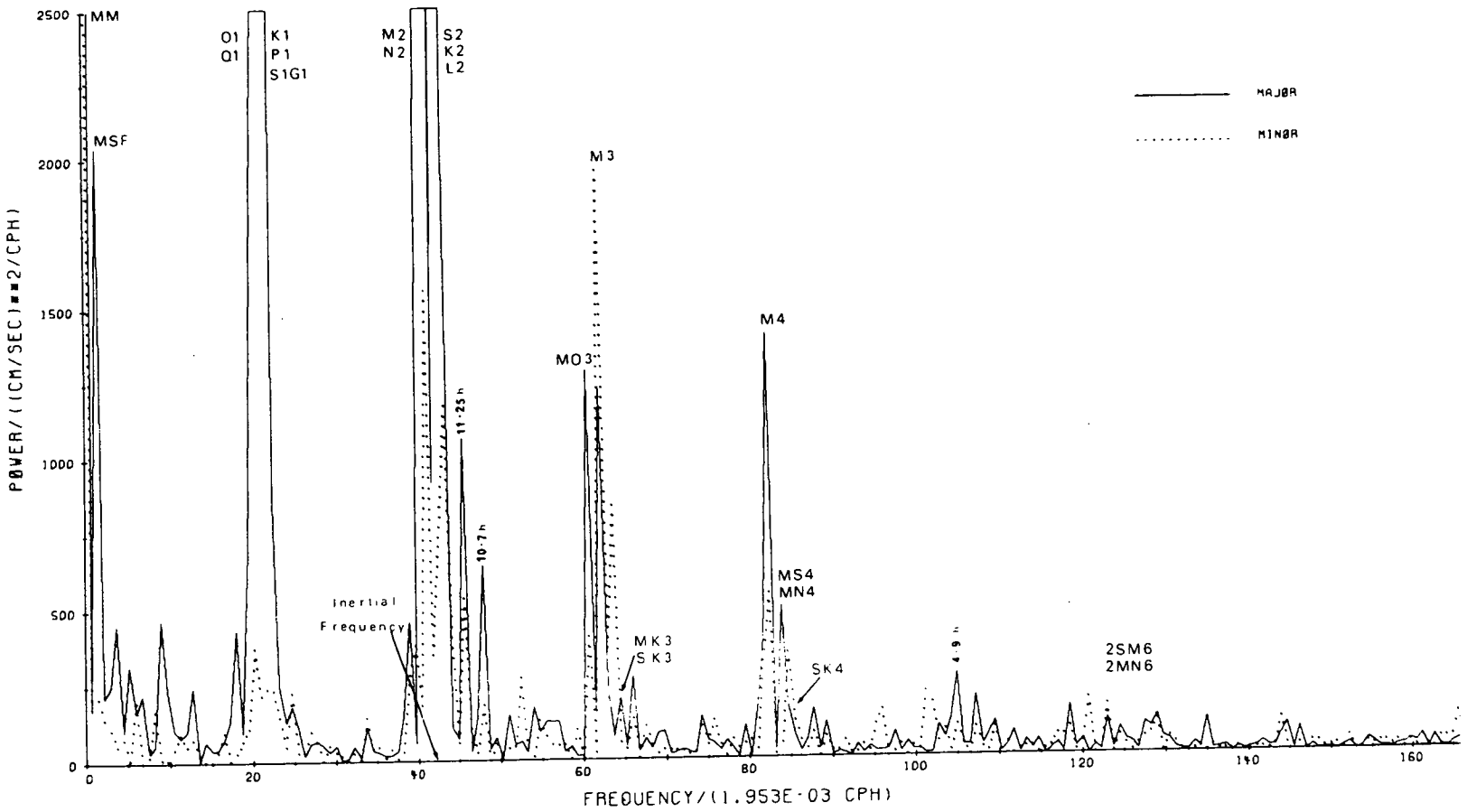

FIGURE 57 *Power spectrum of current velocity components at Meter #235 in Station 2 at 100 metres depth.*

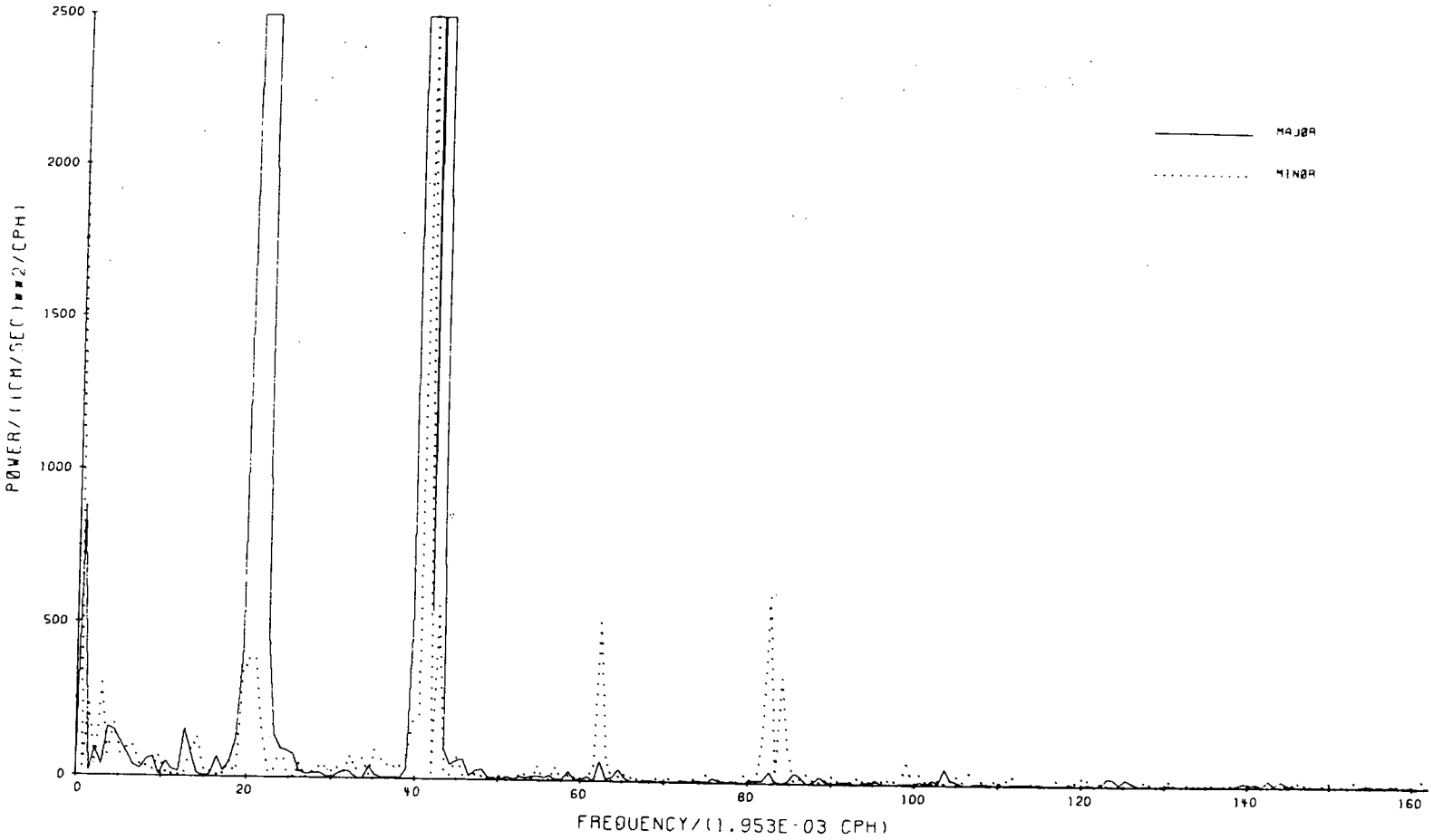

FIGURE 58 *Power spectra of current velocity components at Meter #232 in Station 2 at 500 metres depth.*

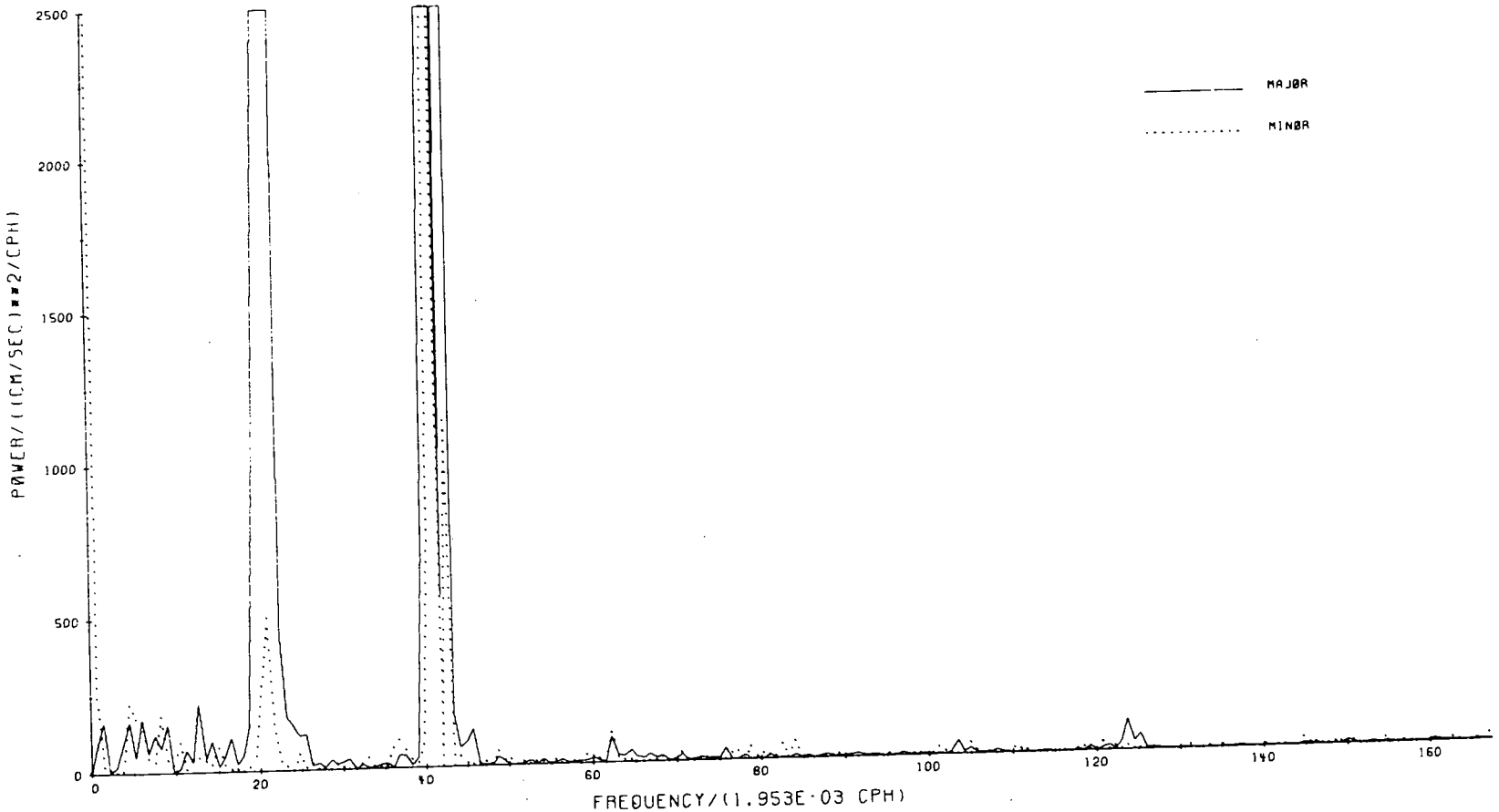

FIGURE 59 *Power spectra of current velocity components at Meter #336 in Station 2 at 600 metres depth.*

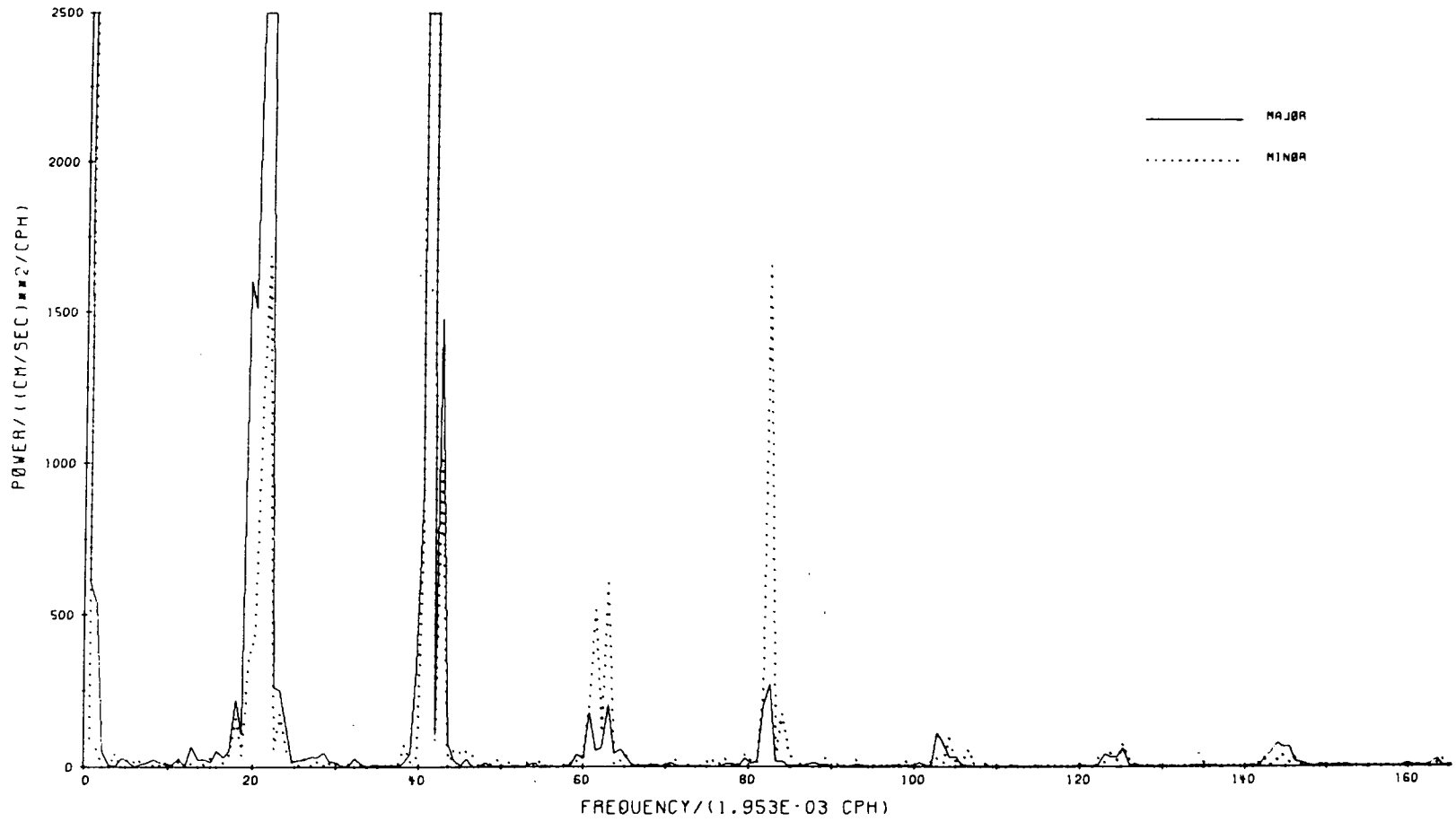

FIGURE 60 *Power spectra of current velocity components at Meter #193 in Station 3 at 10 metres depth.*

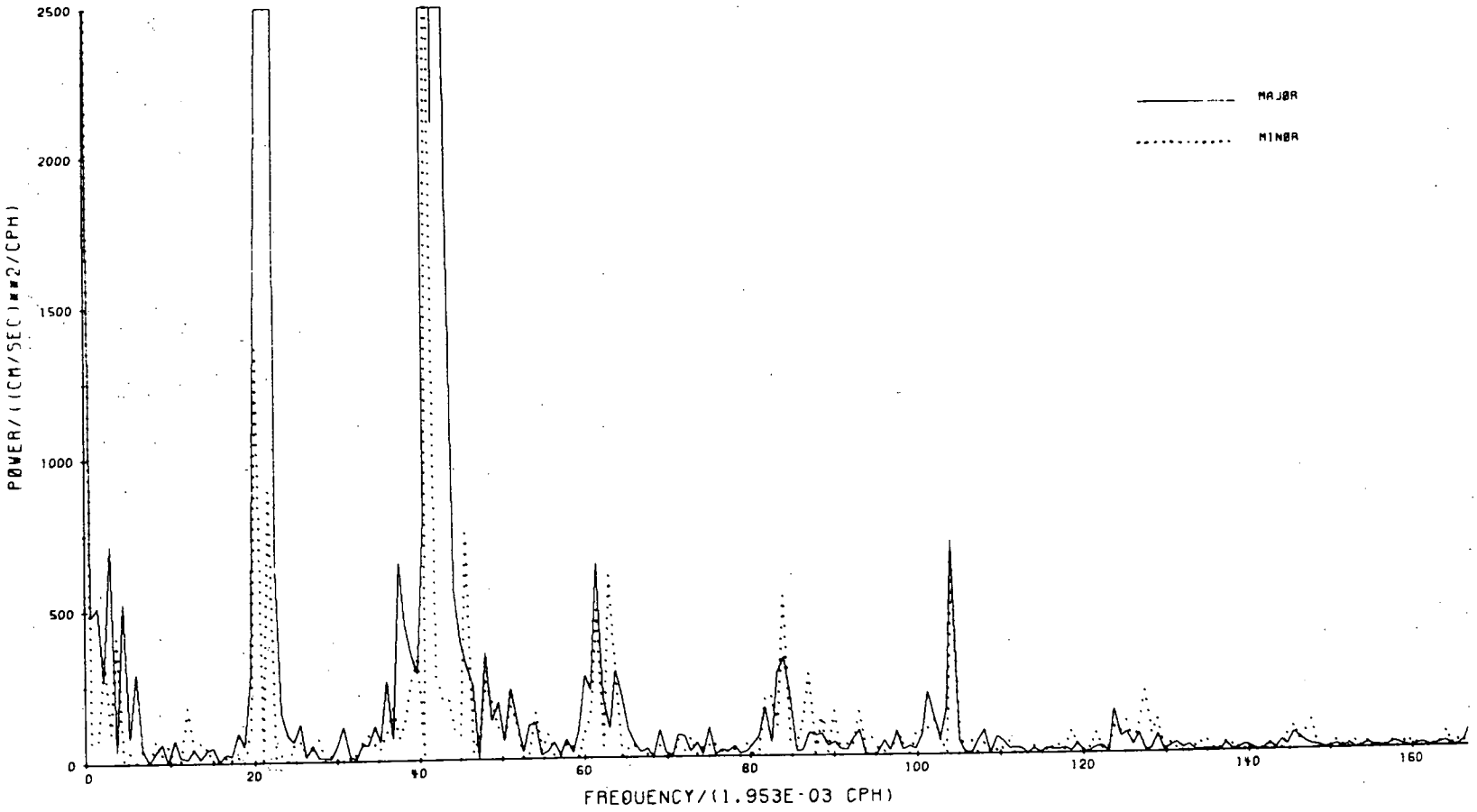

FIGURE 61 *Power spectra of current velocity components at Meter #201 in Station 3 at 100 metres depth.*

where nodal lines lie at each end of the channel for the fundamental frequency. Assuming Robeson Channel to be 60 km long, 24 km wide and with a mean depth of 450 m the fundamental longitudinal seiche period from 4.7 is approximately 30 minutes with a corresponding cross-channel period of 12 minutes. A similar calculation for the whole length of Nares Strait

(513 km) gives a fundamental longitudinal period of 4.5 hours which is close to the peak in the power spectra at just under 5 hours. This agreement is probably fortuitous since the model of a canal of uniform rectilinear cross-section for which Merian's formula was derived is a very poor approximation to the complex form of Nares Strait.

Defant's method (Defant 1960 v2, 165) was applied to the whole length of Nares Strait, the channel being considered as made up of five sections i.e. Robeson Channel, Hall Basin, Kennedy Channel, Kane Basin and Smith Sound and resulted in a value for the seiche period of approximately 4.2 hours. This value is uncorrected for end effects and is not reliable since the bathymetry of the Strait is not well known and the values used for cross-sectional areas were very approximate. In addition the effects of the large inlets opening on to the strait, such as Lady Franklin Bay, Princess Marie Bay and Alexandria Fiord were not included.

In the case of such a seiche the effects of the fundamental frequency of the seiche on the flow in Robeson Channel would be expected to be evident mainly in the axial current records. Robeson Channel, near the end of the Strait would be near a node for surface elevation and the seiche would not be likely to show up on the water level records from Lincoln Bay. Future water level observations in Kennedy Channel, nearer to the probable position of an antinode of the fundamental, may confirm the existence of any longitudinal seiche.

An approximate value for the fundamental frequency of longitudinal internal waves in Robeson Channel was obtained by using the expression

$$\omega_\ell = \frac{\pi}{L}\sqrt{\frac{g\ h_1 h_2(\rho_2 - \rho_1)}{(h_1+h_2)\rho_2}} \qquad 4.8$$

where h is the layer thickness
ρ is the layer density
L is the length of the channel

and the subscripts 1 and 2 refer to the upper and lower layers respectively. The resulting period is 4.8 hours which is again close to that of the peak at 5 hours but in this case the current meter positions were near the mid point of the channel at an antinode of the fundamental and any effects on the current would be expected to be small. Future observations are planned which may produce evidence of internal wave motions in the channel. It seems more likely then that the peak 5 hour period is a result of a longitudinal seiche in the whole of Nares Strait than that of an internal wave in Robeson Channel itself, but both ascriptions are doubtful.

Two further peaks are visible in the record at 100 metres in Station 2 (Fig. 57) having periods of 10.7 and 11.25 hours but the lower confidence limits for both of them are below the noise level and in addition the peaks are visible only on this one record. It is possible that they are artifacts of this one meter or random noise.

No frequency analysis of the type described by Godin (1967) has yet been carried out due to computing difficulties and definite identification of many of the peaks in the power spectra is not possible. Many of the smaller peaks may be due to random noise. The noise level varies considerably between records, being much higher, as might be expected, at those meters recording the greater current magnitude and very low at the deeper locations.

Geostrophic Currents

Because of the very difficult operating conditions no water sampling stations were occupied when the current meter array was laid nor during the recording period. When the meters were removed, three stations were occupied (Appendix 4) but the span of time from first to last of these was two days. In addition one of them could not be extended below 75 metres due to the very strong currents which were encountered. Consequently no useful estimate of geostrophic flow could be made.

SIMPLE TWO-LAYER MODEL

We now apply a two-layer dynamic model to the channel following Defant (1960 v2) i.e.

$$\frac{\partial \xi_s}{\partial y} = - \frac{f}{g} \cdot u_1 \qquad 4.9$$

$$\frac{\partial \xi_I}{\partial} = - \frac{f}{g} \cdot \frac{\rho_2 u_2 - \rho_2 u_1}{\rho_2 - \rho_1} \qquad 4.10$$

where ξ_s is the elevation above normal of the surface
ξ_I^s is the elevation above normal of the interface
$f = 2w\sin\phi$ is the Coriolis acceleration
and the subscripted variables 1 and 2 apply to the upper and lower layers respectively.

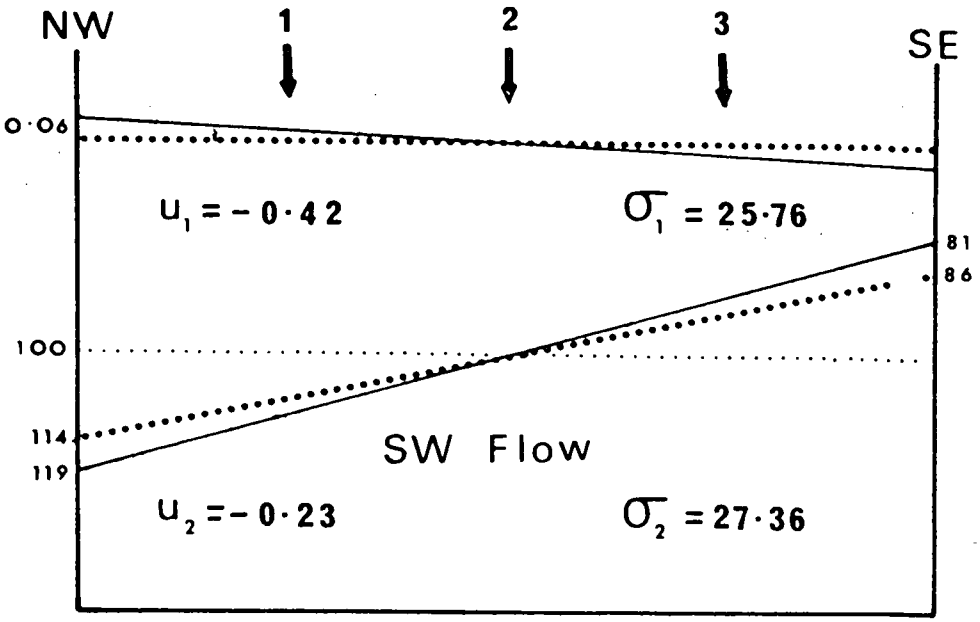

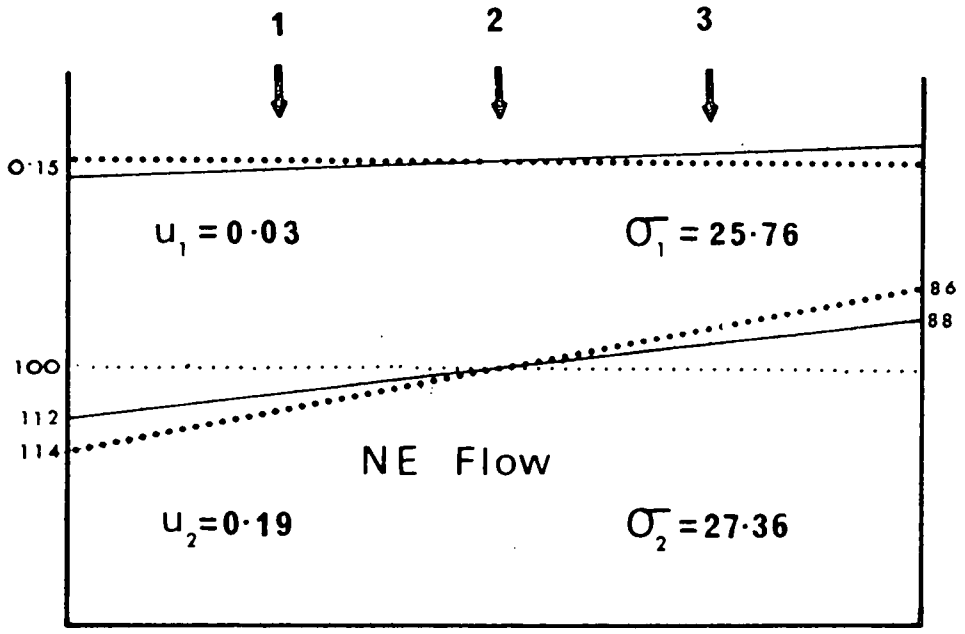

FIGURE 62 Two layer model.

u_1 and u_2 are estimated by summing the mean axial velocity component at each meter (Figure 62) and the mean maximum axial tidal velocity amplitude obtained from Figures 28 to 48. The overall mean value for meters at 100 m depth or less is used to approximate u_1 and that for meters at more than 100 m depth for u_2. The resulting configurations are shown in Figure 62 for south-westerly and north-westerly tidal flows. The surface slope changes sign with changing current direction but these slopes are very small and amplitude of the oscillation of the levels at the sides of the channel is only of the order of 0.1 metres. The slope of the interface does not change sign and the effects of the tidal oscillations is merely to cause an oscillation about the mean position with an amplitude of about 8 metres at the sides of the channel. These oscillations are small since, as discussed above, the tidal motions are almost entirely barotropic and there is no tidal shear across the interface. The slope of the interface is due to the residual flow which is baroclinic with a maximum just above the interface.

However, the simple model does not give a complete description of the structure of Robeson Channel. Figure 62 is drawn for the case where the residual flow is homogeneous across the channel whereas in fact the residual at Station 3 is essentially zero both at 5 m and at 100 metres. Consequently the slope $\partial\xi_I/\partial y$ is not constant across the channel. The limited density data available (Appendix 4) indicates, however, that the pycnocline does slope upward towards south-east between Stations 1 and 2. The upper edge of the pycnocline occurs at between 50 and 70 m in Station 2 while in Station 1 it is below 75 m. In Station 3 it is again between 50 and 75 m, little shallower than it is in Station 2. It appears then from this small sample that the greater part of the advection of water which occurs in the north-western half of the channel, is associated with the greatest slope of the pycnocline.

The model indicates little cross-channel current and the observed components are indeed small and irregular.

MASS TRANSPORT

The mean rate of volume transport $\overline{V}$ over a period of time T through a cross-section A is given by

$$\overline{V} = \frac{1}{T} \int_T \int_A u \; dA.dt \qquad 4.11$$

where $u = u(x, z, t)$.

Writing $u = U + u'$

where $U = U(x, z)$ the time average of $u(x, z, t)$ over time T

and $u' = u'(x, z, t)$

we have
$$\overline{V} = \frac{1}{T}\left[\int_T \int_A U dA dt + \int_T \int_A u' dA\, dt\right] \qquad 4.12$$

if
$$\int_T \int_A u' dA.dt = 0 \qquad 4.13$$

then
$$\overline{V} = \frac{1}{T} \int_T \int_A U\, dA.dt = \int_A U.dA \qquad 4.14$$

i.e.
$$\overline{V} = \sum_i U_i.\Delta A_i \qquad 4.15$$

where
$$\sum_i \Delta A_i = A$$

To satisfy 4.13 we recognize that u' is a linear combination of periodic tidal constituent velocities, small random variations due to turbulence and instrumental and observational errors and any possible long term trends. A mean of the velocity u over 28 days (2016 readings) will remove almost all of the effects of tidal variations with periods of one lunar month or less and at the same time will eliminate the short period random variations. The remaining errors will be due to long period (greater than one lunar month) tidal components and to periodic and non-periodic changes in the residual or non-tidal velocities. These variations in the residual velocity are small over a period of one month and it was assumed that the time series was stationary over the period of observation. The mean of the 28 day progressive means of the residual velocity vectors for each station are shown in Figure 63.

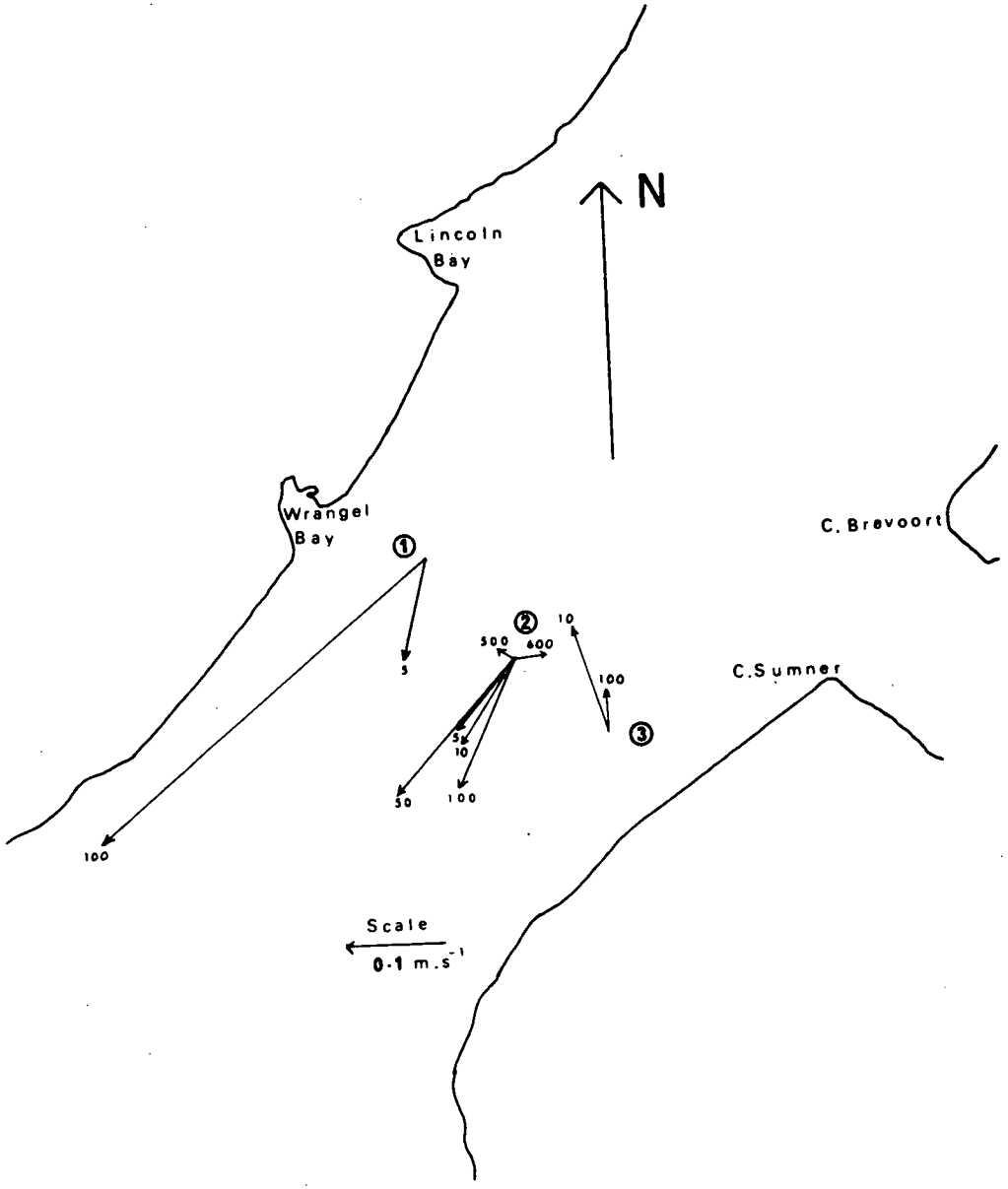

FIGURE 63 28-Day Mean current vectors.

A more serious shortcoming of the data is that there are only ten points over the whole cross-section at which the mean residual velocity is known and some form of approximation must be used to estimate the residual velocities over the whole cross-channel component of the current at each of the meters, together with profiles of the residual currents at each station. The profile at Station 2 has been derived by fitting two third degree curves to the observed current, above and below 100 m respectively. It was then assumed that the profiles at Stations 1 and 3 have the same form as that at Station 2 and the scaled curves were drawn through the two data points available for each station. The profile for Station 2 is based on data from five depths and is considered a good approximation to the actual profile in the centre of the channel. However, the asymetry of the flow through the cross-section shown in Figure 63 and the limited number of data points means that the profiles drawn for Stations 1 and 3 are very approximate, and the uncertainty in the residual velocity at Station 1 must be considered to be at least ± 0.2 $m.s^{-1}$ in the upper 200 metres.

Area of Cross-Section

The volume transport has been calculated over the grid section in Figure 65 using values for the residual current over each grid space taken from the profiles in Figure 64. The values for the elements of area $(\Delta A)_i$ were determined geometrically from a scale drawing of the cross-section. The accuracy of the cross-section depends on the survey given in the Canadian Hydrographic Service Field Sheet No. 3696 and the uncertainty of the bottom contour is considered to be less than ± 20 metres everywhere. Any errors in depth, moreover, have an important effect on the values derived for $(\Delta A)_i$ mainly below 500 metres where the residual currents and volume transports are small. It was found that the estimates of area were reproducible with an estimated uncertainty of less than 3% in the bottom segments.

VOLUME TRANSPORT

Details of the calculation of volume transport are given in Appendix 5. The value arrived at for the mean volume transport during May 1972 is 0.67 x 10^6 $m^3.s^{-1}$ ± 16%.

The amount of seasonal variation which occurs in the volume transports from the Polar Ocean is not known. Certainly the greater part of the fresh water input occurs during the months of June, July and August and one cannot assume that the flow is nearly constant throughout the year. The density changes in the summer are generally confined to the upper layers, mostly less than 50 metres deep but the effects of this seasonal

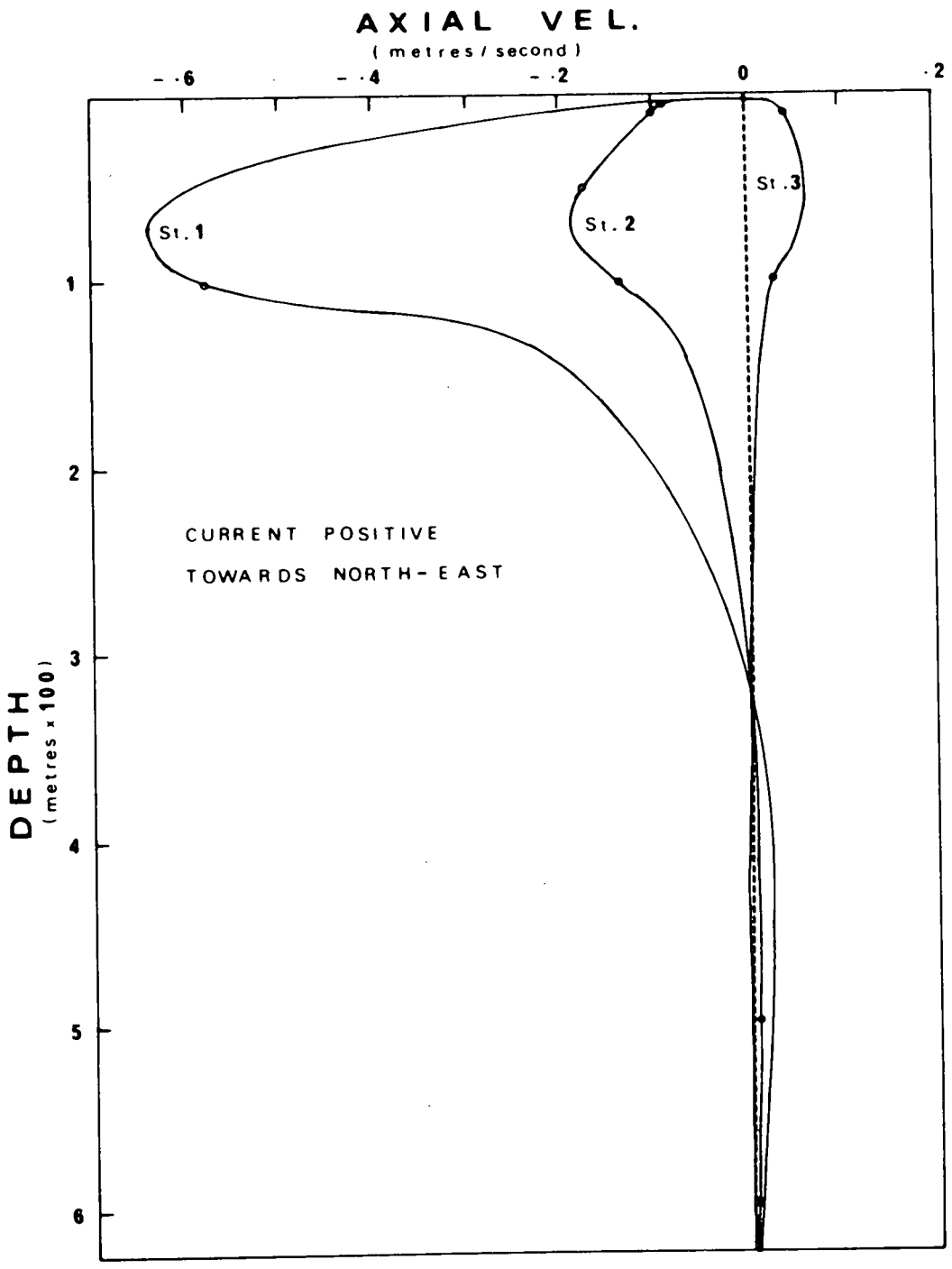

FIGURE 64 *Profiles of the residual axial components of the currents at the three stations.*

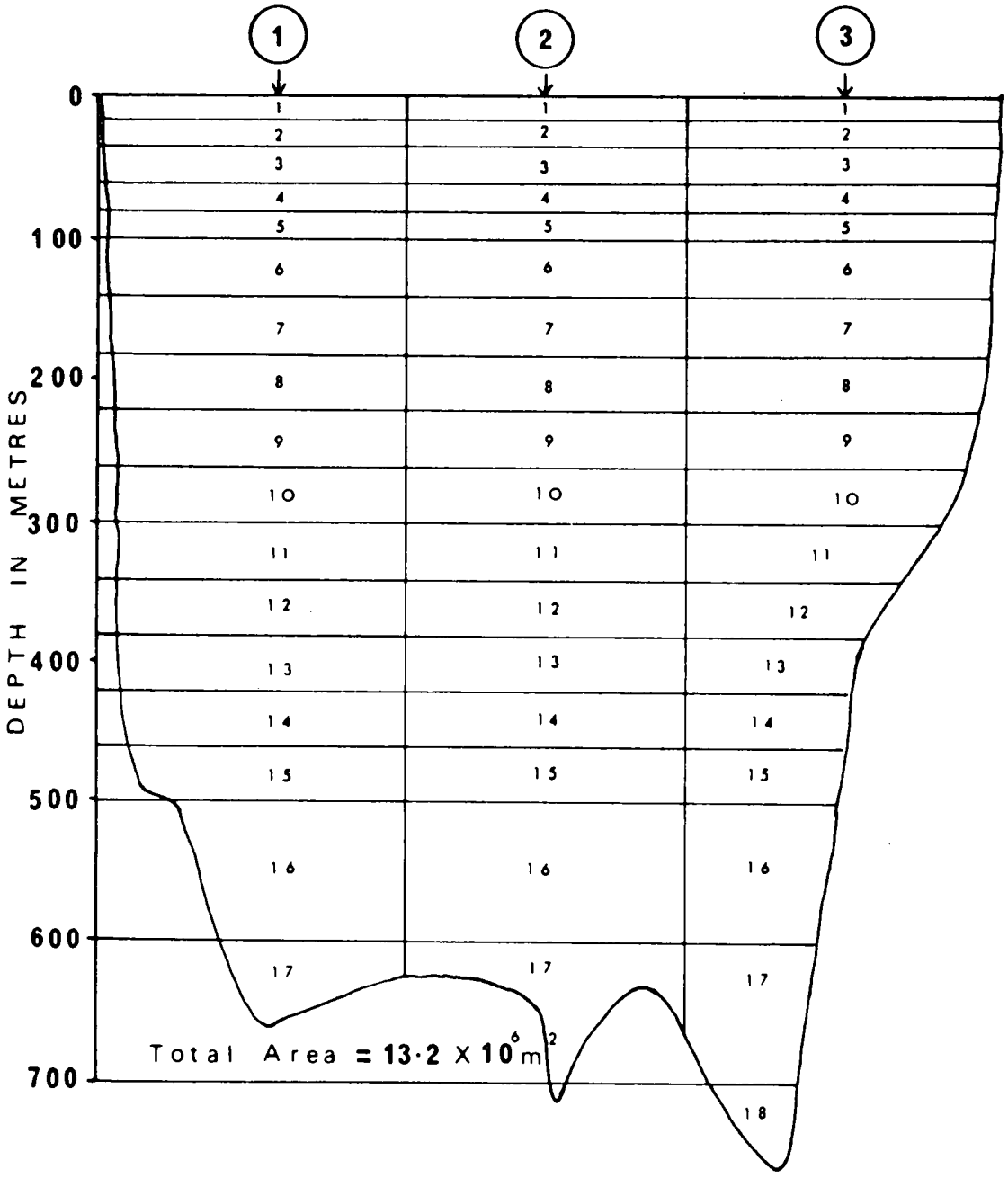

FIGURE 65 *Net used for integration of Water Volume Transports.*

'estuarine' flow are possibly very important in a channel such as Robeson Channel. However, from November to July the channel is completely covered with ice and the observations used here indicate little difference in density structure between April and September. The influence of fresh water is discussed below when dealing with salt transport but for purposes of comparison with previous estimates the rate of flow in May has been considered as a mean value yielding an annual flow of 2.1×10^4 km^3 year^{-1} with an uncertainty of ± 30% which allows for a 50 % discrepancy during July, August and September. The annual differences are probably smaller than the seasonal ones but may still be expected to reach 10%. The value for the mean annual flow of water is therefore assumed to be 2.1×10^4 km^3 year^{-1} ± 30%.

PREVIOUS ESTIMATES

All previous estimates of volume transport were made by geostrophic calculations. Collin (1963 and 1965) using five cross-sections made in the September of several years found a southerly transport of 0.24×10^6 m^3.s^{-1}. Bailey (1957) found a northward transport through Smith Sound in August of 0.42×10^6 m^3.s^{-1}. Day (1968) and Muench (1971) using direct readings of currents, each at one station only reported general southerly flows with reversals due to tidal components. Moynihan (1972) estimates a mean southerly transport of 0.42×10^6 m^3.s^{-1} as a result of three rapidly repeated cross-sections in Smith Sound.

The most comprehensive examination of geostrophic currents in Baffin Bay, that of Kiilerich (1939), gives a value of 0.46×10^6 m.s^{-1} for the southerly transport through Smith Sound and a total flow through all three sounds of 1.4×10^6 m.s^{-1}. Disregarding Bailey's anomalous result, the mean southerly transport from these previous estimates becomes $0.37(\pm 0.10) \times 10^6$ m.s^{-1} which is somewhat smaller than the value found here of $0.67 \times 10^6 (\pm 0.11)$ m.s^{-1}. The difference could well be a result of a barotropic component of the flow undetectable in the density structure, or of the inherent uncertainties of the geostrophic method (Forrester 1972) in the relatively shallow, confined waters of Nares Strait.

Timofeev (1960) estimated the total discharge from the Arctic Ocean through the Canadian Archipelago at 3.1×10^4 km^3. year^{-1} while Treshnikov (1959) reduced this to only 0.8×10^6 km^3. year^{-1} as compared to the flow derived here, for Robeson Channel alone, which is equivalent to 2×10^4 km^3.year^{-1} ± 30%. If the flow through Nares Strait is assumed to be roughly one third of the total, the proportion given by Kiilerich (1939) and Collin (1963), then the estimated total discharge through the archipelago becomes 6×10^4 km^3.year^{-1}. This total discharge is somewhat higher than previous estimates but agrees with the value given by Vowinkel and Orvig (1970) for the net discharge through the Davis Strait (Table 4) below.

THE WATER BALANCE OF THE POLAR OCEAN

For the purpose of this discussion the definition of the Polar Ocean as given by Vowinkel and Orvig (1970) will be used. The Polar Ocean by this definition comprises the Arctic Ocean less the Norwegian and Barents Seas, that is, the advection boundaries are assumed to be the Bering Strait, the Canadian Archipelago and the line running from the north-east point of Greenland by way of Spitzbergen and the northern end of Novaya Zemlya south to the mainland.

It is generally assumed that any exchange east of Spitzbergen is negligible, but there is still much uncertainty as to the magnitude of the fluxes of water across the Greenland - Spitzbergen gap. The values given for the influx via the West Spitzbergen Current by Soviet authors range from 5 x 10^4 $km^3.year^{-1}$ to 16 x 10^4 $km^3.year^{-1}$. (1.6 to 5.1 x $10^6 m^3.s^{-1}$). The transport by the outflowing East Greenland current has been reported by Aagaard and Coachman (1968) as 96 x 10^4 $km^3.year^{-1}$ (30.4 x 10^6 $m^3.s^{-1}$) but it is considered that the greater part of the water in this current is not Polar Water but part of a cyclonic circulation in the Greenland Sea. It may be seen from Table 4 that the amount of water in the East Greenland Current which is required to balance the total influx is only 9.2 x 10^4 $km^3.year^{-1}$, that is, only one tenth of the total flow estimated by Aagard and Coachman. In fact this flow is highly variable and Timofeev's (1956) mean value of 16.1 x 10^4 $km^3.year^{-1}$ (5.1 x 10^6 $m^3.s^{-1}$) for example was obtained from four separate profiles which gave values varying by a factor of 30 or more. It seems probable therefore, that as little as one tenth of the East Greenland Current is made up of Arctic water and that the efflux through Robeson Channel is thus about 14% of the total discharge from the Polar Ocean.

TRANSPORT OF SALT

The total salt transported through Nares Strait has been integrated over the same net as that used for the calculation of the volume transport, the calculations being shown in Appendix 5. The salinity at each depth was estimated from salinity/depth curves drawn from the results of the ice stations in June 1972 (Appendix 4). The total transport was found to be 21.1 x 10^6 $kgms.s^{-1}$ or approximately 6.7 x 10^{14} $kgm.year^{-1}$ out of the Polar Ocean. This value agrees closely with the estimate by Kiilerich (1939) of 16 x 10^{14} $kgm.year^{-1}$ for the total salt flux through all three sounds.

A salt balance for the Polar Ocean was then obtained by making the following assumptions. The variation of salinity with depths in the West Spitzbergen current was obtained from the curve for the North Greenland Sea in Figure 4. It was then assumed the current profile is parabolic

with a maximum velocity at the surface and zero velocity at 2000 m and a value for the weighted mean salinity of 34.8 °/oo was obtained. A mean salinity for the input via the Bering Strait of 32 °/oo was estimated by Sverdrup (1946).

Finally a value of 34 °/oo has been used for the East Greenland Current following Mosby (1963). The resulting salt balance is shown in Table 5.

The difference value of the salinity of fresh water through the rest of the Canadian Archipelago is 31.4 °/oo in fairly good agreement with the observed mean salinity of about 32 °/oo.

Using the above values for salinity of the outflowing currents we may estimate the proportion of the outflow of fresh water through each of the channels. Taking the salinity of the inflowing sea water as 34.2 °/oo the weighted mean of the Bering Strait and West Spitzbergen currents, we have for each channel that S_o the salinity of the outflowing water is given by

$$S_o = (1-p)S_1$$

where 100 p is the percentage of the outflow which consists of fresh water. The results are shown in Table 6.

TABLE 4

ANNUAL WATER BALANCE OF THE POLAR OCEAN

Influx† (in $km^3 \times 10^4$)		Efflux (in $km^3 \times 10^4$)	
West Spitzbergen Current	11.7	Davis Strait	6.3*
Bering Strait	3.3	East Greenland Current	9.2†
Run-Off	0.3		
Net Precipitation	0.2		
TOTAL	15.5		15.5

† From Vowinkel and Orvig (1970)
* Estimated from Robeson Channel transport

TABLE 5

SALT BALANCE OF THE POLAR OCEAN

	Volume Transport in $km^3.yr^{-1} \times 10^4$ (From Table 4)	Mean Salinity $^o/_{oo}$	Salt Transport in $kgm.yr^{-1} \times 10^{14}$
IN			
West Spitzbergen	11.7	34.8	40.7
Bering Strait	3.3	32	10.5
Excess Run off and Ppt.	0.5	0	0
OUT			
East Greenland	9.2	34.0	31.3
Robeson Channel	2.1	32.92	6.7†
Lancaster Sound, Jones Sound, Fury and Hecla Strait	4.2*	31.4*	13.2*

† By integration
* Difference term

TABLE 6

PROPORTION OF FRESH WATER IN OUTFLOW FROM POLAR OCEAN

Channel	% Freshwater	Volume of Freshwater in $km^3.yr^{-1} \times 10^4$	% of Total Freshwater
East Greenland Current	2.3	0.212	42
Robeson Channel	5.4	0.113	23
Canadian Archipelago less Robeson Channel	4.2†	0.115†	35

† Difference term

Table 6 indicates that over half the excess fresh water entering the Polar Ocean leaves by way of the Canadian Archipelago, although less than half of the total outflow of water occurs here.

Seasonal changes are thought to be important particularly with respect to fresh water outflow and the seasonal variations have been discussed previously. If the mean salinity in Robeson Channel weighted for water velocity is calculated for Finlayson's Station 2 and Sadler's Station 6 we find that the salinity on May 3, 1971 was 32.97°/oo and on August 20, 1971 was 32.50°/oo Assuming that the influx of sea water has a constant salinity of 34.2°/oo the proportion of fresh water in Robeson Channel had therefore increased from 3.6°/oo in early May to 4.9°/oo in late August, an increase of about one third of the spring value.

Chapter V

WATER TEMPERATURE RECORDS

GENERAL

Six Braincon recording thermographs were included in the current meter array, each thermograph being suspended directly below one of the current meters in the positions indicated in Figure 26. This type of thermograph photographs, every 20 minutes, the length of the mercury column of a mercury-in-glass thermometer, the record being made on a special green-sensitive 70 mm film. Only one of the thermographs did not obtain a complete record, when the clock drive which advances the film failed in thermograph #5310055 after 30 days (Table 2).

The main purpose of the thermographs was not to obtain absolute values for the temperature at various points since the accuracy of the thermometers themselves is limited to $\pm$ 0.1 ^{o}C. However, it was intended that they should indicate any systematic changes in temperature. In particular it was hoped that they would record the passage through the channel of any distinctive water mass of the kind postulated by Pye (1971) who explained a change in temperature gradient in bottom sediments as the result of the previous passage of a discrete mass of water with a different temperature.

DIGITIZING OF DATA

The method developed for digitizing the film records was analagous to that used to digitize the current meter records. The film was mounted in such a manner as to allow a section of its length to lie across the surface of a Hewlett-Packard 9107A Digitizer. Reference lines parallel to the horizontal axis of the table were marked on the surface and served to line up the film. The cursor was then placed consecutively on the zero mark on the film and on the end of the next 10 images of the mercury column. The process was then repeated for the next 10 images thus providing a reference zero for each set of 10 images and incidentally a time check

by exposure number. The output from the digitizer was used to provide a printed paper tape of the results from a HP 9100B calculator. A number of preliminary trials were made to assess the sensitivity of the system and the reproducibility of the output. It was found that the results obtained by different people agreed to ± 0.01°C. As mentioned above the absolute values of the temperature have an uncertainty of at least ± 0.1°C.

DISCUSSION OF RESULTS

Only four of the six thermographs indicated any temperature variations. The instruments in Station 2 at 10 m and 600 m depth recorded almost constant temperatures through the record. There is thus no indication of the passage during this period of any discrete mass of water of differing characteristics. The records from the other four thermographs all showed periodic variations with amplitudes varying from 0.2°C to 0.4°C. In spite of the relatively small amplitudes these four records all gave useful power spectra which are shown in Figures 66 to 69. When these spectra are compared with the power spectra of the adjacent current meters the appearance of a number of peaks at similar frequencies suggests that the variations in temperature are functions of the tidal frequencies. For example in Station 2 at 100 m depth the power spectra of the water velocity components from Meter #235 (Fig. 57) and that of the temperature record from thermograph #5310030 (Fig. 67) both show peaks corresponding to the semi-monthly, diurnal and semi-diurnal tidal frequencies and also to periods of 8, 6 and 4 hours. The same applies to the other pairs in Stations 1 and 3 at 100 m. Thermograph #5310046 at 200 m in Station 2 (Fig. 68) is much lower in energy with indications of only two or three tidal frequencies of which only the semi-diurnal peak is at all prominent.

There are several possible explanations for the tidal character of the temperature variations. First, if there existed a positive temperature gradient to the south west along the axis of the channel, then a south-westerly flow would tend to move lower temperature water past the thermograph while a north-easterly flow would return slightly warmer water. It is difficult to imagine any mechanism which would account for such a longitudinal gradient. With a tidal excursion of about 6 or 8 km and a temperature range of 0.06°C the necessary gradient would result in a temperature difference, at a depth of 100 m, of 0.5°C over the 60 km length of Robeson Channel. The profile in Figure 12 indicates that the maximum observed temperature difference is about one fifth of that.

A second possibility is that the variations are due to vertical motion of the current meters with respect to the thermocline. The station data from June 1972 given in Appendix 4 was obtained through the holes in the ice from which the meters had just been removed and the resulting profiles are shown in Figure 70. The main thermocline lies between 50 and 150 meters with a mean gradient at 100 m of approximately $0.025^{\circ}C\ m^{-1}$. Due to the strong tidal currents experienced, the depths of the current meters varied as a function of the velocity of the tidal stream. The

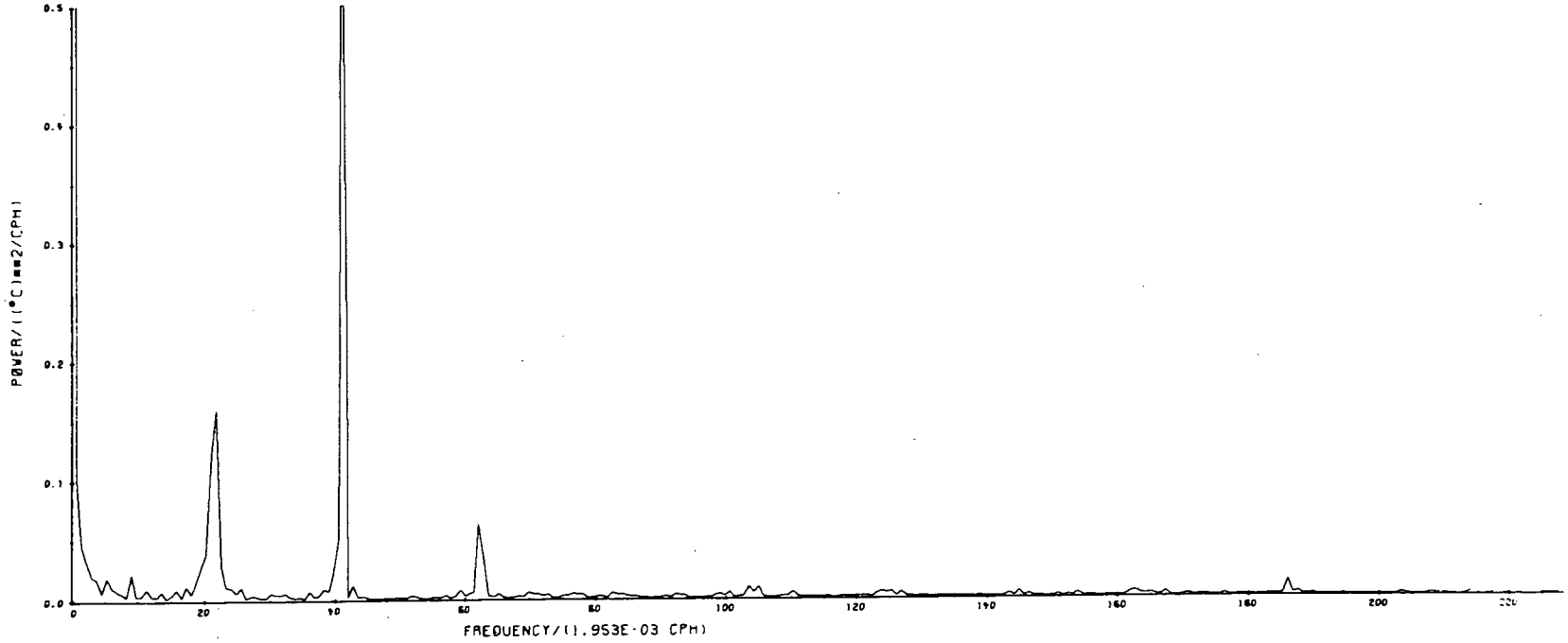

FIGURE 66 *Power spectrum of the temperature record at Station 1 at 100 metres depth.*

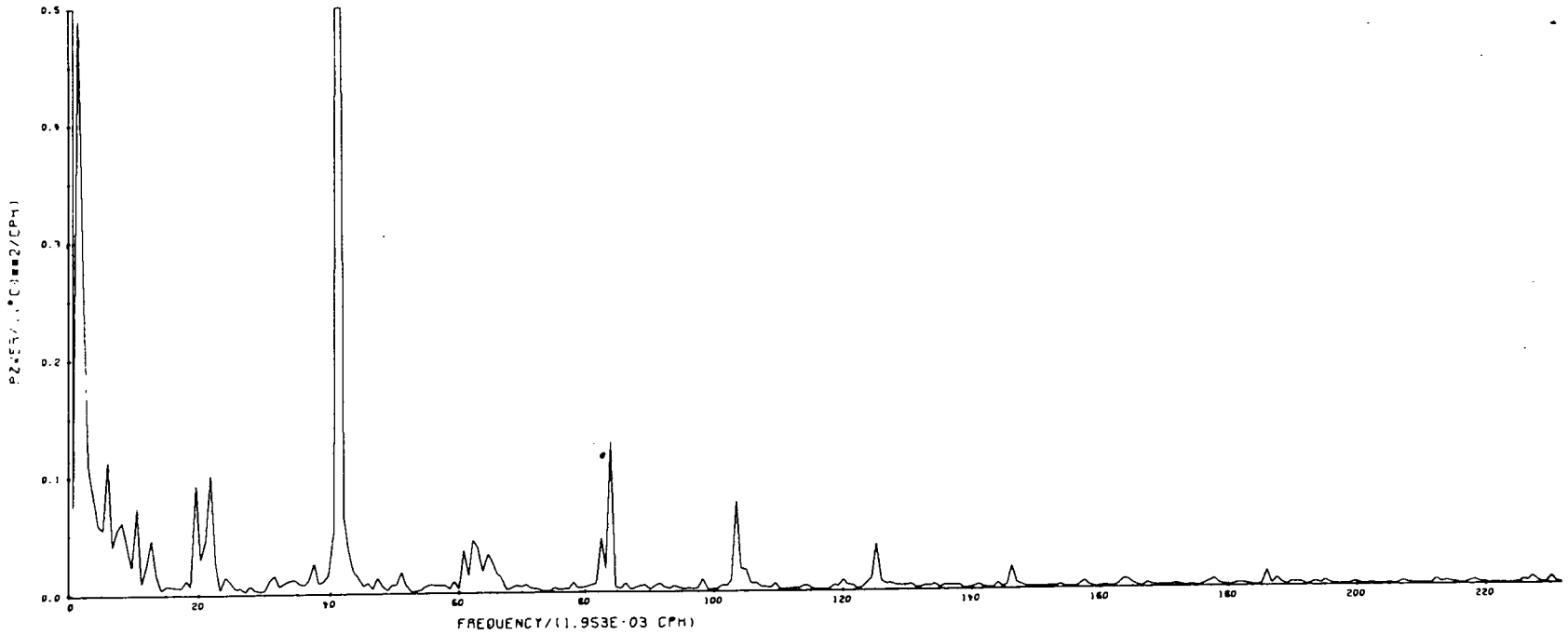

FIGURE 67 *Power spectrum of the temperature record at Station 2 at 100 metres depth.*

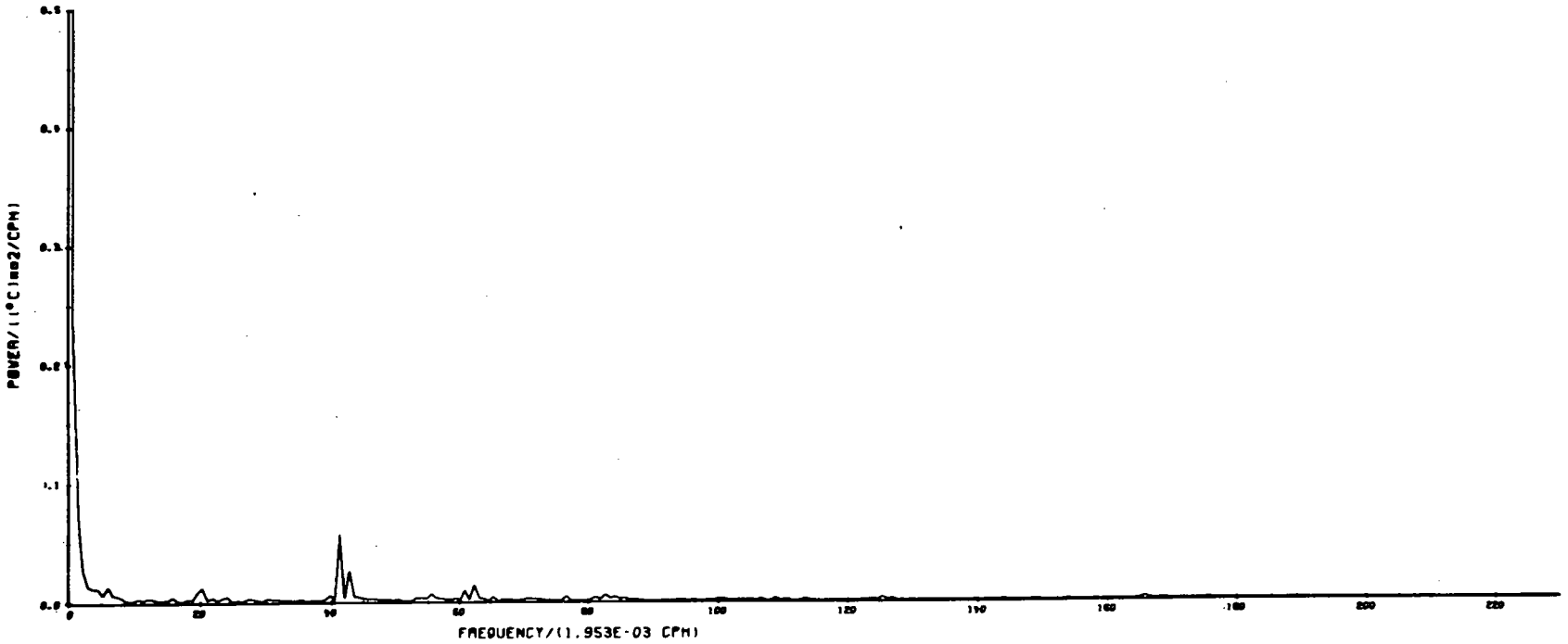

FIGURE 68 *Power spectrum of the temperature record at Station 2 at 200 metres depth.*

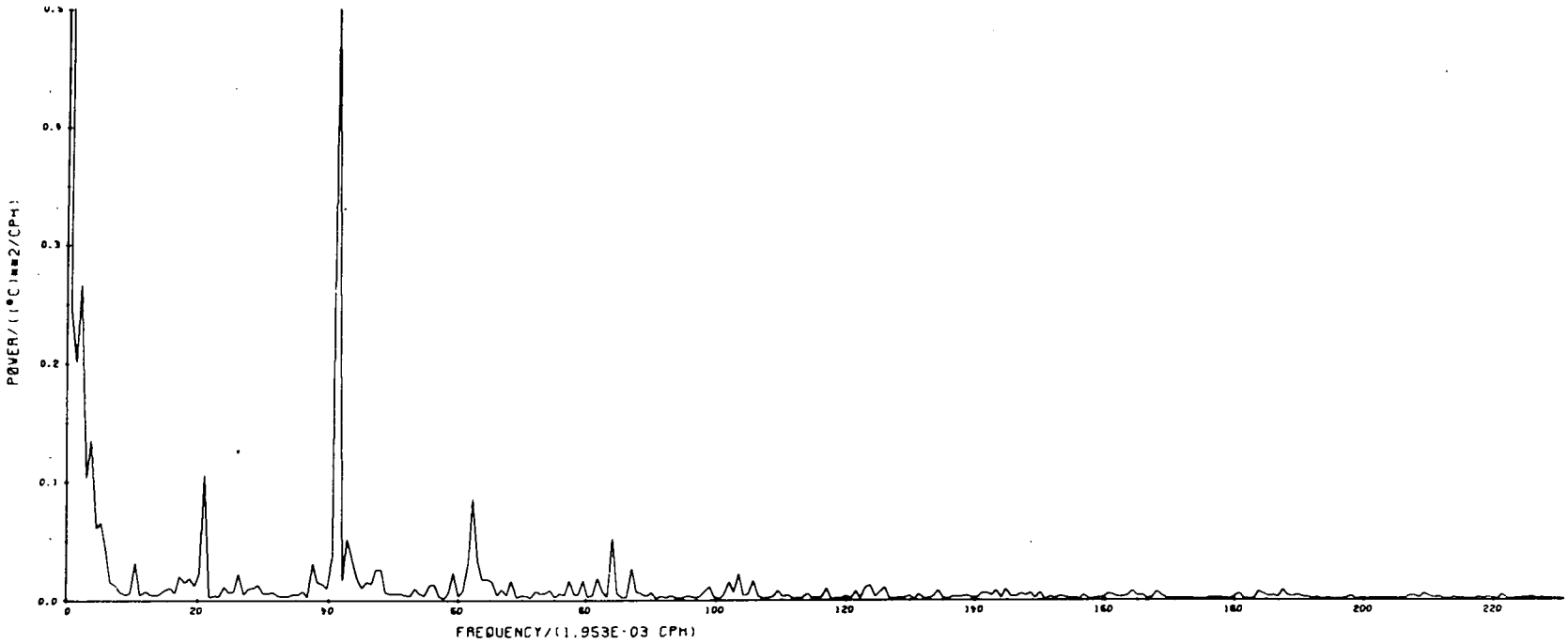

FIGURE 69 *Power spectrum of the temperature record at Station 3 at 100 metres depth.*

extreme values of the tilt recorded by the current meters allow an estimate to be made of the amplitude of this oscillation in depth. In Station 2 the meter at 100 m nominal depth oscillated between about 96 and 100 m. The resulting changes in temperature due to vertical movement through the temperature gradient at this depth should have a range of about $0.1^{\circ}C$ which is about one third of the observed short period variations of recorded temperature. Similar remarks apply to the other two thermographs at 100 m in Stations 1 and 3. The thermograph in Station 2 at 200 m oscillated between 192 and 200 m but at this depth the temperature gradient is only $.004^{\circ}\ m^{-1}$ and the range of the expected temperature variation is therefore only $.03^{\circ}C$ which is about the same as the observed amplitude at that depth. Finally the thermographs at 10 m and 600 m were in nearly isothermal layers and small variations in depth do not affect the temperature. In fact both of these instruments recorded temperatures constant to $0.01^{\circ}C$ throughout the period.

Normally the period of the temperature oscillations due to such changes in depth would be half that of the tidal constituents, as the meter would reach maximum depth at both high and lower water slack i.e. twice per cycle. In cases where the residual current was so strong that it was equal to or greater than the maximum tidal stream the meter would reach maximum depth only at opposing stream i.e. once per cycle and the period of the temperature oscillations would be equal to those of the tidal constituents. While all of the power spectra show a relatively high peak near the semi-diurnal tidal frequency there is little indication of any temperature oscillation with a period of one half of that even at the meter in Station 3 at 100 m depth where the residual current was small and the reversal of the water flow was fairly regular.

If, moreover, the temperature variations are due to the variations in depth caused by the varying drag on the moorings, then they should be in phase with the variation in the tilt angle measured at the meters at the same depth. There is in fact no correlation between these two quantities ($|r| < 0.1$ for all meters) and neither is there any correlation ($|r| < 0.2$) between the current rate itself and either the temperature or the tilt. There is thus little evidence that the temperature oscillations are due entirely to the vertical movement of the meters caused by drag on the moorings.

A third possible explanation of the temperature variations observed is that they are a result of tidal oscillations of the thermocline. It was observed in the last chapter that a simple two layer model of the channel will result in cross-channel oscillation of the thermocline with an amplitude near the channel boundaries of the order of 6 metres (Fig. 62). This implies a vertical oscillation of the interface at Stations 1 and 3 of about 3 metres which is about the same as that due to the deflection of the moorings, the changes in temperature due to the oscillation being 180° out of phase at Stations 1 and 3. However, these two effects are not simply additive. Consider a meter in Station 1 at about 100 metres depth which lies in the thermocline at slack water, that is with the mooring vertical and the slope of the thermocline in the mean position. Suppose the tide now begins to run south-westerly. Then the meter will rise about 4 metres with respect to its original depth because of dynamic drag on the moorings but the level of the thermocline at that station will also rise

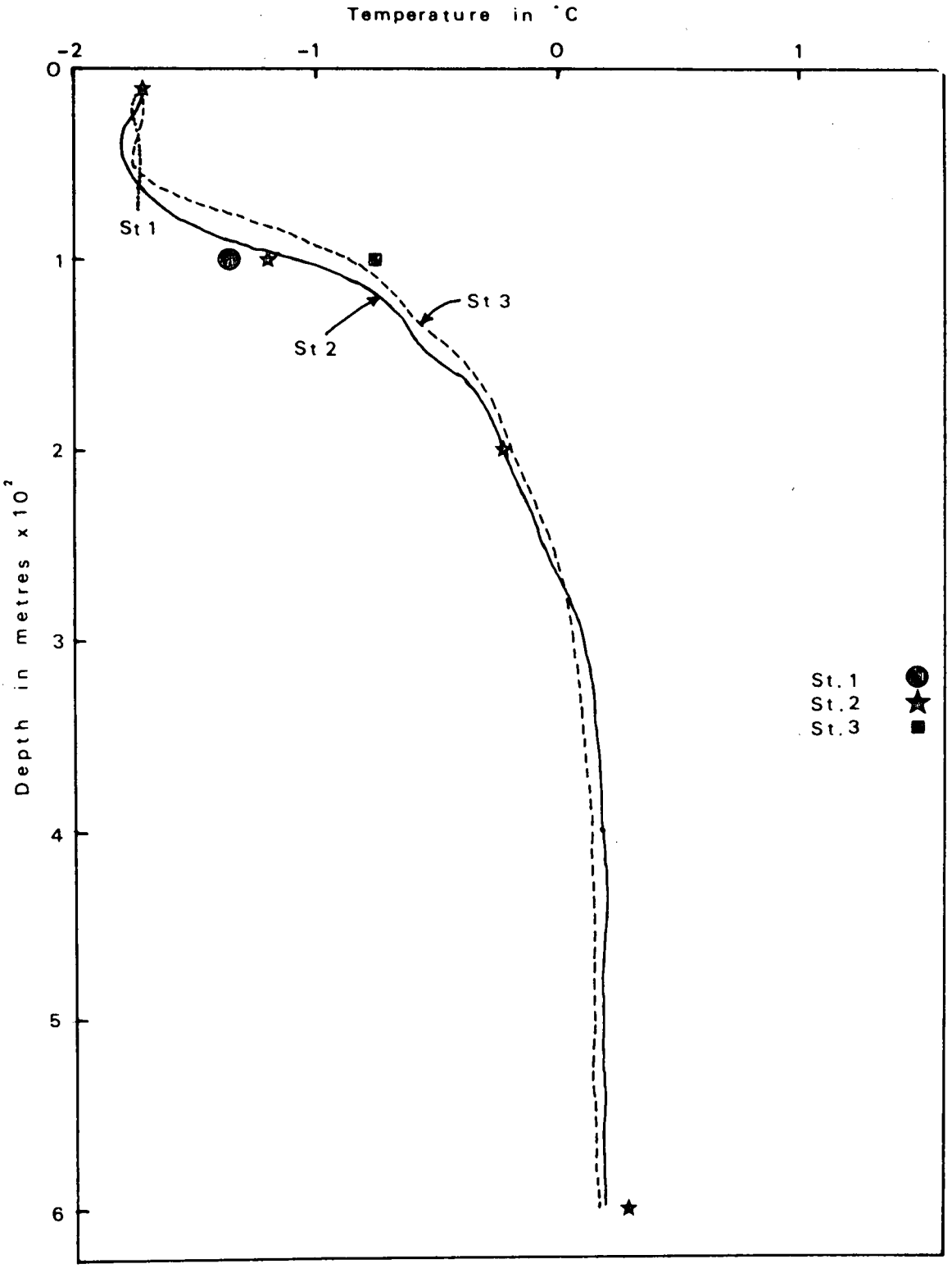

FIGURE 70 *Temperature profiles in Robeson Channel in June 1972 showing also the 28-day mean values of the thermograph readings.*

by about the same amount so that there will be no change in temperature. In Station 3, however, under the same conditions a meter in the thermocline will rise due to dynamic drag while the thermocline will fall by an equal amount resulting in a fall in temperature of about 0.15°C. A similar argument applies to a north-easterly flow and in this case the temperature recorded by the thermograph in Station 3 will remain constant while that at Station 1 will fall about 0.15°C. The temperature variations near the thermocline should therefore show a negative correlation between Stations 1 and 3. Over the period 13th to 14th May the correlation coefficient was -0.37 at phase difference of about 160°. The maximum theoretical correlation coefficient between two sine curves cropped in this manner is -0.66 and it is reasonable to assume that some of the temperature variations are due to the displacement of the current meters with respect to the thermocline.

A fourth explanation might be that the variations were due to internal waves displacing the thermocline. The resonant frequency for a cross-channel standing wave in the thermocline is given by

$$W_R = \frac{H}{W} \sqrt{\frac{g h_1 h_2}{h_1 \pm h_2} \cdot \frac{\rho_2 - \rho_1}{\rho_2}} \qquad 5.1$$

where W is the width of the channel
h is the layer thickness
ρ is the density
and subscripts 1 and 2 refer to the upper and lower layers.

In Robeson Channel with a width of 23 km, a depth of 650 m and the thermocline at 100 m the resonant period is about 1.8 hours. Equation 5.1 with a channel length of 53 km also gives the longitudinal resonant frequency of Robeson Channel as about 4.0 hours. Neither of these frequencies is at all prominent in the temperature power spectra and there is no evidence in the temperature data of the effects of resonant internal waves.

The most likely explanation for the variations of temperature at tidal frequencies is that they are a result of movement relative to the thermocline produced by a combination of dynamic drag on the moorings and changes in the slope of the thermocline, both caused by tidal movements of the water.

DAILY MEAN TEMPERATURES

The existence of a possible seasonal trend in the temperature records was investigated by plotting the 24-hour mean values of the temperature, the results being plotted in Figures 71 and 72. Figure 71

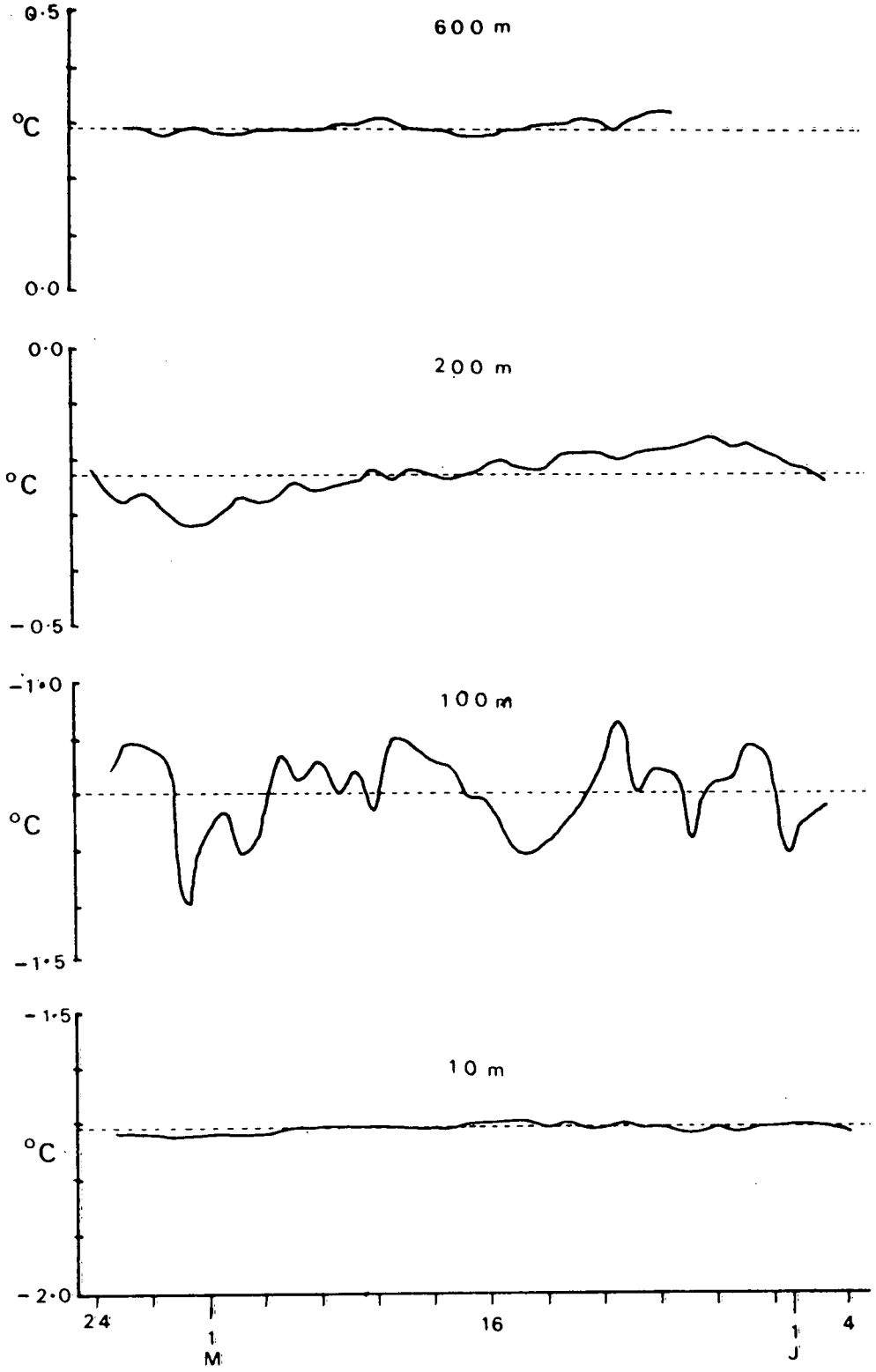

FIGURE 71 *Plots of Daily Means of the thermograph records at 4 depths in Station 2.*

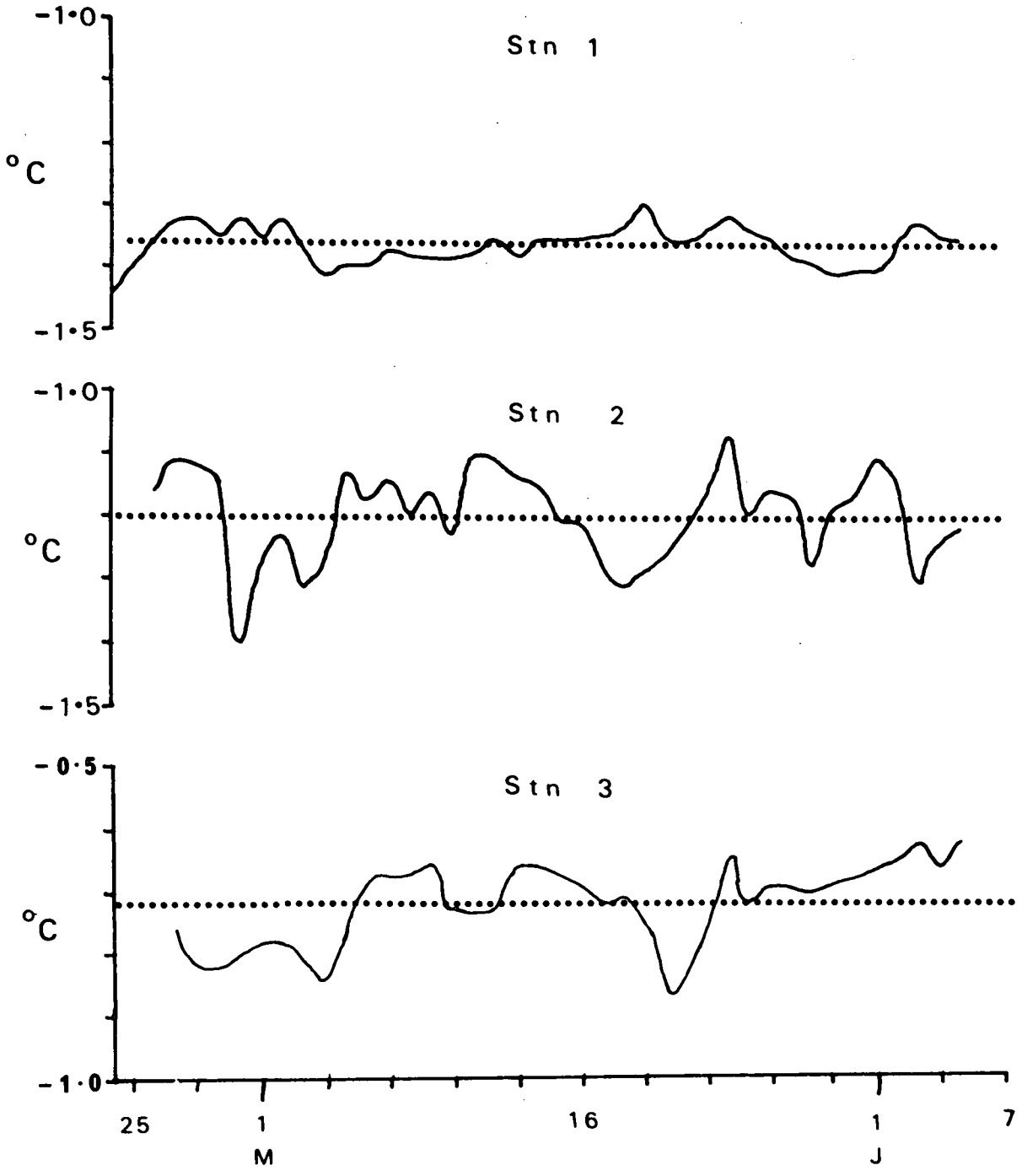

FIGURE 72 *Comparison of the plots of the daily means of the thermograph records at 100 metres depth at all three stations.*

shows the results from the four instruments in Station 2 and Figure 72 those from Stations 1, 2 and 3 at 100 metres depth relative to the mean values. The maximum variability is seen in the records from 100 metres while those from 10 metres and 650 metres are almost isothermal. The record at 200 metres (Figure 71) appears to indicate a possible oscillation with a period of about 40 days but the limited length of the record and the small amplitude of the variation makes its reality very uncertain. The three curves at 100 metres (Figure 72) have no obvious regularity and the correlation coefficients (Table 7) are too small to prove any connection.

To remove any effects of tidal constituents with periods up to one month, the progressive 28-day mean temperatures were calculated and the mean of these 28-day means is given for each thermograph in Table 7. The correlation coefficients of the variations of daily means are also given in Table 7 the coefficient for each pair being shown between them in the table. None of them are of sufficient magnitude to suggest any close relationship between the daily mean temperatures at different locations in the cross-section.

TABLE 7

28 DAY MEANS OF TEMPERATURES
AND THE COEFFICIENTS OF CORRELATION BETWEEN
DAILY MEANS OF TEMPERATURE IN ^{o}C

Depth	Station 1	Station 2	Station 3
10		-1.71	
		(0.00)	
100	-1.36 (-0.19)	-1.20 (+0.28)	-0.73
		(+0.18)	
200		-0.23	
		(-0.09)	
600		+0.31	

HEAT TRANSPORT

The discussion is simplified by confining ourselves to heat exchanges with the Polar Ocean as defined by Vowinkel and Orvig (1970) that is, the Arctic Ocean less the Norwegian and Barents Seas, but including the other peripheral seas (Figure 2). This removes the complication caused by the absorption of latent heat by summer melting of ice in the Norwegian and Barents Seas. It is assumed that the Polar Ocean is in a quasi-static state, that is that the mass of water, the mass of ice and the overall mean temperature of the water are essentially constant from year to year. This implies that any heat lost by radiation or other means must be replaced by solar heating or by advection of heat by the atmosphere or ocean currents.

When estimating a heat balance of such a quasi-static system it is necessary to calculate the net sensible heat advected annually into the basin by ocean currents and this may be done with no reference temperature so long as the net mass inflow is zero. For if M_i and T_i be the mass influx and the temperature through one advection boundary, then the annual net influx of heat $\hat{Q}_W$ through n boundaries is given by

$$\hat{Q}_W = \sum_{i=1}^{n} c_i M_i (T_i - T_R) \qquad 5.2$$

where c_i is the specific heat and T_R the mean temperature of the water in the i basin. If, however,

$$\sum_{i=1}^{n} M_i = 0 \qquad \text{and } c_i \text{ is constant then}$$

$$\hat{Q}_W = c \sum_{i=1} M_i T_i \qquad 5.3$$

which does not involve T_R. Consequently most authors have simply used the measured Celsius temperature of the inflow and outflow to produce a value for net heat input by advection (Vowinkel and Orvig 1970). However, it is incorrect to quote the annual net heat transport through any one advection boundary calculated in this manner since this is equivalent to assuming in the appropriate term in the summation a mean temperature for the basin $T_R = 0^{\circ}C$.

No value for the mean temperature of the Polar Ocean has yet been published but Aagard (1974) estimates from all available data that the value is close to $-0.8^{o}C$ and this reference temperature has been used in this report.

ADVECTIVE SENSIBLE HEAT TRANSPORT

Q_w, the instantaneous advective transport of sensible heat through a single channel into a constant temperature basin may be expressed by

$$Q_w = \int_A \rho_p \, C_p \, (T-T_R) \, v \, dA \qquad 5.4$$

where Q_w is the heat energy transported per unit time by the water,
ρ^w is the water density,
C^p is the specific heat of the water,
T^p is the water temperature as a function of position in the cross-section,
T_R is the mean temperature of the basin,
v is the axial component of water velocity in the channel as a function of position in the cross-section, and
A is the area of the cross-section of the channel.

Within the accuracy of the observations it may be assumed that both ρ_p and C_p are constant with $\rho_p = 10^3$ kg.m^{-3} and $C_p = 10^6$ cal.m^{-3} and with $T_R = -0.8^{o}C$ we have, rewriting 5.4

$$Q_w = 10^9 \int_A (T + 0.8) \, v. \, dA \qquad 5.5$$

where Q_w is in cals.s^{-1}
T^w is in ^{o}C
v is in m.s^{-1}, and
A is in m^2

Then the mean value of heat flow $\overline{Q}_w$ is given by

$$\overline{Q}_w = \frac{10^9}{\tau} \int_\tau \int_A (T + 0.8) \, v. \, dA dt \qquad 5.6$$

where τ is the period of observation and t the time while
T and v are functions both of the position in the cross-section and of time.

In the discrete form

$$\bar{Q}_w = \frac{10^9}{\tau} \sum_{i=1}^{n} \sum_{j=1}^{k} (T_{ij} + 0.8) v_{ij} \Delta A_j \Delta t_i \qquad 5.7$$

or for constant Δt where $\tau = n\Delta t$

$$\bar{Q}_w = \frac{10^9}{n} \sum_{i=1}^{n} \sum_{j=1}^{k} (T_{ij} + 0.8)\ v_{ij} \Delta A_j \qquad 5.8$$

In this case we assume that T_{ij} is constant for all i.e. that the temperature at each location in the cross-section is equal to the mean value $\bar{T}_j$ at that location over a full tidal cycle of 28 days. This is a reasonable assumption since even the largest variations in the temperature at any one point are less than $\pm$ 0.1°C, the uncertainty in the absolute value of the temperature. We then have

$$\bar{Q}_w = \frac{10^9}{n} \sum_{i=1}^{n} \sum_{j=1}^{k} (\bar{T}_j + 0.8)\ v_{ij} \Delta A_j \qquad 5.9$$

If we now substitute for v_{ij} by

$$v_{ij} = \bar{v}_j + v'_{ij} \qquad 5.10$$

where $\bar{v}_j$ is the mean axial current over a full tidal cycle of 28 days through an element of area A_j, while v'_{ij} is the variational current through the same element then

$$\bar{Q}_W = \frac{10^9}{n} \sum_{i=1}^{n} \sum_{j=1}^{k} \bar{v}_j\ (\bar{T}_j + 0.8)\Delta A_j + v'_{ij}(T_j + 0.8)\Delta A_j \qquad 5.11$$

where

$$\sum_{i=1}^{n}\sum_{j=1}^{k} v'_{ij} = 0 \quad \text{for all } j \qquad 5.12$$

This implies that the net tidal transport through each element of area is zero over a full cycle of 28 days. We thus have

$$\bar{Q}_W = 10^9 \sum_{j=1}^{k} (\bar{T}_j + 0.8)\, \bar{v}_j \Delta A_j \qquad 5.13$$

The problem is now reduced to determining $\bar{T}_j$ and $\bar{v}_j$ for all j's. In the previous chapter we obtained values for $\bar{v}_j$ and ΔA_j over the cross-section and the same lattice will be used here. In Figure 70 are displayed the temperature profiles obtained in the three stations by reversing thermometers, the profiles being accurate to $\pm 0.02^{o}C$ at the sampling depths (Appendix 4) and the 28 day mean temperatures obtained from the thermograph records agree closely with these profiles. The temperature read from each of these profiles at depths corresponding to the centre of each element of area in Figure 63 are assumed to be the mean temperatures over the appropriate element of area T_j. Because of the relatively small cross-channel variations in temperature the approximation is considered to be accurate to $\pm 0.05^{o}C$ for each element ΔA_j.

These values substituted in 5.13 (as given in some detail in Appendix 5) produce a value for the mean rate of heat transport into the Polar Ocean through Robeson Channel in May 1972 of

$$\bar{Q}_W = 4.0 \times 10^{11}\ \text{cal.s}^{-1} \pm 25\%$$

using a reference temperature T_R of $-0.8^{o}C$. It should be noted that the calculated value for heat transport is sensitive to errors in the reference temperature. If T_R changes by $0.1^{o}C$ the value for heat transport changes by 15%.

ANNUAL ADVECTIVE SENSIBLE HEAT TRANSPORT

As discussed in Chapter IV, the values obtained here for mass transport of water are probably typical of the entire year. In the case of annual variation of the temperature structure of the water we may make some reasonable assumptions since temperature profiles have been obtained in April (Finlayson 1971), June (Siebert 1967 and Sadler 1972) and late August (Sadler 1971). In effect the water regime is a two season affair; the season of complete or almost complete ice cover and the open season from July to October. The temperature profiles taken in these two seasons,

as discussed in Chapter III, are almost identical except for the immediate surface layer. The probable error in the mean annual heat transport is discussed in Appendix 5 and it is suggested that the error due to seasonal changes in the temperature profile is less than 15% and that the variation from year to year is probably less than 10%. With these assumptions $\hat{Q}_w$ the net annual advective heat flow into the Polar Ocean due to the mass transport of water becomes

$$\hat{Q}_w = 1.3 \times 10^{19} \text{ cal.year}^{-1} \pm 40\%$$

VOLUME TRANSPORT OF ICE

For five or six months each year there is a net outflow of ice from the Polar Ocean through Robeson Channel. Break-up of the winter ice cover begins typically about the middle of July but the date may vary by several weeks each side of that date. The surface water begins to freeze again in September, but the ice continues to move with the tide and wind, and movement in the channel may not cease until January or even February (Dunbar 1973). During this period multi-year floes from the Polar Ocean are driven back and forth with newly frozen ice and a considerable amount of ridging occurs as the floes come under pressure. By the time the ice becomes fixed the unridged first-year ice has reached a thickness of nearly 2 metres, the multi-year floes are three or four metres thick and the typical pressure ridge has a height above the level ice surface of two or three metres.

To estimate the volume transport of ice it is necessary to gain some idea of the mean thickness of ice in the channel and in the Polar Ocean. Vowinkel and Orvig give estimates of ice thickness and of the relative abundance of the various ages of ice (Vowinkel 1970 Tables 5 and 6 page 119). The weighted mean value of ice thickness between July and December calculated from these tables is 2.6 metres. However, this figure does not allow for the effects of ridging. Vowinkel and Orvig consider that in regions of heavy ridging about 10% of the surface is occupied by ridges. Assuming a mean ridge height of 3 metres and isostatic balance the weighted mean thickness of the sea ice in heavily ridged areas may be estimated as 5.0 metres.

Koerner (1973) estimated the mean end-of-winter ice thickness to be 4.6 metres in the Pacific Gyral (Beaufort Sea) and 3.9 metres in the trans-polar drift. These figures allow for 9% of the area in ridges but they are probably lower limits. Wittmann and Schule (1966), working from underwater sonar profiles of the ice obtained from a submarine estimate the area occupied by ridges as between 12% and 18%. For this calculation the mean thickness of the polar ice entering Robeson Channel is assumed to be 4.5 ± 0.5 m.

When the fixed ice in Robeson Channel moves out it is replaced by ice from the Polar Ocean drifting in from the north. Throughout the

so called 'open period' there is ice moving through the channel but the concentration may vary both from day to day and from year to year. In August 1973 for example the polar ice jammed in the northern entrance to Robeson Channel and the channel itself was almost completely free for more than a week. After the jam eventually broke there was almost 100% ice cover in Robeson Channel for days. Time lapse photography by Serson (1973) indicates that a good estimate of average ice cover in Robeson Channel during July and August is 7/10 ± 10%.

The movement of the ice is largely controlled by the currents with the wind having a smaller effect. An investigation of the movement of ice through the channel has been underway for two years and in July and August 1972 a total of 27 floes were tracked by using radar fixes of transponders placed on individual floes (Keys et al 1974). During the first 7 days of this experiment there were very high winds from the south-west the axial component averaging 3.8 $m.s^{-1}$ over the week. The net drift was almost zero during this period. During the last two weeks of August the average axial wind component was about 4 $m.s^{-1}$ from the north-east and during this period the average south-westerly drift of the ice was 0.36 $m.s^{-1}$. A weighted mean over these two periods gives a south-westerly drift of 0.22 $m.s^{-1}$ or 19 km per day.

This drift rate of 19 km per day is probably higher than those which occur later in the year. By October and November fresh ice is forming whenever the wind drops and this will increase the "viscosity" of the flow of ice through the channel. Some of the energy of the moving ice will be dissipated in ridge formation and in distortion of the new ice. Here it is assumed, as a first approximation, that between the beginning of October and the beginning of January, the mean velocity of the ice is reduced in a linear manner from the August value of 19 km per day to zero. The resulting estimate of the mean velocity of ice drift, over the $5\frac{1}{2}$ months from mid July to the end of December 1972, is then 14 km per day.

No great accuracy is claimed for this value since it is possible for the total yearly transport to vary by 50% or more. For example in the summer of 1974 a large floe (15 km in diameter) became wedged across Kennedy Channel between Hans Island and Ellesmere Island. As a result the ice concentration remained unusually high in Robeson Channel and Hall Basin and a much smaller quantity of polar ice than usual entered Robeson Channel from the Lincoln Sea. The result was that the amount of ice leaving, passing through Robeson Channel was reduced by a factor of three or four from that in 1972. Allowing for occasional years such as 1974 the mean velocity of drift ice over a period of several years may be assumed to be 10 km per day ± 30%. For the 5-month open period this implies a volume of 110 km^3 per year. Dunbar (1973) estimated the volume transport of ice through Smith Sound at the southern end of Nares Strait as 75 km^3 per year but this was probably a lower limit as no allowance was made for ridging. The estimated transport of 110 km^3 per year is small compared with the total export of ice from the Polar Ocean. The values proposed by a number of authors for ice export from the whole Polar Ocean are given in Table 8. These values are for export through Fram Strait, between Greenland and Spitzbergen.

TABLE 8

ANNUAL EXPORT OF SEA-ICE THROUGH FRAM STRAIT

Author	Transport in km^3 per year
Zubov (1948)	3000
Gordienko and Karelin (1945)	3000
Gordienko and Laktionov (1960)	8000 - 10,000
Vowinkel (1963)	3000
Antonov (1968)	2000
Koerner (1973)	5600

The arithmetic mean of these estimates is 4300 km^3 per year and the flow through Robeson Channel is only about 3% of this value.

Vowinkel and Orvig (1962) estimate the total outflow of ice through Davis Strait at 491 km^3 per year which is about four times the quantity just derived from Robeson Channel alone. The value includes of course some of the ice coming through Lancaster Sound or Jones Sound and also part of the ice formed in Baffin Bay itself. Although there is some in situ melting of ice in the Bay it is probable that the greater part of the ice formed in situ and of that coming from Lancaster, Jones and Smith Sounds is exported through the Davis Strait by the Labrador Current.

HEAT TRANSPORT BY FLOATING ICE

Q_I, the net heat transport into the Polar Ocean by ice leaving through Robeson Channel is in two forms, sensible heat and the latent heat of fusion. We may write

$$Q_I = \rho_I V_I \{(T_R - T_I) C_I \pm L_I\} \qquad 5.14$$

where Q_I is the heat transported by ice in gram calories

ρ_I is the mean density of the ice in $kg.m^{-3}$

V_I is the volume export in m^3

T_I is the mean temperature of the ice in degrees C

T_R is the mean temperature of the water in the Polar Basin

L_I is the latent heat of fusion in $cal.kg^{-1}$

C_I is the specific heat of ice in $cal.kg^{-1}\ deg^{-1}$ C.

The density, temperature, latent heat and specific heat are all functions of a number of variables and approximations are required for all of them. Pounder (1965) gives 0.91 as a typical value for the specific gravity of first-year ice, reporting values ranging from 0.85 to 0.94. The exact value varies with salinity, the amount of trapped air or brine and the temperature of the ice. The value used here for the mean density of the ice is 0.91×10^3 $kg.m^{-3}$ with a probable uncertainty of ± 3%.

It is assumed that the temperature gradient in the sea ice is linear between air temperature at the upper surface and the water temperature at the lower surface. While this is not a very good approximation, the temperature enters mainly into the estimate of sensible heat transport which is less than 10% of the total. The mean air temperature at Alert (which is 40 km north-west of Robeson Channel) over the $5\frac{1}{2}$ months from July 15 to December 31st is -13^oC (Thompson 1967) and the air temperature in Robeson Channel does not differ greatly from this. Assuming that the water temperature just below the ice averages -1^oC the mean temperature of the ice may be taken to be $-7^oC \pm 2^oC$.

The salinity of the sea ice also varies over a wide range, from almost zero in the higher parts of weathered multi-year ridges to 8 or 10 parts per thousand in new ice. Cox and Weeks (1974) derived two linear equations for salinity as a function of ice thickness for ice thicker than 0.4 m. At the end of the growth season (i.e. May) the mean salinity is given by

$$\bar{S} = 7.88 - 1.59\ h \qquad 5.15$$

where h is the ice thickness in metres. At the end of the melt season,

$$\bar{S} = 1.58 \pm 0.18\ h \qquad 5.16$$

Applying these equations to the relative proportions of ice in the Polar Basin of various thicknesses as given by Vowinkel and Orvig (1970 Tables 5 and 6 pages 129 and 136 respectively) we find a mean salinity for non-ridged ice of 2.7 °/oo in September. The ridges have salinities varying from zero at the top to 4 °/oo at the bottom. Taking the mean value in the ridges as 2 °/oo and the percentage of area ridging as 10% we obtain a value of 2.2 °/oo ± 0.2 °/oo as the mean salinity of the sea ice between May and September.

Pounder (1965 Table 5 p 119) gives a tabulation of values of the specific heat of ice as a function of temperature and salinity. Entering the values obtained above we find a mean specific heat of 0.69×10^3 $cal.kg^{-1}$ C ± 20%.

An expression for the latent heat L_I of sea ice was given by Malmgren (1927) in the form

$$L_I \simeq (1 - \frac{S'}{s}) L \qquad 5.17$$

where L is the latent heat of pure ice
S' is the salinity of the sea ice as a whole i.e. including brine pockets, and
s is the salinity of the sea water.
Using the value obtained above for S' and taking s as 32 $^{o}/oo$ we find

$$L_I \simeq 7.5 \times 10^4 \text{ cal.kg}^{-1} \pm 6\%.$$

Substituting in 5.14 we find $\hat{Q}_I$ the mean annual heat transport

$$\hat{Q}_I = 0.82 \times 10^{19} \text{ cal.year}^{-1} \pm 60\%.$$

Of this total about 8% is in the form of sensible heat in the ice, the remainder being the latent heat of fusion.

TOTAL HEAT TRANSPORT

The combined annual heat flow into the Polar Ocean $\hat{Q}$ due to water and ice advection out of the Ocean is thus

$$\hat{Q} = \hat{Q}_w \pm \hat{Q}_I$$

$$= 2.1 \times 10^{19} \text{ cal.year}^{-1} \pm 50\%$$

Of this total about 30% is due to ice export.

COMPARISON WITH PREVIOUS VALUES

The values obtained here for the mean annual heat transport into the Polar Ocean cannot be compared directly with previous estimates, which were, in the main calculated with a reference temperature of $0^{o}C$. If the integration in Appendix 5 is repeated using a reference temperature of $0^{o}C$ the mean annual heat flow due to the advection of water through Robeson Channel, $(\hat{Q}_w)_o$ becomes 3.2×10^{19} cal.year^{-1} and the total heat transfer $\hat{Q}_o$ is 4.0×10^{19} cal.year^{-1}.

Vowinkel and Orvig (1970) estimated the net influx of heat into the Polar Ocean by water advection to be approximately 30 x 10^{19} cals.year^{-1} for a total of approximately 56 x 10^{19} cals.year^{-1}. However, these values are obtained using estimates for fluxes through the Davis Strait and thus ignore the effects of summer melting and of local ice formation in Baffin Bay. For example they quote a northerly transport of heat through the Davis Strait by water advection of 0.25 x 10^{19} cal.year^{-1}, a full order of magnitude less than that found here for Robeson Channel alone. In Baffin Bay, however, there is a considerable amount of summer melting of ice formed in situ and the latent heat involved is carried southwards in the Canadian Current without ever reaching the Polar Ocean. The effects of this kind of process and others are shown in the difference between the estimates which Vowinkel and Orvig have made for the total heat flux into the Polar Ocean and that into the Arctic Ocean as a whole, that is including the Norwegian and Barents Seas. The mean value for the Polar Ocean is 56 x 10^{19}cals.year^{-1} and that for the Arctic Ocean (Vowinkel and Orvig 1970 Table XXV p 183) is 122 x 10^{19} cals.year^{-1} the extra 66 x 10^{19} cals. year^{-1} being the difference between an excess advective heat flow into the Norwegian Sea of about 80 x 10^{19} cal.year^{-1} used to melt ice.

Consequently the values obtained in this work cannot be compared directly with those given by Vowinkel and Orvig for the Davis Strait. However, this discrepancy will not have a great deal of effect on the estimates of the total fluxes into the Polar Ocean. The values obtained here indicate that the net heat flux through Robeson Channel is about 8% of the total flux into the Polar Ocean. The heat conducted in the water flow is about 11% of the net heat advected by water currents into the Polar Ocean while that due to the export of ice is about 4% of the total heat influx due to the export of ice. Since the transports through Jones and Lancaster Sounds have not been included in the present totals it appears probable that 10% or 15% of the heat influx to the Polar Ocean enters by way of the Canadian Archipelago. This is not really a negligible factor as suggested by Gordienko and Laktionov (1960) and the flows through the Archipelago will be important in the calculation of the heat budget of the Polar Ocean when the present uncertainties in the values for the total fluxes have been reduced from their present large values.

Chapter VI

CONCLUSIONS AND OBSERVATIONS ON FUTURE RESEARCH

The observations made during this work were more limited in both location and time than had been hoped, due to the logistic problems which are inherent in investigations in the High Arctic. Certainly, firmer conclusions could have been drawn if all the readings originally planned could have been made. However, the following conclusions and results follow from the work already completed.

1. The water in Nares Strait is homologous with that in the Lincoln Sea and is apparently advected almost unchanged.

2. No evidence was found of the existence of any water in Nares Strait with the same characteristics as Baffin Bay Bottom Water.

3. Occasional incursions of Baffin Bay water occur, north through Smith Sound. No evidence was found that these incursions are caused by tidal motions or by the barometric gradient along Nares Strait.

4. The tides in Robeson Channel are mixed diurnal-semi-diurnal with the latter constituent predominating. They are barotropic in character being approximately in phase and equal in amplitude from the surface to near the bottom.

5. The water structure in Robeson Channel can be represented approximately by a 2-layer structure with a pycnocline at 100 metres depth. The pycnocline slopes upwards towards the south-east side of the channel the difference in level at opposite boundaries being about 30 metres.

6. The slope of the pycnocline is the result of a baroclinic residual south-westerly flow out of the Polar Ocean. In May 1972 the transport due to this current was $0.67 \times 10^6 m^3.s^{-1} \pm 16\%$ giving an estimate of the mean annual volume transport of water of $2.1 \times 10^4 km^3.yr^{-1}$ which is about 8% of the total volume transport out of the Polar Ocean.

7. The mean annual transport of sea ice through Robeson Channel is 110 $km^3 yr^{-1} \pm 50\%$ which is about 3% of the estimated total annual export from the Polar Ocean.

8. The mean annual transport of heat by advection of water and ice is 2.1×10^{19}cal.yr^{-1} ± 50% which is about 10% of the total annual transport into the Polar Ocean by this means. About 30% of the heat transport through Robeson Channel is in the form of the latent heat of fusion of the ice exported.

9. The mean annual export of salt from the Polar Ocean through Robeson Channel is 6.7×10^{8}kgm.yr^{-1} which is about 13% of the total salt discharge from the Polar Ocean. The proportion of fresh water in the discharge through the Channel varies between 3% and 6% between spring and summer.

These results are of some importance in forming energy and mass balances for the Polar Ocean the transports being somewhat larger than previous estimates. The total transports through the Canadian Archipelago form appreciable fractions of the total transports in and out of the Polar Ocean although they are at present probably less than the uncertainties in the received values for the flows through the Greenland Spitzbergen Gap. These latter are frequently little better than order of magnitude estimates though they are often quoted to four or five significant figures. Recent work such as that by Aagard and Coachman (1968) is reducing the uncertainties to the point where the exchanges across the smaller advection boundaries will have to be considered and realistic estimates of transports through Jones Sound, Lancaster Sound and Fury and Hecla Strait will be required.

The main application of these results at present is to assist in providing a better insight into processes occuring in Baffin Bay where the transports estimated here form a large proportion of the total influx into the northern end of the Bay. Some of the problems and some of the gaps in the data from Baffin Bay which exist at present are discussed below.

THE HEAT AND WATER BALANCE OF BAFFIN BAY

Several models of Baffin Bay have been proposed, by Huyer and Barber (1975), and others. These all require as input well grounded estimates of the flow of water, heat and ice through Lancaster, Jones and Smith Sounds, not only during the summer months but also through the long winter period. Further information is necessary on heat losses in the Bay particularly heat losses to the atmosphere. Estimates of heat losses during the winter are particularly crude because of the many types of surface with widely different albedos and conductivities which can coexist, especially at the northern end of the Bay in the region of the North Water. Müller has found here a considerable heat loss to the atmosphere which has radical effects both on the water and on the precipitation on the surrounding land masses.

Even the mean thickness of ice which freezes each winter is not well known. Kupetskiy (1962) and Dunbar (1974) suggest that the total

thickness of ice which forms annually in the North Water area may exceed the normal first-year ice thickness by a factor of three or four. The continual exposure to extremely cold air of ice-free water, which is a result of the mechanical removal of newly-formed ice by the high winds of the region, will cause extremely rapid freezing over much of the winter, the extent of which is not known at present.

Another factor which is not well known is the extent of the re-melting of sea ice in Baffin Bay in the summer as compared with that exported via the Canada Current, and the additional effect of the glacier ice which is discharged into the Bay also needs investigation. The proportion of solar energy which is actually absorbed by the ice and water of the Bay compared to that absorbed by the frequent summer cloud cover is poorly known and observations need to be extended into the spring and fall periods. Finally more direct observations, particularly winter observations, are desirable at the southern boundary in Davis Strait to determine the mass transports of the West Greenland and Canada Currents and the magnitude of their ice loads. This is so not only for the direct applications to fisheries research, shipping and resource development but also because the total influx into the north end of the Bay appears as a difference term between these two currents.

THE NORTH WATER AND OTHER POLYNYAS

A number of explanations have been proposed to account for the occurrence of the area of open water in the entrances to Smith Sound and Jones Sound and those in the Lancaster Sound. The weakness of all of the proposals is the lack of data during the winter, the exact period when their existence is most prominent. Muench (1971) and others favour the effects of off-shore winds as the main cause of the phenomena but the extent of mixing up of warmer, underlying water has not been measured in winter. Measurement of the water quality and of air-sea energy exchanges during the winter are necessary to determine the mixing depth and to estimate the heat supply to the surface waters by this means.

THE ORIGIN OF BAFFIN BAY DEEP AND BOTTOM WATERS

It has been suggested above that the Bottom Water in the Bay could be produced by a mixture of water from Nares Strait from above sill depth (250m) with Atlantic Water in the Bay, together with excess salinity and a high rate of heat loss due to ice formation in the North Water. This explanation requires that convection mixing in winter should extend to greater depths than the usual 200 metres and winter observations in the North Water itself would be the best method of testing this hypothesis.

EXCHANGES THROUGH SMITH SOUND

Similar observations are required also to investigate the details of the flow through Smith Sound, in particular the sporadic incursions of water northward from Baffin Bay into Kane Basin. The occurence of northerly flows of water in Smith Sound could have a considerable bearing on the date of appearance of the sharply defined northern margin of the North Water.

FUTURE OBSERVATIONS

There is obviously a great deal of experimental work to do before reasonably accurate descriptions can be given of the processes affecting either Baffin Bay or the Polar Ocean. It has been difficult to pursue these objectives in any systematic manner, the area of observation and the kind of experiment to be performed more often than not being selected on a "target of opportunity" basis. If a particular kind of logistic support was available for a particular period and a particular area, then that is when and where the next piece of the work had to be done, and the planning and execution had frequently to be completed in a hurry to meet a deadline.

Attempts are being made, however, to continue in a less haphazard manner and proposals have been made for a number of experiments. It is hoped for example, that a series of observations can be made in Northern Baffin Bay continuously for about 15 months, right through one winter. This series would include measurements of flows through Smith, Jones and Lancaster Sounds, together with measurements of air-sea exchanges, of ice formation and movement and a number of other observations. Such a body of data would go some way towards solving the problems posed by the waters of the Canadian Archipelago, and would be one step towards the kind of large experimental investigation proposed by the Committee on Polar Research of the National Research Council of the United States (1970) for the better understanding of the whole Arctic Ocean.

REFERENCES

Aagaard, K. (1968) with L.K. Coachman. The East Greenland Current North of Denmark Strait. Arctic 21:181-200, 267-290.

(1974) Personal communication.

Anon (1971) Canadian Tide and Current Tables 1971 v.4. Canadian Hydrographic Service, EMR. Ottawa.

Antonov, V.S. (1958) The Role of Continental Drainage in the Current Regime of the Arctic Ocean. Probl. Severa, 1:55-69 (in Russian).

(1968) The Possible Causes of Water Exchange Variations between the Arctic and Atlantic Oceans. Problemy Arktiki i Antarktiki (U.S. Dept. of Commerce Translation 1970).

Bailey, W.B. (1956) On the Origin of Deep Baffin Bay Water. J. Fish R.B. of Canada 13(3).

(1957) Oceanographic Features of the Canadian Archipelago. J. Fish R.B. of Canada 14(5).

Barber, F. (1964) Data Record Eastern Arctic 1960. Can. Oc. Data Centre. Data Record #18 1964.

(1975) Unpublished note.

Bessels, E. (1884) Smith Sound and its Exploration Proc. U.S. N. Inst. 10(3):333-447.

Blackman, R.B. and J.W. Tukey (1958) The Measurement of Power Spectra from the point of view of Communications Engineering. Dover Publ. New York. 1958.

Coachman, L.K. (1962) with C.A. Barnes. Surface Water in the Eurasian Basin of the Arctic Ocean.
Arctic 15:251-277.

(1963) with C.A. Barnes. The Movement of Atlantic Water in the Arctic Ocean.
Arctic 16:9-16.

(1966a) Production of Supercooled Water during Sea Ice Formation.
Proc. Symp. on Arctic Heat Budget and Atmospheric Circulation, Lake Arrowhead, California 31 Jan - 4 Feb 1966. Santa Monica.
Rand Corp. Mem RM-5233 - NSF:497-529.

(1966b) with K. Aagard. On the Water Exchange through Bering Strait.
Limn. & Oc. 11:44-59.

Collin, A.E. (1960) Oceanographic Observations in the Canadian Arctic and the Adjacent Arctic Ocean.
Arctic 13(3). September 1960.

(1963) Waters of the Canadian Arctic Archipelago.
Proc. Arctic Basin Symp. Oct. 1962, Washington, D.C. AINA:128-136.

(1965) Oceanographic Observations in Nares Strait, Northern Baffin Bay, 1963, 1964.
Unpublished Report. B.I. Rep. 65-5, Bedford Institute, 1965.

Cox, G.F.N. and W.F. Weeks (1974) Salinity Variations in Sea Ice.
J. Glac. 13 (67) 1974.

Day, C.G. (1968) Current Measurements in Smith Sound, Summer 1963.
U.S. Coast Guard Oc. Rep. 16. CG-373-16.

Defant, A. (1929) Stabiler Lagerung ozeanischer Wasser Körper und dazu gehörige Stromsysteme.
Veröff. Inst. f. Meereskunde, Univ Berlin.
N.F. Reihe A, No. 19 (Berlin).

(1960) Physical Oceanography 2v. Pergamon Press. 1960.

Dunbar, Moira (1972) Winter Ice Reconnaissance in Nares Strait 1971-1972. Defence Res. Board of Can. DREO Tech Note 72-30.

(1973) Ice Regime and Ice Transport in Nares Strait. Arctic 26 (4) Dec. 1973.

(1973b) Winter Regime of the North Water. Tr. Roy. Soc. Can. Ser IV. v.XI/73.

(1974) Unpublished Note.

Finlayson, D.J. (1971) CODC Data Report Cruise No. 1802-71013.

(1972) Techniques for Laying Instruments in Ice-Covered Waters. Polar Record 16:105. 1973.

Forrester, W.D. (1962) Tidal Transports and Streams in the St. Lawrence River and Estuary. Int. Hydr. Rev. 49(1):95-108.

Godin, Gabriel (1967) L'Analyse d'Observations sur les Courants. Rev. Hydr. Int. v.XLIV no. 1. Jan 1967.

Gordienko, P.A. (1945) with D.B. Karelin. Problems of the Movement and Distribution of Ice in the Arctic Basin. Problemy Arktiki No. 3. (Ref. Vowinkel and Orvig 1962).

(1960) with A.F. Laktionov. Principal Results of the latest Oceanographic Research in the Arctic Basin. Izvestiya Akademii Nauk SSSR, Seriya Geograficheskaya No. 5. (DRBC T350R, 1961).

Herlingveaux, R. (1973) with H.E. Sadler. Oceanographic features in Nares Strait in August 1971. Dept. of Environment, Marine Services Pacific Region Report. July 1973.

Hess, S.L. (1959) Introduction to Theoretical Meteorology. Intersc. New York. 1959.

Hesselburg, T. (1914,1915) with H.U. Sverdrup. Die Stagilitätsverhältnisse des Seewassers bei vertikalen Verschie bungen. Bergens Museums Aarbok, No. 15, (1915).

Hunkins, K. (1966) Ekman Drift Currents in the Arctic Ocean. D.S.R. 13:609-620.

Huyer, J. (1975) Unpublished Note.

Keys, J.E. (1973) Data reduction system for 16 mm film records.
DREO Tech. Note TN 73-14.

(1974) with Moira Dunbar, D.J. Finlayson and J.W. Moffatt. Radar measurement of Ice Drift in Robeson Channel 1972.
Defence Research Establishment Ottawa.
DREO Technical Note 74-21, August 1974.

Kiilerich, A.B. (1939) A theoretical treatment of the hydrographical observational material, Godthaab Expedition 1928.
Medd om Grønl 78:5, 1939.

Koerner, R.M. (1973) The Mass Balance of the Sea Ice of the Arctic Ocean.
J. Glac. 12(65).

Kovacs, A. (1973) with W.F. Weeks, S. Ackley and W.D. Hibler. Structure of a Multi-Year Pressure Ridge.
Arctic 26:1, March 1973.

Kupetskiy, V.N. (1962) The North Water: A Permanent Polynya in Baffin Bay. Moscow State Oceanog. Inst.
Trudy No. 70 1962. Trans. by Moira Dunbar.

Malkus, Joanne S. (1962) Large Scale Interactions.
The Sea v 3:137. M.N. Hill (Ed).
Interscience Publications N.Y.

Malmgren, F. (1927) On the Properties of Sea Ice. Norwegian North Polar Expedition with the Maud 1918-1925. Scientific Results 1(5).

Mosby, H. (1963) Water, Salt and heat balance in the North Polar Sea.
Proc. Arct. Basin Symp. AINA.
Tidewater Pub. Corp. 1963.

Moynihan, M.J. (1972a) Oceanographic Observations in Kane Basin September 1968 and July 1969.
U.S. Coast Guard Oceanographic Report 55 CG-373-55. August 1972.

Moynihan, M.J. (1972b) Oceanographic Conditions in Nares Strait August-September 1970. U.S. Coast Guard Oceanographic Report 57. CG-373-57. August 1972.

Muench, R.D. (1971a) The Physical Oceanography of the Northern Baffin Bay Region. Baffin Bay - North Water Project Scientific Report 1. AINA.

(1971b) Oceanographic Conditions at a Fixed Location in Western Kane Basin, May 1969. U.S. Coast Guard Oceanographic Report 44. CG-373-44.

(1972) Oceanographic Conditions in the Northern Baffin Bay Region. 24 July - 6 August 1970. USCG Oc. Rep. 54. CG-373-54. USCGOU, Washington, D.C. August 1972.

(1973) with H.E. Sadler. Physical Oceanographic Observations in Baffin Bay and Davis Strait. Arctic 26(1). March 1973.

Nares, G.S. (1878) Narrative of a voyage to the Polar Sea. Simpson & Low, London 2 Vol.

Neumann, G. (1948) Bermerkungen zur Zellularkonvektion im Meer und in de Atmosphäre und die Beurteilung des statischen Gleichgewichts. Ann.d.Meteorol July-Aug. pp.235-244 (Hamburg).

Nutt, D.C. (1966) The Drift of Ice Island WH5. Arctic 19(3):244-262.

Pounder, E.R. (1965) The Physics of Ice. Pergamon Press Ltd. 1965.

Pye, G. (1971) Bottom Heatflow in Baffin Bay. Ph.D Thesis. Dalhousie U., Halifax, N.S.

Rudderham, D. (1970) with R.R. Lively. Current Meter Data Reduction Programmes for the CDC 3100 AOL Computer Note 1970-15-C. Dec. 1970. Atlantic Oceanographic Laboratory, Bedford Institute, Dartmouth. N.S.

Sadler, H.E. (1973) On the Oceanography of Makinson Inlet. Arctic 26(1):76-77.

Sater, J.E. (1971) with A.G. Ronhovde and L.C. Van Allen. Arctic Environment and Resources. AINA 1971.

Seibert, G.H. (1968) Oceanographic Observations in the Lincoln Sea, June 1967. Baffin Bay - North Water Project Report No. 2. Arctic Institute of North America Res. Paper No. 46.

Serson, H. (1973) Personal Communication.

Smith, E.H. (1937) with F.M. Soule and O. Mosby. Marion and General Green Expeditions to Davis Strait and Labrador Sea under the direction of the U.S. Coast Guard. USCG Bull 19.

Strickland, J.D.H. (1965) with T.R. Parsons. A Manual of Sea Water Analysis. Fish. Res. B. of Can. Bull 125, 2nd Edition, Ottawa, 1965.

Sverdrup, H.U. (1946) with M.W. Johnson and R.H. Fleming. The Ocean. New York. 1946.

Thompson, H.A. (1967) The Climate of the Canadian Arctic. Canada Year Book 1967 Edition.

Timofeev, V.T. (1956) Annual Water Balance of the Arctic Ocean. Priroda 45:89-91.

Treshnikov, A.F. (1959) Oceanography of the Arctic Basin. Int. Oceanog. Congress Preprints Am. Ass. Adv. Sc.522-3.

Vowinkel, E. (1962) with S. Orvig. Water Balance and Heat Flow of the Arctic Ocean.

(1963) Ice Transport between Greenland and Spitzbergen and its Causes. McGill U. Pub. in Meteorology 59 1963.

(1970) with S. Orvig. The Climate of the North Polar Basin. World Survey of Climatology v 14, H.E. Landsberg (Ed) Elsevier Publishing Company, Amsterdam, London and New York, 1970.

Walmsley, J.L. (1966) Ice Cover and Surface Heat Fluxes in Baffin Bay. Mar. Sc. Centre. McGill U. Man. Rep #2, October 1966.

Wittmann, W.I. (1966) with J.J. Schule. Comments on the Mass Budget of Arctic Pack-Ice . In Proc. Symp. on Arctic Heat Budget and Atmospheric Circulation. Jan 31 - Feb 4, 1966, Lake Arrowhead, California, Santa Monica, California, Rand Corporation Mem. RM-5233-NSF:215-246.

Zubov, N.N. (1948) Arctic Ice and the Warming of the Arctic, from In the Centre of the Arctic, Moscow-Leningrad 1948. (Transl. DRBC T14R 1950).

(1963) Arctic Ice. Transl. U.S. Air Force Cambridge Research Centre.

APPENDIX 1

METHODS USED IN MOORING CURRENT METERS

A. Blowing Holes in Sea-Ice

Because of the size of the Braincon current meters, particularly the older Type 316's, it was necessary to produce a hole of 1.5 to 2 metres diameter. This gives plenty of room not only to lower the meter through the ice but also to recover it when the diameter has been somewhat reduced by ice forming around the margins. The holes had to be blown in first-year ice just under 2 metres thick and they needed to be as near cylindrical as possible and without radial cracks, since the tripod legs had to be set within 50 cm of the edge.

The method used was to drill five holes with an 8" diameter power-driven auger, the holes forming a square of about 70 cm on a side with the fifth hole in the centre. A 1 lb. charge of nitrone was suspended in each of the corner holes at a depth of 1.5 metres from the upper surface of the ice, a 5 lb. charge suspended through the centre hole 0.5 m below the bottom surface of the ice and the fuses were then joined. Wooden battens were used to hold the charges at the proper depth. When the charges exploded, about three quarters of the broken ice fell outside the holes and the surface around the hole had to be cleared quickly to maintain a level working surface. The ice in the hole was cleared using shovels and ice chisels the final layer of crystals being removed by means of a flat sieve with a mesh size of about 2 mm. The average time for a party of four to clear a hole after it was blown was about two hours.

After completing the mooring (see below), the water in the hole was covered with 4" thick sheets of styrofoam and loose snow was then shovelled on top. This insulation proved to be sufficient to prevent the freezing of the surface of the water in the hole during the five weeks they were in place. The diameter of the hole was reduced slightly over this period by freezing around the sides below the surface.

In the case of two of the holes an unusually large amount of broken ice fell back into the hole when it was blasted. An attempt was made to clear this rubble by using another 5 lb. charge below the hole. Although some ice was removed by this method, the diameter of the hole also increased by about 0.5 metres and it is doubtful if the second blast reduced the eventual labour of clearing the hole.

It is possible that a delay of 1/10 of a second or so on the middle charge might improve the efficiency of the blast but no experiments have been made to decide this. The explosive used was not entirely satisfactory and on several occasions pieces of the charges were found unexploded and scattered on the ice. The charges had been in storage at the base camp in Tanquary Fiord through the winter of 1971-72 and the low temperatures (down to -40°C) to which they were exposed may have been the cause of this problem.

B. Method of Laying Moorings

On this occasion the depths at which the meters were to be suspended were decided before going into the field and the 3/8" steel mooring wire was cut to the appropriate length. Each length was fitted with a hard eye at each end and the sections were connected using three shackles in line to make up the mooring line for a specific station. At the base camp before flying out to a station the appropriate cable was wound onto the drum of a small (3 hp) gasoline powered winch.

A tripod with 12 foot legs was mounted over the hole and the feet were prevented from spreading by three 7 foot lengths of ¼" steel wire connecting the bottoms of the legs. A lead block with a wide 'swallow' was shackled to the head of the tripod.

Three additional 8" auger holes were then drilled, two of them opposite each other about half a metre from the edge of the main hole and the third on the same line about 15 metres away. Ice anchors were secured in each of these holes, the anchors consisting of a 50 cm length of steel angle iron shackled at its mid point to a length of 3/8" wire. With the angle irons wedged across the bottom of the auger holes an eye was formed in each of the three wires and secured at the upper surface of the ice. The winch was then set up about 15 metres from the main hole and secured to one of the ice anchors while a second lead block was secured to the anchor at the side of the hole nearest to the winch. One leg of the tripod was set as close as possible to the lead block so that the tension in the mooring wire acted almost parallel to this leg and there was little or no overturning moment on the tripod.

A working platform of heavy planks was constructed beneath the tripod with a gap wide enough for the meter to pass through. The platform also supported a 2 cm diameter safety rod about three metres long which had a length of ¼" steel wire secured to each end. The free ends of these wires could then be shackled to the bottoms of two of the tripod legs. The end of the mooring wire was then passed from the winch, through the two leading blocks, and a 50 lb. sinker was shackled on.

The sinker was then lowered until the first join in the wire was just above the platform. The safety rod was passed through the lowest of the three shackles and secured to the tripod legs. The two upper shackles were unscrewed and the current meter secured between them. All three shackles were then securely 'moused' to prevent accidental unscrewing. The weight was then taken by the winch, the safety rod was removed and the mooring wire paid out until the next join was above the platform when the procedure was repeated for the next current meter.

When all the current meters were suspended at the correct depths, the safety rod was inserted and the lead block at the foot of the tripod leg was removed. The upper end of the mooring was then secured to the ice anchor which had been holding the lead block. A second length of wire was connected to a shackle running on the mooring wire and the other end was then shackled to the third ice anchor. The point of suspension of the mooring was thus removed to the middle of the hole to avoid having the mooring wire frozen in to the side during the period of operation. The planks of the working platform were inserted on either side of the centre to ensure that the mooring did not shift. The hole was then covered and the tripod and winch dismantled.

The hole was marked for recovery by a black pennant about 4 metres long mounted on a 5 metre staff. These pennants proved to be very difficult to see from the air when recovery commenced and in fact all of the moorings were first located by means of other traces left on the surface. The procedure used for recovery was the reverse of that described above.

The method proved to be convenient and fast, the last mooring for example being completed within 30 minutes after the tripod had been rigged. The recovery took only 20 minutes. Two changes will be made, however, in similar operations in the future. The bottom length of the mooring will not be pre-cut but will be prepared in the field after obtaining a sounding through the hole itself. This will avoid the problems due to incomplete hydrographic surveys, particularly the possibility of the deepest meter fouling the bottom. Further, the stations will be marked for recovery by using cloth strips spread horizontally and secured about 3 feet above the ice surface to stakes embedded in the ice.

APPENDIX 2

STATION RECORDS FROM APRIL 1971

ROBESON CHANNEL

Finlayson's Ice Camp

DATA FROM FINLAYSON'S ICE CAMP STATIONS

APRIL 1971

DEPTH m	TEMP. °C	SALIN. °/oo	σ_T	O_2 ml.l^{-1}	DEPTH m	TEMP °C	SALIN °/oo	σ_T	O_2 ml.l^{-1}
Station 1. 1820 25 Apr; 81°54'.0N 62°00'.0W; Depth 270 m					Station 3. 1515 8 May; 81°54'.00N 62°00'; Depth 570 m				
10	-1.76	31.97	25.74		10	-1.75	32.00	25.76	
20	-1.75	31.98	25.75	Not	20	-1.72	32.00	25.76	Not
30	-1.64	31.98	25.75	Obs.	30	-1.22	32.00	25.75	Obs.
50	-1.73	31.99	25.76		50	-1.76	32.01	25.78	
75	-1.57	32.45	26.13		75	-1.68	32.08	25.82	
100	-1.35	33.13	26.66		100	-1.39	33.25	26.78	
125	-1.17	33.53	26.99		125	-1.18	33.65	27.08	
150	-1.04	33.91	27.29		150	-0.73	34.14	27.47	
175	-0.78	34.00	27.39		175	-0.49	34.30	27.64	
200	-0.52	34.10	27.42		200	-0.35	34.46	27.71	
225	-0.37	34.22	27.52		225	-0.25	34.49	27.76	
250	-0.26	34.35	27.62		250	-0.17	34.54	27.80	
300	-0.16	34.58	27.80		300	-0.09	34.62	27.83	
400	-0.04	34.69	27.88						
Station 2. 1900 3 May; 81°54'.0N 62°00'.W; Depth 570 m					Station 4. 1321 10 May; 81°51'.5N 61°43'.0W; Depth N.O				
10	-1.76	32.09	25.84		10	-1.76	31.97	25.74	
20	-1.73	32.09	25.84	Not	20	-1.73	31.98	25.74	Not
30	-1.58	32.10	25.84	Obs.	30	-1.73	31.98	25.75	Obs.
50	-1.74	32.10	25.85		50	-1.73	32.06	25.81	
75	-1.65	32.40	26.08		75	-1.37	32.50	26.16	
100	-1.49	33.12	26.66		100	-1.40	32.91	26.49	
125	-1.11	33.71	27.13		125	-0.79	33.93	27.31	
150	-0.79	34.11	27.44		150	-0.73	34.02	27.37	
175	-0.51	34.25	27.59		175	-0.59	34.21	27.51	
200	-0.29	34.39	27.65		200	-0.42	34.38	27.64	
225	-0.18	34.41	27.68		225	-0.29	34.47		
250	-0.11	34.43	27.70						
300	-0.07	34.46	27.70						
400	0.04	34.70	27.88						
500	0.15	34.72	27.89						

DATA FROM FINLAYSON'S ICE CAMP STATIONS

APRIL 1971

DEPTH m	TEMP. °C	SALIN. °/oo	σ_T	O_2 $ml.l^{-1}$
Station 5. 2032 11 May; 81°59'.0N 62°22'.W; Depth N.O.				
10	-1.72	32.49	26.16	
20	-1.70	32.48	26.15	Not
30	-1.14	32.49	26.14	Obs.
50	-1.70	32.53	26.19	
75	-1.51	32.96	26.54	
100	-1.36	33.40	26.89	
125	-0.98	33.93	27.31	
150	-0.74	34.24	27.55	

APPENDIX 3

STATION RECORDS FROM AUGUST 1971

NARES STRAIT

Cruise of LOUIS S. ST. LAURENT

Cruise No. SL1 - 7104

ST. LAURENT CRUISE - 1971

DEPTH m	TEMP. °C	SALIN. °/oo	σ_T	O_2 ml.l^{-1}
Station 1. 1508 18 Aug; 78°30'.2N 73°42'.OW; Depth 512 m				
0	1.60	31.88	25.53	8.51
10	0.87	31.99	25.66	8.61
20	0.56	32.11	25.77	8.47
30	-0.08	32.73	26.30	8.17
50	-0.96	33.29	26.79	7.63
75	-1.09	33.26	26.77	7.57
100	-1.17	33.39	26.88	7.47
125	-1.18	33.53	26.99	7.30
150	-1.08	33.65	27.08	7.03
175	-1.13	33.71	27.14	-
200	-1.19	33.77	27.19	6.80
225	-1.07	33.84	27.24	-
250	-0.92	33.92	27.29	-
300	-0.60	34.04	27.38	6.76
400	-0.53	34.11	27.44	-
500	-0.46	34.18	27.49	6.76
Station 2. 0430 19 Aug; 79°40'.ON 71°16W; Depth 220 m				
0	-0.64	28.94	24.08	9.68
10	-0.62	30.10	24.20	9.84
20	-0.75	30.98	24.92	10.34
30	-1.18	31.72	25.52	9.32
50	-1.39	32.39	26.07	8.11
75	-1.31	32.93	26.51	7.57
100	-1.11	33.34	26.83	7.19
125	-0.97	33.78	27.18	6.80
150	-0.67	34.10	27.43	6.80
175	-0.52	34.25	27.54	-
200	-0.38	34.39	27.66	6.71

DEPTH m	TEMP. °C	SALIN. °/oo	σ_T	O_2 ml.l^{-1}
Station 3. 0830 19 Aug; 79°42'.ON 69°12'.OW; Depth 110 m				
0	-0.80	30.29	24.36	10.28
10	-1.15	30.56	24.58	10.21
20	-1.23	31.14	25.06	9.74
30	-1.38	31.89	25.66	8.78
50	-1.43	32.27	25.98	8.18
75	-1.36	33.08	26.63	8.05
100	-1.27	33.27	26.78	7.03
Station 4. 1105 19 Aug; 79°47'.1N 67°30'.OW; Depth 73 m				
0	-0.65	14.22	23.40	9.53
10	-1.15	30.27	24.36	10.28
20	-1.33	31.32	25.20	9.60
30	-1.45	31.94	25.71	8.52
50	-1.59	32.51	26.17	7.98

ST. LAURENT CRUISE - 1971

DEPTH m	TEMP. °C	SALIN. °/oo	σ_T	O_2 ml.l^{-1}
Station 5. 1807 19 Aug; 80°45'.1N 65°56'.W; Depth 412 m				
0	±0.50	30.82	24.74	9.66
10	-0.61	30.79	24.76	9.74
20	-1.35	31.56	25.40	9.00
30	-1.43	31.78	25.57	8.78
50	-1.47	32.15	25.89	8.39
75	-1.44	32.72	26.34	7.65
100	-1.23	33.34	26.84	7.30
125	-1.03	33.68	27.11	7.03
150	-0.73	34.04	27.39	6.76
175	-0.56	34.15	27.50	6.76
200	-0.46	34.26	27.55	6.76
225	-0.36	34.34	27.61	6.84
250	-0.28	34.40	27.65	6.88
300	-0.16	34.47	27.71	6.90
500	-0.40	34.58	27.79	6.76
Station 6. 0517 20 Aug; 82°01'.0N 61°29'.5W; Depth 640 m				
0	-1.10	30.10	24.21	9.81
10	-1.64	31.51	25.36	9.39
20	-1.68	31.65	25.48	9.20
30	-1.62	31.69	25.51	9.20
50	-1.67	31.88	25.66	0.06
75	-1.73	32.17	25.90	8.93
100	-1.48	32.66	26.29	7.30
125	-1.31	33.18	26.71	6.96
150	-1.06	33.74	27.17	6.76
175	-1.01	33.87	27.32	-
200	-0.93	34.02	27.38	6.76
225	-0.68	34.19	27.53	-
250	-0.41	34.37	27.66	-
300	-0.01	34.51	27.73	6.76
400	0.01	34.59	27.79	6.76

DEPTH m	TEMP. °C	SALIN. °/oo	σ_T	O_2 ml.l^{-1}
Station 7. 1234 20 Aug; 81°58'.4N 62°18'.0W; Depth 622 m				
0	0.00	30.77	24.72	9.46
10	-1.30	30.71	24.71	9.22
20	-1.59	31.38	25.26	9.06
30	-1.70	31.73	25.55	9.06
50	-1.71	31.95	25.72	8.93
75	-1.44	32.30	26.00	8.11
100	-1.34	32.94	26.51	7.10
125	-1.11	33.59	27.03	6.76
150	-0.80	34.01	27.40	6.61
175	-0.77	34.08	27.45	-
200	-0.75	34.12	27.49	6.49
225	-0.72	34.17	27.47	-
250	-0.60	34.28	27.55	-
350	-0.20	34.50	27.74	6.89
400	-0.08	34.57	27.79	-
500	0.13	34.64	27.83	6.61
Station 8. 1430 20 Aug; 81°56'.4N 61°52'.W; Depth 622 m				
0	-1.67	30.86	25.00	9.53
10	-1.65	31.08	25.02	9.48
20	-1.62	31.11	25.04	9.20
20	-1.64	31.24	25.14	9.06
50	-1.67	31.68	25.50	8.79
75	-1.48	32.60	26.25	7.58
100	-1.38	32.84	26.43	7.37
125	-1.19	33.53	26.81	6.69
150	-0.98	33.80	27.20	6.76
175	-0.84	33.95	27.29	-
200	-0.69	34.08	27.37	6.83
225	-0.55	34.20	27.46	-
250	-0.41	34.31	27.54	-
300	-0.12	34.48	27.71	6.61

ST. LAURENT CRUISE - 1971

DEPTH m	TEMP. °C	SALIN. °/oo	σ_2	O_2 ml/l
Station 9. 1730 20 Aug; 81°49'.8N 61°47'.5W; Depth 348 m				
0	-1.35	30.57	24.46*	9.60
10	-1.40	30.35	24.43	9.81
20	-1.45	30.33	24.40	0.74
30	-1.48	31.06	25.00	9.46
50	-1.54	32.28	25.98	8.25
75	-1.37	32.71	26.33	7.71
100	-1.07	33.45	26.92	7.31
125	-0.82	33.83	27.22	7.03
150	-0.61	34.12	27.44	6.89
175	-0.44	34.33	27.60	-
200	-0.33	34.46	27.70	6.76
225	-0.33	34.46	27.70	-
250	-0.32	34.45	27.70	-
300	-0.31	34.45	27.70	7.03
Station 10. 0230 22 Aug; 82°.32'4N 62°02'.0W; Depth 100 m				
0	-0.60	30.82	24.78	8.70
10	-1.49	31.12	25.05	8.79
20	-1.57	31.56	25.40	8.70
30	-1.57	31.79	25.59	8.70
50	-1.47	32.22	25.94	8.05
75	-1.38	32.61	26.25	7.78

DEPTH m	TEMP. °C	SALIN. °/oo	σ_T	O_2 ml/l
Station 11. 0522 22 Aug; 82°41'.4N 61°07'.0W; Depth 108 m				
0	-0.80	30.75	24.73	9.13
10	-1.38	31.48	25.33	9.13
20	-1.46	31.73	25.54	8.93
30	-1.62	32.18	25.91	8.53
50	-1.65	32.26	25.97	8.39
75	-1.45	33.00	26.57	6.69
Station 12. 0751 22 Aug;82°56'.0N 60°30'.0W; Depth 115 m				
0	0.00	29.17	23.44	9.19
10	-1.60	31.49	25.35	9.13
20	-1.66	31.59	25.43	9.13
30	-1.64	31.80	25.60	8.79
50	-1.62	32.27	25.98	7.91
75	-1.45	32.97	26.55	6.59
Station 13. 1031 22 Aug; 82°36'.0N 59°15'.0W; Depth 196 m				
0	1.00	31.23	25.12	9.06
10	-1.43	31.30	25.19	9.06
20	-1.46	31.34	25.22	9.00
30	-1.56	31.82	25.61	8.64
50	-1.68	32.02	25.78	7.93
75	-1.56	32.51	26.18	7.64
100	-1.36	33.44	26.92	6.76
125	-1.17	33.97	27.35	6.49
150	-0.96	34.08	27.43	6.49

ST. LAURENT CRUISE - 1971

DEPTH m	TEMP. °C	SALIN. °/oo	σ_T	O_2 ml/l
Station 14. 1340 22 Aug; 82°18'.0N 59°05'.0W; Depth 412 m				
0	-1.46	31.32	25.20	9.06
10	-1.51	31.32	25.21	9.06
20	-1.55	31.34	25.22	9.19
30	-1.62	31.43	25.30	9.19
50	-1.69	31.81	25.60	9.06
75	-1.69	31.99	25.76	8.93
100	-1.51	32.56	26.22	8.05
150	-0.80	33.91	27.28	7.03
175	-0.59	34.13	27.50	-
200	-0.42	34.35	27.62	6.90
225	-0.25	34.43	27.72	-
250	-0.10	34.53	27.80	-
300	-0.10	34.70	27.88	6.76
Station 15. 1237 23 Aug; 81°56'.7N 61°57'.0W; Depth 646 m				
0	-0.80	31.75	25.54	8.72
10	-1.54	31.51	25.36	9.00
20	-1.55	31.77	25.58	8.65
30	-1.56	32.04	25.79	8.25
50	-1.51	32.06	25.81	8.45
75	-1.48	32.26	25.91	8.12
100	-1.43	32.69	26.32	7.71
125	-1.17	33.33	26.85	-
150	-0.88	33.88	27.28	6.90
175	-0.72	34.05	27.44	-
200	-0.60	34.20	27.51	6.83
225	-0.47	34.27	27.58	-
250	-0.36	34.35	27.64	-
300	-0.19	34.49	27.73	6.90
400	0.03	34.59	27.83	-
500	0.12	34.69	27.87	6.83
600	0.17	34.75	27.91	6.07

DEPTH m	TEMP. °C	SALIN. °/oo	σ_T	O_2 ml/l
Station 16. 0618 27 Aug; 81°30'.1N 63°51'.9W; Depth 613 m				
0	-0.50	31.44	25.28	8.90
10	-0.98	31.53	25.37	8.99
20	-1.16	31.71	25.51	8.92
30	-1.37	32.26	25.97	8.31
50	-1.44	32.73	26.34	7.71
75	-1.37	32.95	26.52	6.89
100	-1.18	33.48	26.95	6.29
125	-1.07	33.76	27.17	6.35
150	-0.97	33.91	27.29	6.22
175	-0.82	33.95	27.33	-
200	-0.66	34.02	27.36	6.70
225	-0.54	34.16	27.47	-
250	-0.43	34.31	27.58	-
300	-0.25	34.55	27.78	5.95
400	-0.09	34.63	27.84	-
500	-0.08	34.71	27.90	6.42
Station 17. 0830 27 Aug; 81°26'.1N 63°17'.3W; Depth 677 m				
0	-0.50	31.68	25.47	8.45
10	-1.26	31.68	25.50	8.39
20	-1.29	31.99	25.73	8.45
30	-1.37	32.28	25.93	8.27
50	-1.43	32.45	26.13	8.11
75	-1.40	32.81	26.41	7.50
100	-1.17	33.42	26.90	6.22
125	-1.06	33.82	27.23	6.83
150	-0.95	33.97	27.34	6.47
175	-0.73	34.20	27.51	-
200	-0.52	34.35	37.65	6.15
225	-0.40	34.41	27.71	-
250	-0.30	34.47	27.75	-
300	-0.19	34.58	27.80	6.70
400	-0.07	34.72	27.90	-
500	-0.08	34.80	27.97	6.62
600	-0.10	34.86	28.02	6.49

ST. LAURENT CRUISE - 1971

DEPTH m	TEMP. °C	SALIN. °/oo	σ_T	O_2 ml/l
Station 18. 1018 27 Aug; 81°23'.4N 62°58'.5W; Depth 530 m				
0	-1.10	31.37	25.24	8.05
10	-1.00	31.52	25.36	8.58
20	-1.03	31.57	25.40	8.92
30	-1.17	31.74	25.53	8.92
50	-1.49	32.37	26.06	6.42
75	-1.27	33.11	26.65	6.89
100	-1.04	33.60	27.04	6.70
125	-0.87	33.86	27.24	-
150	-0.67	34.02	27.40	6.56
175	-0.50	34.12	27.52	6.76
200	-0.40	34.22	27.62	-
225	-0.33	34.32	27.69	-
250	-0.28	34.42	27.73	6.49
300	-0.21	34.52	27.75	6.20
Station 19. 1806 27 Aug; 80°26'.3N 68°47'.0W; Depth 402 m				
0	0.20	31.03	24.92	9.33
10	-0.98	31.65	25.46	8.99
20	-1.10	31.81	25.59	8.86
30	-1.27	32.02	25.77	8.65
50	-1.38	32.66	26.29	7.84
75	-1.15	33.31	26.81	7.16
100	-1.10	33.57	27.02	6.83
125	-0.94	33.79	27.20	6.83
150	-0.71	33.97	27.33	6.89
175	-0.61	34.18	27.49	6.89
200	-0.58	34.35	27.63	6.89
225	-0.47	34.41	27.68	-
250	-0.36	34.47	27.72	-
300	-0.14	34.59	27.81	6.89

DEPTH m	TEMP. °C	SALIN. °/oo	σ_T	O_2 ml/l
Station 20. 1948 27 Aug; 80°21'.1N 68°24'.0W; Depth 379 m				
0	0.20	31.45	25.50	8.25
10	-1.33	31.90	25.68	8.86
20	-1.43	32.14	25.87	8.51
30	-1.44	32.42	26.10	7.44
50	-1.38	32.76	26.37	7.77
75	-1.17	33.24	26.76	7.30
100	-1.01	33.70	27.12	7.03
125	-0.72	34.09	27.42	6.83
150	-0.57	34.21	27.51	6.83
175	-0.47	34.26	27.55	6.89
200	-0.36	34.39	27.65	6.83
225	-0.28	34.43	27.71	-
250	-0.22	34.48	27.75	-
300	-0.15	34.57	27.78	6.70
Station 21. 2124 27 Aug; 80°15'.1 N 68°29'.3W; Depth 358 m				
0	0.30	31.24	25.09	9.20
10	-0.60	31.46	25.29	9.60
20	-1.26	31.89	25.67	8.86
30	-1.31	32.18	25.90	8.18
50	-1.37	32.84	26.44	7.71
75	-1.23	33.10	26.65	7.37
100	-1.07	33.44	26.91	7.03
125	-0.69	33.91	27.28	7.03
150	-0.57	34.24	27.54	6.62
175	-0.43	34.43	27.69	6.69
200	-0.27	34.44	27.69	6.22
225	-0.17	34.48	27.72	-
250	-0.11	34.52	27.75	-
300	-0.12	34.58	27.79	6.62

ST. LAURENT CRUISE - 1971

DEPTH m	TEMP. °C	SALIN. °/oo	σ_T	O_2 ml/l
Station 22. 0700 29 Aug; 78°11'.0N 73°40'.0W; Depth 622 m				
0	0.50	31.77	25.50	8.25
10	1.38	31.77	25.45	8.39
20	1.24	31.85	25.52	8.39
30	0.48	32.32	25.94	8.53
50	-0.25	33.10	26.60	8.11
75	-0.93	33.41	26.89	7.84
100	-1.08	33.51	26.96	7.64
125	-1.19	33.59	27.03	-
150	-1.19	33.68	27.11	7.16
175	-1.06	33.80	27.20	-
200	-0.92	33.90	27.27	6.89
225	-0.82	33.98	27.34	-
250	-0.73	34.06	27.39	-
300	-0.61	34.15	27.47	6.76
400	-0.50	34.22	27.52	6.69
500	-0.47	34.29	27.58	6.62
Station 23. 0924 29 Aug; 78°13'.5N 74°19'.0W; Depth 631 m				
0	0.60	31.73	25.47	8.53
10	0.48	31.70	25.44	8.53
20	-0.20	31.84	25.59	8.58
30	-1.03	32.15	25.87	8.80
50	-1.26	32.59	26.23	8.18
75	-1.23	33.11	26.66	7.71
100	-1.15	33.50	27.02	7.37
125	-1.05	33.61	27.09	-
150	-0.98	33.71	27.12	6.96
175	-0.92	33.78	27.18	6.76
200	-0.85	33.85	27.24	-
225	-0.78	33.91	27.29	-
250	-0.72	33.97	27.33	6.83
300	-0.62	34.07	27.41	-
400	-0.49	34.21	27.51	6.30
500	-0.41	34.26	27.55	6.40

DEPTH m	TEMP. °C	SALIN. °/oo	σ_T	O_2 ml/l
Station 24. 1130 29 Aug; 78°15'.7N 74°55'.5W; Depth 666 m				
0	1.50	41.49	25.22	8.25
10	1.53	31.49	25.22	8.39
20	1.43	31.54	25.27	8.32
30	0.38	32.20	25.85	8.39
50	0.16	32.62	26.21	8.25
75	-0.36	33.05	26.56	7.78
100	-1.07	33.29	26.79	7.58
125	-1.29	33.38	26.89	-
150	-1.24	33.48	26.95	7.44
175	-1.10	33.62	27.06	-
200	-0.94	33.76	27.17	7.04
225	-0.83	33.87	27.25	-
250	-0.74	33.96	27.33	-
300	-0.61	34.10	27.44	6.76
400	-0.49	34.16	27.52	-
500	-0.48	34.22	27.52	6.63
600	-0.46	34.27	27.56	6.70

APPENDIX 4

STATION RECORDS FROM JUNE 1972

ROBESON CHANNEL

Sadler's Ice Camp

ROBESON CHANNEL ICE CAMP STATIONS

JUNE 1972

DEPTH m	TEMP. °C	SALIN. °/oo	σ_T	O_2 ml/l
Station 1. 2320 5 June; 81°58'.8N 62°06'.5W; Depth 600 m				
10	-1.72	32.34	26.04	
20	-1.76	32.39	26.08	Not
30	-1.74	32.45	26.13	Obs.
50	-1.73	32.49	26.16	
75	-1.73	32.54	26.20	
Note: Currents below 75 m too strong to use sample bottles				
Station 2. 2105 4 June; 81°55'.9N 61°49'.3W; Depth 644 m				
10	-1.72	32.04	25.80	
20	-1.74	32.06	25.81	Not
30	-1.79	32.09	25.84	Obs.
50	-1.78	32.09	25.84	
75	-1.62	32.33	26.03	
100	-0.98	33.46	26.93	
125	-0.65	33.72	27.38	
150	-0.63	33.97	27.67	
175	-0.30	34.23	27.68	
200	-0.28	34.48	27.70	
225	-0.16	34.44	27.71	
250	-0.16	34.39	27.68	
300	0.10	34.39	27.65	
400	0.19	34.55	27.76	
500	0.17	34.81	27.97	
600	0.19	-	-	

DEPTH m	TEMP. °C	SALIN. °/oo	σ_T	O_2 ml/l
Station 3. 1657 5 June; 81°53'.2N 61°16'.4W; Depth N.O				
10	-1.72	31.90	25.68	
20	-1.72	31.90	25.68	Not
30	-1.72	31.93	25.71	Obs.
50	-1.76	31.93	25.71	
75	-1.35	32.73	26.35	
100	-0.91	33.76	27.17	
125	-0.63	33.97	27.55	
150	-0.42	34.17	27.78	
175	-0.28	34.37	27.79	
200	-0.20	34.57	27.83	
225	-0.11	34.61	27.84	
250	-0.03	34.64	27.88	
300	0.06	34.71	27.89	
400	0.14	34.73	27.92	
500	0.14	34.75	27.91	
600	0.17	34.76	27.92	

APPENDIX 5

CALCULATION OF VOLUME AND HEAT TRANSPORT BY ADVECTION OF WATER THROUGH ROBESON CHANNEL

A shortened version of the integration is given on the following pages, the results being

Mean Southerly Volume Transport through Robeson Channel in May 1972	$= 0.67 \times 10^6 m^3 s^{-1}$ ± 16%
Mean Annual Volume Transport	$= 2.1 \times 10^4 km^3 year^{-1}$ ± 30%
and	
Mean Heat Transport into the Polar Ocean due to the transport of water through Robeson Channel in May 1972	$= 4.0 \times 10^{11}$ cals.s^{-1} ± 23%
Mean Annual Heat Transport	$= 1.3 \times 10$ cals.$year^{-1}$ ± 45%

The estimates of error are necessarily approximate but it was concluded that even an approximation would be more useful than the unqualified results in the literature. The method of arriving at these estimates is given below

Uncertainties in Transport for May 1972

It is assumed that the uncertainties in (ΔA) are ± 3% except in the sections including a piece of the bottom of the channel where they are taken as ± 5%. Further it is assumed that the uncertainty in the values of v_i must include not only the estimated ± 6% due to uncertainties of observation but also the uncertainties due to taking the individual values of v_i from the current profiles in Fig. 64 and the assumption that these values are valid for the whole grid square. While the profile at Station 2 is reasonably well based the other two are scaled versions of this profile and may be considerably in error. The assumed values of uncertainty in v_i at each grid point are shown on pages 172 to 175 where an uncertainty of ± 16% is derived for the volume transport in May 1972.

Similarly the value derived for the advective transport of heat due to water transport contains the uncertainties in the values of $(\Delta V)_i$ and those in the values $(\Delta T)_i$. In this case the values of temperature at the station positions taken from the temperature profiles in Figure 68 are considered to be accurate to ± 0.05°C because of the close agreement with the reversing thermometer readings. Further, there is little variation across the channel and it is considered to be a reasonable approximation to assume a similar uncertainty for the sink temperature of -0.8°C. The resulting uncertainty in the value for the temperature difference ΔT_i is thus ± 0.14°C and the uncertainty in the value for advective transport of heat in May 1972 is ± 23%.

Uncertainties in Annual Values

The probable errors given for the annual mean flows are even more uncertain since any seasonal and secular changes must be included. However, the total annual run-off into the whole of the Arctic Ocean is only 2% of the total influx into the ocean and only 15% of the flow through Robeson Channel. The effects of run-off on the flow in Robeson Channel are thus unlikely to exceed two or three per cent of the mean value. The magnitude of any variations which may exist in the volume transport from year to year is unlikely to exceed 10% because of the apparent stability of conditions in the Arctic Ocean. An extra uncertainty in volume flux of 12% due to seasonal and secular changes appears to be a conservative assumption and this value implies a total uncertainty in the value for the mean annual volume transport of ± 28%.

The seasonal variations in temperature might be expected to be more important at first sight. However, the temperature structure in May is probably not very different from the mean for the winter months from November to June inclusive. During the other four months of the year the temperature near the surface rises towards freezing point, but when the profile from Station 2 in Figure 70 is compared in Figure 73 with the mean profile for all those observed in August 1971 (Appendix 3, Stations 6, 7, 8, 9 and 15) it is seen that the maximum difference except at depths shallower than 10 m is 0.3°C. In fact, if the current profiles in August 1971 are assumed to be the same as those in May 1972 and the advective heat transport is calculated by the same method, the result is 3.8×10^{11} cals/s^{-1} which is only 5% different from the value obtained using the May 1972 temperature data. It is therefore probable that the uncertainty in the value for the annual mean advective heat transport is less than ± 33% allowing for a seasonal variation of ± 10%. Variations from year to year are more uncertain but as was discussed for the case of volume transport they are unlikely to exceed 10 or 12%. The total uncertainty of the value for the annual advective flow of heat is therefore about ± 40%.

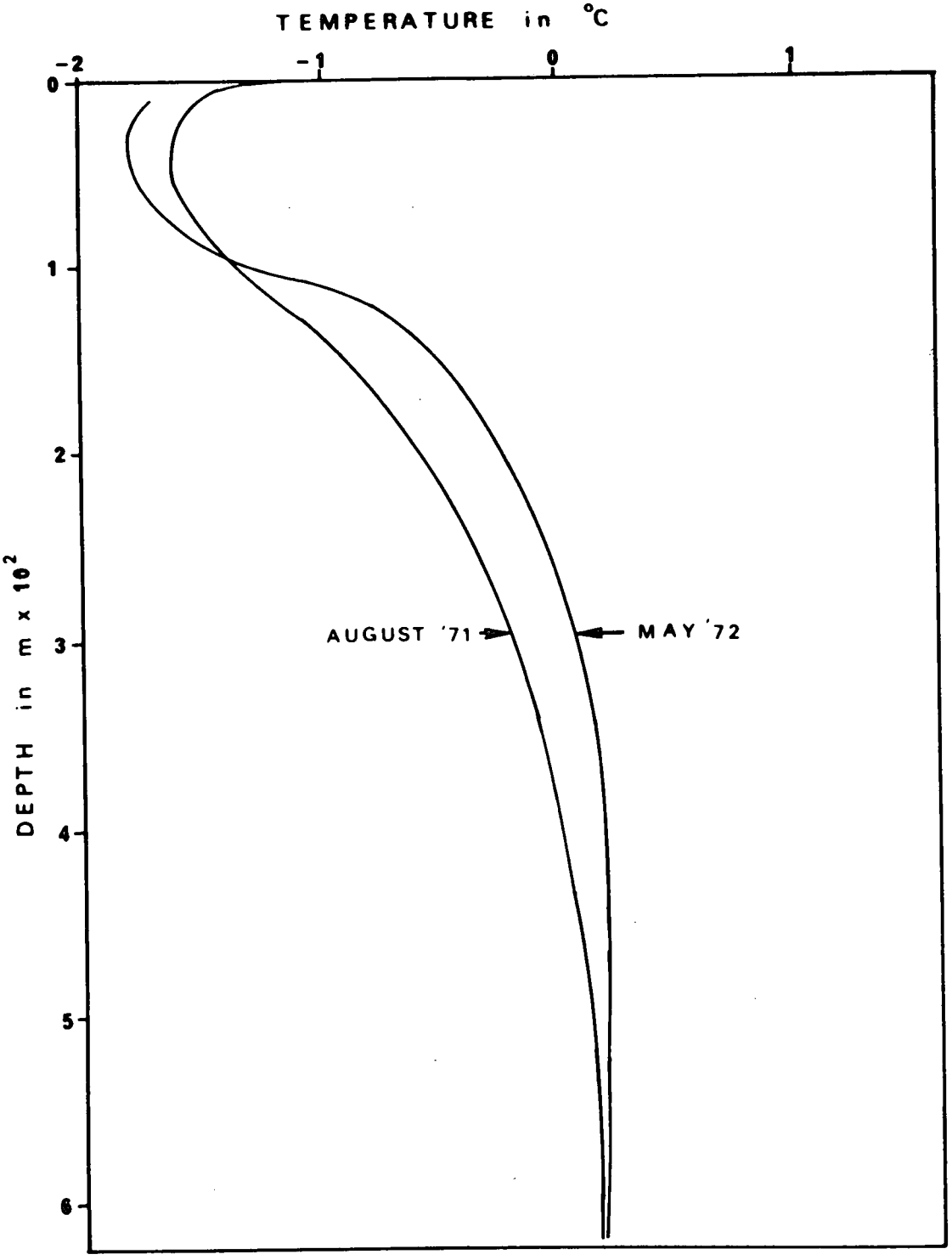

FIGURE 73 *Comparison of Spring and Summer temperature profiles in Robeson Channel.*

CALCULATION OF MASS AND HEAT TRANSPORT

SECTION 1

Section Number		$(\Delta A)_i$ ($m^2 \times 10^6$)	v_i ($m.s^{-1}$)	$(\Delta V)_i$ ($m^3.s^{-1} \times 10^6$)	$(\Delta T)_i$ (^oC) ($T_R = -0.8^oC$)	$(\Delta Q_w)_i$ (cal $\times 10^{10}$)
1.	1	0.1626	-0.172	-0.0280	-0.90	+2.52
	2.	.1625	.464	.0770	.92	7.09
	3.	.1589	.601	.0955	.93	8.88
	4.	.1583	.639	.1012	.93	9.41
	5.	.1581	.620	.0980	.78	7.64
	6.	.3149	.331	.1042	.06	0.63
	7.	.3120	.166	.0518	+0.37	-1.92
	8.	.3097	.102	.1317	.57	1.81
	9.	.3076	.058	.0178	.70	1.25
	10.	.3058	.025	.0077	.84	0.64
	11.	.3055	.000	.0000	.93	0.00
	12.	.3052	+ .015	+ .0046	.97	±0.44
	13.	.3044	.026	.0079	.99	0.78
	14.	.2970	.025	.0074	1.00	0.74
	15.	.2822	.020	.0056	1.00	0.56
	16.	.5788	.010	.0058	.99	0.57
	17.	.1962	.005	.0010	.99	0.10

CALCULATION OF MASS AND HEAT TRANSPORT

SECTION 2

Section Number	$(\Delta A)_i$ ($m^2 \times 10^6$)	v_i ($m.s^{-1}$)	$(\Delta V)_i$ ($m^3.s^{-1} \times 10^6$)	$(\Delta T)_i$ (^oC) ($T_R = -0.8^oC$)	$(\Delta Q_w)_1$ (cal $\times 10^{10}$)
2. 1.	0.1434	-0.098	-0.0140	-0.90	+1.27
2.	.1434	.139	.0199	.99	1.27
3.	.1434	.175	.0251	.98	2.46
4.	.1434	.188	.0269	.86	2.32
5.	.1434	.162	.0232	.60	1.39
6.	.2868	.087	.0250	+ .03	-0.08
7.	.2868	.051	.0146	.38	0.56
8.	.2868	.030	.0086	.56	0.48
9.	.2868	.016	.0046	.71	0.33
10.	.2868	.006	.0017	.84	0.14
11.	.2868	+0.001	+0.0003	.93	+0.03
12.	.2868	.005	.0014	.97	0.14
13.	.2868	.007	.0020	.99	0.20
14.	.2868	.008	.0023	1.00	0.23
15.	.2868	.007	.0020	1.00	0.20
16.	.7110	.004	.0028	.99	0.28
17.	.2995	.002	.0006	.99	0.06

CALCULATION OF MASS AND HEAT TRANSPORT

SECTION 3

Section Number	$(\Delta A)_i$ ($m \times 10^6$)	v_i ($m.s^{-1}$)	$(\Delta V)_i$ ($m^3.s^{-1} \times 10^6$)	$(\Delta T)_i$ (^oC) ($T_R = -0.8^oC$)	$(\Delta Q_w)_i$ ($cal \times 10^{10}$)
3. 1.	0.1605	+0.038	±0.0061	-0.90	-0.55
2.	.1604	.055	.0088	.92	0.81
3.	.1597	.062	.0099	.95	0.94
4.	.1572	.040	.0063	.69	0.43
5.	.1570	.031	.0049	.26	0.13
6.	.3127	.025	.0078	+0.13	+ 0.10
7.	.3119	.015	.0047	.45	0.21
8.	.3113	.011	.0034	.60	0.21
9.	.3002	.006	.0018	.74	0.13
10.	.2831	.004	.0011	.84	0.10
11.	.2440	.000	.0000	.88	0.00
12.	.2173	-0.005	-0.0011	.91	-0.10
13.	.1730	.006	.0010	.94	0.10
14.	.1642	.008	.0013	.94	0.12
15.	.1615	.006	.0010	.94	0.09
16.	.3792	.005	.0019	.95	0.18
17.	.2550	.003	.0008	.96	0.07
18.	.0815	.001	.0001	.96	0.01

CALCULATION OF UNCERTAINTY IN VOLUME AND HEAT TRANSPORT

Section	% Error in $(\Delta A)_i$	$(m.s^{-1})$ Estimated Uncertainty in v_i from profile	Total* % Error in v_i	$(m^3.s^{-1} \times 10^6)$ Uncertainty in $(\Delta T)_i$	$(T_R = 0.8^oC)$** % Error in $(\Delta T)_i$	$(cal.s^{-1} \times 10^{10})$ Uncertainty in $(\Delta Q)_i$
1.1	3	.05	30	.0092	11	1.11
2	3	.10	22	.0193	11	2.55
3	3	.20	34	.0353	11	4.26
4	3	.30	47	.0506	11	5.74
5	3	.10	17	.0916	13	2.52
6	3	.20	60	.0656	167	1.45
7	3	.10	60	.0326	27	1.73
8	3	.05	49	.0165	18	0.88
9	3	.05	86	.0158	14	1.29
10	3	.05	200	.0156	12	1.38
11	3	.02	-	.0000	11	0.00
12	3	.02	133	.0063	10	0.64
13	3	.02	77	.0063	10	0.70
14	3	.03	80	.0061	10	0.69
15	5	.02	100	.0058	10	0.64
16	5	.02	200	.0117	10	1.23
17	5	.02	400	.0040	10	0.42

* Total % error in v_i including the uncertainty of ± 6% found in Chapter 4

** Uncertainty in ΔT is assumed to be ± 0.14^oC for all entries

CALCULATION OF UNCERTAINTY IN VOLUME AND HEAT TRANSPORT

Section	% Error in $(\Delta A)_i$	$(m.s^{-1})$ Estimated Uncertainty in v_i from profile	Total* % Error in v_i	$(m^3.s^{-1} \times 10^6)$ Uncertainty in $(\Delta V)_i$	$(T_R = 0.8^oC)$** % Error in $(\Delta T)_i$	$(cal.s^{-1} \times 10^{10})$ Uncertainty in $(\Delta Q)_i$
2.1	3	.02	21	.0034	11	0.44
2	3	.02	15	.0036	10	.55
3	3	.02	13	.0040	10	.64
4	3	.02	13	.0043	12	.65
5	3	.02	13	.0037	17	.46
6	3	.02	24	.0068	333	.29
7	3	.02	39	.0061	26	.38
8	3	.02	67	.0060	18	.42
9	3	.01	63	.0076	14	.26
10	3	.01	162	.0038	11	.25
11	3	.01	1000	.0030	10	.30
12	3	.01	200	.0028	10	.30
13	3	.01	143	.0029	10	.31
14	3	.01	125	.0029	10	.32
15	3	.01	143	.0029	10	.31
16	3	.01	250	.0071	10	.74
17	5	.01	500	.0030	10	.31

CALCULATION OF UNCERTAINTY IN VOLUME AND HEAT TRANSPORT

Section	% Error in $(\Delta A)_i$	$(m.s^{-1})$ Estimated Uncertainty in v_i from profile	Total* % Error in v_i	$(m^3.s^{-1} \times 10^6)$ Uncertainty in $(\Delta V)_i$	$(T_R = 0.8^oC)$** % Error in $(\Delta T)_i$	$(cal.s^{-1} \times 10^{10})$ Uncertainty in $(\Delta Q)_i$
3.1	3	.02	53	.0034	11	0.37
2	3	.02	36	.0034	11	0.37
3	3	.02	32	.0035	11	.41
4	3	.02	50	.0033	14	.29
5	3	.02	65	.0033	38	.14
6	3	.02	80	.0065	77	.16
7	3	.01	67	.0033	22	.19
8	3	.01	91	.0032	17	.23
9	3	.01	167	.0031	14	.24
10	3	.01	250	.0028	12	.27
11	5	.01	-	.0000	11	.00
12	5	.01	200	.0023	11	.22
13	5	.01	167	.0017	11	.18
14	5	.01	125	.0017	11	.17
15	5	.01	167	.0017	11	.16
16	5	.01	200	.0039	11	.37
17	5	.01	333	.0027	10	.24
18	10	.01	1000	.0010	10	.10

Total uncertainty in Volume Transport $\pm$ 0.107 x $10^6 m.s.^{-1}$

Total uncertainty in Advective Heat Transport = $\pm$ 0.91 x 10^{11} cals s^{-1}

TRANSPORT OF SALT

Section Number	S $^{o}/oo$	Volume Transport ($m^3.s^{-1} \times 10^4$)	Salt Transport ($kgms.s^{-1}$)
1.1	32.34	- 2.80	- 0.91
.2	45	7.70	2.50
.3	.49	9.55	3.10
.4	.54	10.12	3.29
.5	33.10	8.78	2.91
.6	.68	8.41	2.83
.7	34.06	4.71	1.60
.8	.48	3.04	1.05
.9	.62	1.78	0.62
.10	.68	0.77	0.27
.11	.71	0.00	0.00
.12	.73	+ 0.46	+ 0.16
.13	.73	0.79	0.27
.14	.74	0.74	0.26
.15	.74	0.56	0.19
.16	.75	0.58	0.20
.17	.76	0.10	0.03

TRANSPORT OF SALT

Section Number	S °/oo	Volume Transport ($m^3.s^{-1} \times 10^6$)	Salt Transport ($kgms.s^{-1}$)
2.1	32.04	- 1.41	- 0.45
.2	.09	1.99	0.64
.3	.09	2.51	0.81
.4	.28	2.70	0.87
.5	33.32	2.32	0.77
.6	.68	2.50	0.84
.7	34.06	1.46	0.50
.8	.48	0.86	0.30
.9	.40	0.46	0.16
.10	.38	0.17	0.06
.11	.42	+ 0.03	+ 0.01
.12	.47	0.14	0.05
.13	.57	0.20	0.07
.14	.68	0.23	0.08
.15	.76	0.20	0.07
.16	.80	0.28	0.10
.17	.78	0.06	0.02

TRANSPORT OF SALT

Section Number	S °/oo	Volume Transport ($m^3.s^{-1} \times 10^4$)	Salt Transport ($kgm.s^{-1}$)
3.1	31.90	+ 1.01	+ 0.32
.2	93	1.20	.38
.3	.93	1.09	.35
.4	32.54	0.71	.23
.5	33.48	0.49	.16
.6	.94	0.78	.27
.7	34.25	0.47	.16
.8	.57	0.34	.12
.9	.63	0.18	.06
.10	.68	0.11	.04
.11	.71	0.00	.00
.12	.73	- 0.11	- 0.04
.13	.73	0.10	.04
.14	.74	0.13	.05
.15	.75	0.10	.03
.16	.75	0.19	.07
.17	.75	0.08	.03
.18	.75	0.01	.00

Total Salt Transport = 21.09 $kgm.s^{-1}$

out of Polar Ocean ≡ 6.7 x 10 $kgm.yr^{-1}$

Unclassified

Security Classification

DOCUMENT CONTROL DATA - R & D

(Security classification of title, body of abstract and indexing annotation must be entered when the overall document is classified)

1. ORIGINATING ACTIVITY
Defence Research Establishment Ottawa,
National Defence Headquarters,
Ottawa, Ontario. K1A 0Z4

2a. DOCUMENT SECURITY CLASSIFICATION
Unclassified

2b. GROUP

3. DOCUMENT TITLE
THE FLOW OF WATER AND HEAT THROUGH NARES STRAIT,

4. DESCRIPTIVE NOTES (Type of report and inclusive dates)
Report

5. AUTHOR(S) (Last name, first name, middle initial)
Sadler, H. Eric

6. DOCUMENT DATE
October 1975

7a. TOTAL NO. OF PAGES
196

7b. NO. OF REFS
76

8a. PROJECT OR GRANT NO.
97-67-05

9a. ORIGINATOR'S DOCUMENT NUMBER(S)
DREO Report No. 736

8b. CONTRACT NO.

9b. OTHER DOCUMENT NO.(S) (Any other numbers that may be assigned this document)

10. DISTRIBUTION STATEMENT
Normal distribution plus Dr. H. Freeland, Grad.School of Oceanography, U. of Rhode Island, Kingston, R.I. ,02881 and Dr. F. Barber, Environment Cda

11. SUPPLEMENTARY NOTES

12. SPONSORING ACTIVITY
DREO

13. ABSTRACT

(UNCLASSIFIED)

The flow of water from the Polar Ocean through Nares Strait is described by means of observations of water characteristics in the Strait and current meter observations in Robeson Channel. The mean annual volume discharge of water from the Polar Ocean is estimated to be 2.1×10^4 km^3 year^{-1} which is a higher value than previous estimates. The mean annual transport of salt out of the Polar Ocean through the Strait is estimated to be 6.7×10^{14} kg year^{-1}.

Thermograph records and observations of ice movement are used to derive a value for the mean annual heat flux into the Polar Ocean of 2.1×10^{19} cal.year^{-1}, which is also a higher value than previous estimates.

A discussion of tidal variations shows that the tides in Robeson Channel are mixed diurnal/semidiurnal with maximum current velocities along the axis of the channel of the order of 1.5 m.s.$^{-1}$ at 100 m depth.

A new explanation is proposed for the origin of Baffin Bay Bottom Water which depends on the assumption of a greater than usual amount of ice formation in the North Water polynya.

DSIS
72-508

U

Security Classification

KEY WORDS

Nares Strait
Water transport from Arctic Ocean
Heat transport into Arctic Ocean
Arctic islands
Sea-ice out of polar ocean

INSTRUCTIONS

1. ORIGINATING ACTIVITY: Enter the name and address of the organization issuing the document.

2a. DOCUMENT SECURITY CLASSIFICATION: Enter the overall security classification of the document including special warning terms whenever applicable.

2b. GROUP: Enter security reclassification group number. The three groups are defined in Appendix 'M' of the DRB Security Regulations.

3. DOCUMENT TITLE: Enter the complete document title in all capital letters. Titles in all cases should be unclassified. If a sufficiently descriptive title cannot be selected without classification, show title classification with the usual one-capital-letter abbreviation in parentheses immediately following the title.

4. DESCRIPTIVE NOTES: Enter the category of document, e.g. technical report, technical note or technical letter. If appropriate, enter the type of document, e.g. interim, progress, summary, annual or final. Give the inclusive dates when a specific reporting period is covered.

5. AUTHOR(S): Enter the name(s) of author(s) as shown on or in the document. Enter last name, first name, middle initial. If military, show rank. The name of the principal author is an absolute minimum requirement.

6. DOCUMENT DATE: Enter the date (month, year) of Establishment approval for publication of the document.

7a. TOTAL NUMBER OF PAGES: The total page count should follow normal pagination procedures, i.e., enter the number of pages containing information.

7b. NUMBER OF REFERENCES: Enter the total number of references cited in the document.

8a. PROJECT OR GRANT NUMBER: If appropriate, enter the applicable research and development project or grant number under which the document was written.

8b. CONTRACT NUMBER: If appropriate, enter the applicable number under which the document was written.

9a. ORIGINATOR'S DOCUMENT NUMBER(S): Enter the official document number by which the document will be identified and controlled by the originating activity. This number must be unique to this document.

9b. OTHER DOCUMENT NUMBER(S): If the document has been assigned any other document numbers (either by the originator or by the sponsor), also enter this number(s).

10. DISTRIBUTION STATEMENT: Enter any limitations on further dissemination of the document, other than those imposed by security classification, using standard statements such as:

    (1) "Qualified requesters may obtain copies of this document from their defence documentation center."

    (2) "Announcement and dissemination of this document is not authorized without prior approval from originating activity."

11. SUPPLEMENTARY NOTES: Use for additional explanatory notes.

12. SPONSORING ACTIVITY: Enter the name of the departmental project office or laboratory sponsoring the research and development. Include address.

13. ABSTRACT: Enter an abstract giving a brief and factual summary of the document, even though it may also appear elsewhere in the body of the document itself. It is highly desirable that the abstract of classified documents be unclassified. Each paragraph of the abstract shall end with an indication of the security classification of the information in the paragraph (unless the document itself is unclassified) represented as (TS), (S), (C), (R), or (U).

    The length of the abstract should be limited to 20 single-spaced standard typewritten lines; 7½ inches long.

14. KEY WORDS: Key words are technically meaningful terms or short phrases that characterize a document and could be helpful in cataloging the document. Key words should be selected so that no security classification is required. Identifiers, such as equipment model designation, trade name, military project code name, geographic location, may be used as key words but will be followed by an indication of technical context.